

Metabolism of doping agents using *in vitro* and *in vivo* models

Lore Geldof

Thesis submitted in fulfilment of the requirements for the degree of

Doctor (PhD) in Biomedical Sciences

Promotor

Prof. Dr. ir. Peter Van Eenoo

Co-promotor

Dr. Leen Lootens

2016

Metabolism of doping agents

using *in vitro* and *in vivo* models

Lore Geldof¹

Public defence on 1 July 2016

Promotor

Prof. Dr. ir. Peter Van Eenoo¹

Co-promotor

Dr. Leen Lootens¹

Examination Committee

Chairman:

Prof. Dr. Johan Van de Voorde²

Reading Committee:

Dr. Pieter Van Renterghem¹

Prof. Dr. Alain Verstraete³

Prof. Dr. Veronique Stove⁴

Prof. Dr. Christophe Stove⁵

Dr. Wim Van Thuyne⁶

Prof. Dr. Martial Saugy⁷

¹ Doping Control Laboratory (DoCoLab), Department of Clinical Chemistry, Microbiology and Immunology (GE06), Ghent University, Ghent, Belgium

² Department of Pharmacology (GE09), Ghent University, Ghent, Belgium

³ Laboratory of Toxicology, Department of Clinical Chemistry, Microbiology and Immunology (GE06), Ghent University, Ghent, Belgium

⁴ Laboratory of Clinical Biology – Metabolic diseases, Department of Clinical Chemistry, Microbiology and Immunology (GE06), Ghent University, Ghent, Belgium

⁵ Laboratory of Toxicology, Department of Bio-analysis (FW03), Ghent University, Ghent, Belgium

⁶ Eastman Chemical Company, Ghent, Belgium

⁷ Swiss Laboratory for Doping Analyses, University of Lausanne, Switzerland

“De korste weg is een illusie, de langste weg hobbelig traag. Volg je Hart en vindt het pad waar je onderweg lerend geniet...”

Patrick Mundus

Dankwoord

Het ganse traject van mijn doctoraat is een heel boeiende reis geweest die zowel mijn groei als wetenschapper als mijn persoonlijke groei gestimuleerd heeft. Ik ben dan ook ontzettend dankbaar voor deze leerrijke ervaring.

Het is niet altijd een even gemakkelijke weg geweest, af en toe werden er enkele omwegen toegevoegd. Gelukkig werd ik steeds omringd door mensen die mij opnieuw de juiste richting konden aangeven. Zonder al hun steun onderweg had ik de eindbestemming zeker niet bereikt! Ik wil hier dan ook iedereen stuk voor stuk oprecht bedanken voor hun, misschien soms onbewuste, bijdrage die ze hebben geleverd aan deze thesis.

Als eerste zou ik graag mijn promotor Prof. Peter Van Eenoo willen bedanken om mij de kans te geven om mijn doctoraat te starten na mijn masterproef in DoCoLab. Bovendien stond hij mij telkens opnieuw met raad en daad bij en vormde hij een onuitputbare bron van inspiratie voor zowel nieuwe experimenten als te onderzoeken componenten. Ik ben hem eveneens dankbaar om mij op wetenschappelijk vlak verder te laten ontwikkelen door deelnames aan congressen en de bijhorende presentaties. Ik wil hem ook bedanken om mij de verantwoordelijkheid te geven om studenten te begeleiden tijdens hun masterproef. Het mogen meehelpen met het routine werk, zorgden voor een leuke variatie met het onderzoek.

Ik wil eveneens mijn co-promotor Leen bedanken om mij op weg te zetten met de *in vitro* en *in vivo* modellen. En mij met haar kennis en ervaring bij te staan voor het uitvoeren van de muizenproeven.

Deze gelegenheid wil ik zeker en vast ook aangrijpen om Koen te bedanken om mij zo veel kennis bij te brengen over LC-MS. Ik ben hem eveneens heel dankbaar om mij door zijn aanstekelijk wetenschappelijk enthousiasme telkens te blijven motiveren en me terug op weg te helpen als ik even het noorden kwijt was.

Kris en Wim ben ik dankbaar om mij in te leiden in de wondere wereld van LC-MS en GC-MS respectievelijk en om mijn kennis omtrent de toestellen bij te schaven waar nodig. Ze hebben me telkens ook ontzettend goed bijgestaan bij mijn analyses en ze verleenden mij eveneens een uitstekende pechverhelping met de toestellen.

Leen en Pieter wil ik eveneens als mede-eilandbewoners en Nik, Michaël, Simone, Peter J. van het andere eiland bedanken om het bureauwerk aangenamer te maken. Nik wil ik zeker ook nog eens extra bedanken voor al zijn hulp tijdens mijn masterproef en de zo opgebouwde kennis, die een goede basis vormden voor mijn verder onderzoek in DoCoLab.

Ik zou Eva ook in het bijzonder een welgemeende dankjewel willen zeggen om haar levensvreugde en –visies met mij te delen. Je hebt me ongelofelijk geïnspireerd, zowel op wetenschappelijk als persoonlijk vlak. Ik wil je dan ook het allerbeste en een mooie toekomst wensen (hier in België of waar dan ook...)!!!

Alle andere collega's van DoCoLab Jan, Dominique, Fiona, Ann, Trui, Monica, Pascaline, Ruth en Steven wil ik bedanken voor alle teamwork en hulp met het labo en administratieve werk. Ik wil hen eveneens bedanken voor de leuke sfeer in DoCoLab met de vele fantasierijke pauzes en de bijhorende pronostieken (voorjaarsklassiekers, ronde van Frankrijk en de mol). Het was leuk dat ik in het laatste jaar toch ook eens met de overwinning mocht gaan lopen. Mede dankzij jullie was dit ganse traject een boeiende maar vooral ook leuke ervaring.

De studenten Jasper, Wouter en Ann-Sofie die ik heb mogen begeleiden tijdens hun masterproef wil ik bedanken voor hun inzet. Ik vond dit alvast heel leerrijk en leuk om jullie te mogen bijstaan. Dankjewel Lieselot Decroix voor de samenwerking in verband met de prostanozol studie. Ik wil hier eveneens alle andere studenten die in DoCoLab ontmoet heb gedurende hun stage/thesis bedanken. Ik wil hen dan ook het beste wensen bij hun verdere carrière en hoop dat hun ervaring in DoCoLab hierbij nog van pas komt.

I want to thank all the people that I met during my stay at DoCoLab: Lance, Vinicius, Vinod, Juliana and many more. My thanks go also to all participants of the Cologne workshop for their useful contributions in the field of doping and the interesting discussions. This workshop keeps researchers open-minded and encourages researchers, including myself, to perform further research in this field.

I am all the co-authors grateful for their cooperation and support.

Thank you Prof. Francesco Botrè and Dr. Amy B. Cadwallader for your support to set up the *in vitro* protocol and Prof. Daniel Eichner, Thane Campbell and Vinod Nair for your cooperation with regard to the methylstenbolone and estradienedione study. Special thanks to Dr. Óscar Pozo for the help with the interpretation of LC-MS/MS product ion scan spectra, the identification of the fragmentation patterns and the corresponding figures.

Ik wil hierbij ook Prof. Geert-Leroux Roels en Prof. Philip Meuleman bedanken om ons de mogelijk te bieden om met het chimeer muismodel te werken. Lieven Verhoye wil ik eveneens bedanken voor de assistentie met de muizenproeven en de verzorgsters van het animalarium voor het verzorgen van de muizen en onderhoud van de kooien.

Prof. José Martins en Tim Courtin wil ik eveneens bedanken voor het uitvoeren van de NMR analyses.

The members of the reading committee, Prof. Johan Van de Voorde, Dr. Pieter Van Renterghem, Prof. Alain Verstraete, Prof. Veronique Stove, Prof. Christophe Stove, Dr. Wim Van Thuyne and Prof. Martial Saugy, are acknowledged for their time to review this thesis and their valuable comments to improve this work.

Ik wil bovendien ook mijn (plus)ouders bedanken voor de mogelijkheid die ze me gaven om verder te studeren en zo mijn kennis te laten verruimen. Ik wil hen bedanken voor hun onvoorwaardelijke steun tijdens mijn doctoraat.

Mijn mama wil ik eveneens bedanken voor de vele kommetjes soep en kopjes thee met een zoetigheidje tijdens het studeren en bij het schrijven van mijn doctoraat. Ik wil mijn zus Inne ook bedanken voor de vele momenten van steun, leuke praatjes en belevenissen. Ik ben jou eveneens enorm dankbaar voor het ontwerpen van de kaft van mijn doctoraat, het ziet er echt prachtig uit!

De rest van mijn familie (oma's, opa's, plusbroers, tantes, nonkels, neven en nichten,...) wil ik uiteraard ook bedanken voor de interesse in mijn onderzoek, om in mij te blijven geloven en om er steeds voor mij te zijn.

Een bijkomende dankjewel aan de sterretjes in de hemel, Freddy en opa Julien. Bedankt Freddy om mij de Hakuna Matata filosofie bij te brengen! Bedankt opa om zo een warme, moedige, liefdevolle opa te zijn! Weet dat ik jullie bewonder en nog steeds naar jullie opkijk!

Ik ben ook mijn vrienden en vriendinnen ontzettend dankbaar voor hun luisterend oor en interesse in mijn onderzoek, weet dat dit telkens veel voor mij betekend heeft.

Een dikke merci aan Venera om mij te steunen en het vertrouwen te geven om jouw getuige te mogen zijn, de paardrijdvrienden die zorgden voor de nodige ontspanning op en naast de paarden, de Izegemse vrienden voor de vele leuke avonden in en buiten het marktkafee, Evelyn voor de toffe etentjes en babbeltjes tussendoor en Marlies, Stephanie en Irène om mij al vanaf de start aan de UGent te steunen en voor de vele plezante citytrips/etentjes/babbeltjes samen,...

Ik wil eveneens de vele personen en vrienden vanop de trein bedanken om het pendelen op te vrolijken met een babbel en een lach.

Ik wil de ongetwijfeld vele anderen die ik hierboven nog niet heb vermeld eveneens bedanken voor hun steun!

Tenslotte wil ik uiteraard Kris bedanken om zo een geduldig, hulpvaardig en steunend kompas voor mij te zijn. Bedankt om mij zo de juiste richting aan te geven voor het afwerken van deze thesis! Een bijkomende dankjewel voor de vele kleine, muzikale, fietsende, wandelende, reizende afslagen die mijn energiepeil/stressniveau in balans hielden...

Hartelijk Dank! Warm Thanks!

Lore

Table of Contents

Table of Contents	I
List of Tables	V
List of Figures	IX
List of Abbreviations.....	XV
<u>Part 1 - Introduction</u>	1
Chapter 1: General introduction	3
1 (Anti-)Doping and sport	4
2 World Anti-Doping Agency (WADA)	5
3 Doping control laboratories	7
4 Anabolic androgenic steroids (AAS)	8
5 New evolutions of performance enhancing substances	27
6 Doping and research ethics.....	31
7 Metabolism studies	32
References.....	45
Chapter 2: Outline of the study.....	55
1 <i>In vitro</i> and <i>in vivo</i> models for metabolism studies.....	56
2 Metabolism studies of (designer) steroids	57
3 Metabolism studies of other performance enhancing substances	58
4 Research objectives	60
References	61
<u>Part 2 - Metabolism studies of (designer) steroids</u>	65
Chapter 3: <i>In vitro</i> and <i>in vivo</i> metabolism studies of Prostanazol...	67
Abstract	68
1 Introduction	69
2 Materials and Methods	71
3 Results and Discussion	74
4 Conclusions.....	85
Acknowledgements.....	86
References	87
Chapter 4: <i>In vitro</i> and <i>in vivo</i> metabolism studies of Methylstenbolone	
.....	91
Abstract	92

1 Introduction	93
2 Materials and Methods	94
3 Results and Discussion	98
4 Conclusions.....	110
Acknowledgements.....	110
References	111
Chapter 5: <i>In vitro</i> and <i>in vivo</i> metabolism studies of Dimethazine	115
Abstract	116
1 Introduction	117
2 Materials and Methods	118
3 Results and Discussion	121
4 Conclusions.....	130
Acknowledgements.....	130
References	131
Chapter 6: <i>In vitro</i> and <i>in vivo</i> metabolism studies of Estra-4,9-diene-3,17-dione	133
Abstract	134
1 Introduction	135
2 Materials and Methods	136
3 Results and Discussion	139
4 Conclusions.....	144
Acknowledgements.....	144
References	145
Chapter 7: Dilute-and-shoot LC-HRMS method for the detection of (un)conjugated AAS - <i>In vitro</i> application: synthesis of glucuronide conjugates	147
Abstract	148
1 Introduction	149
2 Materials and Methods	150
3 Results and Discussion	154
4 Conclusions.....	167
Acknowledgements.....	168
References	169

<u>Part 3 - Metabolism studies of other performance enhancing substances</u>	173
Chapter 8: <i>In vitro</i> metabolism studies of LGD-4033.....	175
Abstract	176
1 Introduction	177
2 Materials and Methods	179
3 Results and Discussion	182
4 Conclusions.....	193
Acknowledgements.....	193
References	194
Chapter 9: <i>In vitro</i> metabolism studies of REV-ERB agonists: SR9009 and SR9011	197
Abstract	198
1. Introduction	199
2. Materials and Methods	201
3. Results and Discussion	204
4. Conclusions.....	215
Acknowledgements.....	215
References	216
<u>Part 4 - Epilogue</u>	219
Chapter 10: General discussion	221
1 Metabolism studies of (designer) steroids	222
2 Metabolism studies of other performance enhancing substances	230
3 Detection and identification of metabolites.....	233
References.....	235
Chapter 11: Conclusions and future perspectives	237
1 Conclusions.....	238
2 Future perspectives	239
References.....	241
Summary	243
Samenvatting	247
Curriculum Vitae	251

List of Tables

Chapter 1: General introduction

Table 1.1. Overview of prohibited substances and prohibited methods from the Prohibited List [8].

Table 1.2. Substances identified as AAFs in each drug class, for all sports, during 2014 (adapted from [14]).

Table 1.3. Phase I metabolic reactions in the four rings of AAS. The chemical structure of testosterone with indication of the A, B, C and D rings and numbering of the carbon atoms is also presented.

Table 1.4. Phase II metabolic reactions in the A- and D-rings of AAS.

Table 1.5. Overview of GC-MS and LC-MS techniques and their (dis)advantages for the screening of AAS.

Table 1.6. Overview of metabolic enzymes present in human liver fractions: S9, HLM and cytosol [25, 27, 117].

Table 1.7. Protocol for the *in vitro* metabolism studies.

Chapter 3: *In vitro* and *in vivo* metabolism studies of Prostanazol

Table 3.1. Prostanazol metabolites detected in the *in vitro* and *in vivo* metabolism studies by full scan GC-MS analysis. The metabolites are ranked according to their RRT.

Table 3.2. Overview of prostanazol metabolites detected in the *in vitro* and *in vivo* studies compared with reported metabolites in literature (human excretion studies).

Chapter 4: *In vitro* and *in vivo* metabolism studies of Methylstenbolone

Table 4.1. Overview of metabolites detected after incubation of isolated methylstenbolone and reference standard of methasterone to HLM and the chimeric mouse model by GC-MS. Ion transitions of selected compounds in the developed multiple reaction monitoring (MRM) method (GC-MS/MS) for the detection of methylstenbolone and methasterone misuse are listed.

Chapter 5: *In vitro* and *in vivo* metabolism studies of Dimethazine

Table 5.1. Overview of dimethazine metabolites detected in metabolism studies with HLM and the chimeric mouse model by LC-HRMS. See Figure 5.1 for tentative structures of the metabolites.

Chapter 6: *In vitro* and *in vivo* metabolism studies of Estra-4,9-diene-3,17-dione

Table 6.1. Overview of estra-4,9-diene-3,17-dione metabolites detected in metabolism studies with HLM and the chimeric mouse model by LC-HRMS and GC-MS.

Chapter 7: Dilute-and-shoot LC-HRMS method for the detection of (un)conjugated AAS - *In vitro* application: synthesis of glucuronide conjugates

Table 7.1. Structure, chemical formula, detected ion and theoretical mass, retention time and standard deviation (n=10) and matrix effects for the commercially available investigated compounds.

Table 7.2. Structure, chemical formula, detected ions, theoretical and experimental masses and retention time for the non-commercially available investigated compounds.

Table 7.3. Obtained LOD (ng/mL) for the investigated compounds.

Chapter 8: *In vitro* metabolism studies of LGD-4033

Table 8.1. Detected metabolites after HLM incubation with LGD-4033. Both LC-HRMS as GC-MS results are indicated.

Table 8.2. Results derived from LC-HRMS/MS (ESI) product ion scans in negative and positive ionization mode of LGD-4033 and its metabolites.

Chapter 9: *In vitro* metabolism studies of REV-ERB agonists: SR9009 and SR9011

Table 9.1. LC-HRMS product ion scans of SR9009 and SR9011. Common product ions of the parent compounds and metabolites are also indicated.

Table 9.2. Characterization of metabolites detected in HLM incubation samples with SR9009 by LC-HRMS analysis.

Table 9.3. Characterization of metabolites detected in HLM incubation samples with SR9011 by LC-HRMS analysis.

Chapter 10: General discussion

Table 10.1. Overview of black market products examined in this study.

List of Figures

Chapter 1: General introduction

Figure 1.1. Evolution in the number of human (urine) samples analyzed per year by DoCoLab from 1973 until 2015.

Figure 1.2. Mechanism of action of AAS and estrogens (extracted from [19]).

Figure 1.3. Core structure of AAS with indication of the A, B, C and D rings and the numbering of the carbon atoms (left side) and chemical structure of testosterone (right side).

Figure 1.4. Relationships of the four steps in disposition of xenobiotic compounds within an organism.

Figure 1.5. Glucuronide conjugation of testosterone by UGT.

Figure 1.6. Sulfate conjugation of testosterone by SULT.

Figure 1.7. Sample preparation procedure of urine samples.

Figure 1.8. TMS derivatization of testosterone.

Figure 1.9. Configuration of GC-MS and LC-MS triple quadrupole instruments and the different scan modes.

Figure 1.10. Approach for the detection and characterization of unknown compounds (adapted from [55]).

Figure 1.11. Mammalian circadian clock.

Figure 1.12. Overview of *in vitro* and *in vivo* models for metabolism studies. The advantages (+) and disadvantages (-) of the models are also indicated, including the positioning of the models in comparison with human excretion studies.

Figure 1.13. Isolation of HLM and S9 liver fractions.

Figure 1.14. NADPH regeneration by glucose-6-phosphate dehydrogenase (G6PD).

Figure 1.15. Eppendorf Thermomixer applied for the incubation of the *in vitro* metabolism studies.

Figure 1.16. Protocol of the *in vitro* metabolism studies with HLM and S9 liver fractions.

Figure 1.17. Administration protocol for the chimeric mouse model.

Figure 1.18. Metabolic cage (left side) and filter top cage (right side).

Figure 1.19. Sample preparation protocol for the *in vitro* and *in vivo* assays.

Chapter 2: Outline of the study

Figure 2.1. Chemical structures of prostanazol, estradiendione, methylstenbolone, methasterone, and dimethazine.

Figure 2.2. Chemical structure of SARM LGD-4033.

Figure 2.3. Chemical structures of REV-ERB agonists SR9009 and SR9011.

Chapter 3: *In vitro* and *in vivo* metabolism studies of Prostanazol

Figure 3.1. Chemical structures of (A) prostanazol-THP, (B) prostanazol and (C) stanazolol and commercially available reference standards: (D) 4-hydroxy-17-ketoprostanazol, (E) 3'-hydroxy-17-ketoprostanazol and (F) 16 β -hydroxy-17-ketoprostanazol.

Figure 3.2. Mass spectra of prostanazol and the categories of prostanazol metabolites (I-VII; see Table 2 for the classification of the metabolites) detected in chimeric mice and/or HLM studies by GC-MS analysis and tentative structure presentation of the metabolites in correspondence with the molecular masses.

Figure 3.3. Extracted ion chromatogram (EIC) of the ions with m/z (A) 168, 456 and 458; (B) 544; (C) 546 (D) 632 and (E) 634 in a 4 h HLM sample and overlay with 4 h blank control sample (upper panel). EIC of m/z 254, 458, 544, 546, 632 and 634 in chimeric mouse urine collected after prostanazol administration (lower panel).

Figure 3.4. LC-MS/MS precursor ion scan chromatograms of (A) blank control sample and (B) HLM sample 4 h incubated with prostanazol. For legend of the categories I-VII see Table 3.2. In (A) also the proposed fragmentation pathways for the selected product ions are shown.

Figure 3.5. LC-MS/MS precursor ion scan chromatograms of (A) chimeric mouse urine collected before prostanazol administration and (B) chimeric mouse urine collected after prostanazol administration. For legend of the categories I-VII see Table 3.2. In (B) a detail is shown of the extra metabolite of category V (m/z 329) detected with m/z 81 as product ion next to the metabolite of category II (m/z 331), when applying a Zorbax C8 column. This latter metabolite corresponds to metabolite M9 (16 β -hydroxy-17-ketoprostanazol) detected by GC-MS

Chapter 4: *In vitro* and *in vivo* metabolism studies of Methylstenbolone

Figure 4.1. Chemical structures of (A) methasterone (marketed as 'Superdrol') and (B) methylstenbolone (marketed as 'Ultradrol').

Figure 4.2. GC-MS mass spectra of the detected metabolites of methylstenbolone after HLM incubation or administration to the chimeric mouse model of the purified steroid product.

Figure 4.3. LC-MS/MS precursor ion scan chromatograms of (A) blank (substrate stability) sample and (B) 4 h microsomal incubation sample of isolated methylstenbolone (m/z 317). IS = 17 α -methyltestosterone (m/z 303).

Figure 4.4. EIC (m/z 143) after 4 h incubation of steroid product containing methasterone and methylstenbolone and incubation of the reference standard of methasterone with HLM. Metabolites S1, S2 and S3 of methasterone are indicated. The mass spectrum of S3 is shown.

Figure 4.5. Developed MRM method to detect misuse of methylstenbolone via parent compound, U1, U4, U6, U7, U11, U12 and U13. This method was applied to a mix of microsomal incubation samples and chimeric mouse urine after administration of isolated methylstenbolone.

Figure 4.6. GC-MS/MS chromatograms obtained in the application of the developed MRM method to (A) negative human urine sample and (B) human urine sample declared positive for methasterone.

Chapter 5: *In vitro* and *in vivo* metabolism studies of Dimethazine

Figure 5.1. Chemical structures of dimethazine (A), methasterone (B), M1 (S1) and tentative structures for metabolites M2-M6.

Figure 5.2. Extracted ion LC-HRMS chromatograms of methasterone and metabolites M2, M3, M4 and M6 in a negative control sample (without dimethazine) (A), a blank control sample (without HLM) (B) and a 4 h HLM incubation sample of dimethazine (C).

Figure 5.3. Product ion scan mass spectra (LC-HRMS) of DMZ (A) and methasterone (B) obtained from their reference standard with as selected precursor ion m/z 633.5354 (CE of 55eV) and 319.2632 (CE of 25eV) respectively.

Figure 5.4. Product ion scan mass spectra (LC-HRMS) of metabolites M2, M3(b) and M6(a) obtained from *in vitro* samples and M4 from *in vivo* sample at a CE of 25eV (M2, M3(b) and M4) or 35 eV (M6(a)).

Chapter 6: *In vitro* and *in vivo* metabolism studies of Estra-4,9-diene-3,17-dione

Figure 6.1. Chemical structures of (A) estradienedione, (B) dienolone and (C) trenbolone.

Figure 6.2. LC-HRMS extracted ion chromatogram of estra-4,9-dien-3,17-dione in the steroid product and LC-MS/MS product ion scan mass spectrum at 25 eV.

Figure 6.3. Extracted LC-HRMS ion chromatograms of the parent compound and metabolites M1-M4 in a (A) negative control sample and a (B) 4 h HLM incubation sample of estra-4,9-dien-3,17-dione.

Figure 6.4. Product ion scan mass spectrum of (A) M1a (m/z 287) at 15 eV and (B) M2 (m/z 273) at 25eV and proposed fragmentation pathways.

Chapter 7: Dilute-and-shoot LC-HRMS method for the detection of (un)conjugated AAS - *In vitro* application: synthesis of glucuronide conjugates

Figure 7.1. Optimized gradient.

Figure 7.2. Simulated chromatogram of a spiked urine at 50 ng/mL with the compounds included in the DS-LC-HRMS method in positive (A) and negative (B) ionization mode. (The scale was adjusted to visualize all compounds. LOD's are presented in Table 3).

Figure 7.3. Detection of methyltestosterone: (A) Negative urine. (B) METm2G detected in a methyltestosterone excretion urine where only METm2 at 2 ng/mL was detected by GC-MS.

Figure 7.4. Detection of CMD misuse. (A) Negative urine. (B) Spiked urine with CMD (100 ng/mL). (C) CMD excretion urine.

Chapter 8: *In vitro* metabolism studies of LGD-4033

Figure 8.1. LC-HRMS and GC-MS analysis of black market product containing LGD-4033. LC-HRMS: both the TIC and EIC are shown. GC-MS: EIC, EI mass spectrum of LGD-4033 and proposed fragmentation pattern after TMS-derivatization is also presented.

Figure 8.2. Phase I and phase II (UGT) LGD-4033 metabolism studies with HLM. The 4 h HLM incubation samples are presented in comparison with the blank control samples.

Figure 8.3. LC-HRMS/MS mass spectra of LGD-4033 are shown in both negative and positive ionization mode at a collision energy of 35 eV and 45 eV respectively. The tentative fragmentation patterns are also presented.

Figure 8.4. LC-HRMS/MS mass spectra of LGD-4033 metabolites M2 and M4 are shown in both negative and positive ionization mode at a collision energy of 35 eV and 45 eV respectively. The tentative fragmentation patterns are also presented.

Figure 8.5. Tentative fragmentation pathways of LGD-4033 metabolite M2 in both negative and positive ionization mode. Only one possible configuration of metabolite M2 is presented here.

Figure 8.6. Tentative fragmentation pathways of LGD-4033 metabolite M4 in both negative and positive ionisation mode. Only one possible configuration of metabolite M4 is presented here.

Chapter 9: *In vitro* metabolism studies of REV-ERB agonists: SR9009 and SR9011

Figure 9.1. Chemical structures of REV-ERB α agonists SR9009 (left side) and SR9011 (right side). The tentative fragmentation patterns are also indicated.

Figure 9.2. *In vitro* metabolism studies with SR9009. The extracted ion LC-HRMS chromatograms of the 4 h HLM incubation samples (right column) are presented in comparison with blank (without HLM) control samples (left column).

Figure 9.3. *In vitro* metabolism studies with SR9011. The extracted ion LC-HRMS chromatograms of the 4 h HLM incubation samples (right column) are presented in comparison with blank (without HLM) control samples (left column).

Figure 9.4. Overview of *in vitro* metabolism studies with SR9009 and SR9011. The proposed metabolic modifications are also indicated. For the position of hydroxylations only one possible configuration is shown.

Chapter 10: General discussion

Figure 10.1. Overview of prostanazol metabolic pathways observed via *in vitro* and *in vivo* metabolism studies. The question marks indicate proposed positions for hydroxylations based on common AAS hydroxylation pathways described in literature.

Figure 10.2. Overview of metabolic pathways observed for dimethazine, methasterone and methylstenbolone via *in vitro* and *in vivo* metabolism studies.

Figure 10.3. Overview of metabolic pathways observed for estra-4,9-diene-3,17-dione via *in vitro* and *in vivo* metabolism studies. The proposed positions for hydroxylations are at C2, C6 or C16 (indicated with a *).

Figure 10.4. Integrated approach for metabolism studies.

Figure 10.5. Overview of metabolic pathways observed for LGD-4033 via *in vitro* metabolism studies.

Figure 10.6. Overview of metabolic pathways observed for SR9009 and SR9011 via *in vitro* metabolism studies. The structures of A, B, C, D and F' are indicated in Chapter 9 (Figure 9.1 and Table 9.4).

List of Abbreviations

List of Abbreviations

A	Area
AAFs	Adverse analytical findings
AAS	Anabolic androgenic steroids
ABP	Athletes biological passport
ADAMS	Anti-Doping Administration and Management System
ADME	Absorption, distribution, metabolism and excretion
APMU	Athletes Passport Management Unit
AM(-2201/2233)	Synthetic cannabinoids first synthesized by Alexandros Makriniannis
Amu	Atomic mass units
AR	Androgen receptor
BMAL1	Brain and muscle aryl hydrocarbon receptor nuclear translocator-like protein 1
CI	Chemical ionization
CID	Collision induced dissociation
CE	Collision energy
CEVAC	Center for Vaccinology
CLOCK	Circadian locomotor output cycles kaput
COMT	Catechol-O-methyltransferase
CRY	Cryptochrome
CYP450	Cytochrome P450
DHT	5 α -dihydrotestosterone
DMZ	Dimethazine
DoCoLab	Doping control laboratory at Ghent University
DOSY	Diffusion ordered spectroscopy
<i>E. coli</i>	<i>Escherichia coli</i>

EH	Epoxide hydrolase
EI	Electron ionization
EIC	Extracted ion chromatogram
EPO	Erythropoietin
ER*	Estrogen receptor
ER	Endoplasmatic reticulum
ESAs	Erythropoiesis stimulating agents
ESI	Electrospray ionization
EtOH	Ethanol
FIFA	Fédération Internationale de Football Association
FMO	Flavin monooxygenase
GC-MS	Gas chromatography – mass spectrometry
GHRP	Growth hormone-releasing peptide
GST	Glutathione transferase
G6PD	Glucose-6-phosphate dehydrogenase
HCD	Higher energy collision dissociation
HESI	Heated electrospray ionization
HLM	Human liver microsomes
HOAc	Acetic acid
HPLC	High performance liquid chromatography
<i>H. pomatia</i>	<i>Helix pomatia</i>
HRMS	High resolution mass spectrometry
Hsp90	Heat shock protein 90
IAAF	International Association of Athletics Federations

List of Abbreviations

I.d.	Internal diameter
IEC	International Electrotechnical Commission
IFs	International Sports Federations
IOC	International Olympic Committee
IRMS	Isotope Ratio Mass Spectrometry
IS	Internal standard
ISL	International Standard for Laboratories
ISO	International Standard Organization
JWH(-122/200)	Synthetic cannabinoids first synthesized by John W Huffman
LC-MS	Liquid chromatography – mass spectrometry
LGD-4033	SARM first synthesized by Ligand Pharmaceuticals
LHRH	Luteinizing hormone-releasing hormone
LLE	Liquid-liquid extraction
MAO	Mono-amine oxidase
MeOH	Methanol
MRPLs	Minimum required performance limits
MRM	Multiple reaction monitoring
MS	Mass spectrometry
MS/MS	Tandem mass spectrometry
MSTFA	N-methyl-N-trimethylsilyltrifluoroacetamide
MW	Molecular weight
m/z	Mass to charge ratio
NADOs	National Anti-Doping Organizations
NADPH	Nicotinamide adenine dinucleotide phosphate

NADPH-A	NADPH solution A
NADPH-B	NADPH solution B
NAT	N-acetyl transferase
NMR	Nuclear Magnetic Resonance
NPD	Nitrogen Phosphorous Detetector
NR1D1	Nuclear Receptor Subfamily 1 Group D, member 1
OFN	Oxygen free nitrogen
PAP	3'-phosphoadenosine-5'-phosphate
PAPS	3'-phosphoadenosine-5'-phosphosulfate
PBS	Phosphate Buffered Saline
PER	Period
RADOs	Regional Anti-Doping Organizations
REV-ERB	Reverse – viral erythroblastosis oncogene product
ROR α	Retinoic acid-related orphan nuclear receptors α
RT	Retention time
RRT	Relative retention time
SARMs	Selective androgen receptor modulators
SCID	Severe Combined Immuno Deficiency
SCN	Suprachiasmatic nucleus
SIM	Selected ion monitoring
S/N	Signal to noise ratio
SPE	Solid-phase extraction
SR(-9009/9011)	REV-ERB agonists first synthetized by SCRIPPS Research institute
SRE	Steroid response element

List of Abbreviations

SRM	Selected reaction monitoring
SULT	Sulfotransferase
T	Testosterone
TB	Thymosin- β 4
T/E	Testosterone to epitestosterone ratio
THG	Tetrahydrogestrinone
THP	Tetrahydropyranyl
TIC	Total ion chromatogram
TMS	Trimethylsilyl
TMSI	Iodotrimethylsilane
TOF	Time-of-flight
UCI	Union Cycliste Internationale
UDPGA	Uridine 5'-diphospho-glucuronic acid
UDPGA-A	UDPGA solution A
UDPGA-B	UDPGA solution B
UGT	Uridine diphosphoglucuronosyl transferases
uPA	Urokinase plasminogen activator
V _{DC}	Direct current
V _{RF}	Radio frequency voltage
WAADS	World Association of Anti-Doping Scientists
WADA	World Anti-Doping Agency

PART 1

Introduction

Chapter 1

General introduction

1 (Anti-)Doping and sport

The word doping would etymologically be derived from 'dope', a spirit prepared from grape residues by Zulu warriors used as a stimulant during fights and religious procedures. In Afrikaans / Dutch this was reportedly also called 'doop' [1, 2].

The use of substances or beverages to enhance performance is as old as competitive sport itself [2, 3]. Various plants, mushrooms and mixtures of wine and herbs were used by ancient Greek Olympic athletes and Roman gladiators for their stimulant effects (overcome fatigue), to improve their strength and to mask pain [3, 4]. The Indians and the Huns also consumed testicles to enforce virility [1]. Nowadays, factors as economic benefits, social and psychological pressure are still tempting athletes to use doping to enhance their performance in competitions [5]. In the beginning the use of doping was not considered as cheating, but rather as a tool to extend human capacities. Nor was there any attempt to discourage the use of these substances [3, 5]. It was only during the 1920s that opinions were raised that doping was unfair and that restrictions were needed, not only to protect the ethics of sport, but also the health of athletes [2, 4].

Several International Sports Federations (IFs) e.g. the International Association of Athletics Federations (IAAF) started banning doping in 1928 [1, 2]. Several national governments also prohibited doping. The first of these were France and Belgium in 1963 and 1965, respectively. However, the first doping tests were only introduced in 1966 by the Union Cycliste Internationale (UCI) and the Fédération Internationale de Football Association (FIFA) [1, 2]. In 1967 a first list of prohibited substances (stimulants and narcotics) was set up by the medical commission of the International Olympic Committee (IOC). The first drug tests by the IOC were introduced at the Olympic Winter Games in Grenoble and at the Olympic Games in Mexico in 1968 [1, 2]. By the 1970s most IFs followed by introducing drug testing of athlete samples [2]. Although indications of extensive use of anabolic androgenic steroids (AAS) existed, these compounds were not initially added to the list of prohibited substances of the IOC. This is probably due to a combination of the lack of detection methods and the prevalent medical opinion, at that time, which stated that the use of AAS had no advantage in athletic performance [6]. The first reliable test for anabolic agents was introduced in 1974 and two years later anabolic steroids were also added to the list of prohibited substances of the IOC [2]. However, these measures did not stop the use of AAS as demonstrated by several doping scandals over history, for example the misuse of stanozolol by Ben Johnson at the 1988 Olympic Games in Seoul [1, 2]. Other (well-organized) doping practices came out and indicated that the struggle against doping was not over [2]. Moreover, on top of the AAS there was also a focus to blood doping and erythropoiesis stimulating agents (ESAs) (such as erythropoietin (EPO)). Both

were banned by the IOC in 1986 and 1990 respectively. The first effective EPO detection test was implemented ten years after the ban of EPO at the Sydney Olympic Games [2].

In 1989 the first step was made towards an international harmonization in the fight against doping by the establishment of the Anti-Doping Convention of the Council of Europe. However, national legislation and rules of IFs still varied substantially. Spurred by the doping scandal at the 1998 Tour de France, where large amounts of performance enhancing substances were discovered, a World Conference on Doping in Sport was organized by the IOC in Lausanne in 1999 seeking a partnership between governments and IFs in the fight against doping. This conference led to the foundation of the World Anti-Doping Agency (WADA), an international independent governing body [1, 2, 4].

2 World Anti-Doping Agency (WADA)

WADA's mission is to promote and coordinate the fight against doping in sport internationally. WADA wants to preserve the intrinsic value of sport, the so-called 'spirit of the sport'. Therefore, WADA protects the athlete to participate in a doping-free, healthy sport and harmonizes the fight against doping by implementation of a universal anti-doping program with regards to detection, education and prevention of doping. The World Anti-Doping Code ensures a uniform application of the anti-doping regulations across all sports and all countries. WADA also stimulates scientific doping research worldwide and cooperation of IFs, National Anti-Doping Organizations (NADOs) and Regional Anti-Doping Organizations (RADOs) [1, 2, 4, 7].

2.1 Definition of doping

The extended definition of doping by WADA is: the occurrence of one or more of the anti-doping rule violations in the Anti-doping Code [7].

These anti-doping rule violations include:

1. Presence of a prohibited substance or its metabolites or markers in an athlete's sample
2. Use or attempted use by an athlete of a prohibited substance or a prohibited method
3. Evading, refusing or failing to submit to sample collection
4. Whereabouts failures
5. Tampering or attempted tampering with any part of doping control
6. Possession of a prohibited substance or a prohibited method
7. Trafficking or attempted trafficking in any prohibited substance or prohibited method
8. Administration or attempted administration of any prohibited substance or prohibited method to an athlete in- or out-of-competition
9. Complicity in an anti-doping rule violation
10. Prohibited association with sanctioned athlete support personnel

2.2 Prohibited List

Since 2004, WADA publishes yearly a list of prohibited substances and methods [1]. These substances and methods are not only prohibited to warrant fair play and the spirit in sports but also to safeguard the health of athletes [7].

Prohibited substances of categories S0 till S5 and all prohibited methods (M1 till M3) are prohibited at all times, in- and out-of-competition (Table 1.1). Substances of categories S6 till S9 are only prohibited in-competition. Substances of categories P1 and P2 are only prohibited in particular sports such as automobile and archery [8]. This list is not a nominative list and can be updated at any time.

Table 1.1. Overview of prohibited substances and prohibited methods from the 2016 Prohibited List [8].

PROHIBITED SUBSTANCES
<i>Prohibited in- and out-of-competition</i>
S0. Non-approved substances
S1. Anabolic agents
S2. Peptide hormones, growth factors, related substances and mimetics
S3. Beta-2 agonists
S4. Hormone and metabolic modulators
S5. Diuretics and masking agents
<i>Prohibited in-competition</i>
S6. Stimulants
S7. Narcotics
S8. Cannabinoids
S9. Glucocorticoids
SUBSTANCES PROHIBITED IN PARTICULAR SPORTS
P1. Alcohol
P2. Beta-blockers
PROHIBITED METHODS
M1. Manipulation of blood and blood components
M2. Chemical and physical manipulation
M3. Gene doping

2.3 Athletes biological passport (ABP)

In 2009 the ABP was introduced to enable indirect detection of doping misuse besides the direct detection of prohibited substances and methods [2]. Indirect markers can reveal modifications in biological parameters induced by a doping product e.g. increased hematocrit values can indicate use of ESAs and suppressed endogenous steroid profiles can indicate administration of exogenous steroids [9, 10].

Initially, the ABP only consisted out of a hematological module including a longitudinal evaluation of blood parameters (e.g. hematocrit) of individual athletes, which may be indicative for blood doping. In 2014 the steroidal module was incorporated into the ABP to detect doping with synthetic analogues of endogenous steroids [2]. Further extension of the ABP with other modules (e.g. hormones and genetic profiling) is likely.

Since the ABP is based on longitudinal follow up it has the advantage over the previous stand-alone evaluation of results applied so far because individual reference ranges can be calculated for each parameter. The application of these individual ranges rather than population based thresholds facilitates the detection of abnormal values for every individual athlete [2, 9]. Indeed, the intra-individual variation for the monitored compounds is lower than the combined intra- and inter-individual variation.

3 Doping control laboratories

Currently there are 34 laboratories accredited by WADA to conduct human doping control samples. The International Standard for Laboratories (ISL) is mandatory for all accredited doping laboratories and implies application of International Standard Organization / International Electrotechnical Commission (ISO/IEC) 17025 [11] and compliance with WADA's Technical documents, including the minimum required performance limits (MRPLs) [11]. Additionally, laboratories are expected to perform research which contributes to the development and implementation of an effective doping control. WADA accredited laboratories are subjected to an intensive proficiency testing scheme to maintain accreditation and need to report all results in a WADA controlled database, called ADAMS (Anti-Doping Administration and Management System).

To harmonize the efforts of the doping control laboratories the World Association of Anti-Doping Scientists (WAADS) was established. WAADS provides a forum to exchange knowledge and to enhance the contribution to clean and fair sports [1, 12].

The research for this doctoral dissertation was performed at the doping control laboratory of Ghent University (DoCoLab), the only WADA accredited laboratory in the Benelux. Since 1973 DoCoLab analyzes human doping control samples (Figure 1.1). DoCoLab was first accredited by the IOC in 1992 and later on by WADA. The percentage of adverse analytical findings (AAFs) and atypical findings (ATF) ranged from 1.6 to 7.2 during the period of 1973 till 2015. It should however be noted that after 2014, the number of ATFs dropped significantly due to the implementation of the steroidal module of the ABP, thereby no longer automatically identifying samples with a testosterone-to-epitestosterone ratio (T/E) higher than 4 as an ATF.

DoCoLab also analyzes blood samples in support of the hematological module of the ABP. Moreover, DoCoLab holds a WADA approved Athlete Passport Management Unit (APMU) for both the hematological as the steroidal module of the ABP [2].

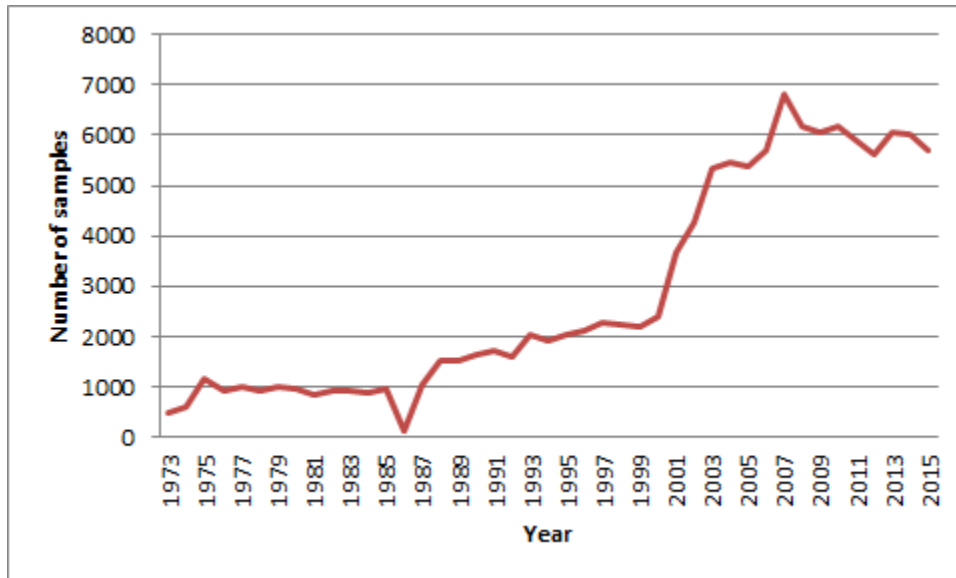


Figure 1.1. Evolution in the number of human (urine) samples analyzed per year by DoCoLab from 1973 until 2015.

4 Anabolic androgenic steroids (AAS)

4.1 AAS as doping

The use of AAS by consuming testicles was already reported in documents from ancient history. The 'discovery' of testosterone and its synthesis in the 1930s accelerated scientific investigations on the effects of testosterone administrations [3, 4, 13]. During the 1950s, the first misuse in sport of male steroid hormones to increase strength and power, namely by the Soviet Olympic team and bodybuilders (strength-intensive sports), was reported [3, 4, 13]. Nowadays, AAS continue to be the most detected class of prohibited substances in the testing statistics of WADA accredited doping control laboratories, as indicated in Table 1.2 [14].

Table 1.2. Substances identified worldwide as AAFs in each drug class, for all sports, during 2014 (adapted from[14]).

Substance group	Number of findings	% of all ADAMS reported findings
S1. Anabolic agents	1479	48
S6. Stimulants	474	15
S5. Diuretics and other masking agents	389	13
S9. Glucocorticosteroids	252	8
S4. Hormone and metabolic modulators	145	5
S3. Beta-2 agonists	122	4
S2. Peptide hormones, growth factors and related substances	91	3
S8. Cannabinoids	73	2
S7. Narcotics	26	0.8
P2. Beta-blockers	25	0.8
M2. Chemicals and physical manipulation	3	0.1
P1. Alcohol	0	0
M1. Enhancement of oxygen transfer	0	0
TOTAL: 3079		

4.2 Mechanism of action of AAS

The inactive androgen receptor (AR) is located in the cytosol and is associated with molecular chaperones such as heat shock protein 90 (Hsp 90) (Figure 1.2). Interaction of suitable steroids leads to migration of the ligand-AR complex to the nucleus. The activated AR interacts as homodimer with a specific DNA sequence, the steroid response element (SRE). Attachment of this homodimer to the SRE triggers the formation of a transcription complex by recruitment of several coregulators or comodulators. These coregulators can mediate transcriptional regulation in either positive (co-activators) or negative (corepressors) way. Generally, liganded receptors recruit co-activators which results in transcription and translation of the gene and synthesis of

specific proteins [6, 13, 15, 16]. The activation of the estrogen receptor (ER*) by estrogenic compounds has a similar mechanism [17] (Figure 1.2).

Ligand binding to the AR would induce specific conformational changes dependent on the particular structure of the ligand. These conformational changes would affect interactions with different coregulators in different tissues and would enable tissue-specific gene regulation [13, 15, 18].

Steroids can also induce an anti-catabolic effect by interfering with the glucocorticoid receptor expression and establish non-genomic effects by induction of signaling pathways and changes in ion transport [15].

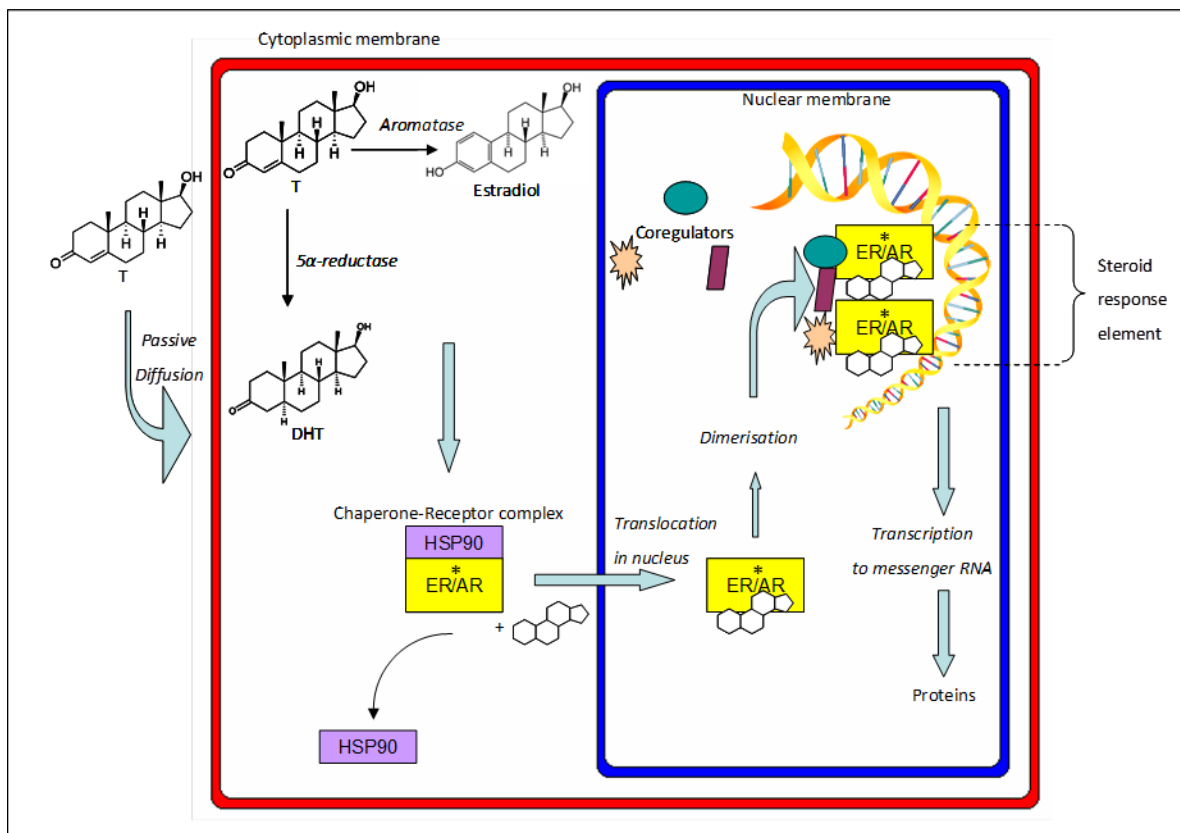


Figure 1.2. Mechanism of action of AAS and estrogens (extracted from [19]).

4.3 General properties and effects of AAS

Based on the capability of the body to produce these substances naturally or not, AAS are classified into two categories according to their origin: endogenous and exogenous steroids. Endogenous steroids are produced by the body, while exogenous steroids are not produced by the human body. A few steroids, although natural are currently not considered endogenous, meaning that production in the human has not been proven although they do appear in other

species. Exogenous steroids are purely synthetic, but endogenous steroids can also be manufactured synthetically. Both classes are prohibited in sports. Testosterone (T) and 5 α -dihydrotestosterone (DHT) are examples of endogenous steroids, whereas methandienone (Dianabol) and stanozolol (Winstrol) are examples of exogenous steroids.

Both categories are characterized by the same perhydrocyclopentanophenanthrene or sterane core structure. This carbon core structure is composed of four fused rings: three cyclohexane rings (A, B and C) and one cyclopentane ring (D) (Figure 1.3).

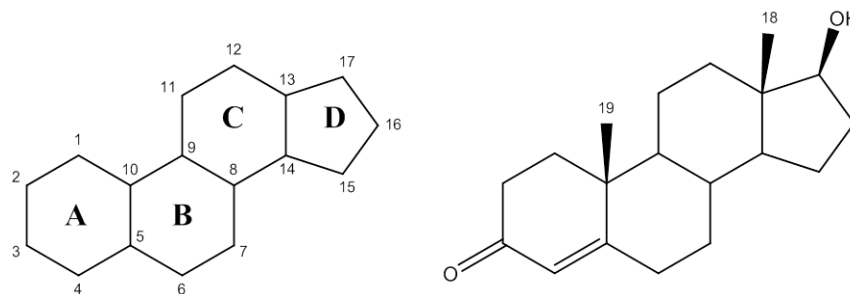


Figure 1.3. Core structure of AAS with indication of the A, B, C and D rings and the numbering of the carbon atoms (left side) and chemical structure of testosterone (right side).

As indicated in the name, AAS have both anabolic (increasing protein synthesis, muscle size and strength) and androgenic properties (increasing virilization and aggression) [6, 20, 21].

Administration of AAS leads to down-regulation of the endogenous steroid synthesis by a negative feedback loop of the hypothalamic-pituitary-gonadal axis. This negative feedback mechanism can also result in infertility, impotence, testicular atrophy and disturbances of menstrual cycles [6, 13, 15, 16].

Other undesirable effects include acne, irreversible virilization of women, stunting of linear growth of adolescents, gynecomastia and enlargement of the prostate for males [6, 16]. In addition there is an increased cardiovascular risk by augmented low-density lipoprotein (LDL)- and decreased high-density lipoprotein (HDL)-cholesterol levels [6, 16, 18]. Chronic administration, especially of the orally active (17 α -alkylated) steroids can lead to liver dysfunction or liver tumors [6, 16]. Moreover, some premature mortality has been described after AAS use, mostly by myocardial infarction or hepatic failure [6, 16].

Pharmaceutical companies started developing synthetic analogues of testosterone and DHT to improve the dissociation of the 'beneficial anabolic' effects from the unwanted androgenic effects (in particular the virilizing effects) [6, 22]. Therapeutic indications for these analogues were patients in 'catabolic state' e.g. after severe burning or associated with muscle wasting diseases such as cancer and HIV [6]. With the growing availability of licensed compounds, athletes began to experiment with these analogues to enhance the skeletal muscle performance and to balance the catabolic condition in the body to speed-up recovery from stress [6, 22].

Although AAS can stimulate EPO synthesis, improvement of endurance performance by AAS has not been demonstrated [20].

The 17β -hydroxy and 3-keto groups are essential for the interaction of AAS with the AR and for their anabolic effects. However, it is assumed that the 3-keto group has a supportive role and can be replaced by a double bond at C2 [16]. As 5α -reduction of the A-ring of AAS is considered to be a typical feature of androgens, synthetic analogues with modifications to stabilize the A-ring conformation are in general less androgenic. Besides several modifications in the A-ring of testosterone and DHT (e.g. attachment of a pyrazole ring (stanozolol) to the A-ring or methylgroup at C1) the improved anabolic/androgenic dissociation of synthetic AAS can also be achieved by removal of the C19 methyl group to obtain the so-called 19-nor steroids [6].

The aim of synthesizing analogues is to enhance the anabolic/androgenic dissociation and to improve the oral availability. Orally active AAS can be obtained by 17α -alkyl substituents, which protect the 17β -hydroxy group from first-pass hepatic metabolism by sterical hindrance, or by methylation at C1, as is the case for methenolone and mesterolone [6]. Other administration routes include transdermal application, intravenous administration and intramuscular injection of steroid esters, which results in prolonged release [6].

Estrogenic side effects, such as gynecomastia, are often observed after AAS use and are caused by aromatization of the AAS to estrogens. Therefore the self-(co)administration of compounds with anti-estrogenic effects like tamoxifen is often observed [16]. The following modifications can interfere with the conversion into estrogens: condensation of the A-ring (e.g. stanozolol), 5α -reduction of the C4 double bond, methylene substitution in C2 (e.g. oxymetholone) or additional double bonds in A-ring (e.g. trenbolone, tetrahydrogestrinone (THG)) [16]. It should be noted that although 17α -alkylation is beneficial for the oral activity of compounds, this modification can lead to stronger estrogenic effects by preventing deactivation of the 17β -estradiol to the (less potent) 17-keto or 17α -hydroxy estrogens [16].

4.4 Metabolism of AAS

The disposition of xenobiotic compounds in the human body is generally divided into four, interrelated, phases: absorption, distribution, metabolism and excretion (ADME) (Figure 1.4).

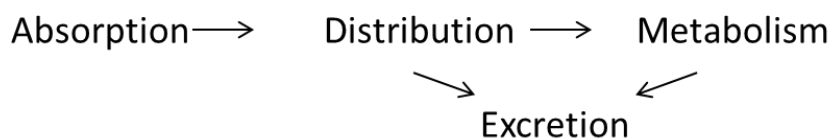


Figure 1.4. Relationships of the four steps in disposition of xenobiotic compounds within an organism.

Excretion is an important step for elimination of exogenous compounds from the organism after administration. For most compounds, such as AAS, urinary excretion is the main excretion route [6, 23]. Other routes are excretion in saliva or via the gastrointestinal tract [23]. A small fraction of AAS metabolites is excreted into the bile, in particular sulfate conjugates which can be reabsorbed as part of the enterohepatic circulation [13].

The main organ for metabolism of xenobiotic compounds is the liver. Extrahepatic sites for metabolism include skin, kidney, intestines and lungs [24].

In general, the metabolic reactions lead to transformation into a less active and more polar metabolite, which facilitates excretion and thus elimination [25]. However, as observed for the testosterone metabolite DHT, which has greater affinity for the androgen receptor than testosterone itself, metabolism can also increase the biological activity [13, 15]. As xenobiotic AAS have highly non-polar characteristics, these compounds are often extensively metabolized prior to their urinary excretion [6, 24].

The metabolism of AAS can be divided into phase I and phase II reactions. Phase I reactions are functionalization reactions (e.g. oxidation, reduction or hydrolysis) whereas phase II reactions are conjugation reactions (e.g. glucuronidation or sulfonation) [24-26]. Although phase I reactions can introduce additional functional groups, which can be conjugated in phase II, phase I and phase II should not necessarily occur together or in this order [25]. For example not all AAS are excreted as conjugated metabolites. Therefore, excreted AAS and their metabolites can be categorized as unconjugated ('free') and/or conjugated metabolites [26]. Sometimes there is also referred to phase III reactions, to indicate further biotransformation of phase II metabolic products [25].

In the following paragraphs the general phase I and phase II pathways will be described. The metabolic pathways of testosterone will be used as a representative example.

4.4.1 Phase I

4.4.1.1 Oxidation reactions

The majority of the phase I oxidation reactions are catalyzed by cytochrome P450 (CYP450) enzymes. CYP450 is a collection of isoenzymes and the highest concentration of these enzymes can be found in the liver. These CYP enzymes are located in the endoplasmatic reticulum (ER) and can be isolated as the so-called microsomal fraction by cell fractionation [25].

These oxidation reactions require nicotinamide adenine dinucleotide phosphate (NADPH), magnesium and molecular oxygen. NADPH is the cofactor for the NADPH cytochrome oxidoreductase, which donates the electron to the CYP enzymes during the oxidation reactions [25, 27].

The CYP450 mediated oxidation reactions include [25]:

- hydroxylation reactions of several substrates such as C atoms of aliphatic and aromatic compounds
- oxidation of a hydroxyl group to a keto function
- dealkylation reactions of alkyl groups attached to N, O or S atoms, for which removal requires oxidation of the alkyl group and then rearrangement and loss as the respective aldehyde.

Certain oxidation reactions are also catalyzed by other enzymes such as alcohol dehydrogenase, xanthine oxidase, microsomal amine oxidase, monoamine oxidase, diamine oxidase and peroxidases [25].

4.4.1.2 Reduction reactions

The phase I reduction reactions are catalyzed by either microsomal or cytosolic reductases. These reduction reactions include reductions of double bonds, nitro, azo, epoxides, aldehyde and keto groups [25].

4.4.1.3 Hydrolysis

Esterases and amidases catalyze the hydrolysis of esters and amides respectively. These enzymes are usually located in the cytosol of cells in a variety of tissues but some are present in plasma. However, microsomal esterases have also been described [25].

4.4.1.4 Hydration

The enzyme epoxide hydrolase, present in the microsomal fraction, can catalyze the hydration of epoxides which yields dihydrodiol products [25].

4.4.1.5 Example: phase I metabolic reactions of testosterone

As all synthetic AAS follow similar metabolic pathways compared to endogenous steroids, the metabolism of testosterone will be discussed as example. In Table 1.3 common phase I reactions for AAS are indicated per ring [26].

The rate-limiting reaction of testosterone (3-keto-4-ene-steroid) degradation is reduction of the C4 double bond by 5 α -/5 β -reductases. The 5 α -reductase is primarily located in the ER and the 5 β -reductase in the cytoplasm. The ratio of 5 α -/5 β -isomers depends on the structure of the steroid, for example 3-keto-androsta-1,4-dien steroids (e.g. methandienone) will only be converted into 5 α -metabolites. Subsequent to this irreversible step, the 3-keto group of 5 α -steroids is rapidly reduced by 3 α /3 β -hydroxysteroid dehydrogenases. Mainly 3 α -hydroxy isomers are produced and only small amounts of the 3 β -hydroxy-5 α metabolite. For 5 β -steroids only 3 α -hydroxy-reduction has been reported [26]. This reduction of the 3-keto group leads to

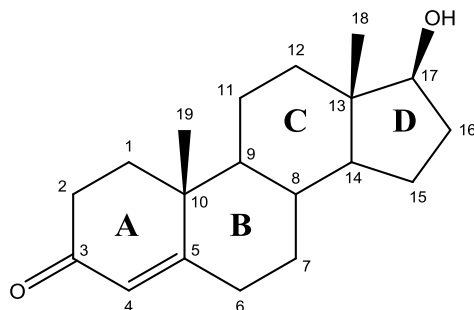
some loss of the biological activity [13]. For AAS with a secondary 17 β -hydroxy group (e.g. testosterone) oxidation to a 17-keto AAS, catalyzed by 17 β -hydroxysteroid dehydrogenase, is an important metabolic pathway [26]. This 17 β -hydroxy oxidation results in a considerable loss of activity [13]. For orally active steroids this 17-oxidation step is sterically hindered by the presence of 17 α -alkyl groups [6, 18, 26]. 17 β -hydroxysteroid dehydrogenase can also reconvert the 17-keto group to a 17 β -hydroxyl group [26].

AAS can be converted to estrogens by the steroid aromatase enzyme [13, 16]. A proposed mechanism of A-ring aromatization would involve oxidation (hydroxylation) of C19 with formation of a geminal diol, followed by dehydration and cleavage of the C19 methyl group and subsequent enolisation of the 3-keto group [13, 16].

Besides the phase I reactions indicated in Table 1.3 hydroxylations can also occur at positions C18 and C19 [26]. The described oxidoreductive phase I reactions for AAS are catalyzed by CYP enzymes [13, 15]. However, it should be noted that the proposed mechanism of 17-epimer formation is via a sulfoconjugate (phase II) intermediate (Table 1.4).

Table 1.3. Phase I metabolic reactions in the four rings of AAS. The chemical structure of testosterone with indication of the A, B, C and D rings and numbering of the carbon atoms is also presented.

A-ring	B-ring	C-ring	D-ring
- 5 α -/5 β -reduction	- 6 β -hydroxylation	- 12-hydroxylation	- 17-dehydrogenation (17 β -hydroxy)
- 3 α -/3 β -hydroxy-reduction	- 6,7-dehydrogenation (methandienone)		- 17 β -/17 α -hydroxy-reduction (17-keto AAS)
- 1,2-hydrogenation			- 16 α -/16 β -hydroxylation
- 1,2-dehydrogenation			- 16-dehydrogenation (16 α -/16 β -hydroxy AAS)
- aromatization			- 17-epimerization
- other metabolic reactions of AAS with modified A-ring e.g. 4 β -hydroxylation (stanozolol), oxidation to a 2 β -carboxylic acid metabolite (oxymetholone)			- other metabolic reactions e.g. 17 β -hydroxylation (17 α -ethyl AAS)



4.4.1.6 Genetic polymorphisms

CYP450 consists of a family of isoenzymes, which are responsible for approximately sixty different types of reactions with a broad and overlapping substrate specificity. The families CYP 1 until 4 are involved in the metabolism of xenobiotic compounds [25]. CYP3A4 is an important

isoenzyme and catalyzes the metabolism of the majority of all drugs (>50%) such as the 6 β -hydroxylation of testosterone [28, 29]. CYP19 is also known as the steroid aromatase [13].

CYP450 shows a number of genetic polymorphisms which may affect metabolic pathways and thus individual human ability to metabolize drugs and other chemicals. For example the genetic polymorphism of CYP2D6 is well-characterized and results in poor, extensive and ultrarapid metabolizers [25, 30]. Poor metabolizers are individuals who have reduced metabolic activity towards certain substrates and may therefore suffer from increased toxicity for some drugs such as penicillamine, which can result in skin rashes. This poor metabolizer phenotype occurs in approximately 5–10 % of the white Caucasian population. Genetic variations have also been observed for other enzymes involved in drug metabolism such as alcohol dehydrogenase and esterases [25].

4.4.2 Phase II

4.4.2.1 Glucuronidation

Glucuronidation is a major phase II metabolic pathway and involves conjugation with glucuronic acid. Glucuronic acid is a polar and water soluble carbohydrate molecule which may be attached to a wide variety of substrates containing hydroxyl groups, carboxylic acid groups, amino groups, thiols or single carbon (C-C) bonds [24, 25]. These glucuronidation reactions, yielding β -glycosidic bonds, are catalyzed by uridine diphosphoglucuronosyl transferases (UGTs) and utilize uridine 5'-diphospho-glucuronic acid (UDPGA) as cofactor (Figure 1.5) [24, 25].

The UGTs are microsomal enzymes, but their active sites are in contrast to the CYP450 enzymes localized on the luminal side and not at the cytosolic side of the ER [27, 31].

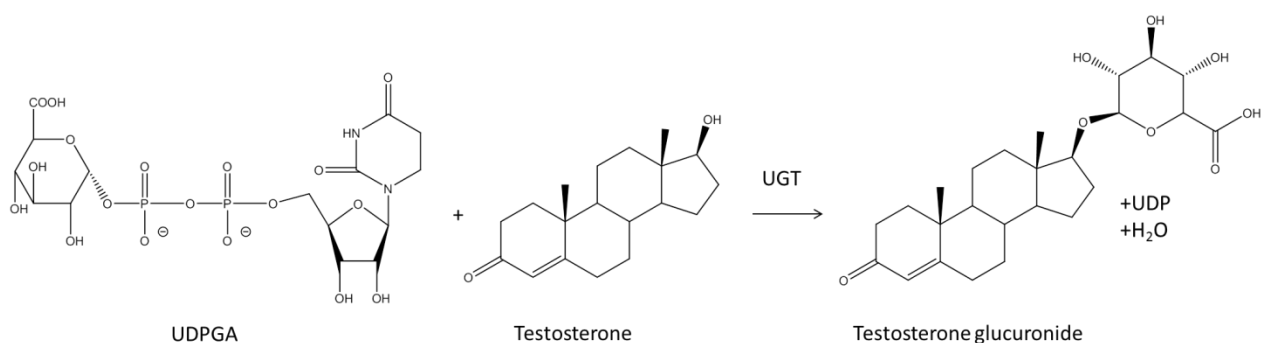


Figure 1.5. Glucuronide conjugation of testosterone by UGT.

The main site of glucuronidation is the liver [24]. In general, the UGT enzymes which catalyze the glucuronidation reaction can be divided into two families: UGT1 and UGT2. The most important UGT enzymes involved in phase II glucuronidation of AAS are members of subfamilies UGT1A and UGT2B [24, 32, 33].

4.4.2.2 Sulfonation

The addition of a sulfo moiety (SO_3) is also a major route of conjugation for xenobiotic compounds. Both aromatic and aliphatic hydroxyl groups as N-hydroxy groups and amino groups may be sulfonated. The sulfonated product is an ester which is very polar and water soluble.

The sulfate conjugation reactions are catalyzed by cytosolic sulfotransferase (SULT) enzymes and utilize the coenzyme 3'-phosphoadenosine-5'-phosphosulfate (PAPS) (Figure 1.6) [25].

Unlike with UGTs, each SULT enzyme displays a more unique tissue distribution e.g. SULT1A1 is the main hepatic isoenzyme for catalyzing sulfonation reactions. The SULTs-1E1, 2A1, 2B1a and 2B1b have been reported to be involved in the sulfonation of AAS, which are partially located in the liver [24].

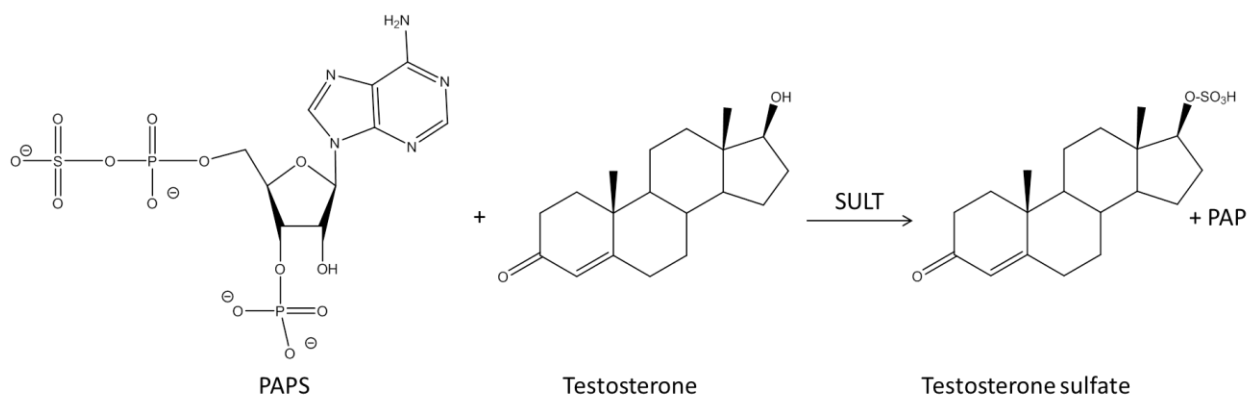


Figure 1.6. Sulfate conjugation of testosterone by SULTs.

4.4.2.3 Other conjugation reactions

The most important phase II pathways of AAS consist of conjugation with glucuronic acid or sulfonation [26]. Other phase II reactions that were described for AAS include conjugation with cysteine and N-acetylcysteine [34, 35]. The postulated metabolic pathway, for (N-acetyl)cysteine conjugates, would involve glutathione conjugation and subsequent (phase III) transformation to (N-acetyl)cysteine conjugates [25, 34].

Conjugation with glutathione, a tripeptide, plays a major protective role in the body as a scavenger for various reactive compounds. Glutathione may react, either chemically or enzyme-catalyzed (glutathione transferases), with reactive compounds and electrophilic metabolites produced in phase I reactions. The glutathione transferases can be located in both the soluble fraction and the microsomal fraction of the cell [25].

Methyltransferases may methylate hydroxyl, amino and thiol groups in molecules [25]. Methylation by catechol-O-methyltransferase (COMT) has been described for estrogens [36,

37]. Soluble COMT enzymes are located in the cytosol and membrane bound COMT enzymes can be found in the microsomal fraction [38]. Acetylation of aromatic amino compounds, sulfonamides, hydrazines and hydrazides may also occur by acetyltransferases. The latter enzymes are e.g. found in the cytosol of cells and utilize acetyl Coenzyme A as cofactor [25]. Although metabolic reactions have the aim to promote excretion, methylation and acetylation tend to decrease, rather than increase, water solubility [25].

4.4.2.4 Example: phase II metabolic reactions of testosterone

For AAS glucuronidation and sulfonation are the major phase II metabolic reactions. The majority of androgen metabolites are excreted as glucuronide conjugates. However, 3 β -hydroxylated steroids, such as DHEA, are predominantly excreted as sulfate conjugates [13, 15, 24, 26]. In Table 1.4 common phase II reactions for the A- and D-ring of AAS are indicated [26].

For testosterone glucuronidation of 3 α -hydroxy- and sulfonation of 3- β -hydroxymetabolites have also been described, regardless of 5 α -/5 β -configuration. However, the major phase II metabolite for testosterone, following 3 α -hydroxy reduction, is a 3 α -O- β -glucuronide [26]. In addition, both glucuronidation and sulfonation of the 17 β -hydroxy group have been reported [26].

Table 1.4. Phase II metabolic reactions in the A- and D-rings of AAS.

A-ring	D-ring
- sulfonation of 3 β -hydroxy group	- glucuronidation of secondary 17 β -hydroxy group
- glucuronidation of 3 α -hydroxy group	- glucuronidation of tertiary 17 β -hydroxy group (17 β -hydroxy-17 α -methyl AAS)
	- sulfonation of secondary 17 β -hydroxy group
	- sulfonation of tertiary 17 β -hydroxy group and subsequent 17-epimerization (17 β -hydroxy-17 α -methyl AAS)

4.4.2.5 Genetic polymorphism

The genetic deletion polymorphism of UGT2B17 (del/del genotype) leads to lower glucuronidation rates of testosterone, but would not affect epitestosterone glucuronides. The resulting del/del genotype affects the evaluation of the T/E ratio as marker for testosterone administration, as this ratio can remain below the threshold even after misuse of testosterone. This demonstrates the usefulness of the ABP which evaluates the individual steroid profiles longitudinally, and hence can exclude the effect of several genetic polymorphisms. The UGT2B17 del/del genotype is more common in Asian than in Caucasian populations [13, 24, 32].

4.5 Detection of AAS

The ISL of WADA focusses on urine and blood collection for the detection of prohibited substances and methods [11]. Urine is the biological fluid of choice for sample collection because it is less invasive than blood collection and many drugs and/or their metabolites are more concentrated in urine than in blood after administration [6]. This is also the case for AAS. Blood samples are collected for doping control purposes to determine blood parameters and to detect misuse of e.g. human growth hormone [6]. Currently, the use of less invasive blood collection techniques compared to the conventional techniques such as dried blood spots (DBS) are investigated for the detection of AAS [39, 40].

Alternative specimens that are investigated for the detection of AAS are hair and oral fluid ('saliva') [40-43]. Advantages of these alternative specimens include their non-invasive nature and that these specimens can be collected under close supervision, which prevents adulteration and substitution of samples [44-46]. An additional advantage of hair testing is that it can prolong the detection times in comparison to urine or blood [44-47]. Drawbacks that are related to hair testing include potential external contamination, influence of cosmetic treatments (e.g. bleaching, dyeing) to the drug stability in hair, wash-out of drugs, and the necessity of athletes to have scalp hairs [6, 41, 44-47]. Moreover, the incorporation rate of prohibited substances into hair is affected by the melanin content of the hair, the hydrophilicity and the membrane permeability of the drug [6, 46, 48]. The use of oral fluid has the advantage that the plasma concentration can be estimated without requiring invasive blood sampling [44]. According to a study of Thieme *et al.* the use of oral fluid seems promising for the detection of transdermal testosterone gel application [41]. However, it should be taken into account that the drug concentration in oral fluid can be influenced by the sample collection procedure, leakage of blood into saliva, storage conditions and individual differences [44, 49]. Although hair and oral fluid are already successfully applied outside the field of doping controls more data is necessary to determine the potential of these alternative biological fluids for doping control purposes [44, 47]. The WADA ISL clearly indicates that testing results from alternative biological matrices such as hair and oral fluid shall not be used to counter AAFs from urine and blood [11].

The detection windows of AAS depend on the route of administration, the type and concentration of the administered AAS. In general, detection windows of AAS observed in urine samples range from some hours-days for oral endogenous steroids, some days-weeks for oral exogenous steroids and until one year after administration for injectable long-acting steroid esters. Hair testing would allow a detection of AAS misuse for a period of six months till one year, depending on the length of hair shaft analyzed [44-46]. Oral fluid and blood are assumed to have the shortest detection windows [46].

Due to the extensive metabolism of AAS there is often only a small percentage of (or even no) parent AAS excreted into the urine [6, 24]. Additionally, it has been shown that the excretion of metabolites often shows a pattern which shifts with time. Some metabolites are excreted rapidly, while other secondary metabolites might only be excreted at a later stage. Therefore it is important to identify metabolites for doping control purposes to improve the detection (windows) of AAS misuse.

The still growing list of prohibited substances, both regarding number and kind, is challenging the doping control laboratories to develop detection methods with good sensitivity and selectivity to meet the MRPLs set by WADA. The improvements of detection strategies are based on sample preparation and detection techniques, which is related with instrumental innovations [47], but also with respect to elucidation of drug metabolism and identification of long-term metabolites [50].

Qualitative analyses are applied for non-threshold substances (e.g. exogenous steroids) since their presence in athlete urine samples leads directly to an AAF. However, for threshold substances a quantitative approach is required. This also holds true for endogenous steroids, since it is required to identify if their presence is related to an endogenous production or originates from administration of synthetic endogenous steroids [6]. To distinguish endogenous steroids from their synthetic analogue, Isotope Ratio Mass Spectrometry (IRMS) is applied by doping control laboratories [1, 6]. As IRMS is an expensive and time-consuming technique, IRMS analysis is only used as confirmation methodology. To identify suspicious samples, screening is performed by measuring several urinary concentrations and ratios of endogenous steroids [51]. The T/E ratio is an important biomarker for testosterone misuse [6, 51, 52]. Other markers were added to enable detection of misuse of other endogenous steroids, such as DHT, DHEA and 4-androstenedione and form the so-called 'traditional' steroid profile [51]. These parameters include the urinary concentrations of testosterone, epitestosterone, DHT, DHEA and 4-androstenedione, and their main urinary metabolites (androsterone, etiocholanolone, 5 β -androstane-3 α ,17 β -diol and 5 α -androstane-3 α ,17 β -diol) [51]. This steroid profile is traditionally obtained by gas chromatography - mass spectrometry (GC-MS) analysis. In addition to the steroid profile several cofounding factors, including finasteride, ketoconazole and alcohol (ethanol) are screened for [51, 53]. The introduction of the ABP refined the evaluation of steroid profiles by enabling comparison with individual reference limits [53]. For the qualitative analysis of exogenous AAS both GC-MS and liquid chromatography - mass spectrometry (LC-MS) instruments are generally applied [47, 54].

4.5.1 Sample preparation

As screening methods are based on the simultaneous detection of a wide range of substances with a single sample preparation procedure, generic protocols are applied to cover all

compounds with a reasonable recovery [24, 55]. In general, this sample preparation procedure (Figure 1.7) consists of hydrolysis of the urine samples and an extraction based on liquid-liquid extraction (LLE) or solid-phase extraction (SPE) [6, 55].



Figure 1.7. Sample preparation procedure of urine samples.

The hydrolysis step involves the hydrolysis of conjugated substances to enable their extraction from the urine sample (and detection by GC-MS) [6, 55]. In this step the main focus is on the glucuronide-conjugated fraction since the enzymatic hydrolysis is performed with β -glucuronidase derived from *Escherichia coli* (*E. coli*). In some cases extracts from *Helix pomatia* (*H. pomatia*), which contain both β -glucuronidase and arylsulfatase, are used to include the sulfate conjugates. However, these sulfate conjugates are not efficiently enzymatically hydrolyzed [24, 56, 57] and problems associated with the production of artifacts [56, 57] and conversion between steroids [6, 57, 58] have been described for *H. pomatia* extracts, which makes the use of *E. coli* mandatory for endogenous steroids (steroid profiling). The alternative solvolysis (e.g. methanolysis), although more efficient, might lead to degradation of certain substances [24, 57].

Extraction of AAS from the urine matrix is generally performed by LLE with an apolar organic solvent such as diethylether or t-butylmethylether [6, 59]. The neutral AAS are favorably partitioned in this organic solvent [6]. After separation of the organic phase, the solvent is evaporated.

The dried extracts are then reconstituted (in water/methanol or water/acetonitrile) in case LC-MS analysis will be performed. For GC-MS analysis an extra derivatization step is needed to improve the chromatographic properties, volatility and thermostability of the substances [6, 60]. A common applied derivatization is based on trimethylsilylation of AAS [6, 60]. To convert both hydroxyl and keto functions of AAS to their trimethylsilyl (TMS) ether and enol derivatives respectively a TMS derivatization mixture consisting of N-methyl-N-trimethylsilyl-trifluoroacetamide (MSTFA), ethanethiol and ammonium iodide (NH_4I) is used (Figure 1.8). Derivatization of hydroxyl functions can be performed by adding MSTFA. However, for the derivatization of the more stable keto functions a catalyst such as iodotrimethylsilane (TMSI) is required. Since NH_4I is more stable than TMSI, TMSI is generated in-situ by the reaction of MSTFA with NH_4I . To inhibit the formation of iodine an anti-oxidant such as ethanethiol is added to the derivatization mixture [6, 60]. This derivatization step requires anhydrous conditions to assure complete derivatization [6] since both the reagents and the formed derivatives are

sensitive towards water [60]. Therefore the extracts are evaporated to dryness and anhydrous sodium sulphate (Na_2SO_4) is added to ensure removal of all water [6].

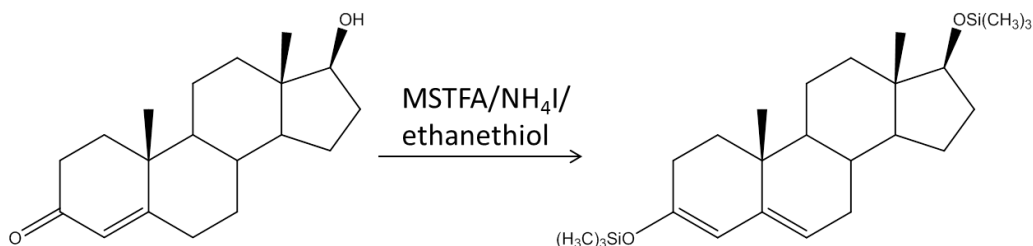


Figure 1.8. TMS derivatization of testosterone.

Recently, direct injection (dilute-and-shoot) methods combined with LC-MS analysis were developed in order to face the increasing number of samples and to minimize turnaround time and reagent cost [61-65]. This substantially reduced sample preparation is possible thanks to more improved detection instruments.

4.5.2 Analysis of samples

GC-MS and LC-MS are the technologies of choice for the detection of most prohibited substances, including AAS, in doping control laboratories [47, 54]. LC-MS offers in many cases the advantage over GC-MS that sample preparation can be reduced [10, 55, 60] (Table 1.5). Indeed, GC-MS often requires additional steps during sample preparation, including hydrolysis to detect conjugated metabolites and derivatization of compounds to improve their chromatographic properties [6]. Moreover, some compounds are thermolabile, non-volatile or have marginal GC chromatographic properties (e.g. THG and stanozolol), even after derivatization [47, 54, 66]. For these compounds LC-MS analysis can be applied, which does not require derivatization and enables the direct detection of conjugated compounds via dilute-and-shoot methods, which circumvent problems related to hydrolysis [24, 55, 61, 66, 67]. However, GC-MS remains a valuable technique especially for saturated AAS (e.g. 5 α -/5 β -androstane-3 α ,17 β -diols), which represent ionization difficulties by LC-MS [55, 60, 68].

LC-MS and GC-MS instruments have a similar configuration consisting of a chromatograph, ion source and detector (MS). Chromatography is a separation technique in which the analytes are differently distributed or partitioned between a stationary phase (e.g. coated on a column) and a mobile phase. For GC the mobile phase is a gas (carrier gas) and for LC the mobile phase is a liquid. The separation of the analytes is performed due to differential interaction with the stationary phase and mobile phase, which leads to retention of the compounds. Therefore the compounds elute at different retention times [69]. For the GC and LC screening of AAS apolar columns are generally applied. These GC columns are capillary columns based on fused silica (such as dimethylpolysiloxane e.g. J&W Ultra 1 and HP-1MS). Since the GC column is located in

an oven temperature program can be applied to optimize the separation of the compounds [47].

Table 1.5. Overview of GC-MS and LC-MS techniques and their (dis)advantages for the screening of AAS.

Parameter	GC-MS	GC-MS/MS	LC-MS/MS	LC-HRMS
Analytes	Volatile, thermally stable, non-polar, small compounds + Detection of saturated AAS feasible (e.g. androstenediols) - Improve GC properties: derivatization - Hydrolysis (deconjugation) needed		Non-volatile, thermally unstable, polar, small/large compounds + Direct detection of conjugated AAS + Detection of AAS such as trenbolone, THG	
Sample preparation	Hydrolysis & LLE/SPE & derivatization		Hydrolysis & LLE/SPE + Dilute-and-shoot possible	
Column	Apolar		Apolar	
Mobile phase	Gas (He, H₂, N₂)		Polar solvent (H₂O, MeOH, acetonitrile)	
Ionization	EI + Fragmentation: additional structural information - Less abundant molecular ion	EI (See GC-MS) CI + More abundant molecular ion - Less structural information	ESI + Abundant molecular ion - Less structural information - Ionizable groups needed - More prone to matrix effects	
Screening AAS	SIM + More sensitive compared to full scan - Targeted detection	MRM + More sensitive compared to SIM - Targeted detection	MRM + More sensitive compared to SIM - Targeted detection	Full scan + Retrospective data analysis feasible
Identification analytes	RT, EI mass spectrum	RT, MS/MS fragmentation	RT, MS/MS fragmentation	RT, exact mass, fragmentation
Resolution	1 amu	1 amu	1 amu	0.001-0.0001 amu + Reduced background
Cost	€	€€	€€	€€€- €€€€

+ = advantage; - = disadvantage

LC-MS/MS methods for the detection of AAS are based on apolar C18 or C8 columns and a mobile phase containing water and methanol (MeOH) or acetonitrile. The application of an apolar column with a polar solvent for the LC separation is called 'reversed phase' LC [47, 69]. Several mobile phase modifiers can be added to the mobile phase (e.g. formic acid or acetic acid and ammonium formate or ammonium acetate) to optimize the chromatographic behavior and ionization [55]. Gradient elution (changing composition of mobile phase throughout the run) is applied to modify the separation of the compounds [69].

After the chromatographic separation of the analytes the compounds are ionized in the ion source. For GC-MS electron ionization (EI) and chemical ionization (CI) are often applied, whereas electrospray ionization (ESI) is commonly used for LC-MS instruments [47]. EI is a rather hard ionization technique, resulting in additional fragmentation of the compounds [47]. This has the advantage that additional structural information can be obtained in the corresponding EI mass spectrum. However, a disadvantage of this 'destructive' ionization technique is that less abundant molecular ions can be observed [47]. CI and ESI are soft ionization techniques which advantageously leads to less fragmentation and a more abundant molecular ion, but consequently provides less structural information [47]. A more abundant molecular ion is beneficial for the development of multiple reaction monitoring (MRM) as more diagnostic precursor ions (high mass to charge ratio (m/z) at relative high abundance) can be selected [70]. During ESI competitive ionization can occur, which makes the technique more prone to matrix effects (ion enhancement/suppression) [47, 55]. Therefore the determination of matrix effects is important in LC-MS/MS method validation and the use of stable isotope labeled internal standards is recommended for quantitative LC-MS/MS methods [47]. For the efficient ionization of AAS by ESI and thus LC-MS/MS analysis ionizable groups such as a conjugated carbonyl function or heteroatoms are required [68]. Consequently, the detection of saturated AAS such as 5α -/ 5β -androstane- 3α , 17β -diols is impeded by LC-MS/MS analysis. For the detection of these compounds GC-MS analysis is applied.

The detector is a mass selective detector or mass spectrometer, which separates the ionized analytes into an electromagnetic field depending on their m/z [47]. There are several types of mass analyzers including (single/triple) quadrupoles, ion traps, time-of-flight (TOF) and orbitraps [47]. A brief description of the mass analyzers applied in this thesis (single/triple quadrupole and Orbitrap) is given below.

The quadrupole analyser consists of four parallel rods. Each opposing rod pair is electrically connected and an oscillation radio frequency voltage (V_{RF}) is applied between the pair of rods. In addition to this V_{RF} a positive/negative direct current (V_{DC}) is applied. Ions entering the quadrupole undergo oscillating movements between the rods due to these V_{RF} and V_{DC} electric fields. For a given ratio of voltages only ions with a particular m/z undergo stable oscillations and will reach the detector. Other ions will have unstable movements and will collide with the rods [47]. Triple quadrupole MS instruments consist of three quadrupoles (Q1, Q2 and Q3; figure 1.9). Q1 and Q3 are conventional quadrupoles, which can be operated in full scan or selected ion monitoring (SIM) mode [47]. Q2 act as a collision cell which enables fragmentation of selected precursor ions to product ions [47].

An Orbitrap is a special type of ion trap MS consisting of an outer barrel-like electrode and central spindle-like electrode. Ions are, due to their electrostatic attraction to the central

electrode, trapped in an orbital motion around the central electrode. The m/z value of the ions is related to the frequency of oscillation [47]. This Orbitrap technology is applied in LC-high resolution MS (HRMS) instruments (e.g. Exactive and Q-Exactive). A higher energy collision dissociation (HCD) cell enables all ion fragmentation. The advantage of the Q-Exactive is the presence of an additional quadrupole which allows performing fragmentation of selected ions in the HCD cell.

In GC-(EI)MS full scan mass spectra of AAS the molecular ion and several fragment ions can be observed. It should be taken into account that for GC-MS the compounds are derivatized with TMS prior to the GC-MS analysis. For example if both the 3-keto and 17-hydroxy groups of testosterone are derivatized with TMS a molecular ion of m/z 432 ($288+(2 \times 72)$) will be observed. Besides the molecular ion, the fragment ion m/z 73, which represents the trimethylsilyl radical, is commonly observed in the mass spectra of TMS derivatives [54]. Losses of methyl radicals ($[M-15]^+$) and TMSOH ($[M-90]^+$) groups are frequently observed in the GC-MS mass spectra of AAS [47, 70].

In the LC-MS full scan mass spectra of AAS protonated $[M+H]^+$ and deprotonated $[M-H]^-$ molecules can be observed, depending on the ionization mode that is applied. For molecules exhibiting a high proton affinity (basic molecules) $[M+H]^+$ will be the most abundant species while for molecules which can transfer a proton to the solvent (acidic molecules) $[M-H]^-$ will be more abundant. Other species that can be observed include sodium ($[M+Na]^+$), potassium ($[M+K]^+$), ammonium ($[M+NH_4]^+$) and acetate adducts ($[M+OAc]^-$) [68].

To fulfill the higher demands regarding sensitivity, selectivity and sample throughput there has been some evolution in MS techniques [1, 10, 47]. Initially by use of classical MS, full scan analyses evolved to the use of the more selective SIM mode. Subsequently detection limits were further improved by implementation of tandem MS (MS/MS) (Figure 1.9). This MS/MS analysis involves collision induced dissociation (CID) of compounds with an inert gas (e.g. nitrogen, helium and argon), which results in characteristic MS/MS spectra. With these MS/MS instruments product ion scan mass spectra (quadrupole linked to ion trap or time of flight (TOF) detector) or selected reaction monitoring (SRM)/MRM (triple quadrupoles) can be applied [10]. Although these improved MS techniques lead to an efficient detection of a range of known compounds, a drawback from the high selectivity is that it does not allow the detection of non-targeted or unknown compounds [10]. These target methods require information about compounds and their metabolites such as a selection of the most appropriate ions and its retention time.

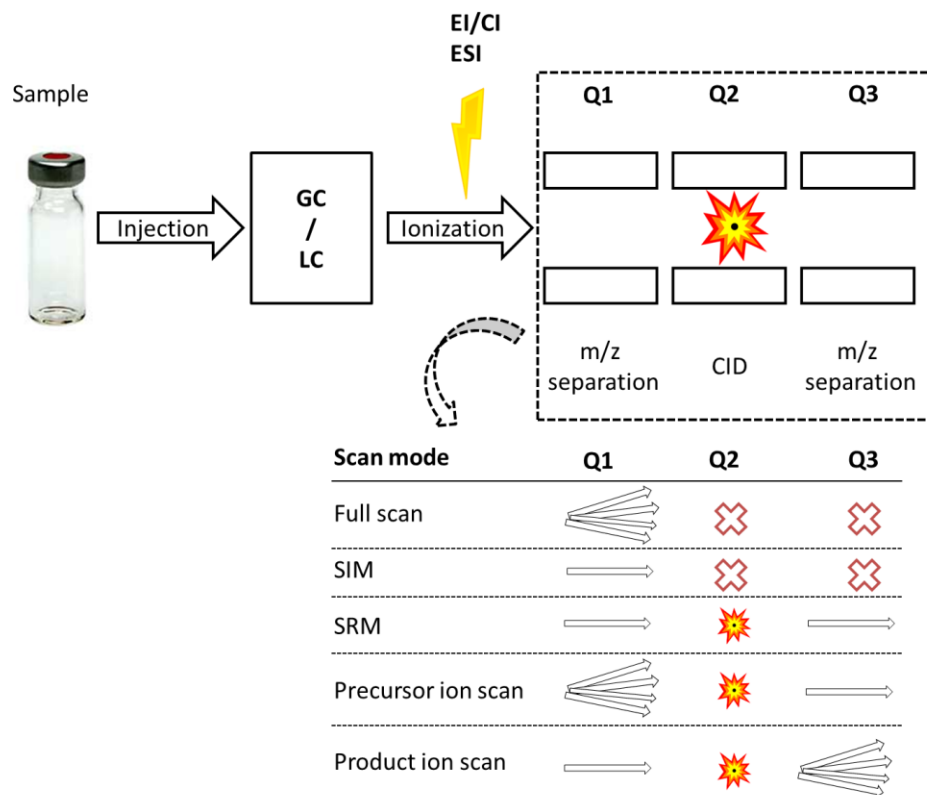


Figure 1.9. Configuration of GC-MS and LC-MS triple quadrupole instruments and the different scan modes.

The application of LC-HRMS instruments can lead to a reduction of background noise by measuring of specific ions with an accurate mass [10]. This in turn enables the detection of quite low levels of substances and requires less sample clean up [10]. Evaluation of HRMS data requires post-acquisition processing methods to select target substances. However, an advantage of the use of HRMS instruments is that they allow retrospective data analysis as data processing is a post-acquisition rather than pre-acquisition process. Eventually the full scan HRMS data can also be combined with fragmentation data to obtain more structural information of unknown compounds [10].

Taking into account the drawbacks related to targeted screening methods, other strategies were developed to enable the detection of unknown doping substances [1, 10]. These strategies were applied for AAS and include androgen bioassays, based on their androgenic activity [71] or interaction with the AR [72], and open screening strategies [10]. The open screening strategies are based on the finding that related steroids have similar MS/MS fragmentation patterns which give rise to common ion fragments [10, 73, 74]. Pozo *et al.* developed an approach for the detection and characterization of unknown AAS (Figure 1.10) [75].

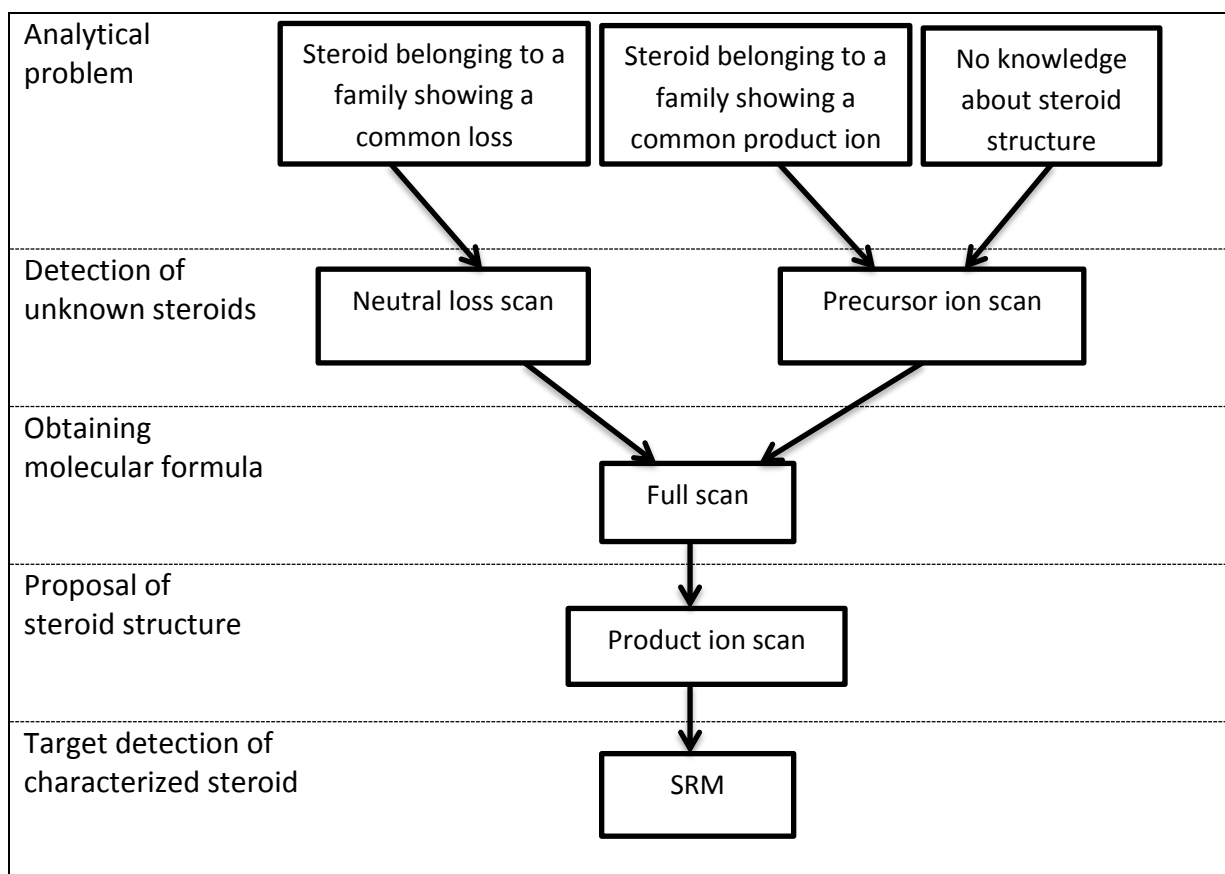


Figure 1.10. Approach for the detection and characterization of unknown compounds (adapted from [75]).

5 New evolutions of performance enhancing substances

Since illicit producers are regularly inspired by (pipeline) products of pharmaceutical companies, pharmaceutical innovations are often related to evolutions in black market products. The black market provides cheaper preparations of pharmacological products or products containing slightly modified substances [76-79]. These black market products are often distributed without sales permission or without safety or efficacy studies [10, 24]. Therefore, a wide range of performance enhancing substances is currently available over the internet. While in the 1990s and 2000s these substances were predominantly products containing AAS and designer steroids, nowadays new classes of performance enhancing substances are observed including peptides [77, 80-84], non-steroidal selective androgen receptor modulators (SARMs) [18, 76, 85], REV-ERB (reverse – viral erythroblastosis oncogene product) agonists [86] and small molecule ESAs [87, 88].

5.1 Designer steroids

Synthetic AAS analogues were produced to improve the pharmacological profile of AAS by pharmaceutical companies. However, while knowledge was growing, so-called underground laboratories started to manufacture designer steroids, which structures closely resemble existing, known products but with sufficient chemical diversity to evade detection and legislation [10, 89]. The circumvention of legislation was based on misuse of gaps in legal regulations, which scope is based on defined compounds or structures [10, 89]. Moreover, attempts to hide the true identity of compounds are applied by incorrect, misspelled names or refusing to use the androstane nomenclature (e.g. alloetiocholane or perhydrophenanthrene derivatives) and reappearance of banned products under other trade names has been observed [10]. These gaps were recognized in the Prohibited List of WADA and were closed by widening the scope of prohibited compounds by e.g. adding the expression 'and other substances with similar chemical structure or similar biological activity' and changing the term anabolic steroids to anabolic agents [1].

Substances developed by pharmaceutical companies undergo full clinical studies to prove their efficacy and safety and their production is also strictly regulated. The designer steroids often marketed as so-called prohormones or 'dietary supplements' lack generally such defined toxicological profiles. The clandestine production process jeopardizes the purity of these products [10, 76, 90, 91] and labeling is often incorrect as products do sometimes either not contain any of the active ingredients indicated on the label or contain structural analogues [76, 91]. Although athletes should be careful with using 'dietary supplements' to prevent a positive doping control, it should be noted that not all dietary supplements contain designer steroids/prohormones or are linked to contamination issues. Examples of these designer steroids are THG, prostanazol and dimethazine (DMZ) [10].

5.2 SARMs

To further improve the pharmacological properties of (synthetic) AAS non-steroidal SARMs were developed. SARMs selectively interact with the AR and allow a tissue-selective activation or inhibition of the AR [18, 22, 92-96]. Moreover, these compounds are not a substrate for 5 α -reductases and aromatases. Therefore administration of SARMs does not lead to undesirable effects resulting from amplification of androgenic and estrogenic effects [18]. A proposed mechanism for their tissue-selective activation of the AR would be related to specific conformational changes of the AR induced by SARMs, which affects the interactions with coregulators as described above (4.3 Mechanism of action of AAS) [13, 18]. SARMs allegedly exhibit improved oral bioavailability and represent more metabolically stable compounds with reduced liver toxicity [97, 98].

The chemical structures of SARMs are quite different from the steroid structures, as SARMs have chemical pharmacophore structures such as arylpropionamides, bicyclic hydantoin, quinolines, and tetrahydroquinolines [18, 22, 93, 94]. However, this diverse group is continuously expanding with new substances and other pharmacophores. For example, recently a new class of SARMs was introduced with a pyrrolidin-benzonitrile structure (LGD-4033) [99-101].

Andarine and ostarine (also known as Enobosarm) are the first described SARMs. Other examples of SARMs include ACP-105 and LGD-4033 [79]. Clinical applications for SARMs include hypogonadism, sarcopenia, prevention and treatment of muscle wasting, osteoporosis, breast cancer and as hormone replacement therapy [18, 96, 102]. Although SARMs are currently still undergoing clinical trials the promising anabolic effects of SARMs result in a high potential of misuse by athletes [18]. Moreover, the misuse of non-approved substances has already been reported before and several SARMs are available in black market products over the internet [76, 78]. Therefore in 2008 WADA added SARMs to the Prohibited List in the subcategory of S1-Anabolic agents, S1-2 other anabolic agents.

5.3 REV-ERB agonists

In 2012 REV-ERB agonists SR9009 and SR9011 were described as promising drug candidates to treat several metabolic disorders [103-105]. SR9009 and SR9011 modulate the activity of the nuclear receptors REV-ERB- α and - β , which regulate the expression of core clock proteins of the mammalian circadian clock [103, 105-108]. The circadian rhythm organizes behavior and physiological processes, including activity/rest, feeding times, body temperature and metabolism, on a cycle of approximately 24 h [103, 109, 110].

In Figure 1.11 the mammalian circadian clock with its major molecular components is presented. A central clock located in the suprachiasmatic nucleus (SCN) is responsible to coordinate independent peripheral clocks to obtain a coherent circadian rhythm [109]. The central clock is entrained by environmental influences such as light, which enables adjustment to the solar day and seasonal changes [106, 111, 112].

Heterodimeric complexes of the transcription factors BMAL 1 (brain and muscle aryl hydrocarbon receptor nuclear translocator-like protein 1) and CLOCK (circadian locomotor output cycles kaput) initiate the transcription of period (PER) and cryptochrome (CRY) genes [103, 105-110]. Transcriptional feedback loops result in a rhythmic expression of BMAL 1/CLOCK and PER/CRY.

REV-ERB- α or Nuclear Receptor Subfamily 1 Group D, member 1 (NR1D1) and retinoic acid-related orphan nuclear receptors α (ROR α) regulate the expression of BMAL 1/CLOCK. REV-ERB- α is a negative regulator, whereas ROR α is a positive regulator [109, 110].

The peripheral clock receives signals from the central clock and is also adjusted by feeding and fasting [111, 113]. Many processes, including glucose and lipid metabolism, food absorption and insulin secretion, are regulated by the peripheral clocks located in several organs (e.g. liver, skeletal muscles, kidney and pancreas) [106, 111, 113].

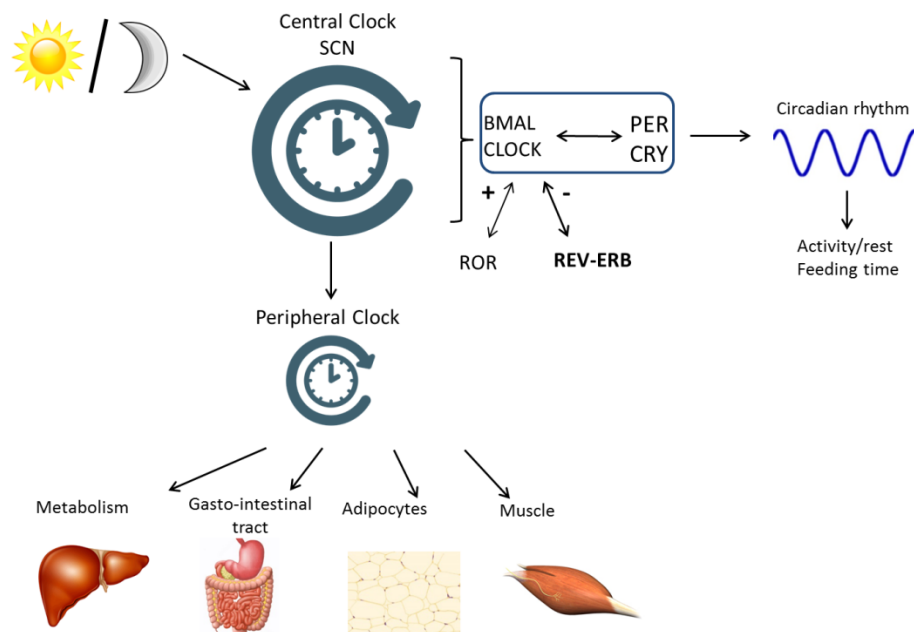


Figure 1.11. Mammalian circadian clock.

Effects observed via *in vitro* and *in vivo* animal studies with REV-ERB agonists SR9009 and SR9011 included increased basal oxygen consumption, decreased lipogenesis in the liver, increased mitochondrial content, glucose and fatty acids oxidation in the skeletal muscle and decreased lipid storage in the white adipose tissue [103-108, 114].

Their role in energy homeostasis and the observed increase in exercise capacity via *in vivo* animal studies, make these compounds attractive for doping purposes [104]. Moreover, soon these compounds were discussed as 'exercise in a pill' compounds [115-117] and SR9009 was marketed in black market products [86]. Although the effects of SR9009 and SR9011 in human still need to be investigated illicit use for doping purposes can be anticipated. These compounds are not explicitly mentioned on the list of prohibited substances but are prohibited under the category S0 which represents 'non-approved substances' such as drugs under clinical development or designer drugs [8]. SR9009 and SR9011 could potentially also be classified as metabolic modulators under category S4 [8].

6 Doping and research ethics

The (extreme) pressure and desire to perform, drives athletes to win at all costs and might tempt them to short-sighted solutions like doping [4, 5]. The presence of a wide variety of performance enhancing substances over the internet makes these easily available for both elite athletes as for non-professional recreational sportsmen [4, 5, 10, 20]. These substances are provided as both pharmaceutical and non-pharmaceutical grade products [10]. The latter group of products is often made in clandestine ways containing substances sometimes designed with structural similarity to published compounds but with little or no knowledge about their potential toxic effects. Therefore, athletes are used as 'guinea pigs' without any ethical considerations to determine side effects and the potential for performance enhancement of these substances [10, 76]. In many cases these products are self-administered by recreational athletes with self-determined doses and sometimes in combination with several doping products without regular check-up by medical doctors. Side-effects and performance enhancing effects are often discussed on internet fora, like observed with some designer steroids [10, 20]. Moreover, as described for the designer steroids, these products have often poor purity, which raises considerable concerns for the safety of the consumers [10, 76, 90].

Education programs and effective detection methods to reveal misuse of performance enhancing substances are important for the fight against doping, not only to protect the ethics of sports but also the health of athletes [5]. Preventive anti-doping research can also be helpful to close the gap between doping control laboratories and the appearance of new doping agents [10]. Therefore, vigilance by doping control laboratories is recommended for early detection of

designer drugs and new evolutions of potential performance enhancing substances, both from the pharmaceutical industry as the black market [10, 76, 79].

To allow detection of substances with the longest retrospectivity, knowledge is required about the metabolic behavior and the detection of the parent compound and potential metabolites. Traditionally, elucidation of the metabolism is performed in excretion studies with human subjects. However, for pipeline products or compounds from illicit producers ethical constraints and safety aspects limit the use of human volunteers. To ensure a fast response and prompt implementation of new, non-pharmaceutical grade products, alternative models are needed for these metabolism studies [10, 24, 89]. These alternative models include animal models, tissue slices or crude enzyme preparations from animal or human origin [22, 24, 29, 118, 119].

7 Metabolism studies

The purpose of metabolism studies for doping control and pharmacology are different. For the pharmacological activity of candidate compounds the metabolic reactions leading to active/toxic metabolites are of major interest. In contrast, the main interest for doping control purposes is to characterize (major) metabolites and their physicochemical properties to facilitate detection in routine screening [22].

7.1 Alternative models

For the metabolism of xenobiotic compounds, hepatic enzyme activity plays a significant role. Therefore alternative (*in vitro*) models for metabolism studies are predominantly based on the liver. Examples of such alternative models are supersomes [29, 120, 121], liver fractions [22, 24, 29, 118, 122], hepatocyte cell cultures [123-125], mice with humanized livers [126-130] and primates [131, 132]. These *in vivo* and *in vitro* model systems all have advantages as well as disadvantages (Figure 1.12). For example hepatocytes can be used to study phase I and phase II reactions sequential or in parallel but they show a relative rapid decline in CYP450 activities [119]. Supersomes, microsomes derived from baculovirus transfected insect cells with human CYP and UGT enzymes, provide usually higher enzyme activity than human liver fractions [29].

The *in vivo* models have the advantage that metabolism studies are performed in an intact organism. Therefore a complete overview of the ADME processes can be obtained. Moreover, the normal architectural relationship is preserved in the *in vivo* models, which promotes the resemblance with the *in vivo* human situation. However, the use of animal models is related to interspecies differences which hamper extrapolation of the results to humans. The humanized mouse model offers the advantage that metabolism studies can be performed in an intact organism with reduced interspecies differences.

In vitro techniques do not serve as replacement for *in vivo* studies due to the difficult extrapolation to the *in vivo* situation arising from the lack of an intact biological system [133]. However, both techniques can complement each other since *in vitro* studies can be helpful to reduce and refine the number of animal experiments. The *in vitro* approach offers some additional advantages such as the production of cleaner and more concentrated extracts, which facilitates the characterization of metabolites and allows a fast response to potential new threats. Moreover, the *in vitro* models could be applied to biologically generate reference material for compounds for which no synthesized standard is available or that cannot be easily chemically synthesized [124, 133, 134]. Therefore *in vitro* samples could also be used as an alternative to *in vivo* post-administration urine samples for comparative purposes during routine screening procedures, in accordance with the 2009 ILAC-G7 guidelines [133, 135].

	<i>In vitro</i>						<i>In vivo</i>		
	Supersomes	Microsomes/cytosol	S9 liver fractions	Homogenised liver	Hepatocytes cultures	Liver slices	Animal models	Humanized mouse model	Human
<i>In vivo</i> human resemblance	--- → +++)								
Ethical acceptance	← +++) ---								
Complexity	--- → +++)								
Ease of use	← +++) ---								
Viability	++	← ---				-	++	+	++
Cost	← +++)							-	+

Figure 1.12. Overview of *in vitro* and *in vivo* models for metabolism studies. The advantages (+) and disadvantages (-) of the models are also indicated, including the positioning of the models in comparison with human excretion studies.

The research for this doctoral dissertation focused on *in vitro* models based on liver fractions (human liver microsomes (HLM) and S9 fractions) and the *in vivo* mouse model with a humanized liver [136].

7.1.1 Human liver microsomes (HLM)

HLM are a subcellular fraction of the human liver, derived by differential centrifugation [27] (Figure 1.13). HLM consist predominantly of the membranes of the ER [25, 27] and provide therefore an enriched source of membrane bound drug metabolizing enzymes, such as CYP450, UGT and flavin monooxygenase (FMO) enzymes (Table 1.6) [28].

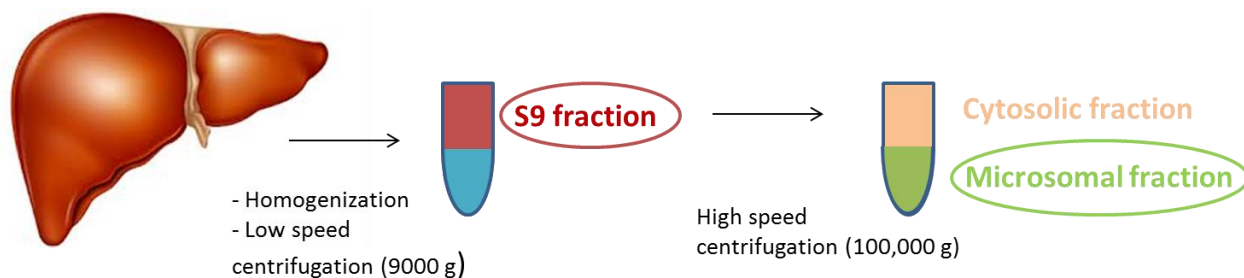


Figure 1.13. Isolation of HLM and S9 liver fractions.

HLM can be applied to study phase I and phase II (UGT) metabolism studies, both separately and in parallel, by adding the appropriate cofactors. For the phase I experiments (e.g. CYP and FMO) these cofactors are NADPH and magnesium and for the phase II (UGT) experiments UDPGA should be added [27]. The UGT system is a ‘low affinity - high capacity pathway’, which requires a high substrate concentration [24].

The advantages of HLM compared to other *in vitro* models (including liver slices and hepatocytes) and *in vivo* animal models is that they are user-friendly and not that expensive. HLM can be stored at -80 °C for several years and they do not require a sterile environment. The metabolism studies can also be performed with a straightforward procedure. Moreover, there are less ethical constraints for metabolism studies with non-pharmaceutical grade substances compared to humans and primates [28, 29].

Disadvantages of the HLM are that they cannot be applied for quantitative estimations of specific metabolic pathways as they consist of enriched CYP and UGT enzymes, which restricts competition for other enzymes. HLM do not take into account extrahepatic metabolism and the whole ADME process. Therefore, extrapolation to the real human *in vivo* situation is more difficult only based on the HLM results [29].

7.1.2 S9 liver fractions

S9 liver fractions are obtained after a low speed centrifugation of homogenized human liver and contain both HLM and cytosolic fractions (Figure 1.13) [29]. Therefore, in addition to CYP and UGT enzymes the cytosolic SULTs are present in the S9 liver fractions (Table 1.6). In contrast to the UGT system, sulfonation is a ‘high affinity - low capacity’ pathway as the activity of SULTs is

restricted by product inhibition. Therefore, the sulfate conjugation should be performed at low substrate concentration [24]. The cofactor of the SULTs is PAPS [24].

The (dis)advantages related with the use of S9 liver fractions are similar to the HLM. However, S9 liver fractions offer a more complete representation of the metabolic profile by the presence of both microsomal and cytosolic enzymes (Table 1.5). The overall lower enzyme activity in the S9 fraction compared to microsomes or cytosol may be considered as an additional disadvantage, as this may leave some metabolites unnoticed [29].

Table 1.6. Overview of metabolic enzymes present in human liver fractions: S9, HLM and cytosol [25, 27, 137, 138].

Metabolic enzymes present in the human liver	S9	HLM	Cytosol
CYP450	√	√	
Flavin monooxygenase (FMO)	√	√	
NADPH cytochrome oxidoreductase	√	√	
Aldehyde oxidase	√		√
Mono-amine oxidase (MAO)	√		√
Epoxide hydrolase (EH)	√	√	√
Esterases	√	√	√
Amidases	√		√
Peptidase	√	√	√
UGT	√	√	
SULT	√		√
Glutathione transferase (GST)	√		√
N-acetyl transferase (NAT)	√		√
Methyltransferase (COMT)	√	√	√
Amino acid transferase	√	√	

7.1.3 Chimeric mouse model

The *in vivo* model used in this study is a humanized mouse model which was developed in cooperation with the Center for Vaccinology (CEVAC) of Ghent University Hospital. This model

involves the transplantation of primary human hepatocytes into uPA^{+/-}-SCID mice within two weeks after birth, resulting in a chimeric animal [139]. Chimeric is defined as consisting of cells from two genetically different organisms (e.g. human and mouse) [140].

uPA stands for urokinase-type plasminogen activator and is also known as Plasminogen Activator, urokinase-type (PLAU). The uPA gene encodes for a protease, which converts inactive plasminogen into active plasmin. Plasmin is involved in degradation of extracellular matrix and fibrinolysis, a process which restores blood flow after thrombotic events by breaking down fibrin. Therefore, overexpression of the uPA gene results in cell damage and bleeding disorders by inhibition of blood coagulation. In this transgenic mouse model the uPA gene is linked to the albumin enhancer/promotor. Since albumin is produced in the liver, this leads to liver specific overexpression of the uPA gene.

The resulting high plasma uPA levels cause severe and sometimes fatal intestinal and abdominal bleeding and extensive hepatocellular damage. This latter leads to chronic hepatic insufficiency and creates a supportive niche and growth advantage for liver regeneration by transplanted healthy hepatocytes.

To by-pass the risk of graft rejection the human hepatocytes are transplanted to genetically immunodeficient (Severe Combined Immuno Deficiency (SCID)) mice (uPA^{+/-}-SCID) [139, 141-144]. Primary human hepatocytes are transplanted by injection into the mouse spleen, after which the hepatocytes migrate via the spleen and portal veins into the liver, where the cells diffusely spread into the hepatic sinusoids [145-147]. The transplanted primary human hepatocytes will repopulate the diseased liver and restore the normal liver function [139, 145].

To determine the success of human hepatocyte engraftment and therefore restoration of the normal liver function the human albumin concentration is measured in the mouse plasma. This human albumin concentration correlates to the percentage of liver replacement by the human hepatocytes [141, 145]. The functionality of the transplanted hepatocytes can be evaluated by using a proteomic approach, which involves the identification of other human proteins in the mouse plasma [139]. As no complete replacement of the mouse liver tissue by human hepatocytes can be obtained non-chimeric mice (uPA^{+/-}-SCID mice without transplantation) are also included as control group to check for interspecies differences [136].

The chimeric mouse model was already successfully applied for metabolism studies of steroids in our laboratory [136] and has proven to be a good alternative for human excretion studies [126-130]. In this project the chimeric mouse model was applied, predominantly to verify the metabolism studies performed by the *in vitro* (HLM/S9 liver fractions) models. In this way the use of the chimeric mouse model can be refined and the number of animal experiments can be reduced.

The advantage of performing metabolism studies in an intact biological system is that all pharmacokinetic processes (ADME) are included and the preservation of cellular architecture of the complete liver provides a better resemblance to the *in vivo* human situation. The *in vivo* model has the additional advantage that a wide range of phase I and phase II metabolic pathways can be studied. Similar to the liver fractions they are ethically more acceptable to use in comparison to human or primates. In contrast to the *in vitro* models the *in vivo* mouse model does not require addition of cofactors and the model can also be applied for consecutive administrations if a wash out period is respected.

However, the mice are vulnerable for infections due to their immunodeficient (SCID) background. Other drawbacks of this chimeric mouse model include that the *in vivo* experiments are more labor-intensive, the well-fare of the animals must be ensured, only limited urine volumes can be obtained (via specially designed metabolic cages) and the higher background in the concentrated urine samples. Moreover, the production of this chimeric mouse model is technically very challenging and the efficiency of repopulation is highly variable, leading to high overall production costs to obtain chimeric mice with high percentages of liver replacement by human hepatocytes [140, 145]. As no complete repopulation by the human hepatocytes can be obtained, specific human metabolites can remain unnoticed by the high metabolic rate typical for mouse hepatocytes.

7.2 Protocols of the *in vitro* and *in vivo* metabolism studies

The protocols for the *in vitro* and *in vivo* metabolism studies will be described in this section. Only differences to these protocols will be indicated in the materials and methods section of Chapters 3 till 9.

7.2.1 Analysis of test compound

Prior to the metabolism studies with the *in vitro* and *in vivo* models it is important to verify the content and purity of the solution of the test compounds, especially if black market products will be used. Therefore, analysis by both GC-MS and LC-(HR)MS techniques were applied for all tested compounds. If possible the content of the black market product was also compared with reference material of the test compounds. Product ion scans can also be helpful as they provide additional proof of the structure of the test compound. Ultimately, further evidence of the chemical structure can be obtained by Nuclear Magnetic Resonance (NMR) analysis. The solutions, containing the test compounds, prepared for *in vitro* and *in vivo* metabolism studies were verified by GC-MS and/or LC-MS analysis.

7.2.2 *In vitro* metabolism studies

7.2.2.1 Materials and instrumentation

- **Human liver fractions:**

HLM and S9 liver fractions used for this doctoral research were commercially available and were purchased from BD-Gentest with a protein concentration of 20 mg/mL in 250 mM sucrose. To take into account inter-individual variation related to genetic polymorphisms and to reduce lot-to-lot variability pooled HLM and S9 liver fractions derived from 20-30 male and female donors were used [27]. The HLM and S9 liver fractions are stored at -80 °C and are thawed on ice before use. To reduce the number of freeze thaw cycles aliquots were prepared.

- **Test compound:**

The test compounds were dissolved in ethanol (EtOH). To prevent inhibition of the metabolic enzymes, the final concentration of the solvent was kept at 1% EtOH [27, 28, 118]. Therefore a solution of the test compound should be prepared at a concentration of 100 times the desired final concentration in the assay, since a volume of 2.5 μ L is added to perform the incubation experiment (to obtain a total volume of 250 μ L). In general reference material of the test compound was dissolved in EtOH at a concentration of 4 mg/mL. If only limited material of the test compound was available, 100 μ L of a 100 μ g/mL solution of the test compound in MeOH was evaporated (to obtain a total volume of 250 μ L).

- **Buffer and cofactors:**

Phase I: 0.1 M Phosphate buffer at pH 7.4; NADPH.

For this study a NADPH regeneration system was applied. The regeneration of NADPH by glucose-6-phosphate dehydrogenase (G6PD) is shown in Figure 1.14. Both the phosphate buffer and the NADPH regeneration system (NADPH solutions A and B) were purchased from BD-Gentest.

NADPH solution A (NADPH-A) contains: NADP⁺ (26 mM); glucose-6-phosphate (66 mM) and MgCl₂ (66 mM).

NADPH solution B (NADPH-B) contains: G6PD (40 U/mL) in sodium citrate (5 mM).

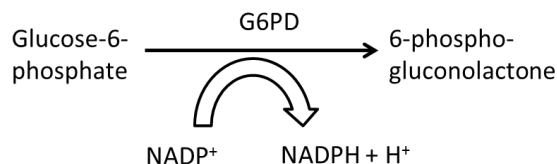


Figure 1.14. NADPH regeneration by glucose-6-phosphate dehydrogenase (G6PD).

Phase II: purified water (buffer (TrisHCl) is included in cofactor solutions); UDPGA

For the UGT enzyme the cofactor UDPGA solutions A and B from BD-Gentest were used.

UDPGA Solution A (UDPGA-A) contains: UDPGA (25 mM).

UDPGA Solution B (UDPGA-B) contains: Tris-HCl (250 mM); MgCl₂ (40 mM); alamethicin (0.125 mg/mL).

Since the UGT enzymes are located at the luminal side of the ER [31], the pore-forming peptide alamethicin was added to reduce latency of the phase II (UGT) reactions, this would not affect phase I enzymes located in the ER [27, 148]. The presence of Mg would be beneficial for the UGT conjugation rate [149].

- **Stop solutions:**

To terminate the metabolic reactions the samples were transferred to an ice-bath and a stop solution was added, for example MeOH, acetonitrile or perchloric acid (4M).

Besides inactivation of the enzymes, the stop solution also precipitates the proteins so they cannot interfere with the metabolite analysis [27].

- **Incubation instrument:**

The *in vitro* samples were incubated at 37 °C (simulating body temperature and optimum temperature for the enzyme activity), while constant gently mixing (300 rpm) by an Eppendorf Thermomixer comfort (Eppendorf, Rotselaar, Belgium) (Figure 1.15).



Figure 1.15. Eppendorf Thermomixer applied for the incubation of the *in vitro* metabolism studies.

7.2.2.2 Protocol *in vitro* metabolism studies

The protocol of the phase I and phase II assays is represented in Figure 1.16 and Table 1.7. The indicated volumes are for a total incubation volume of 250 µL in an Eppendorf thermomixer.

In a first step the test compound and the appropriate cofactors are added in a tube and pre-incubated during 5 min at 37 °C. The enzymatic reactions are initiated by adding the HLM or S9 liver fractions. At the desired incubation time MeOH is added to terminate the enzymatic reactions. For the phase I samples incubation times of 2, 4, 6, 8 and 18 h were applied and the phase II samples were incubated for 2 h. Finally the enzymatic proteins are removed by centrifugation of the incubation samples and subsequent transfer of the supernatant to new tubes.

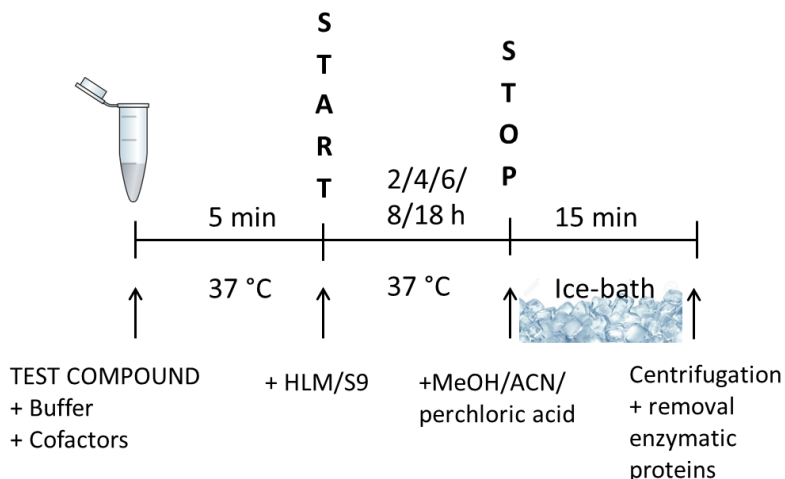


Figure 1.16. Protocol of the *in vitro* metabolism studies with HLM and S9 liver fractions.

For the combined phase I and phase II (UGT) metabolism studies, both NADPH and UDPGA are needed as cofactor. However, first the phase I incubations were initiated and after 2 h the phase II glucuronide conjugation reactions were initiated, for another 2 h, by the addition of UDPGA-A. UDPGA-B is already added in the pre-incubation step as this contains the Tris-HCl buffer.

Besides the *in vitro* incubation samples with the test compound control incubations (positive, negative and blank) were also performed to verify the enzymatic reactions. For the positive control samples the test compound was replaced by methandienone. The negative or system blank control samples did not contain any test compound and to the blank or substrate stability control samples no enzymatic proteins are added. These latter control samples were incubated to monitor non-enzymatic reactions and the stability of the test compound. To keep final volumes for all tubes identical, phosphate buffer was added to negative and blank control samples to adjust the volumes.

Table 1.7. Protocol for the *in vitro* metabolism studies.

Step	Phase I	Phase II (UGT)	Phase I + II (UGT)
Pre-incubation: 5 min at 37°C	2.5 µL Test compound (4 mg/mL in EtOH)		
	226 µL phosphate buffer (0.1 M; pH 7.4)	171 µL purified water	156 µL purified water
	12.5 µL NADPH-A	20 µL UDPGA-A	12.5 µL NADPH-A
	2.5 µL NADPH-B (final [NADPH] = 1.3 mM)	50 µL UDPGA-B (final [UDPGA] = 2 mM)	2.5 µL NADPH-B 50 µL UDPGA-B
Incubation: Phase I: 2-18 h Phase II and I+II: 2 h	6.5 µL HLM/S9 (20 mg protein / mL)		
	×	×	20 µL UDPGA-A
Stop	250 µL ice-cold MeOH; 15 min ice bath		
Removal of enzymatic proteins	Centrifugation (5 min; 4°C; 12,000 g) and transfer into new tubes		

7.2.3 *In vivo* metabolism studies

The *in vivo* metabolism studies were performed in cooperation with the CEVAC of Ghent University Hospital. The required ethical approval was obtained by the ethical committee for laboratory animal experiments of the Faculty of Medicine and Health Sciences of Ghent University (ECD 06/09). The protocol for the *in vivo* experiments with the chimeric mouse model was adapted from previous research performed with this model [136] (Figure 1.17).

Measurement of the human albumin concentration in the mouse plasma was performed to evaluate the success of the human liver cell engraftment. Both chimeric and non-chimeric mice were applied for the *in vivo* metabolism studies.

The test compounds were administered in a single dose to the mice by oral gavage. This forced oral administration route allows knowledge of the exact administered dose and was performed outside the cage to avoid direct contamination. The test compounds were dissolved in EtOH (10-20%) and further diluted in phosphate buffered saline (PBS). The mice were administered a maximum volume of 200 µL of this solution.

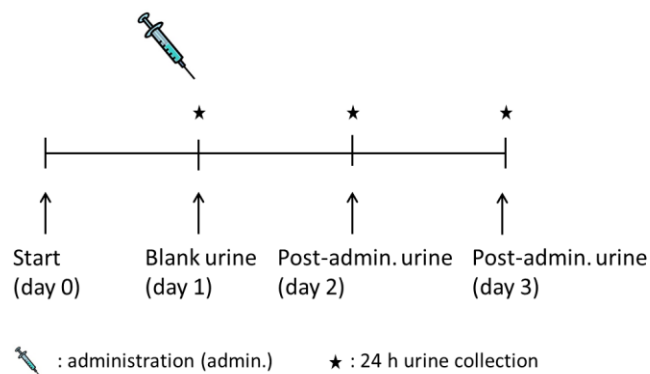


Figure 1.17. Administration protocol for the chimeric mouse model.

The dose for oral administration was chosen based on pilot studies with non-chimeric mice to allow detection of parent compound and metabolites in the mouse urine. To collect mouse urine the administration studies were performed in metabolic cages from Tecniplast (Sommeren, the Netherlands) (Figure 1.18). These cages are specially designed to separate urine and faeces, which enables proper urine collection. Urine samples were collected every 24 h due to the low amount of urine produced per day by one mouse (< 1.5 mL). Before the administration of the test compound ‘blank’ urine samples were collected. After the administration, urine samples were collected daily for two days.

The mice were kept in these metabolic cages for a maximum of three days and their welfare was daily monitored. During this period, the mice had free access to autoclaved water and powdered food. The mice were kept in type II filter top cages with nesting material, in the periods between the experiments (Figure 1.18).

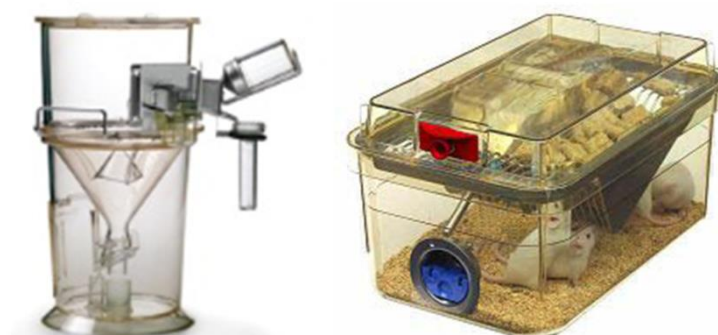


Figure 1.18. Metabolic cage (left side) and filter top cage (right side).

7.2.4 Sample preparation and analysis of *in vitro* and *in vivo* metabolism samples

The general sample preparation scheme is presented in Figure 1.19.

For the chimeric mouse urine samples hydrolysis and LLE were combined as both phase I and phase II metabolic pathways are performed in the *in vivo* model. The phase I *in vitro* incubation samples only underwent LLE. For GC-MS analysis an extra derivatization step is required, while for LC-MS analysis reconstitution of the samples in water/MeOH (50/50) is sufficient. Eventually direct injection of the (phase I/phase II) HLM incubation samples by LC-MS were performed.

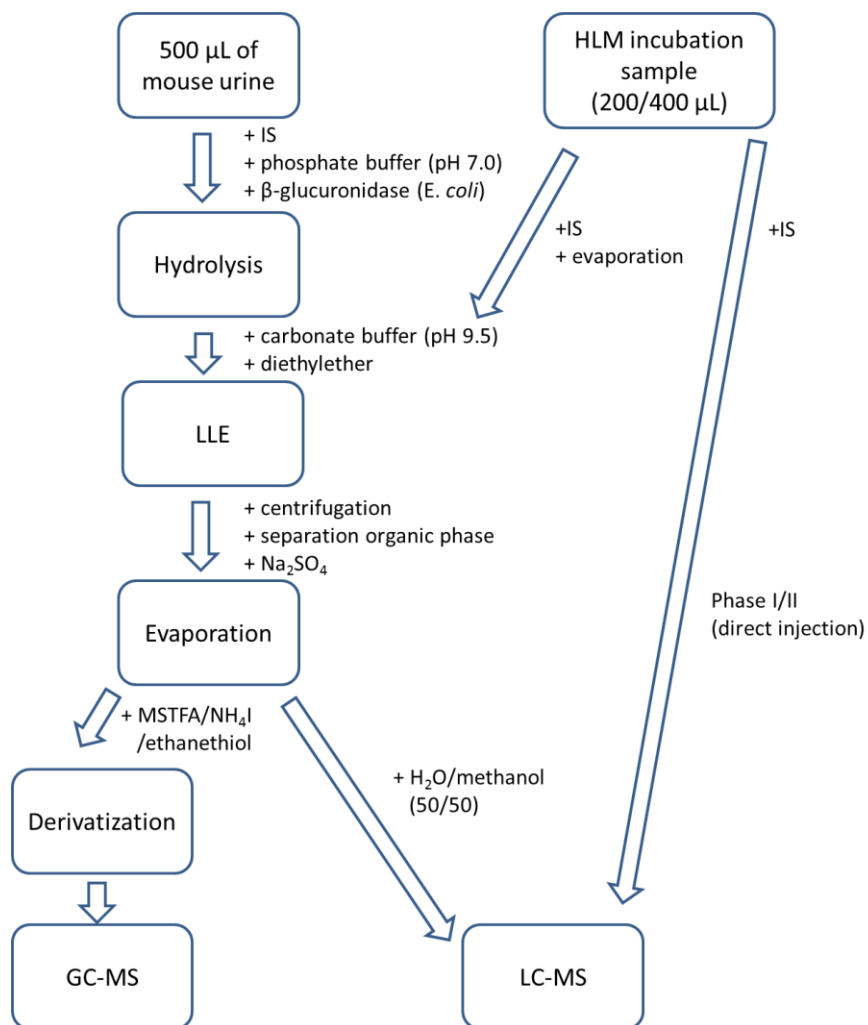


Figure 1.19. Sample preparation protocol for the *in vitro* and *in vivo* assays.

GC-MS(/MS) and/or LC-MS (both low and high resolution) instruments were applied for the analysis of the samples. Metabolites were identified by comparison of incubation samples and (blank and negative) control samples for the *in vitro* experiments and pre- and post-administration urine samples for the *in vivo* experiments. Both total ion chromatograms (TIC)

and extracted ion chromatograms (EIC) were compared. These extracted ions included (both single and combined) metabolic transformation such as reduction (+H₂), oxidation (-H₂; + OH), dealkylation (e.g. - CH₂), deacetylation (-C₂OH₂) and hydrolysis. Besides the full scan analysis strategies for the detection of unknown (steroids) were also applied such as precursor ion and neutral loss scan. If no reference material was available, further structure elucidation of the detected metabolites was performed by GC-MS/MS and/or LC-(HR)MS product ion scans.

References

1. Müller RK (2010). History of doping and doping control. In *Handb Exp Pharmacol* (Thieme, D., and Hemmersbach, P., Eds.) 195, 1-23.
2. WADA. WADA website. Montreal (2016) <https://www.wada-ama.org/> (access date 04/01/2016).
3. Yesalis CE, and Bahrke MS (2002). History of doping in sport. *International sports studies* 24, 42-76.
4. Baron DA, Martin DM, and Magd SA (2007). Doping in sports and its spread to at-risk populations: an international review. *World Psychiatry* 6, 54-59.
5. Ehrnborg C, and Rosen T (2009). The psychology behind doping in sport. *Growth Horm. IGF Res.* 19, 285-287.
6. Kicman AT, and Gower DB (2003). Anabolic steroids in sport: biochemical, clinical and analytical perspectives. *Ann. Clin. Biochem.* 40, 321-356.
7. WADA. The World Anti-Doping Code. Montreal (2015) <https://wada-main-prod.s3.amazonaws.com/resources/files/wada-2015-world-anti-doping-code.pdf> (access date 04.01.16).
8. WADA. The 2016 Prohibited List, International Standard. Montreal (2016) <https://wada-main-prod.s3.amazonaws.com/resources/files/wada-2016-prohibited-list-en.pdf> (access date 04.01.16).
9. Sottas P-E, Robinson N, and Saugy M (2010). The athlete's biological passport and indirect markers of blood doping. In *Handb Exp Pharmacol* (Thieme D, and Hemmersbach P, Eds.) 195, 305-326.
10. Kazlauskas R (2010). Designer steroids. In *Handb Exp Pharmacol* (Thieme D, and Hemmersbach P, Eds.) 195, 155-185.
11. WADA. International Standard for Laboratories. Montreal (2015) <https://www.wada-ama.org/en/resources/laboratories/international-standard-for-laboratories-isl> (access date 04.01.16).
12. WAADS. WAADS website. (2016) <http://waads.org/> (access date 06/01/2016).
13. Kicman AT (2010). Biochemical and physiological aspects of endogenous androgens. In *Handb Exp Pharmacol* (Thieme D, and Hemmersbach P, Eds.) 195, 25-64.
14. WADA. 2014 Anti-Doping Testing Figures - Laboratory report. Montreal (2015) https://wada-main-prod.s3.amazonaws.com/wada_2014_anti-doping-testing-figures_full-report_en.pdf (access date 27/12/2015).
15. Kicman AT (2008). Pharmacology of anabolic steroids. *Br. J. Pharmacol.* 154, 502-521.
16. Büttner A, and Thieme D (2010). Side effects of anabolic androgenic steroids: pathological findings and structure-activity relationships. In *Handb Exp Pharmacol* (Thieme D, and Hemmersbach P, Eds.) 195, 459-484.
17. Hall JM, Couse JF, and Korach KS (2001). The multifaceted mechanisms of estradiol and estrogen receptor signaling. *J. Biol. Chem.* 276, 36869-36872.

Chapter 1 - Introduction

18. Thevis M, and Schänzer W (2010). Synthetic anabolic agents: steroids and nonsteroidal selective androgen receptor modulators. In *Handb Exp Pharmacol* (Thieme D, and Hemmersbach P, Eds.) 195, 99-126.
19. Van Renterghem P (2010). Alternative steroid profiling: advances in detection of misuse with endogenous steroids in sports, In *Faculty of Medicine and Health Sciences, Ghent University, PhD thesis*, Ghent.
20. Hartgens F, and Kuipers H (2004). Effects of androgenic-anabolic steroids in athletes. *Sports Med.* 34, 513-554.
21. Mottram DR, and George AJ (2000). Anabolic steroids. *Baillieres Best Pract Res Clin Endocrinol Metab* 14, 55-69.
22. Kuuranne T, Leinonen A, Schänzer W, Kamber M, Kostianen R, and Thevis M (2008). Aryl-propionamide-derived selective androgen receptor modulators: Liquid chromatography-tandem mass spectrometry characterization of the in vitro synthesized metabolites for doping control purposes. *Drug Metab. Dispos.* 36, 571-581.
23. Timbrell J (2002). Disposition of toxic compounds. In *Introduction to toxicology* 3, 19-38, London.
24. Kuuranne T (2010). Phase-II metabolism of androgens and its relevance for doping control analysis. In *Handb Exp Pharmacol* (Thieme D, and Hemmersbach P, Eds.) 195, 65-75.
25. Timbrell J (2002). Metabolism of foreign compounds. In *Introduction to toxicology* 3, 39-56, London.
26. Schänzer W (1996). Metabolism of anabolic androgenic steroids. *Clin. Chem.* 42, 1001-1020.
27. Bioscience B (2012). Mammalian liver microsomes - Guidelines for use.
28. Jia L, and Liu X (2007). The conduct of drug metabolism studies considered good practice (II): in vitro experiments. *Curr. Drug Metab.* 8, 822-829.
29. Brandon EFA, Raap CD, Meijerman I, Beijnen JH, and Schellens JHM (2003). An update on in vitro test methods in human hepatic drug biotransformation research: pros and cons. *Toxicol. Appl. Pharmacol.* 189, 233-246.
30. Ingelman-Sundberg M (2005). Genetic polymorphisms of cytochrome P450 2D6 (CYP2D6): clinical consequences, evolutionary aspects and functional diversity. *Pharmacogenomics J* 5, 6-13.
31. Radominska-Pandya A, Czernik PJ, Little JM, Battaglia E, and Mackenzie PI (1999). Structural and functional studies of UDP-glucuronosyltransferases. *Drug Metab. Rev.* 31, 817-899.
32. Sten T, Bichlmaier I, Kuuranne T, Leinonen A, Yli-Kauhalaoma J, and Finel M (2009). UDP-Glucuronosyltransferases (UGTs) 2B7 and UGT2B17 Display Converse Specificity in Testosterone and Epitestosterone Glucuronidation, whereas UGT2A1 Conjugates Both Androgens Similarly. *Drug Metab. Dispos.* 37, 417-423.
33. Sten T, Kurkela M, Kuuranne T, Leinonen A, and Finel M (2009). UDP-Glucuronosyltransferases in Conjugation of 5 alpha- and 5 beta-Androstane Steroids. *Drug Metab. Dispos.* 37, 2221-2227.
34. Fabregat A, Kotronoulas A, Marcos J, Joglar J, Alfonso I, Segura J, Ventura R, and Pozo OJ (2013). Detection, synthesis and characterization of metabolites of steroid hormones conjugated with cysteine. *Steroids* 78, 327-336.

35. Pozo OJ, Gomez C, Marcos J, Segura J, and Ventura R (2012). Detection and characterization of urinary metabolites of boldione by LC-MS/MS. Part II: Conjugates with cysteine and N-acetylcysteine. *Drug Test. Anal.* 4, 786-797.
36. Martucci CP, and Fishman J (1993). P450 enzymes of estrogen metabolism. *Pharmacol. Ther.* 57, 237-257.
37. Zhu BT, and Lee AJ (2005). NADPH-dependent metabolism of 17 beta-estradiol and estrone to polar and nonpolar metabolites by human tissues and cytochrome P450 isoforms. *Steroids* 70, 225-244.
38. Lundstrom K, Tenhunen J, Tilgmann C, Karhunen T, Panula P, and Ulmanen I (1995). Cloning, expression and structure of catechol-O-methyltransferase. *Biochim Biophys Acta* 1251, 1-10.
39. Tretzel L, Thomas A, Geyer H, Gmeiner G, Forsdahl G, Pop V, Schänzer W, and Thevis M (2014). Use of dried blood spots in doping control analysis of anabolic steroid esters. *J Pharm Biomed Anal* 96, 21-30.
40. Thevis M, Geyer H, Tretzel L, and Schänzer W (2016). Sports drug testing using complementary matrices: Advantages and limitations. *J Pharm Biomed Anal.*
41. Thieme D, Rautenberg C, Grosse J, and Schoenfelder M (2013). Significant increase of salivary testosterone levels after single therapeutic transdermal administration of testosterone: suitability as a potential screening parameter in doping control. *Drug Test Anal* 5, 819-825.
42. Thieme D, Grosse J, Sachs H, and Müller RK (2000). Analytical strategy for detecting doping agents in hair. *Forensic Sci Int* 107, 335-345.
43. Gaillard Y, Vayssette F, Balland A, and Pepin G (1999). Gas chromatographic-tandem mass spectrometric determination of anabolic steroids and their esters in hair. Application in doping control and meat quality control. *J Chromatogr B Biomed Sci Appl* 735, 189-205.
44. Kintz P, and Samyn N (2002). Use of alternative specimens: drugs of abuse in saliva and doping agents in hair. *Ther Drug Monit* 24, 239-246.
45. Kintz P (2003). Testing for anabolic steroids in hair: a review. *Legal Medicine (Tokyo)* 5 Suppl 1, S29-33.
46. Gallardo E, and Queiroz JA (2008). The role of alternative specimens in toxicological analysis. *Biomed Chromatogr* 22, 795-821.
47. Thevis M (2010). *Mass spectrometry in sports drug testing*, Wiley, New Jersey.
48. Kintz P, Cirimele V, and Ludes B (2000). Pharmacological criteria that can affect the detection of doping agents in hair. *Forensic Sci Int* 107, 325-334.
49. Granger DA, Shirtcliff EA, Booth A, Kivlighan KT, and Schwartz EB (2004). The "trouble" with salivary testosterone. *Psychoneuroendocrinology* 29, 1229-1240.
50. Geyer H, Schänzer W, and Thevis M (2014). Anabolic agents: recent strategies for their detection and protection from inadvertent doping. *Br J Sports Med* 48, 820-826.
51. WADA. WADA technical document - TD2016EAAS v 1.0, Endogenous anabolic androgenic steroids measurement and reporting. Montreal (2016) <https://wada-main-prod.s3.amazonaws.com/resources/files/wada-td2016eaas-eaas-measurement-and-reporting-en.pdf> (access date 15/01/2016).

52. Dehennin L, and Matsumoto AM (1993). Long-term administration of testosterone enanthate to normal men - Alterations of the urinary profile of androgen metabolites potentially useful for detection of testosterone misuse in sport. *J. Steroid Biochem. Mol. Biol.* 44, 179-189.
53. Kuuranne T, Saugy M, and Baume N (2014). Confounding factors and genetic polymorphism in the evaluation of individual steroid profiling. *Br J Sports Med* 48, 848-855.
54. Thevis M, and Schänzer W (2007). Mass spectrometry in sports drug testing: Structure characterization and analytical assays. *Mass Spectrom. Rev.* 26, 79-107.
55. Marcos J, and Pozo OJ (2015). Current LC-MS methods and procedures applied to the identification of new steroid metabolites. *J Steroid Biochem Mol Biol.*
56. Houghton E, Grainger L, Dumasia MC, and Teale P (1992). Application of gas-chromatography mass-spectrometry to steroid analysis in equine sports - Problems with enzyme hydrolysis. *Org. Mass Spectrom.* 27, 1061-1070.
57. Gomes RL, Meredith W, Snape CE, and Sephton MA (2009). Analysis of conjugated steroid androgens: Deconjugation, derivatisation and associated issues. *J. Pharm. Biomed. Anal.* 49, 1133-1140.
58. Hauser B, Schulz D, Boesch C, and Deschner T (2008). Measuring urinary testosterone levels of the great apes - Problems with enzymatic hydrolysis using *Helix pomatia* juice. *Gen. Comp. Endocrinol.* 158, 77-86.
59. Gomez C, Fabregat A, Pozo OJ, Marcos J, Segura J, and Ventura R (2014). Analytical strategies based on mass spectrometric techniques for the study of steroid metabolism. *Trac-Trends Anal. Chem.* 53, 106-116.
60. Marcos J, and Pozo OJ (2015). Derivatization of steroids in biological samples for GC-MS and LC-MS analyses. *Bioanalysis* 7, 2515-2536.
61. Tudela E, Deventer K, Geldof L, and Van Eenoo P (2015). Urinary detection of conjugated and unconjugated anabolic steroids by dilute-and-shoot liquid chromatography-high resolution mass spectrometry. *Drug Test. Anal.* 7, 95-108.
62. Deventer K, Pozo OJ, Verstraete AG, and Van Eenoo P (2014). Dilute-and-shoot-liquid chromatography-mass spectrometry for urine analysis in doping control and analytical toxicology. *Trac-Trends Anal. Chem.* 55, 1-13.
63. Fabregat A, Pozo OJ, Marcos J, Segura J, and Ventura R (2013). Use of LC-MS/MS for the Open Detection of Steroid Metabolites Conjugated with Glucuronic Acid. *Anal. Chem.* 85, 5005-5014.
64. Schänzer W, Guddat S, Thomas A, Opfermann G, Geyer H, and Thevis M (2013). Expanding analytical possibilities concerning the detection of stanozolol misuse by means of high resolution/high accuracy mass spectrometric detection of stanozolol glucuronides in human sports drug testing. *Drug Test. Anal.* 5, 810-818.
65. Gorgens C, Guddat S, Orlovius AK, Sigmund G, Thomas A, Thevis M, and Schänzer W (2015). "Dilute-and-inject" multi-target screening assay for highly polar doping agents using hydrophilic interaction liquid chromatography high resolution/high accuracy mass spectrometry for sports drug testing. *Anal. Bioanal. Chem.* 407, 5365-5379.
66. Thevis M, and Schänzer W (2007). Current role of LC-MS(/MS) in doping control. *Anal. Bioanal. Chem.* 388, 1351-1358.

67. Borts DJ, and Bowers LD (2000). Direct measurement of urinary testosterone and epitestosterone conjugates using high-performance liquid chromatography/tandem mass spectrometry. *J. Mass Spectrom.* 35, 50-61.
68. Pozo OJ, Van Eenoo P, Deventer K, and Delbeke FT (2007). Ionization of anabolic steroids by adduct formation in liquid chromatography electrospray mass spectrometry. *J. Mass Spectrom.* 42, 497-516.
69. Arsenault J, and Mcdonald P (2007). *Beginners guide to liquid chromatography*, Waters Corporation.
70. Van Gansbeke W, Polet M, Hooghe F, Devos C, and Van Eenoo P (2015). Improved sensitivity by use of gas chromatography-positive chemical ionization triple quadrupole mass spectrometry for the analysis of drug related substances. *Journal of Chromatography B-Analytical Technologies in the Biomedical and Life Sciences* 1001, 221-240.
71. Nielen MWF, Bovee TFH, van Engelen MC, Rutgers P, Hamers ARM, van Rhijn IHA, and Hoogenboom L (2006). Urine testing for designer steroids by liquid chromatography with androgen bioassay detection and electrospray quadrupole time-of-flight mass spectrometry identification. *Anal. Chem.* 78, 424-431.
72. Yuan XF, B. M. (2005). Detection of designer steroids. *Nucl. Recept. Signal.* 3, 1-5.
73. Pozo OJ, Deventer K, Eenoo PV, and Delbeke FT (2008). Efficient approach for the comprehensive detection of unknown anabolic steroids and metabolites in human urine by liquid chromatography-electrospray-tandem mass spectrometry. *Anal. Chem.* 80, 1709-1720.
74. Thevis M, Geyer H, Mareck U, and Schänzer W (2005). Screening for unknown synthetic steroids in human urine by liquid chromatography-tandem mass spectrometry. *J. Mass Spectrom.* 40, 955-962.
75. Pozo OJ, Van Eenoo P, Deventer K, and Delbeke FT (2008). Detection and characterization of anabolic steroids in doping analysis by LC-MS. *Trac-Trends Anal. Chem.* 27, 657-671.
76. Kohler M, Thomas A, Geyer H, Petrou M, Schänzer W, and Thevis M (2010). Confiscated black market products and nutritional supplements with non-approved ingredients analyzed in the Cologne Doping Control Laboratory 2009. *Drug Test. Anal.* 2, 533-537.
77. Thevis M, Kuuranne T, Geyer H, and Schänzer W (2013). Annual banned-substance review: analytical approaches in human sports drug testing. *Drug Test. Anal.* 5, 1-19.
78. Thevis M, Kuuranne T, Geyer H, and Schänzer W (2014). Annual banned-substance review: analytical approaches in human sports drug testing. *Drug Test. Anal.* 6, 164-184.
79. Thevis M, Kuuranne T, Geyer H, and Schänzer W (2015). Annual banned-substance review: analytical approaches in human sports drug testing. *Drug Test. Anal.* 7, 1-20.
80. Esposito S, Deventer K, Goeman J, Van der Eycken J, and Van Eenoo P (2012). Synthesis and characterization of the N-terminal acetylated 17-23 fragment of thymosin beta 4 identified in TB-500, a product suspected to possess doping potential. *Drug Test. Anal.* 4, 733-738.
81. Esposito S, Deventer K, and Van Eenoo P (2012). Characterization and identification of a C-terminal amidated mechano growth factor (MGF) analogue in black market products. *Rapid Commun. Mass Spectrom.* 26, 686-692.

82. Henninge J, Pepaj M, Hullstein I, and Hemmersbach P (2010). Identification of CJC-1295, a growth-hormone-releasing peptide, in an unknown pharmaceutical preparation. *Drug Test. Anal.* 2, 647-650.
83. Kohler M, Thomas A, Walpurgis K, Terlouw K, Schänzer W, and Thevis M (2010). Detection of His-tagged Long-R-3-IGF-I in a black market product. *Growth Horm. IGF Res.* 20, 386-390.
84. Thomas A, Kohler M, Mester J, Geyer H, Schänzer W, Petrou M, and Thevis M (2010). Identification of the growth-hormone-releasing peptide-2 (GHRP-2) in a nutritional supplement. *Drug Test. Anal.* 2, 144-148.
85. Thevis M, Thomas A, Kohler M, Beuck S, and Schänzer W (2009). Emerging drugs: mechanism of action, mass spectrometry and doping control analysis. *J. Mass Spectrom.* 44, 442-460.
86. Alibaba.com. http://www.alibaba.com/product-detail/SR9009-1379686-30-2-increase-exercise_1684435259.html?spm=a2700.7724838.30.1.ZgphMt&s=p (access date 10.07.2014).
87. Jelkmann W (2009). Erythropoiesis Stimulating Agents and Techniques: A Challenge for Doping Analysts. *Curr. Med. Chem.* 16, 1236-1247.
88. Beuck S, Schänzer W, and Thevis M (2012). Hypoxia-inducible factor stabilizers and other small-molecule erythropoiesis-stimulating agents in current and preventive doping analysis. *Drug Test. Anal.* 4, 830-845.
89. Scarth JP, Clarke AD, Teale P, and Pearce CM (2010). Comparative in vitro metabolism of the 'designer' steroid estra-4,9-diene-3,17-dione between the equine, canine and human: Identification of target metabolites for use in sports doping control. *Steroids* 75, 643-652.
90. Van Thuyne W, Van Eenoo P, and Delbeke FT (2006). Nutritional supplements: prevalence of use and contamination with doping agents. *Nutr. Res. Rev.* 19, 147-158.
91. Geyer H, Parr MK, Koehler K, Mareck U, Schänzer W, and Thevis M (2008). Nutritional supplements cross-contaminated and faked with doping substances. *J. Mass Spectrom.* 43, 892-902.
92. Thevis M, and Schänzer W (2008). Mass spectrometry of selective androgen receptor modulators. *J. Mass Spectrom.* 43, 865-876.
93. Fragkaki AG, Angelis YS, Koupparis M, Tsantili-Kakoulidou A, Kokotos G, and Georgakopoulos C (2009). Structural characteristics of anabolic androgenic steroids contributing to binding to the androgen receptor and to their anabolic and androgenic activities Applied modifications in the steroidal structure. *Steroids* 74, 172-197.
94. Chen JY, Kim J, and Dalton JT (2005). Discovery and therapeutic promise of selective androgen receptor modulators. *Mol. Interv.* 5, 173-188.
95. Gao WQ, and Dalton JT (2007). Expanding the therapeutic use of androgens via selective androgen receptor modulators (SARMs). *Drug Discov. Today* 12, 241-248.
96. Zhi L (2012). Selective androgen receptor modulators (sarms) and uses thereof, Ligand Pharmaceuticals Incorporated.
97. Wu D (2005). Pharmacokinetics and metabolism of a selective androgen receptor modulator (SARM) in rats--implication of molecular properties and intensive metabolic profile to investigate ideal pharmacokinetic characteristics of a propanamide in preclinical study. *Drug Metab. Dispos.*

98. Grata E, Perrenoud L, Saugy M, and Baume N (2011). SARM-S4 and metabolites detection in sports drug testing: A case report. *Forensic Sci.Int.* 213, 104-108.
99. Krug O, Thomas A, Walpurgis K, Piper T, Sigmund G, Schänzer W, Laussmann T, and Thevis M (2014). Identification of black market products and potential doping agents in Germany 2010-2013. *Eur. J. Clin. Pharmacol.* 70, 1303-1311.
100. Thevis M, and Schänzer W (2014). Analytical approaches for the detection of emerging therapeutics and non-approved drugs in human doping controls. *J Pharm Biomed Anal* 101, 66-83.
101. Thevis M, Lagojda A, Kuehne D, Thomas A, Dib J, Hansson A, Hedeland M, Bondesson U, Wigger T, Karst U, and Schänzer W (2015). Characterization of a non-approved selective androgen receptor modulator drug candidate sold via the Internet and identification of in vitro generated phase-I metabolites for human sports drug testing. *Rapid Commun. Mass Spectrom.* 29, 991-999.
102. Basaria S, Collins L, Dillon EL, Orwoll K, Storer TW, Miciek R, Ulloor J, Zhang AQ, Eder R, Zientek H, Gordon G, Kazmi S, Sheffied-Moore M, and Bhasin S (2013). The Safety, Pharmacokinetics, and Effects of LGD-4033, a Novel Nonsteroidal Oral, Selective Androgen Receptor Modulator, in Healthy Young Men. *J. Gerontol. Ser. A-Biol. Sci. Med. Sci.* 68, 87-95.
103. Solt LA, Wang YJ, Banerjee S, Hughes T, Kojetin DJ, Lundasen T, Shin Y, Liu J, Cameron MD, Noel R, Yoo SH, Takahashi JS, Butler AA, Kamenecka TM, and Burris TP (2012). Regulation of circadian behaviour and metabolism by synthetic REV-ERB agonists. *Nature* 485, 62-68.
104. Woldt E, Sebti Y, Solt LA, Duhem C, Lancel S, Eeckhoutte J, Hesselink MKC, Paquet C, Delhaye S, Shin YS, Kamenecka TM, Schaart G, Lefebvre P, Neviere R, Burris TP, Schrauwen P, Staels B, and Duez H (2013). Rev-erb-alpha modulates skeletal muscle oxidative capacity by regulating mitochondrial biogenesis and autophagy. *Nat. Med.* 19, 1039-1046.
105. Bass J (2012). DRUG DISCOVERY Time in a bottle. *Nature* 485, 45-46.
106. Shea SA (2012). Obesity and Pharmacologic Control of the Body Clock. *N. Engl. J. Med.* 367, 175-178.
107. Duez H, and Staels B (2008). Rev-erb alpha gives a time cue to metabolism. *FEBS Lett.* 582, 19-25.
108. Ramakrishnan SN, and Muscat GE (2006). The orphan Rev-erb nuclear receptors: a link between metabolism, circadian rhythm and inflammation? *Nucl. Recept. Signal.* 4, 1-5.
109. Ko CH, and Takahashi JS (2006). Molecular components of the mammalian circadian clock. *Hum Mol Genet* 15 Spec No 2, R271-277.
110. Preitner N, Damiola F, Lopez-Molina L, Zakany J, Duboule D, Albrecht U, and Schibler U (2002). The orphan nuclear receptor REV-ERBalpha controls circadian transcription within the positive limb of the mammalian circadian oscillator. *Cell* 110, 251-260.
111. Griffett K, and Burris TP (2013). The mammalian clock and chronopharmacology. *Bioorg. Med. Chem. Lett.* 23, 1929-1934.
112. Reppert SM, and Weaver DR (2002). Coordination of circadian timing in mammals. *Nature* 418, 935-941.
113. Cagampang FR, and Bruce KD (2012). The role of the circadian clock system in nutrition and metabolism. *Br J Nutr* 108, 381-392.

114. Shin Y, Noel R, Banerjee S, Kojetin D, Song XY, He YJ, Lin L, Cameron MD, Burris TP, and Kamenecka TM (2012). Small molecule tertiary amines as agonists of the nuclear hormone receptor Rev-erb alpha. *Bioorg. Med. Chem. Lett.* 22, 4413-4417.
115. Li S, and Laher I (2015). Exercise Pills: At the Starting Line. *Trends Pharmacol Sci* 36, 906-917.
116. Fan W, Atkins AR, Yu RT, Downes M, and Evans RM (2013). Road to exercise mimetics: targeting nuclear receptors in skeletal muscle. *J Mol Endocrinol* 51, T87-T100.
117. Handschin C (2016). Caloric restriction and exercise "mimetics": Ready for prime time? *Pharmacol Res* 103, 158-166.
118. Kuuranne T, Aitio O, Vahermo M, Elovaara E, and Kostiaainen R (2002). Enzyme-assisted synthesis and structure characterization of glucuronide conjugates of methyltestosterone (17 alpha-methylandrost-4-en-17 beta-ol-3-one) and nandrolone (estr-4-en-17 beta-ol-3-one) metabolites. *Bioconjug. Chem.* 13, 194-199.
119. Tingle MD, and Helsby NA (2006). Can in vitro drug metabolism studies with human tissue replace in vivo animal studies? *Environ. Toxicol. Pharmacol.* 21, 184-190.
120. Kuuranne T, Kurkela M, Thevis M, Schänzer W, Finel M, and Kostiaainen R (2003). Glucuronidation of anabolic androgenic steroids by recombinant human UDP-glucuronosyltransferases. *Drug Metab. Dispos.* 31, 1117-1124.
121. Kurkela M, Garcia-Horsman JA, Luukkanen L, Morsky S, Taskinen J, Baumann M, Kostiaainen R, Hirvonen J, and Finel M (2003). Expression and characterization of recombinant human UDP-glucuronosyltransferases (UGTs). UGT1A9 is more resistant to detergent inhibition than other UGTs and was purified as an active dimeric enzyme. *J Biol Chem* 278, 3536-3544.
122. Wong JKY, Tang FPW, and Wan TSM (2011). In vitro metabolic studies using homogenized horse liver in place of horse liver microsomes. *Drug Test. Anal.* 3, 393-399.
123. Levesque JF, Gaudreault M, Houle R, and Chauret N (2002). Evaluation of human hepatocyte incubation as a new tool for metabolism study of androstenedione and norandrostenedione in a doping control perspective. *J. Chromatogr. B* 780, 145-153.
124. Levesque JF, Gaudreault M, Aubin Y, and Chauret N (2005). Discovery, biosynthesis, and structure elucidation of new metabolites of norandrostenedione using in vitro systems. *Steroids* 70, 305-317.
125. Gauthier J, Goudreault D, Poirier D, and Ayotte C (2009). Identification of drostanolone and 17-methyldrostanolone metabolites produced by cryopreserved human hepatocytes. *Steroids* 74, 306-314.
126. Lootens L, Meuleman P, Leroux-Roels G, and Van Eenoo P (2011). Metabolic studies with promagnon, methylclostebol and methasterone in the uPA(+/-)-SCID chimeric mice. *J. Steroid Biochem. Mol. Biol.* 127, 374-381.
127. Lootens L, Meuleman P, Pozo OJ, Van Eenoo P, Leroux-Roels G, and Delbeke FT (2009). uPA(+/-)-SCID Mouse with Humanized Liver as a Model for In Vivo Metabolism of Exogenous Steroids: Methandienone as a Case Study. *Clin. Chem.* 55, 1783-1793.
128. Lootens L, Van Eenoo P, Meuleman P, Leroux-Roels G, and Delbeke FT (2009). The uPA(+/-)-SCID Mouse with Humanized Liver as a Model for in Vivo Metabolism of 4-Androstene-3,17-dione. *Drug Metab. Dispos.* 37, 2367-2374.

129. Pozo OJ, Lootens L, Van Eenoo P, Deventer K, Meuleman P, Leroux-Roels G, Parr MK, Schänzer W, and Delbeke FT (2009). Combination of liquid-chromatography tandem mass spectrometry in different scan modes with human and chimeric mouse urine for the study of steroid metabolism. *Drug Test. Anal.* 1, 554-567.
130. Lootens L, Van Eenoo P, Meuleman P, Pozo OJ, Van Renterghem P, Leroux-Roels G, and Delbeke FT (2009). Steroid metabolism in chimeric mice with humanized liver. *Drug Test. Anal.* 1, 531-537.
131. Catlin DH, Sekera MH, Ahrens BD, Starcevic B, Chang YC, and Hatton CK (2004). Tetrahydrogestrinone: discovery, synthesis, and detection in urine. *Rapid Commun. Mass Spectrom.* 18, 1245-1249.
132. Sekera MH, Ahrens BD, Chang YC, Starcevic B, Georgakopoulos C, and Catlin DH (2005). Another designer steroid: discovery, synthesis, and detection of 'madol' in urine. *Rapid Commun. Mass Spectrom.* 19, 781-784.
133. Scarth JP, Spencer HA, Timbers SE, Hudson SC, and Hillyer LL (2010). The use of in vitro technologies coupled with high resolution accurate mass LC-MS for studying drug metabolism in equine drug surveillance. *Drug Test. Anal.* 2, 1-10.
134. Scarth JP, Spencer HA, Hudson SC, Teale P, Gray BP, and Hillyer LL (2010). The application of in vitro technologies to study the metabolism of the androgenic/anabolic steroid stanozolol in the equine. *Steroids* 75, 57-69.
135. ILAC (2009). ILAC G7: 06/2009 Accreditation requirements and operating criteria for horseracing laboratories, International Laboratory Accreditation Cooperation (ILAC).
136. Lootens L (2010). The mouse with the humanized liver: A new model for metabolic studies of anabolic steroids in man, In Faculty of Medicine and Health Sciences, Ghent University, PhD thesis, Ghent.
137. Esposito S, Deventer K, Geldof L, and Van Eenoo P (2015). In vitro models for metabolic studies of small peptide hormones in sport drug testing. *J. Pept. Sci.* 21, 1-9.
138. Yanni S (2015). Metabolism: Principle, Methods, and Applications. In *Translational ADMET for drug therapy - Principles, Methods, and Pharmaceutical applications* 3, 63-110, New Jersey.
139. Meuleman P, Libbrecht L, De Vos R, de Hemptinne B, Gevaert K, Vandekerckhove J, Roskams T, and Leroux-Roels G (2005). Morphological and biochemical characterization of a human liver in a uPA-SCID mouse chimera. *Hepatology* 41, 847-856.
140. Scheer N, and Wilson ID (2015). A comparison between genetically humanized and chimeric liver humanized mouse models for studies in drug metabolism and toxicity. *Drug Discov Today*.
141. Tateno C, Yoshizane Y, Saito N, Kataoka M, Utoh R, Yamasaki C, Tachibana A, Soeno Y, Asahina K, Hino H, Asahara T, Yokoi T, Furukawa T, and Yoshizato K (2004). Near completely humanized liver in mice shows human-type metabolic responses to drugs. *Am. J. Pathol.* 165, 901-912.
142. Petersen J, Dandri M, Gupta S, and Rogler CE (1998). Liver repopulation with xenogenic hepatocytes in B and T cell-deficient mice leads to chronic hepadnavirus infection and clonal growth of hepatocellular carcinoma. *Proc Natl Acad Sci U S A* 95, 310-315.
143. Dandri M, Burda MR, Torok E, Pollok JM, Iwanska A, Sommer G, Rogiers X, Rogler CE, Gupta S, Will H, Greten H, and Petersen J (2001). Repopulation of mouse liver with human hepatocytes and in vivo infection with hepatitis B virus. *Hepatology* 33, 981-988.

Chapter 1 - Introduction

144. Mercer DF, Schiller DE, Elliott JF, Douglas DN, Hao C, Rinfret A, Addison WR, Fischer KP, Churchill TA, Lakey JR, Tyrrell DL, and Kneteman NM (2001). Hepatitis C virus replication in mice with chimeric human livers. *Nat Med* 7, 927-933.
145. Vanwolleghem T, Libbrecht L, Hansen BE, Desombere I, Roskams T, Meuleman P, and Leroux-Roels G (2010). Factors determining successful engraftment of hepatocytes and susceptibility to hepatitis B and C virus infection in uPA-SCID mice. *J Hepatol* 53, 468-476.
146. Sandgren EP, Palmiter RD, Heckel JL, Daugherty CC, Brinster RL, and Degen JL (1991). Complete hepatic regeneration after somatic deletion of an albumin-plasminogen activator transgene. *Cell* 66, 245-256.
147. Meuleman P, and Leroux-Roels G (2008). The human liver-uPA-SCID mouse: a model for the evaluation of antiviral compounds against HBV and HCV. *Antiviral Res* 80, 231-238.
148. Fisher MB, Campanale K, Ackermann BL, Vandenbranden M, and Wrighton SA (2000). In vitro glucuronidation using human liver microsomes and the pore-forming peptide alamethicin. *Drug Metab. Dispos.* 28, 560-566.
149. Fisher MB, Yoon K, Vaughn ML, Strelevitz TJ, and Foti RS (2002). Flavin-containing monooxygenase activity in hepatocytes and microsomes: In vitro characterization and in vivo scaling of benzydamine clearance. *Drug Metab. Dispos.* 30, 1087-1093.

Chapter 2

Outline of the study

1 *In vitro* and *in vivo* models for metabolism studies

Driven by pharmaceutical innovations, there is a fast evolution in the number and kind of performance enhancing substances which are available on the internet. These substances can be obtained as pharmaceutical preparations and black market products. Since the latter products are often produced by clandestine 'underground' laboratories, their purity is not guaranteed and toxicological profiles are often missing. Although this raises concerns about the safety of these products, both professional and amateur athletes might still be tempted to use these substances for doping purposes. Because of the deterrent effects, prompt implementation of markers for these substances into existing screening methods is recommended to warrant the ethics of sports and health of the athletes. Preventive anti-doping research plays therefore an important role to determine the metabolism of these compounds, which is essential to improve the detection (windows). For the non-approved substances ethical and safety aspects limit the use of human volunteers for metabolism studies. To overcome these constraints and to ensure a fast response to the evolutions of performance enhancing substances there is a quest for alternatives to human excretion studies to establish the metabolic profile of doping agents.

DoCoLab has access to the uPA^{+/+}-SCID chimeric mouse model with humanized liver for the study of the metabolism of drugs, thanks to the collaboration with CEVAC (Ghent University Hospital). The model has proven to be an excellent alternative for this kind of research [1-5]. The high-end model however has some practical limitations such as the limited volume of urine that is daily excreted (± 1 mL/day) and the low doses that can be applied. Furthermore, the production of the chimeric mouse model is technically very challenging and leads to the high cost of the model. Although there are less ethical constraints in comparison with the use of humans and primates, some ethical questions related to the use of animal models remain.

Therefore, the aim of this study was to examine the use of *in vitro* techniques for metabolism studies. In this way the welfare of the animals can be improved respecting the 3R's concept: refinement, replacement and reduction. The focus of this study was to develop an integrated approach, in which human liver microsomes (HLM) and/or S9 liver fractions support the chimeric mouse model. The use of HLM and S9 liver fractions is less expensive and more user-friendly, because of the straightforward protocol and the cleaner extracts that can be obtained in comparison with the chimeric mouse model. However, the correlation with the real *in vivo* human situation must be investigated.

2 Metabolism studies of (designer) steroids

Since the turn of the millennium (designer) steroids are marketed in so-called nutritional supplements to circumvent legislation and doping controls [6] and till today the anabolic androgenic steroids (AAS) are one of the most detected classes of prohibited substances [7]. Therefore, in Part 2 of this study the integrated *in vitro* and *in vivo* approach was applied to elucidate the metabolism of AAS and designer steroids. The exogenous AAS or designer steroids that were studied include prostanazol (Chapter 3), methylstenbolone (Chapter 4) and methasterone (Chapter 4 and 5), dimethazine (DMZ) (Chapter 5) and estradienedione (Chapter 6) (Figure 2.1).

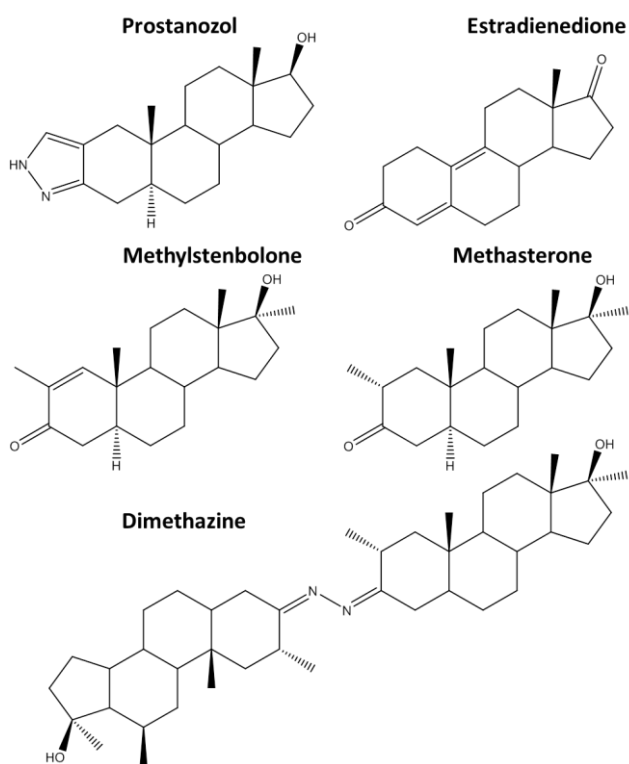


Figure 2.1. Chemical structures of prostanazol, estradienedione, methylstenbolone, methasterone and dimethazine.

Prior to the metabolism studies, black market products which declare to contain the designer steroids and are marketed as so-called supplements were purchased to verify their content. The confirmed presence of the labeled substances in the black market products highlights the potential risk for their misuse and the need for optimized screening methods. Therefore metabolism studies are essential to identify markers which allow detection of these substances with the longest retrospectivity.

For the metabolism studies, the *in vitro* models (phase I) always preceded the *in vivo* model. Both GC-MS(/MS) and LC-(HR)MS/MS analyses were applied to determine phase I and phase II metabolites in the *in vitro* and *in vivo* assays. To facilitate the comparison of GC and LC techniques, fractions were collected of the metabolism samples. Product ion scans were performed to further characterize the structure of the detected metabolites.

Besides these phase I *in vitro* metabolism studies with (designer) steroids, the *in vitro* model was also applied for the synthesis of (non-commercially available) AAS glucuronides (Chapter 7). The *in vitro* synthesized phase II compounds were used as reference materials (via direct injection by LC-MS) and allowed to establish the metabolic nature and further characterization of the metabolites observed in excretion urine samples. HLM were used to simulate the phase II metabolism of following AAS: gestrinone, tetrahydrogestrinone, trenbolone, 4 β -hydroxystanozolol and 16 β -hydroxystanozolol.

3 Metabolism studies of other performance enhancing substances

Nowadays an evolution from designer steroids to new performance enhancing substances such as SARMs [8-10], REV-ERB agonists [11] and peptides [12-17] is observed. To anticipate the potential misuse of these substances, the test compounds of the metabolism studies were extended from designer steroids to other classes of performance enhancing substances (Part 3).

3.1 SARMs

Andarine and ostarine were the first SARMs that were described and detected in ‘supplements’. Both have an aryl-propionamide structure [8, 18-20]. More recently a new SARM was introduced on the black market with a pyrrolidin-benzonitrile structure: LGD-4033 [21-23]. LGD-4033 was invented by Ligand pharmaceuticals and is still under clinical investigation [24]. The chemical structure of the substance which is distributed as LGD-4033 in black market products is presented in Figure 2.2. However, it should be noted that the exact structure of LGD-4033 is still not confirmed by Ligand pharmaceuticals [21-23], but this structure was present on a patent application of Ligand pharmaceuticals for SARMs [23, 25].

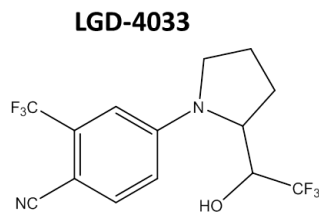


Figure 2.2. Chemical structure of SARM LGD-4033.

This preventive anti-doping research was initiated by purchasing a black market product over the internet, which was advertised to contain LGD-4033 (Chapter 8). The presence of LGD-4033 and the purity of the black market product was verified by LC-MS/MS (both low and high resolution), GC-MS(/MS) and GC-NPD. As no reference material is available for LGD-4033, also NMR analysis was performed.

To anticipate misuse of LGD-4033, its metabolism was elucidated using *in vitro* models: HLM and S9 liver fractions. Phase I as well as combined phase I and II assays were studied. The *in vitro* incubation samples were analyzed by GC-MS and LC-HRMS. To characterize the structures of the detected metabolites high resolution product ion scans (LC-HRMS/MS) were performed.

3.2 REV-ERB agonists

In 2012 the REV-ERB agonists SR9009 and SR9011 (Figure 2.3) were described by the SCRIPPS Research institute as promising drug candidates to treat metabolic disorders [26]. Although these compounds are still undergoing clinical evaluation, the observed beneficial effects on energy homeostasis and increase in exercise capacity via *in vivo* animal studies make these compounds attractive for doping purposes [26-32]. Moreover, SR9009 is already advertised as ‘exercise in a pill’ compound on the black market [11].

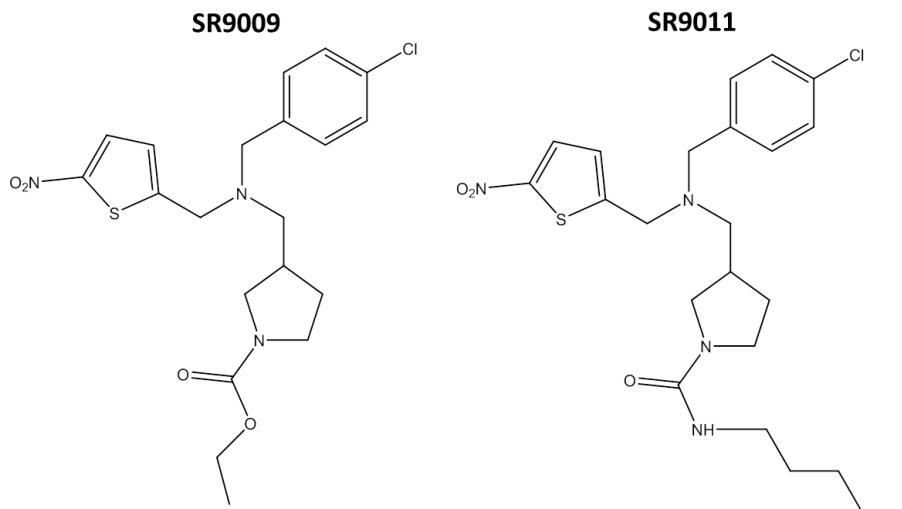


Figure 2.3. Chemical structures of REV-ERB agonists SR9009 and SR9011.

A black market product containing SR9009 was purchased over the internet. In addition also reference material for both SR9009 and SR9011 was obtained.

The metabolism studies with SR9009 and SR9011 using HLM are described in Chapter 9. The *in vitro* incubation samples were analyzed by LC-HRMS (direct injection). LC-HRMS product ion scans were applied to elucidate the structures of the metabolites. Furthermore, an assay validation for the detection of SR9009 and SR9011 using a routine LC-HRMS screening method was performed. The presence of SR9009, SR9011 and their metabolites in routine doping control samples was verified by retrospective data analysis.

4 Research objectives

1. Can the *in vitro* model based on HLM and S9 liver fractions complement the chimeric mouse model to predict human steroid metabolism and therefore help to reduce the number of animal experiments?
2. Can the *in vitro* model based on HLM and S9 liver fractions assist in the elucidation of the metabolism of designer steroids where ethical questions limit the use of human volunteers for metabolism studies?
Can this *in vitro* model also be applied for the metabolic investigation of other classes of non-approved (doping) substances?
3. Can the *in vitro* incubation samples be applied in screening methods for comparative purposes and to synthesize reference material?

References

1. Lootens L, Meuleman P, Leroux-Roels G, and Van Eenoo P (2011). Metabolic studies with promagnon, methylclostebol and methasterone in the uPA(+/-)-SCID chimeric mice. *J. Steroid Biochem. Mol. Biol.* 127, 374-381.
2. Lootens L, Meuleman P, Pozo OJ, Van Eenoo P, Leroux-Roels G, and Delbeke FT (2009). uPA(+/-)-SCID Mouse with Humanized Liver as a Model for In Vivo Metabolism of Exogenous Steroids: Methandienone as a Case Study. *Clin. Chem.* 55, 1783-1793.
3. Lootens L, Van Eenoo P, Meuleman P, Leroux-Roels G, and Delbeke FT (2009). The uPA(+/-)-SCID Mouse with Humanized Liver as a Model for in Vivo Metabolism of 4-Androstene-3,17-dione. *Drug Metab. Dispos.* 37, 2367-2374.
4. Pozo OJ, Lootens L, Van Eenoo P, Deventer K, Meuleman P, Leroux-Roels G, Parr MK, Schänzer W, and Delbeke FT (2009). Combination of liquid-chromatography tandem mass spectrometry in different scan modes with human and chimeric mouse urine for the study of steroid metabolism. *Drug Test. Anal.* 1, 554-567.
5. Lootens L, Van Eenoo P, Meuleman P, Pozo OJ, Van Renterghem P, Leroux-Roels G, and Delbeke FT (2009). Steroid metabolism in chimeric mice with humanized liver. *Drug Test. Anal.* 1, 531-537.
6. Kazlauskas R (2010). Designer steroids. In *Handb Exp Pharmacol* (Thieme, D., and Hemmersbach, P., Eds.) 195, 155-185.
7. WADA. 2014 Anti-Doping Testing Figures - Laboratory report. Montreal (2015) https://wada-main-prod.s3.amazonaws.com/wada_2014_anti-doping-testing-figures_full-report_en.pdf (access date 27/12/2015).
8. Thevis M, and Schänzer W (2010). Synthetic anabolic agents: steroids and nonsteroidal selective androgen receptor modulators. In *Handb Exp Pharmacol* (Thieme D, and Hemmersbach P, Eds.) 195, 99-126, Heidelberg Germany.
9. Kohler M, Thomas A, Geyer H, Petrou M, Schänzer W, and Thevis M (2010). Confiscated black market products and nutritional supplements with non-approved ingredients analyzed in the Cologne Doping Control Laboratory 2009. *Drug Test. Anal.* 2, 533-537.
10. Thevis M, Thomas A, Kohler M, Beuck S, and Schänzer W (2009). Emerging drugs: mechanism of action, mass spectrometry and doping control analysis. *J. Mass Spectrom.* 44, 442-460.
11. Alibaba.com. http://www.alibaba.com/product-detail/SR9009-1379686-30-2-increase-exercise_1684435259.html?spm=a2700.7724838.30.1.ZgphMt&s=p (access date 10.07.2014).
12. Thevis M, Kuuranne T, Geyer H, and Schänzer W (2013). Annual banned-substance review: analytical approaches in human sports drug testing. *Drug Test. Anal.* 5, 1-19.

13. Esposito S, Deventer K, Goeman J, Van der Eycken J, and Van Eenoo P (2012). Synthesis and characterization of the N-terminal acetylated 17-23 fragment of thymosin beta 4 identified in TB-500, a product suspected to possess doping potential. *Drug Test. Anal.* 4, 733-738.
14. Esposito S, Deventer K, and Van Eenoo P (2012). Characterization and identification of a C-terminal amidated mechano growth factor (MGF) analogue in black market products. *Rapid Commun. Mass Spectrom.* 26, 686-692.
15. Henninge J, Pepaj M, Hullstein I, and Hemmersbach P (2010). Identification of CJC-1295, a growth-hormone-releasing peptide, in an unknown pharmaceutical preparation. *Drug Test. Anal.* 2, 647-650.
16. Kohler M, Thomas A, Walpurgis K, Terlouw K, Schänzer W, and Thevis M (2010). Detection of His-tagged Long-R-3-IGF-I in a black market product. *Growth Horm. IGF Res.* 20, 386-390.
17. Thomas A, Kohler M, Mester J, Geyer H, Schänzer W, Petrou M, and Thevis M (2010). Identification of the growth-hormone-releasing peptide-2 (GHRP-2) in a nutritional supplement. *Drug Test. Anal.* 2, 144-148.
18. Fragkaki AG, Angelis YS, Koupparis M, Tsantili-Kakoulidou A, Kokotos G, and Georgakopoulos C (2009). Structural characteristics of anabolic androgenic steroids contributing to binding to the androgen receptor and to their anabolic and androgenic activities Applied modifications in the steroidal structure. *Steroids* 74, 172-197.
19. Chen JY, Kim J, and Dalton JT (2005). Discovery and therapeutic promise of selective androgen receptor modulators. *Mol. Interv.* 5, 173-188.
20. Kuuranne T, Leinonen A, Schänzer W, Kamber M, Kostianen R, and Thevis M (2008). Aryl-propionamide-derived selective androgen receptor modulators: Liquid chromatography-tandem mass spectrometry characterization of the in vitro synthesized metabolites for doping control purposes. *Drug Metab. Dispos.* 36, 571-581.
21. Krug O, Thomas A, Walpurgis K, Piper T, Sigmund G, Schänzer W, Laussmann T, and Thevis M (2014). Identification of black market products and potential doping agents in Germany 2010-2013. *Eur. J. Clin. Pharmacol.* 70, 1303-1311.
22. Thevis M, and Schänzer W (2014). Analytical approaches for the detection of emerging therapeutics and non-approved drugs in human doping controls. *J Pharm Biomed Anal* 101, 66-83.
23. Thevis M, Lagojda A, Kuehne D, Thomas A, Dib J, Hansson A, Hedeland M, Bondesson U, Wigger T, Karst U, and Schänzer W (2015). Characterization of a non-approved selective androgen receptor modulator drug candidate sold via the Internet and identification of in vitro generated phase-I metabolites for human sports drug testing. *Rapid Commun. Mass Spectrom.* 29, 991-999.
24. Basaria S, Collins L, Dillon EL, Orwoll K, Storer TW, Miciek R, Ulloor J, Zhang AQ, Eder R, Zientek H, Gordon G, Kazmi S, Sheffied-Moore M, and Bhasin S (2013). The Safety,

- Pharmacokinetics, and Effects of LGD-4033, a Novel Nonsteroidal Oral, Selective Androgen Receptor Modulator, in Healthy Young Men. *J. Gerontol. Ser. A-Biol. Sci. Med. Sci.* 68, 87-95.
25. Zhi L (2012). Selective androgen receptor modulators (sarms) and uses thereof, Ligand Pharmaceuticals Incorporated.
 26. Solt LA, Wang YJ, Banerjee S, Hughes T, Kojetin DJ, Lundasen T, Shin Y, Liu J, Cameron MD, Noel R, Yoo SH, Takahashi JS, Butler AA, Kamenecka TM, and Burris TP (2012). Regulation of circadian behaviour and metabolism by synthetic REV-ERB agonists. *Nature* 485, 62-68.
 27. Bass J (2012). DRUG DISCOVERY Time in a bottle. *Nature* 485, 45-46.
 28. Shea SA (2012). Obesity and Pharmacologic Control of the Body Clock. *N. Engl. J. Med.* 367, 175-178.
 29. Duez H, and Staels B (2008). Rev-erb alpha gives a time cue to metabolism. *FEBS Lett.* 582, 19-25.
 30. Ramakrishnan SN, and Muscat GE (2006). The orphan Rev-erb nuclear receptors: a link between metabolism, circadian rhythm and inflammation? *Nucl. Recept. Signal.* 4, 1-5.
 31. Woldt E, Sebti Y, Solt LA, Duhem C, Lancel S, Eeckhoutte J, Hesselink MKC, Paquet C, Delhaye S, Shin YS, Kamenecka TM, Schaart G, Lefebvre P, Neviere R, Burris TP, Schrauwen P, Staels B, and Duez H (2013). Rev-erb-alpha modulates skeletal muscle oxidative capacity by regulating mitochondrial biogenesis and autophagy. *Nat. Med.* 19, 1039-1046.
 32. Shin Y, Noel R, Banerjee S, Kojetin D, Song XY, He YJ, Lin L, Cameron MD, Burris TP, and Kamenecka TM (2012). Small molecule tertiary amines as agonists of the nuclear hormone receptor Rev-erb alpha. *Bioorg. Med. Chem. Lett.* 22, 4413-4417.

PART 2

Metabolism studies with (designer) steroids

Chapter 3

In vitro and *in vivo* metabolism studies of prostanazol

Adapted from:

Geldof L, Lootens L, Decroix L, Botrè F, Meuleman P, Leroux-Roels G, Deventer K and Van Eenoo P (2016). Metabolic studies of prostanazol with the uPA-SCID chimeric mouse model and human liver microsomes. *Steroids* 107, 139-148.

Abstract

Anabolic androgenic steroids are prohibited by the World Anti-Doping Agency because of their adverse health and performance enhancing effects. Effective control of their misuse by detection in urine requires knowledge about their metabolism. In case of designer steroids, ethical objections limit the use of human volunteers to perform excretion studies. Therefore the suitability of alternative models needs to be investigated.

In this study pooled human liver microsomes (HLM) and an uPA^{+/+}-SCID chimeric mouse model were used to examine the metabolism of the designer steroid prostanazol as a reference standard. Metabolites were detected by gas chromatography-mass spectrometry (GC-MS; full scan) and liquid chromatography-tandem mass spectrometry (LC-MS/MS; precursor ion scan).

In total twenty-four prostanazol metabolites were detected with the *in vitro* and *in vivo* metabolism studies, which could be grouped into two broad classes, those with a 17-hydroxy- and those with a 17-keto-substituent. Major first phase metabolic sites were tentatively identified as C3', C4 and C16. Moreover, 3'- and 16 β -hydroxy-17-ketoprostanazol could be unequivocally identified, since authentic reference material was available, in both models.

Comparison with published data from humans showed a good correlation, except for phase II metabolism. In contrast to the human studies, the metabolites detected in the chimeric mouse model were predominantly present in the unconjugated fraction. Two types of metabolites ((di)hydroxylated prostanazol metabolites) that have not been described before could be confirmed in a real positive doping control sample. Hence, the results provide further evidence for the applicability of chimeric mice and HLM to perform metabolism studies of designer steroids.

1 Introduction

Some athletes resort to the use of prohibited substances to achieve performance enhancement, regardless of health effects, values and ethics that are essential to sports. To warrant fair play and ethics in sports as well as to safeguard health of athletes, the World Anti-Doping Agency (WADA) publishes a list of prohibited substances yearly [1]. To enforce these regulations WADA accredited doping-control laboratories consequently analyze biological samples from athletes for the presence of these substances. Anabolic androgenic steroids (AAS) are the most frequently detected compounds [2].

In order to try to evade detection, designer steroids are developed. These steroids are manufactured to closely resemble existing known compounds, but with sufficient chemical diversity to circumvent doping controls and legislation [3].

Since 2002 new 'designer' steroids have been marketed as so-called 'nutritional supplements' [4, 5]. Prostanazol (Figure 3.1) is such a designer steroid and is a 17-demethylated analogue of stanozolol (Winstrol®) [5] and is present as tetrahydropyranyl (THP) derivative ((17 β -[(tetrahydropyran-2-yl)oxy]-1'H-pyrazolo[3,4:2,3]-5 α -androstane) in the steroid product Orastan-E [6].

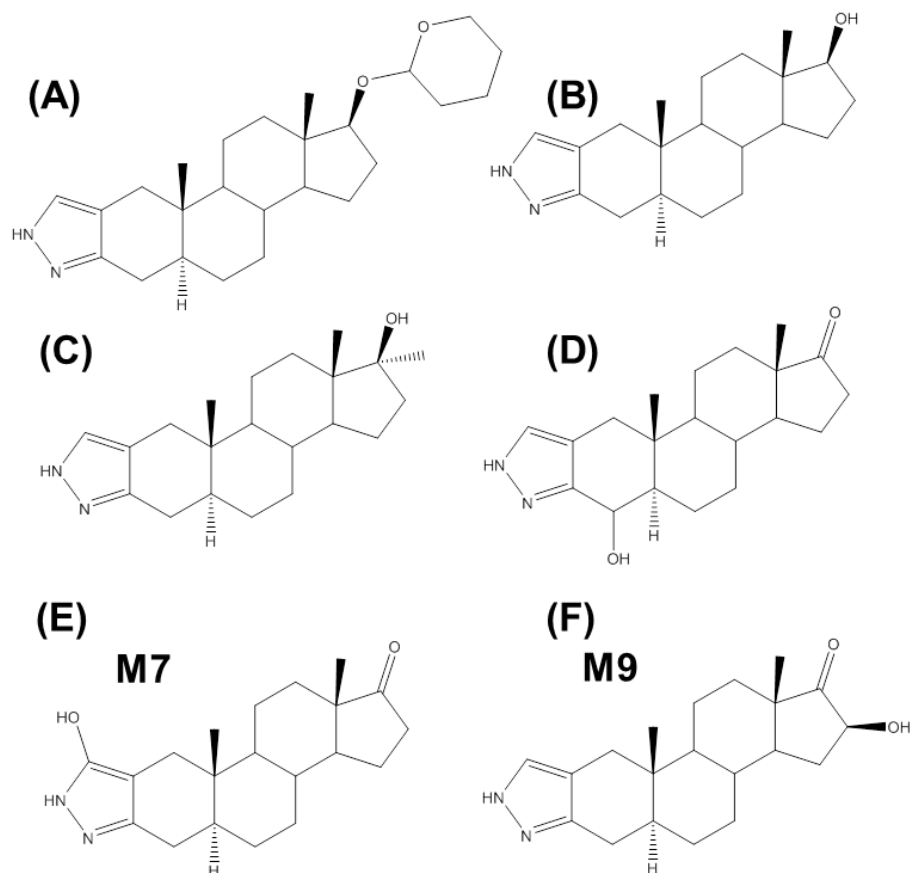


Figure 3.1. Chemical structures of (A) prostanazol-THP, (B) prostanazol and (C) stanozolol and commercially available reference standards: (D) 4-hydroxy-17-ketoprostanazol, (E) 3'-hydroxy-17-ketoprostanazol and (F) 16 β -hydroxy-17-ketoprostanazol.

Designer steroids are often sold over the internet or on the black market, sometimes when these compounds are still in early or advanced clinical trials. These facts bear several dangers because they are offered without information about their toxicological effects or their metabolism [7]. Indeed, the use of prostanazol has been related to an adverse health effect (cerebral infarction) [8]. In 2012 prostanazol was also added as steroid to the Controlled Substances Act [9] and as such to the Prohibited List of WADA [1].

As AAS are often extensively metabolized, it is important to identify the metabolites which can facilitate the detection of the steroid misuse for a longer time period [10]. This requires knowledge of the steroid metabolism. The metabolism of AAS can, just like other drugs, be divided in phase I and phase II reactions. Phase I reactions are functionalization reactions (e.g. oxidation or reduction) whereas phase II reactions are conjugation reactions (e.g. glucuronidation or sulfonation) [11]. In case of designer steroids, the application of *in vivo* human excretion studies is restricted due to ethical constraints and safety aspects. To overcome this problem there is a quest for alternatives to human administration for metabolism studies. Examples of such alternatives are liver fractions [12-16], hepatocyte cell cultures [17, 18], chimeric mice with humanized livers [19-21] and primates [22, 23].

These *in vivo* and *in vitro* model systems all have advantages as well as disadvantages. For example hepatocytes can be used to study phase I and phase II reactions sequentially or in parallel but they show a relative rapid decline in cytochrome P450 (CYP450) activities [24]. When a difference between them arises, the *in vivo* results should always take precedence over *in vitro* findings [25]. The aim of this study is to use human liver microsomes (HLM) as *in vitro* model and the uPA^{+/+}-SCID chimeric mouse as *in vivo* model to study the metabolism of the designer steroid prostanazol. In this way, two alternatives for human excretion studies are tested and the results of both models will be compared to provide a better overview on possible metabolic pathways.

The liver is the principal site of drug metabolism, where the CYP450 superfamily of oxidative enzymes plays an important role. HLM are a subcellular fraction of the human liver; they are principally derived from the membranes of the endoplasmatic reticulum. HLM provide an enriched source of membrane bound drug metabolizing enzymes, such as CYP450, uridine glucuronosyl transferase and flavin monooxygenase enzymes [26]. The *in vivo* model used in this study is a chimeric mouse model with human hepatocytes, developed in cooperation with CEVAC (Ghent University Hospital). This model involves the transplantation of primary human hepatocytes into immunodeficient (SCID) mice, to by-pass the risk of graft rejection [27]. Besides, the mice suffer from a liver disease because of liver-specific overexpression of a 'noxious' protein, namely urokinase plasminogen activator (uPA). The transplanted primary human hepatocytes will repopulate the diseased liver and restore the normal liver function [27].

By our knowledge this is the first time prostanazol is studied with a combination of an *in vitro* model and an *in vivo* animal model. Therefore it is interesting to elucidate its

metabolism in order to discover possible new metabolites and to verify if these alternative models result in comparable metabolites as already described in human studies [6, 28, 29]. Kazlauskas *et al.* [6] and Rodchenkov *et al.* [29] reported results from human administration studies with a single volunteer in a condensed format in conference proceedings with limited distribution. For all these studies [6, 28, 29] metabolites were tentatively identified, although they were the stimulus for this work and organic synthesis of the detected metabolites by others.

2 Materials and methods

2.1 Chemicals and reagents

The steroids needed for this study, prostanazol-tetrahydropyranyl (prostanazol-THP) (17 β -tetrahydropyranyl-5 α -androst-2-eno(3,2-c)-pyrazole) and prostanazol (17 β -hydroxy-5 α -androst-2-eno(3,2-c)-pyrazole), were purchased from 'Toronto Research Chemicals' (TRC, Toronto, Canada). The reference standards of methandienone and the following prostanazol metabolites: 3'-hydroxy-17-ketoprostanazol (3'-hydroxy-5 α -androst-2-eno[3,2-c]pyrazol-17-one), 16 β -hydroxy-17-ketoprostanazol (16 β -hydroxy-5 α -androst-2-eno[3,2-c]pyrazol-17-one), 4 α - and 4 β -hydroxy-17-ketoprostanazol (4 α - and 4 β -hydroxy-5 α -androst-2-eno[3,2-c]pyrazol-17-one) were obtained from the National Measurement Institute (NMI, North Ryde, Australia). The internal standard (IS) 17 α -methyltestosterone was a gift from Organon (Oss, the Netherlands).

Pooled HLM from 20-30 donors (HLM; 452161), the nicotinamide adenine dinucleotide phosphate (NADPH) regenerating system solutions A (451220) and B (451200) and phosphate buffer with pH 7.4 (451201) were purchased from BD Gentest (Erembodegem, Belgium).

Perchloric acid came from Sigma Aldrich (Steinheim, Germany). Ethanol, LC grade water and ammonium acetate (NH₄OAc) were purchased from Biosolve (Valkenswaard, the Netherlands). Diethyl ether and methanol (MeOH) were obtained from Fisher Scientific (Loughborough, UK). Sodium sulfate (Na₂SO₄), sodium hydrogen carbonate (NaHCO₃), potassium carbonate (K₂CO₃), disodium hydrogen phosphate dihydrate (Na₂HPO₄.2H₂O), sodium dihydrogen phosphate monohydrate (NaH₂PO₄.H₂O), orthophosphoric acid, acetic acid (HOAc), ammonium iodide (NH₄I), LC grade water and LC grade MeOH were from Merck (Darmstadt, Germany). The β -glucuronidase preparations from *Escherichia coli* (E. coli) K12 and from *Helix pomatia* (H. pomatia) were purchased from Roche Diagnostics (Mannheim, Germany) and Sigma-Aldrich (Steinheim, Germany), respectively. N-methyl-N-trimethylsilyltrifluoroacetamide (MSTFA) was from Karl Bucher (Waldstetten, Germany). Ethanethiol was obtained from Acros (Geel, Belgium). Phosphate Buffered Saline (PBS) was from Invitrogen (Merelbeke, Belgium). The helium (He) and oxygen-free nitrogen (OFN) gasses were delivered by Air Liquide (Bornem, Belgium).

2.2 Instrumentation

2.2.1 GC-MS

An Agilent 6890 gas chromatograph (Agilent Technologies, Palo Alto, CA, USA) was interfaced to an Agilent 5973 mass spectrometer. 1 μL of sample was injected into the system using a 7683 series Autosampler with a splitless injector (Agilent). The GC separation was performed using a JW Ultra-1 (Agilent) capillary column (17 m x 200 μm i.d., 0.11 μm) and He as mobile phase at a flow rate of 0.6 mL/min at 10.15 psi (constant flow). The temperature program was as follows: initial temperature was 120 $^{\circ}\text{C}$ and increased at a rate of 70 $^{\circ}\text{C}/\text{min}$ until 180 $^{\circ}\text{C}$ is reached. Temperature was then further increased with 4 $^{\circ}\text{C}/\text{min}$ to 234 $^{\circ}\text{C}$ and finally the temperature raises with 30 $^{\circ}\text{C}/\text{min}$ to 300 $^{\circ}\text{C}$. This final temperature was held during 2 min. The total run time was 18.76 min. The temperature of the source was set at 250 $^{\circ}\text{C}$ and for the electron impact ionization, electron energy of 70 eV was used. Full scan analysis was performed with the mass spectrometer (50-800 m/z , 2 cycles/sec).

2.2.2 LC-MS/MS

The precursor ion scan method was conducted using a Thermo Finnigan Surveyor Autosampler Plus, MS Pump Plus and TSQ Quantum Discovery MAX triple quadrupole mass spectrometer (all from Thermo Separation Products, Thermo, San Jose, USA). Electrospray ionization (ESI) was used for the ionization of the steroids. The mobile phase consisted of LC grade water (solvent A) and LC grade MeOH (solvent B) both with 1 mM NH_4Ac and 0.001% HOAc. The LC separation was performed using a SunFire™ C18 column (50 mm x 2.1 mm i.d., 3.5 μm) from Waters (AH Etten-Leur, the Netherlands). For comparison of the detected metabolites with the commercially available reference standards also a Zorbax RX C8 column (150 mm x 2.1 mm i.d., 5 μm) from Agilent Technologies (Palo Alto, CA, USA) was used. Both columns were applied at a flow rate of 250 $\mu\text{L}/\text{min}$. 20 μL of sample was injected into the instrument. A gradient program was applied, the percentage of solvent B changed as follows: 0 min, 30%; 1.5 min, 30%; 8 min, 55%; 15 min, 55%; 29.5 min, 95%; 30.5 min, 95%; 31 min, 30%; 34 min, 30%. The other instrumental parameters were adopted from Pozo *et al.* [30]. The method has a total run time of 33 min. The ions with m/z 81, 97 and 145 were selected as product ions. The collision energy was 45 eV for m/z 81 and 97 and 30 eV for m/z 145.

2.3 In vitro studies with HLM

The phase I metabolism studies of prostanazol were performed as described in Chapter 1 (7.2.2.2 *Protocol in vitro metabolism studies*; Table 1.6).

In short, reference standard of prostanazol (final concentration of 40 $\mu\text{g}/\text{mL}$) was incubated with HLM as test compound. Substrate stability samples (blank; without HLM) and system blank samples (without test compound) control samples were used to verify the enzymatic

reactions. Methandienone was used as test compound in the positive control samples. At the appropriate time (after 0, 1, 2, 3, 4, 5, 6 and 18 h) the enzymatic reactions were stopped by adding 25 μL 4 M perchloric acid.

2.4 Excretion studies with uPA+/-SCID chimeric mice

The protocol of the *in vivo* administration studies was applied as described in Chapter 1 (7.2.3 *In vivo* metabolism studies).

The chimeric mouse model was developed in cooperation with CEVAC of Ghent University Hospital [27]. The *in vivo* metabolism studies were approved by the Animal Ethical Committee of the Faculty of Medicine of Ghent University (ECD 06/09).

Prostanazol was administered to one non-chimeric and four chimeric mice by oral gavage. 100 μL of the reference standard of prostanazol (at a concentration of 10 mg/mL solved in PBS with 10% ethanol) was administered to the mice. This dose and route of administration was selected based on previous metabolism studies in the same model [19-21]. Before administration this solution was analyzed by GC-MS.

2.5 Sample preparation

2.5.1 Liquid-liquid extraction (LLE)

For the *in vitro* metabolic incubations the samples are first centrifuged at 4 °C (12,000 g, 5 min) then 200 μL was used for LLE. From the mouse urine 500 μL was used. 50 μL of the IS 17 α -methyltestosterone (2 $\mu\text{g}/\text{mL}$) was added to all samples.

For the HLM incubation samples only the unconjugated fraction (free fraction) was studied. Therefore LLE was performed by adding 1 mL liquid carbonate buffer pH 9.5 ($\text{NaHCO}_3/\text{K}_2\text{CO}_3$ (2/1)) and 5 mL diethyl ether and rolling during 20 min. The samples were then centrifuged (1500 g, 5 min). After centrifugation the organic layer was separated and dried by adding \pm 100 mg Na_2SO_4 . The organic layer was separated from the Na_2SO_4 and evaporated under OFN at 40 °C. To study the total fraction (conjugated and unconjugated steroids) in the mouse urine samples enzymatic hydrolysis was performed by adding 1 mL phosphate buffer (0.1 M, pH 7) and 50 μL β -glucuronidase from *E. coli* K12 (\pm 80 U/mg or 0.1 U/ μL). The samples were hydrolyzed during 2.5 h at 56 ± 5 °C. After cooling to room temperature, extraction was performed as described above.

To study phase II metabolism of prostanazol the free, glucuronidated and sulfated fractions were analyzed of a blank sample and a urine sample collected 24 h after administration. Therefore LLE without hydrolysis was first performed to study the free (unconjugated) fraction. After separation of the organic fraction LLE was performed on the same samples with hydrolysis with β -glucuronidase from *E. coli* (glucuronidated fraction). This was also

repeated with β -glucuronidase from *H. pomatia* (also arylsulfatase activity) and 1 mL acetate buffer (pH 5.2) instead of phosphate buffer.

For GC-MS analysis the samples were derivatized by adding 100 μ L derivatization solution containing MSTFA, NH_4I and ethanethiol (500/4/2) and incubation during 1 h at 80 ± 5 °C. For LC-MS analysis samples were dissolved in 100 μ L $\text{H}_2\text{O}/\text{MeOH}$ (70/30).

3 Results and discussion

3.1 Analysis of prostanazol

The presence of prostanazol-THP and prostanazol in the steroid product Orastan-E was observed by Kazlauskas *et al.* [6]. Both in this study (results not shown here) and by Kazlauskas *et al.* it was also observed that the THP-derivative readily hydrolyses to prostanazol, even in MeOH [6]. Therefore the reference standard of prostanazol instead of prostanazol-THP was chosen to be administered to the mouse model and HLM. Moreover, according to Yum *et al.* [28] oral administration would lead to hydrolysis of prostanazol-THP to prostanazol by gastric acid.

The mass spectrum of prostanazol after TMS-derivatization (MW 458; bis-TMS) is shown in Figure 3.2 and exhibits a characteristic ion at m/z 168, originating from fragmentation of the A- and N-ring [28].

3.2 In vitro metabolism studies of prostanazol with HLM

3.2.1 Full scan GC-MS analysis of in vitro metabolism samples of prostanazol

In order to eliminate inhibition of the microsomal enzymes, the final solvent concentration of prostanazol (reference standard) was limited to 1% [12, 26]. Methandienone was selected as steroid for positive control because the metabolism of methandienone has been thoroughly investigated in the past and undergoes metabolism via a wide variety of metabolic pathways [21].

After 4 h incubation of prostanazol the largest number of metabolites with the highest abundance could be detected (Figure 3.3 and Table 3.1). In total 19 metabolites (M1 and M5-M22), were found that were absent in the control samples (0 h, blank and negative samples). These HLM produced metabolites were grouped in seven categories (I-VII) based on their mass spectra (Table 3.2). The mass spectrum and tentative structures of each category are shown in Figure 3.2. Furthermore, also the parent compound and 17-ketoprostanazol (M1) could be detected.

Characteristic ions for the detection of prostanazol derivatives after trimethylsilylation are the ions m/z 254 and 168 (Figure 3.2). The ion m/z 254 is an indicator for 3'/4-hydroxylmetabolites [6, 28, 29], while m/z 168 indicates metabolites having no

hydroxylation in the A- or pyrazole (N-) rings [28]. The proposed positions of the hydroxyl group, when m/z 168 is present, are C6, C12 or C16, according to known hydroxylation positions in literature [11], and are indicated with 'x'.

Two new categories, hydroxylated and dihydroxylated prostanazol metabolites (I and VII respectively), were found in the HLM incubation samples which have so far not been reported in human excretion studies [6, 28, 29]. Detection of metabolites of prostanazol in human urine is however hampered by the corticosteroid area of the chromatogram [6, 29]. An overview of reported prostanazol metabolites in literature is given in Table 3.2.

Only one metabolite was detected for categories I (M8) and IV (M7), which are possibly 3'-hydroxy- or 4-hydroxy-prostanazol derivatives. Comparison with a certified reference standard led to the identification of M7 as 3'-hydroxy-17-ketoprostanazol.

Most metabolites were detected for categories II (M6, M10, M12, M14 and M16) and V (M5, M9, M11 and M15) with as characteristic ion m/z 168 indicating hydroxylations outside the A- and N-rings. M9 could be identified as 16 β -hydroxy-17-ketoprostanazol by comparison with the corresponding reference standard. A comparable metabolite was described as the main prostanazol metabolite in the study of Rodchenkov *et al.* [29], in their study a 6- or 16-hydroxy-17-ketoprostanazol structure was proposed. Our data clearly show it is 16 β -hydroxy-17-ketoprostanazol.

Although both categories (II and V) correspond to metabolites with m/z 546 and 544 after trimethylsilylation respectively, metabolites M10/M11 and M14/M15 are difficult to distinguish as they are co-eluting. So, using GC-MS these metabolites could not be resolved.

Metabolites of categories III (M18 and M20) and VII (M13, M17 and M22) with m/z 634 as molecular ion are definitely present. But as a result of the lower abundance of the peaks (S/N) of these metabolites it is more difficult to determine the abundance of the ions in the mass spectrum and to distinguish the ions m/z 168 and 254 in the full scan spectra. These metabolites are certainly not found in the blank and negative control samples.

Two metabolites (M19 and M21) of category VI (m/z 632/168) were detected but no metabolites of category VI', with as characteristic ions m/z 632 and 254 were found. So, the suggested positions of hydroxylations are outside the A- and N-rings for both metabolites.

3.2.2 Precursor ion scan analysis of *in vitro* metabolism samples of prostanazol by LC-MS/MS

To confirm the structures of the metabolites detected by GC-MS, the HLM incubation samples were also analyzed using LC-MS/MS (Figure 3.4). A precursor ion scan method was used, with m/z 81, 97 and 145 as selected product ions. The ion m/z 81 is an indicator for metabolites of stanozolol without any modifications in the A- and N-ring. Stanozolol derivatives with a hydroxyl group in the N-ring have ion m/z 97 as characteristic ion. Ion m/z 145 is common for 4-hydroxy stanozolol derivatives [30-32]. Because of the structural

similarity between stanozolol and prostanazol in their A- and N-ring this method was used for the detection of prostanazol metabolites. Moreover, analysis of reference standards of prostanazol and hydroxylated (3'-/4 α -/4 β -/16 β -)17-ketoprostanazol metabolites confirmed the applicability of this precursor ion scan method (results not shown here). Hence this precursor ion scan method can be applied to distinguish 3'-hydroxy from 4-hydroxy prostanazol metabolites. Possible metabolites of prostanazol that can be detected by ion m/z 81 are prostanazol itself and metabolites of categories II, V, VI and VII. Categories I, III and IV can be detected by ions m/z 97 and 145.

Prostanazol ($[M+H]^+ = m/z 315$) could be detected at a retention time (RT) of 18.08 min with ion m/z 81 as selected ion (Figure 3.4). All the categories of prostanazol metabolites (I-VII), except for category IV, could be confirmed by LC-MS/MS. By the precursor ion scan method only one metabolite of category I could be detected, with m/z 145 as most abundant ion which is indicative for a 4-hydroxy-prostanazol metabolite. As by GC-MS analysis also just one metabolite (M8) was detected for this category (I), a 4-hydroxylated prostanazol structure is suggested for this compound.

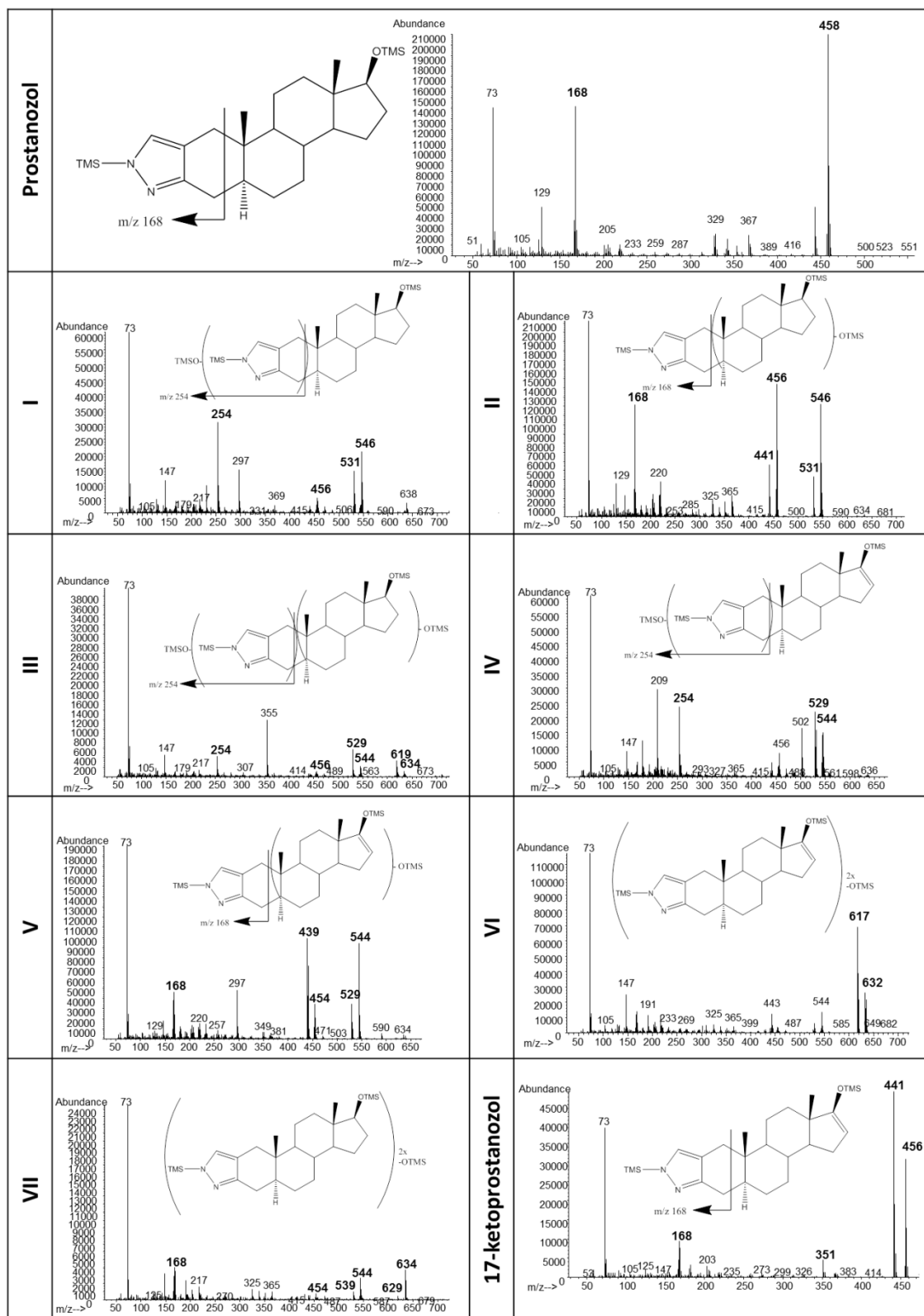


Figure 3.2. Mass spectra of prostanazol and the categories of prostanazol metabolites (I-VII; see Table 3.2 for the classification of the metabolites) detected in chimeric mice and/or HLM studies by GC-MS analysis and tentative structure presentation of the metabolites in correspondence with the molecular masses.

Table 3.1. Prostanazol metabolites detected in the *in vitro* and *in vivo* metabolism studies by full scan GC-MS analysis. The metabolites are ranked according to their RRT.

Metabolite ^a	Category ^b	Tentative structures	Characteristic ion(s) after TMS-derivatization	RRT	HLM	Chimeric mice	Phase II ^d
Prostanazol			458/443/168	1.15	√	√	
M1		17-ketoprostanazol	456/441/168	1.14	√	×	
M2	I	3'/4-hydroxy-prostanazol	546/254	1.16	×	√	free
M3	I	3'/4-hydroxy-prostanazol	546/254	1.17	×	√	free
M4	I	3'/4-hydroxy-prostanazol	546/254	1.18	×	√	free
M5	V	x-hydroxy-17-ketoprostanazol	544/529/168	1.18	√	×	
M6	II	x-hydroxy-prostanazol	546/531/168	1.18	√	×	
M7^c	IV	3'-hydroxy-17-ketoprostanazol	544/529/254	1.18	√	√	free, gluc
M8	I	4-hydroxy-prostanazol	546/531/254	1.18	√	√	free
M9^c	V	16β-hydroxy-17-ketoprostanazol	544/529/168	1.19	√	√	free
M10	II	x-hydroxy-prostanazol	546/531/168	1.20	√	√	free
M11	V	x-hydroxy-17-ketoprostanazol	544/529/168	1.20	√	×	
M12	II	x-hydroxy-prostanazol	546/531/168	1.21	√	√	free
M13	VII	x,x-dihydroxy-prostanazol	634/619/168	1.22	√	√	free, gluc, sulf
M14	II	x-hydroxy-prostanazol	546/531/168	1.22	√	×	
M15	V	x-hydroxy-17-ketoprostanazol	544/529/168	1.22	√	×	
M16	II	x-hydroxy-prostanazol	546/531/168	1.22	√	×	
M17	VII	x,x-dihydroxy-prostanazol	634/619/168	1.24	√	×	
M18	III	4,x-dihydroxy-prostanazol	634/617/254	1.25	√	×	
M19	VI	x,x-dihydroxy-17-ketoprostanazol	632/617/168	1.26	√	×	
M20	III	4,x-dihydroxy-prostanazol	634/619/254	1.26	√	×	
M21	VI	x,x-dihydroxy-17-ketoprostanazol	632/617/168	1.27	√	√	free, gluc, sulf
M22	VII	x,x-dihydroxy-prostanazol	634/619/168	1.28	√	√	free, gluc, sulf
M23	III	3'/4,x-dihydroxy-prostanazol	634/254	1.29	×	√	x
M24	III	3'/4,x-dihydroxy-prostanazol	634/254	1.29	×	√	x

RRT = Relative Retention Time, RRT IS = 1; IS = 17α-methyltestosterone (RT IS: 14.07 min);

√ = detected; × = not detected

^a For tentative structures and mass spectra of the metabolites see Figure 3.2.

^b See Table 3.2 for the classification of the metabolites (I-VII).

^c Reference standards available.

^d Phase II metabolism studied by GC-MS analysis of chimeric mouse urine samples with and without hydrolysis (β-glucuronidase and β-glucuronidase/arylsulfatase) after LLE; gluc: glucuronidated and sulf: sulfate conjugate.

For category II one more metabolite could be found by the precursor ion scan method in comparison with the GC-MS analysis (6 versus 5 metabolites respectively). However, no extra information was obtained about the position of hydroxylation for these compounds.

Only one metabolite was detected by LC-MS/MS for category III with ion m/z 145 as the most abundant ion, indicating a 4,x-dihydroxylated prostanazol structure for one of these metabolites previously detected by GC-MS (M18 and M20). For categories V (2 by LC versus 4 by GC) and VI (1 by LC versus 2 by GC) also fewer metabolites were detected by the precursor ion scan method. No additional information was gained for the possible position of the hydroxylations. However, one metabolite of category V, at a retention time of 9.37 min, could be identified as 16 β -hydroxy-17-ketoprostanazol (M9) by comparison with the corresponding reference standard.

For the first time a metabolite of category VI' could be detected with characteristic ions m/z 345 and 145, a potential 4,x-dihydroxy-17-ketoprostanazol metabolite. This category could not be detected by GC-MS as no metabolite with characteristic ions m/z 632 and 254 was found. The three metabolites of category VII detected by GC-MS in the HLM incubation samples could also be confirmed, but the structure could not be further elucidated.

3.3 In vivo metabolism studies of prostanazol with chimeric mouse model

3.3.1 Full scan GC-MS analysis of in vivo metabolism samples of prostanazol

To complement the results obtained in the HLM incubation samples, prostanazol was also administered to the chimeric mouse model. In this way the suitability of HLM incubation studies as alternative for *in vivo* metabolism studies was investigated.

Since prostanazol is not an endogenous steroid the pre-administration urine was used for comparative purposes with post-administration urines to discover possible metabolites of prostanazol.

The administration of prostanazol was performed in four chimeric mice. Only the results of the 'best' chimeric mice, i.e. with highest human albumin levels, are presented (Figure 3.3 and Table 3.1). The other mice gave similar results, however with less abundance.

Administration of prostanazol to chimeric mice resulted in the detection of thirteen metabolites, eight in common with the *in vitro* samples, by full scan GC-MS analysis (Table 3.1). These metabolites could also be divided in the seven categories (I-VII) presented in Table 3.2.

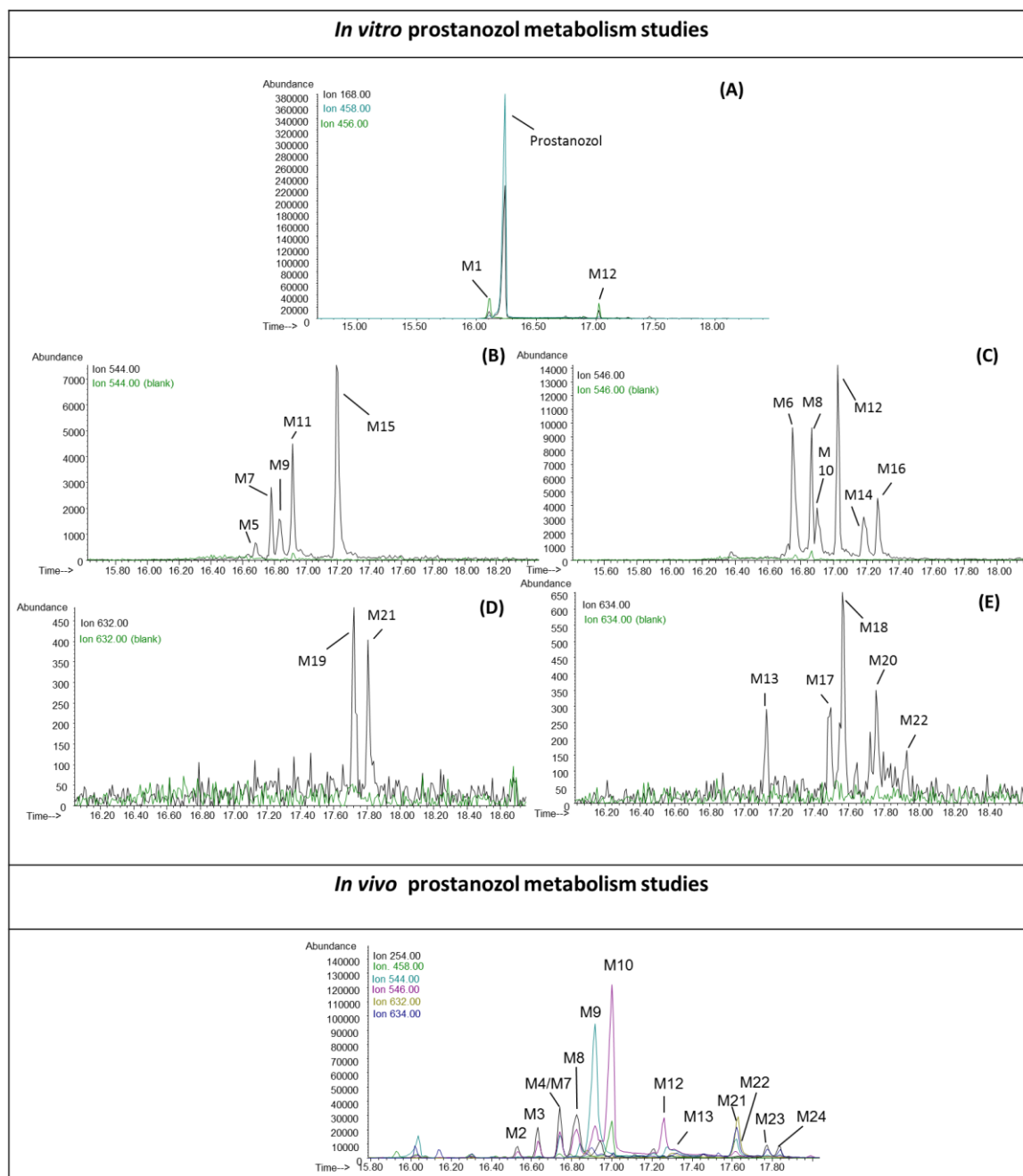


Figure 3.3. Extracted ion chromatogram (EIC) of the ions with m/z (A) 168, 456 and 458; (B) 544; (C) 546 (D) 632 and (E) 634 in a 4 h HLM sample and overlay with 4 h blank control sample (upper panel). EIC of m/z 254, 458, 544, 546, 632 and 634 in chimeric mouse urine collected after prostanazol administration (lower panel).

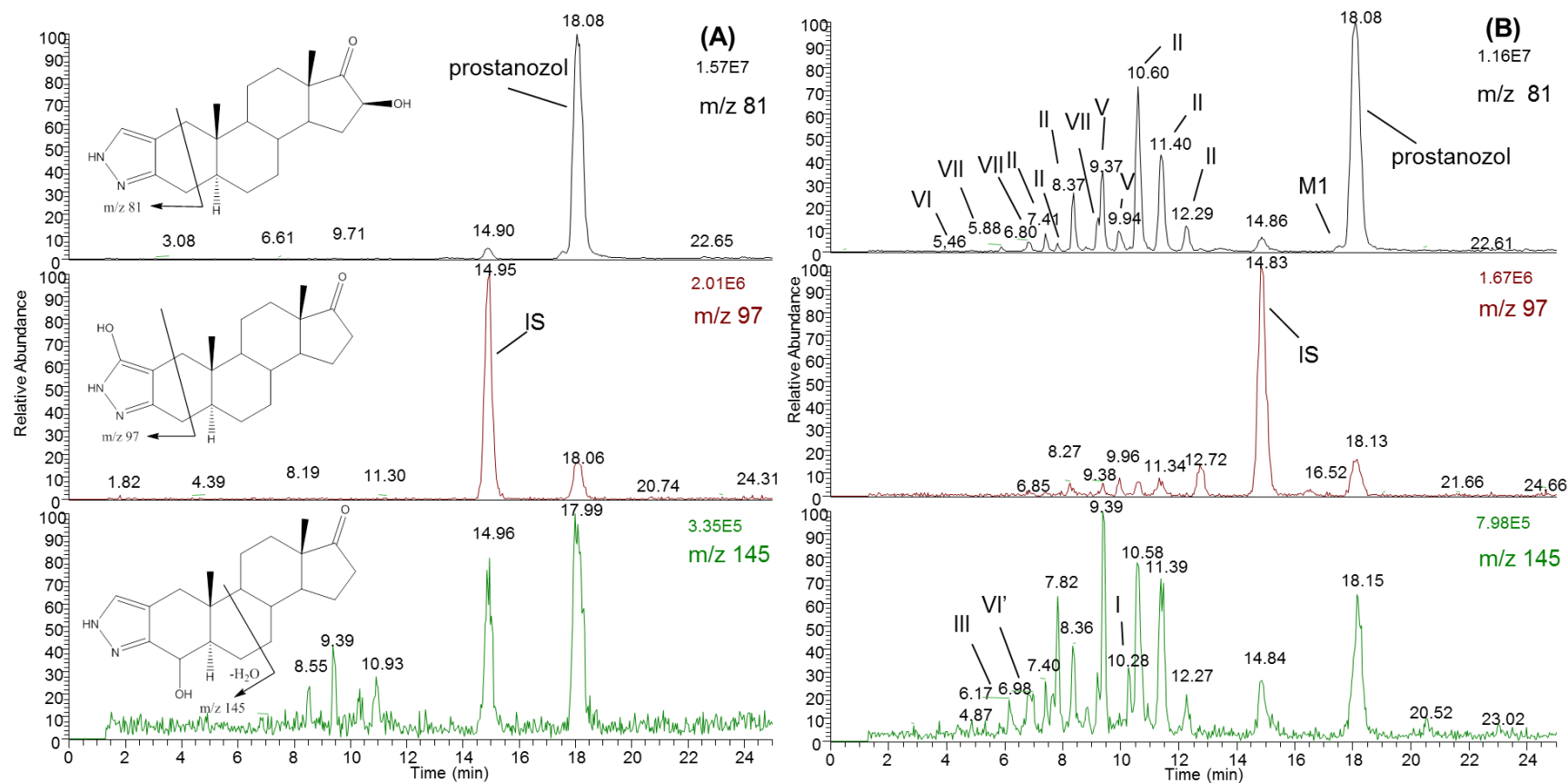


Figure 3.4. LC-MS/MS precursor ion scan chromatograms of (A) blank control sample and (B) HLM sample 4 h incubated with prostanazol. For legend of the categories I-VII see Table 3.2. In (A) the proposed fragmentation pathways for the selected product ions are also shown.

In contrast to the human excretion study of Yum *et al.* [28] and the HLM studies described above, 17-ketoprostanazol (M1) was not detectable in chimeric mouse urine. However, several (di)hydroxylated 17-ketoprostanazol derivatives (categories IV, V and VI) were found. A possible explanation is that 17-ketoprostanazol is immediately hydroxylated because of the higher metabolic rate of mice, e.g. 48 h after administration no traces of prostanazol or metabolites of the parent were detected.

For all categories, except for category III, at least one metabolite detected in the HLM incubation samples could be confirmed with the chimeric mice model. The metabolites M18 and M20 were not detected for category III, but two new metabolites M23 and M24 were found in the chimeric mouse urine samples. More metabolites were detected with the chimeric mice model only for category I, in addition to M8 also metabolites M2-M4 were found. The presence of *m/z* 254 in the mass spectra of the category I and III metabolites indicates a hydroxylation in the A- or N-rings. However, no further information about possible positions of hydroxyl groups could be obtained. In these *in vivo* samples, the presence of *m/z* 168 in the mass spectra of metabolites M13 and M22 (category VII) suggests hydroxylation(s) outside the A- and N-rings, but the exact position could not be determined.

Table 3.2. Overview of prostanazol metabolites detected in the *in vitro* and *in vivo* metabolism studies compared with reported metabolites in literature (human excretion studies).

Metabolite	Category	Characteristic ions GC ^b	Characteristic ions LC ^c	Chimeric mice	HLM	Human [6, 28, 29]
17-ketoprostanazol		456/168	313	×	√	√
3'/4-hydroxy-prostanazol	I	546/254	331/97 or 331/145	√	√	×
x-hydroxy ^a -prostanazol	II	546/168	331/81	√	√	√
3'/4,x-dihydroxy ^a -prostanazol	III	634/254	347/97 or 347/145	√	√	√
3'/4-hydroxy-17-ketoprostanazol	IV	544/254	329/97 or 329/145	√	√	√
x-hydroxy ^a -17-ketoprostanazol	V	544/168	329/81	√	√	√
x,16-dihydroxy ^a -17-ketoprostanazol	VI	632/168	345/81	√	√	√
3'/4,x-dihydroxy ^a -17-ketoprostanazol	VI'	632/254	345/97 or 345/145	×	± ^d	√
x,x-dihydroxy ^a -prostanazol	VII	634/168	347/81	√	√	×

√ = detected; × = not detected

^a x-hydroxy and x,x-dihydroxy: x = C6, C12 or C16

^b after TMS-derivatization

^c in positive ionization mode

^d ±: only one metabolite of this category was detected by LC-MS/MS analysis (precursor ion scan), which could not be confirmed by GC-MS analysis.

Some metabolites were also found 24 h after prostanazol administration in the non-chimeric mouse urine. In comparison with the results in chimeric mouse urine, the abundance of the metabolites was lower and there were also fewer metabolites found (e.g. categories III and IV were not detected). Therefore, these latter categories (III and IV) can be considered as typical human metabolites. Both categories have indeed been described in human metabolism studies [6, 28, 29].

Monohydroxylated prostanazol (II; M10 and M12) and monohydroxylated 17-ketoprostanazol (V; M9 and M15) metabolites have the highest abundance and can be considered as the most important prostanazol metabolites in both models. Both alternative models can confirm monohydroxylated and dihydroxylated prostanazol metabolites (categories II and III) which were also found by Yum *et al.* [28] in a human excretion study.

The phase II reactions of prostanazol were also studied in chimeric mouse urine (Table 3.1) by comparison of hydrolyzed and non-hydrolyzed fractions after GC-MS analysis. All metabolites were excreted at least partially in the free fraction, but category III metabolites were not detected at all. Metabolites of categories VI, VII and a small fraction of category IV were glucuronidated. Conjugated derivatives of categories I, II and V were not present after enzymatic hydrolysis. These results are in contrast with the results of the study of Yum *et al.* where all metabolites formed glucuronic conjugates and just some metabolites were excreted without conjugation [28]. These contradictory results can eventually originate from differences between mice and humans or because of differences in genetic background (Asian versus Caucasian) [33, 34]. Only categories VI and VII were detected after hydrolysis with β -glucuronidase/arylsulfatase. In a previous human excretion study [28] metabolites with molecular ion m/z 632, like category VI were also excreted as sulfate conjugates.

3.3.2 Precursor ion scan analysis of *in vivo* metabolism samples of prostanazol by LC-MS/MS

The LC-MS/MS precursor ion scan method was also applied to the *in vivo* samples incubated with prostanazol (Figure 3.5). The parent compound was detected and all categories of metabolites that were detected by GC-MS (I-VII) could also be confirmed by LC-MS/MS analysis.

Although only 4-hydroxyprostanazol metabolites were detected in the *in vitro* samples for categories I and III, both 3'- and 4-hydroxyprostanazol metabolites could be detected in the *in vivo* samples. For category IV metabolite M7 could be confirmed as 3'-hydroxy-17-ketoprostanazol with selected product ion m/z 97.

By this precursor ion scan method four metabolites of category II were detected, two more compared to GC-MS analysis, which indicates several possible positions for hydroxylation.

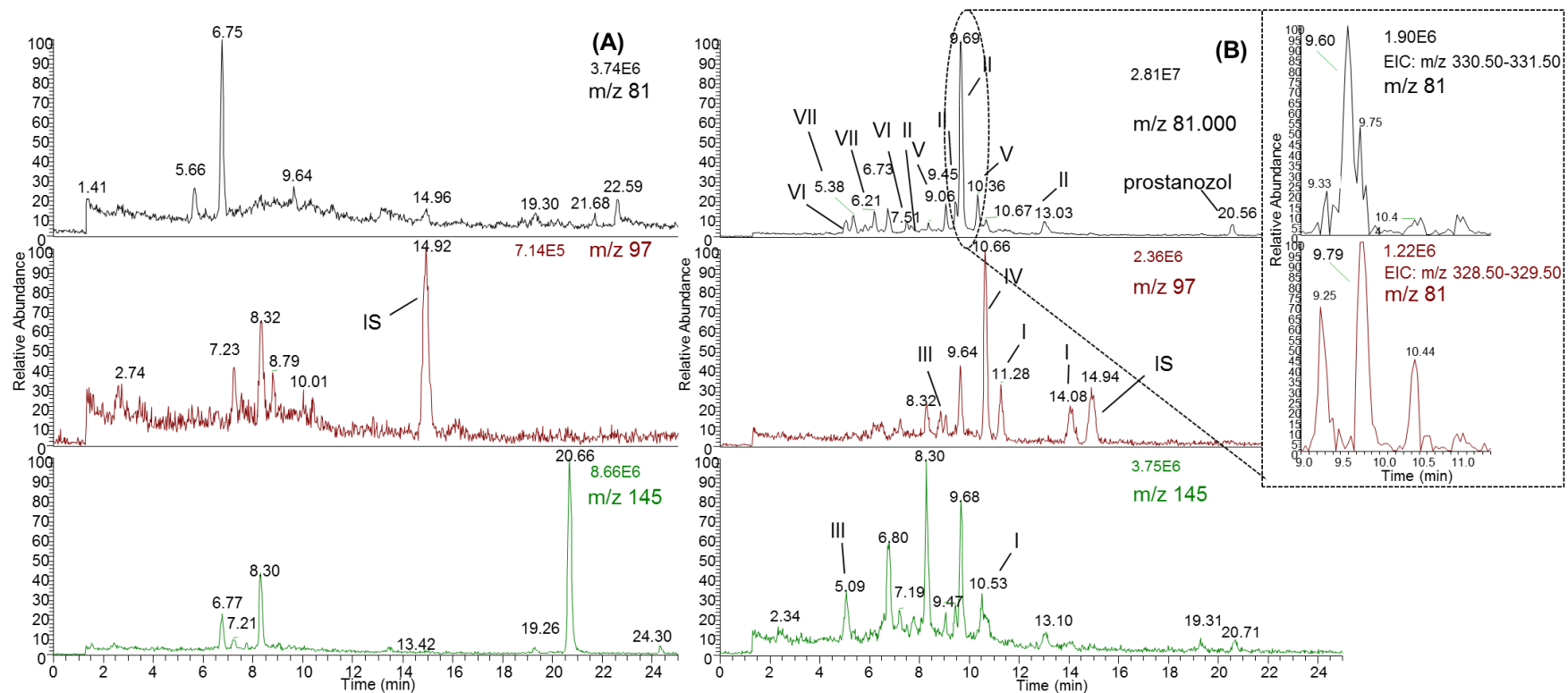


Figure 3.5. LC-MS/MS precursor ion scan chromatograms of (A) chimeric mouse urine collected before prostanazol administration and (B) chimeric mouse urine collected after prostanazol administration. For legend of the categories I-VII see Table 3.2. In (B) a detail is shown of the extra metabolite of category V (m/z 329) detected with m/z 81 as product ion next to the metabolite of category II (m/z 331), when applying a Zorbax C8 column. This latter metabolite corresponds to metabolite M9 (16 β -hydroxy-17-ketoprostanazol) detected by GC-MS.

Two metabolites were detected for category V, but when applying a Zorbax C8 column for comparison with commercial available reference standards an extra metabolite could be detected. This latter metabolite was identified as 16 β -hydroxy-17-ketoprostanazol and confirmed the presence of M9 in the chimeric mouse urine samples (Figure 3.5).

For each of the categories VI and VII two metabolites were detected, but no extra information about the hydroxylation position was obtained. In contrast to the *in vitro* results, no metabolites of category VI' (Table 3.2) were detected by this precursor ion scan method in chimeric mouse urine.

3.4 Application to a real doping control sample

To verify the relevance of the detected metabolites for doping control purposes a previous positive human urine sample for prostanazol was reanalyzed. In this human urine all categories of prostanazol metabolites, including 17-ketoprostanazol, were detected. In the urine sample monohydroxylated 17-ketoprostanazol metabolites were, similar to the studies of Rodchenkov *et al.* and Kazlauskas *et al.* [6, 29], more abundant than the monohydroxylated prostanazol metabolites. 16 β -, 3'- and 4-hydroxy-17-ketoprostanazol were identified by comparison with commercially available reference material.

Based on the *in vitro* metabolism studies two new metabolites were detected which seem, based on their relative abundances, interesting for doping control purposes. These metabolites correspond to category II (RT 8.37 min) and V (RT 9.94 min) metabolites detected in the *in vitro* samples by LC-MS/MS.

4 Conclusions

In both the HLM and the chimeric mice model seven categories (I-VII) of prostanazol metabolites were detected by GC-MS. Only traces of category VI' could be seen with the precursor ion scan by LC-MS/MS in the *in vitro* samples. Furthermore M1, with 17-ketoprostanazol as proposed structure, was also detected in HLM. Both alternative models exhibited similar results like the human excretion studies already performed [6, 28, 29]. Moreover, some previously unreported metabolites have been identified, namely metabolites of categories I and VII which were confirmed in a human urine positive for prostanazol.

Based on the relative abundances observed in these prostanazol metabolism studies it seems that metabolites of categories II and V (e.g. M9, M10 and M12) are most likely to be relevant for routine analysis. It is nevertheless not known if these metabolites may serve for long-term detection of prostanazol. It is difficult to determine the exact positions of the hydroxyl groups of the metabolites because of lack of reference standards to confirm the specific structures. However, with the available reference standards, M9 could be identified as 16 β -hydroxy-17-ketoprostanazol and M7 as 3'-hydroxy-17-ketoprostanazol in both

models (Figure 3.1). As some differences were observed for phase II metabolism (glucuronidation) performed in mouse urine with earlier reported human data [28], further research will be needed to verify these conjugation reactions.

The range of new unapproved drugs, available on the black market, is expanding rapidly. For these substances it is difficult to obtain ethical committee approval for administration to humans. Both the HLM and the chimeric mouse model offer the scientist an alternative. The advantage of the use of pooled HLM is that there are in general less ethical constraints and that both male and female HLM of different persons are combined in this pool. In this way a more complete profile of catalytic activities is represented and lot-to-lot variability is reduced. The uPA^{+/+}-SCID mice model transplanted with human hepatocytes have the merit to represent the real *in vivo* human situation including, besides metabolism, absorption, distribution and excretion processes. Moreover, unlike the HLM, the phase I and phase II pathways are not controlled by adding the appropriate cofactors. By administering the drug to both chimeric and non-chimeric mice and comparison of the results, metabolic pathways exclusive from human hepatocytes can be identified. A limitation of the chimeric mouse model and the microsomes is that the liver as major organ for drug metabolism is emphasized and that both methodologies do not take into account the contribution of extra-hepatic metabolism [24, 25]. In general this represents only a minor part of the urinary steroid metabolism. Hence, HLM and chimeric mice can be powerful tools for the study of steroid metabolism and both models can certainly be used as alternative for human excretion studies, when there are ethical restraints, e.g. for designer steroids or steroid products sold on the black market.

Although one should be careful in extrapolating the results derived from HLM incubation experiments, and even from the chimeric mouse model, following considerations can be helpful to predict *in vivo* human metabolism. (Poly)hydroxylated derivatives of the parent compounds are commonly found in HLM incubation samples, but cautious extrapolation to the human situation should be performed, especially for a higher number of hydroxylations. Combination of hydroxylation and another modification of the parent compound (e.g. hydroxylated 17-ketoprostanazol) might be more easily interpreted as typical *in vivo* human metabolite.

Acknowledgements

WADA is gratefully acknowledged for financial support. The authors thank Dr. Amy B. Cadwallader for the excellent technical support and Lieven Verhoye for the administrations to the mice.

References

1. WADA. The 2016 Prohibited List, International Standard. Montreal (2016) <https://wada-main-prod.s3.amazonaws.com/resources/files/wada-2016-prohibited-list-en.pdf> (access date 04.01.16).
2. WADA. 2013 Anti-Doping Testing Figures - Laboratory report. Montreal (2014) <https://wada-main-prod.s3.amazonaws.com/resources/files/WADA-2013-Anti-Doping-Testing-Figures-LABORATORY-REPORT.pdf> (access date 08/01/2015).
3. Kazlauskas R (2010). Designer steroids. In *Handb Exp Pharmacol* (Thieme D, and Hemmersbach P, Eds.) 195, 155-185.
4. Geyer H, Parr MK, Koehler K, Mareck U, Schänzer W, and Thevis M (2008). Nutritional supplements cross-contaminated and faked with doping substances. *J. Mass Spectrom.* 43, 892-902.
5. Van Eenoo P, and Delbeke FT (2006). Metabolism and excretion of anabolic steroids in doping control - New steroids and new insights. *J. Steroid Biochem. Mol. Biol.* 101, 161-178.
6. Kazlauskas R (2006). Miscellaneous projects in sports drug testing at the National Measurement Institute, Australia, 2005, In *Recent Advances in Doping Analysis (14)*, Proceedings of the 24th Cologne Workshop on dope analysis (Schänzer W, Geyer H, Gotzmann A, and Mareck-Engelke U, Eds.), pp 129-140, Sport & Buch Strauss, Cologne, Germany.
7. Kohler M, Thomas A, Geyer H, Petrou M, Schänzer W, and Thevis M (2010). Confiscated black market products and nutritional supplements with non-approved ingredients analyzed in the Cologne Doping Control Laboratory 2009. *Drug Test. Anal.* 2, 533-537.
8. Shimada Y, Yoritaka A, Tanaka Y, Miyamoto N, Ueno Y, Hattori N, and Takao U (2012). Cerebral infarction in a Young Man Using High-dose Anabolic Steroids. *J. Stroke Cerebrovasc. Dis.* 21.
9. Government of the United States. Designer anabolic steroid control act of 2012. (2012) <https://www.govtrack.us/congress/bills/112/s3431/text> (access date 04/04/2014).
10. Kicman AT, and Gower DB (2003). Anabolic steroids in sport: biochemical, clinical and analytical perspectives. *Ann. Clin. Biochem.* 40, 321-356.
11. Schänzer W (1996). Metabolism of anabolic androgenic steroids. *Clin. Chem.* 42, 1001-1020.
12. Kuuranne T, Aitio O, Vahermo M, Elovaara E, and Kostianen R (2002). Enzyme-assisted synthesis and structure characterization of glucuronide conjugates of methyltestosterone (17 alpha-methylandro-4-en-17 beta-ol-3-one) and nandrolone (estr-4-en-17 beta-ol-3-one) metabolites. *Bioconjug. Chem.* 13, 194-199.
13. Kuuranne T, Kurkela M, Thevis M, Schänzer W, Finel M, and Kostianen R (2003). Glucuronidation of anabolic androgenic steroids by recombinant human UDP-glucuronosyltransferases. *Drug Metab. Dispos.* 31, 1117-1124.
14. Kuuranne T, Pystynen KH, Thevis M, Leinonen A, Schänzer W, and Kostianen R (2008). Screening of in vitro synthesised metabolites of 4,9,11-trien-3-one steroids by liquid chromatography-mass spectrometry. *Eur. J. Mass Spectrom.* 14, 181-189.
15. Hintikka L, Kuuranne T, Aitio O, Thevis M, Schänzer W, and Kostianen R (2008). Enzyme-assisted synthesis and structure characterization of glucuronide conjugates of eleven anabolic steroid metabolites. *Steroids* 73, 257-265.

16. Wong JKY, Tang FPW, and Wan TSM (2011). In vitro metabolic studies using homogenized horse liver in place of horse liver microsomes. *Drug Test. Anal.* 3, 393-399.
17. Levesque JF, Gaudreault M, Houle R, and Chauret N (2002). Evaluation of human hepatocyte incubation as a new tool for metabolism study of androstenedione and norandrostenedione in a doping control perspective. *J. Chromatogr. B* 780, 145-153.
18. Levesque JF, Templeton E, Trimble L, Berthelette C, and Chauret N (2005). Discovery, biosynthesis, and structure elucidation of metabolites of a doping agent and a direct analogue, tetrahydrogestrinone and gestrinone, using human hepatocytes. *Anal. Chem.* 77, 3164-3172.
19. Lootens L, Van Eenoo P, Meuleman P, Pozo OJ, Van Renterghem P, Leroux-Roels G, and Delbeke FT (2009). Steroid metabolism in chimeric mice with humanized liver. *Drug Test. Anal.* 1, 531-537.
20. Pozo OJ, Lootens L, Van Eenoo P, Deventer K, Meuleman P, Leroux-Roels G, Parr MK, Schänzer W, and Delbeke FT (2009). Combination of liquid-chromatography tandem mass spectrometry in different scan modes with human and chimeric mouse urine for the study of steroid metabolism. *Drug Test. Anal.* 1, 554-567.
21. Lootens L, Meuleman P, Pozo OJ, Van Eenoo P, Leroux-Roels G, and Delbeke FT (2009). uPA(+/-)-SCID Mouse with Humanized Liver as a Model for In Vivo Metabolism of Exogenous Steroids: Methandienone as a Case Study. *Clin. Chem.* 55, 1783-1793.
22. Catlin DH, Sekera MH, Ahrens BD, Starcevic B, Chang YC, and Hatton CK (2004). Tetrahydrogestrinone: discovery, synthesis, and detection in urine. *Rapid Commun. Mass Spectrom.* 18, 1245-1249.
23. Sekera MH, Ahrens BD, Chang YC, Starcevic B, Georgakopoulos C, and Catlin DH (2005). Another designer steroid: discovery, synthesis, and detection of 'madol' in urine. *Rapid Commun. Mass Spectrom.* 19, 781-784.
24. Tingle MD, and Helsby NA (2006). Can in vitro drug metabolism studies with human tissue replace in vivo animal studies? *Environ. Toxicol. Pharmacol.* 21, 184-190.
25. Liu X, and Jia L (2007). The conduct of drug metabolism studies considered good practice (I): analytical systems and in vivo studies. *Curr. Drug Metab.* 8, 815-821.
26. Jia L, and Liu X (2007). The conduct of drug metabolism studies considered good practice (II): in vitro experiments. *Curr. Drug Metab.* 8, 822-829.
27. Meuleman P, Libbrecht L, De Vos R, de Hemptinne B, Gevaert K, Vandekerckhove J, Roskams T, and Leroux-Roels G (2005). Morphological and biochemical characterization of a human liver in a uPA-SCID mouse chimera. *Hepatology* 41, 847-856.
28. Yum T, Lee J, Paeng K, and Kim Y (2011). Determination of metabolites of prostanazol in human urine by LC/ESI/MS and GC/TOF-MS. *Analytical Science and Technology* 24, 173-182.
29. Rodchenkov G, Sobolevsky T, and Sizoi V (2006). New designer anabolic steroids from internet, In *Recent Advances in Doping Analysis (14)* , Proceedings of the 24th Cologne Workshop on dope analysis (Schänzer W, Geyer H, Gotzmann A, and Mareck-Engelke U, Eds.), pp 141-150, Sport & Buch Strauss, Cologne, Germany.
30. Pozo OJ, Van Eenoo P, Deventer K, Lootens L, Grimalt S, Sancho JV, Hernandez F, Meuleman P, Leroux-Roels G, and Delbeke FT (2009). Detection and structural investigation of metabolites of stanozolol in human urine by liquid chromatography tandem mass spectrometry. *Steroids* 74, 837-852.

31. Thevis M, Fussholler G, Geyer H, Rodchenkov G, Mareck U, Sigmund G, Koch A, Thomas A, and Schänzer W (2006). Detection of stanozolol and its major metabolites in human urine by liquid chromatography-tandem mass spectrometry. *Chromatographia* 64, 441-446.
32. Thevis M, Makarov AA, Horning S, and Schänzer W (2005). Mass spectrometry of stanozolol and its analogues using electrospray ionization and collision-induced dissociation with quadrupole-linear ion trap and linear ion trap-orbitrap hybrid mass analyzers. *Rapid Commun. Mass Spectrom.* 19, 3369-3378.
33. Strahm E, Sottas PE, Schweizer C, Saugy M, Dvorak J, and Saudan C (2009). Steroid profiles of professional soccer players: an international comparative study. *Br. J. Sports Med.* 43, 1126-1130.
34. Jakobsson J, Ekstrom L, Inotsume N, Garle M, Lorentzon M, Ohlsson C, Roh HK, Carlstrom K, and Rane A (2006). Large differences in testosterone excretion in Korean and Swedish men are strongly associated with a UDP-glucuronosyl transferase 2B17 polymorphism. *J. Clin. Endocrinol. Metab.* 91, 687-693.

Chapter 4

***In vitro* and *in vivo* metabolism studies of methylstenbolone**

Adapted from:

Geldof L, Lootens L, Polet M, Eichner D, Campbell T, Nair V, Botrè F, Meuleman P, Leroux-Roels G, Deventer K and Van Eenoo P (2014). Metabolism of methylstenbolone studied with human liver microsomes and the uPA^{+/+}-SCID chimeric mouse model. *Biomedical Chromatography* 28 (7), 974-985.

Abstract

Anti-doping laboratories need to be aware of evolutions on the steroid market and elucidate their metabolism to identify markers of misuse. Owing to ethical considerations, *in vivo* and *in vitro* models are preferred to human excretion for non-pharmaceutical grade substances. In this study the chimeric mouse model and human liver microsomes (HLM) were used to elucidate the phase I metabolism of a new steroid product containing, according to the label, methylstenbolone. Analysis revealed the presence of both methylstenbolone and methasterone, a structurally closely related steroid.

Via high performance liquid chromatography (HPLC) fraction collection, methylstenbolone was isolated and studied with both models. Using HLM 10 mono-hydroxylated derivatives (U1-U10) and a still unidentified derivative of methylstenbolone (U13) were detected. In chimeric mouse urine only dihydroxylated metabolites (U11-U12) were identified. Although closely related, neither methasterone nor its metabolites were detected after administration of isolated methylstenbolone.

Administration of the steroid product resulted mainly in the detection of methasterone metabolites, which were similar to those already described in the literature. Methylstenbolone metabolites previously described were not detected.

A GC-MS/MS multiple reaction monitoring method was developed to detect methylstenbolone misuse. In one out of three samples, previously tested positive for methasterone, methylstenbolone and U13 were additionally detected, indicating the applicability of the method.

1 Introduction

Over the last decade a wide range of new designer steroids were introduced to the market masquerading as supplements owing to the loose regulation of the industry. These compounds are challenging for the anti-doping laboratories to develop appropriate detection methods. The chemical structures of these designer substances are based on known compounds but with minor modifications to evade detection or to enable them to be marketed freely on the internet [1]. These designer steroids are often sold without defined toxicological profiles or when these products are still under clinical investigation. This raises ethical concerns to perform human administration studies, which are needed to identify specific metabolites for sensitive target analytical methods. To allow a fast incorporation of markers of new steroid compounds into routine screening methods, alternative *in vivo* and *in vitro* models should be used. *In vitro* techniques do not serve as a replacement for the more complex *in vivo* studies, which give a better correlation with the human metabolism [2]. However, these studies can help to identify new metabolites in a fast and efficient way. Moreover *in vitro* models produce cleaner extracts for analysis and they could also reduce and refine the number of animal experiments needed [3, 4]. Data obtained from animal models cannot always be extrapolated to humans [2]. However, the chimeric mouse model has shown to be an excellent model to study human-based like steroid metabolism *in vivo* [5-9]. In this study the chimeric mouse model will be complemented with the use of human liver microsomes (HLM). Both models focus mainly on the liver, as this organ is the major site of drug metabolism [2].

The *in vivo* mouse model involves the transplantation of primary human hepatocytes into immunodeficient (SCID) mice. The mice also suffer from a severe liver disease which is induced by liver specific over-expression of the mouse urokinase plasminogen activator (uPA) gene. The transplantation of human hepatocytes is not rejected in the transgenic uPA^{+/+}-SCID mice and so normal liver function can be restored [10]. This chimeric mouse model proved to be a good alternative for human excretion studies based on steroid research in the past [5-9]. HLM provide an enriched source of membrane bound drug metabolizing enzymes, such as the cytochrome P450 superfamily (CYP450) [11]. Application of pooled microsomes results in a representative enzyme activity and limits individual variations [12]. The major advantages with the use of HLM are the low cost, simplicity in use and less ethical objections [11, 12]. A disadvantage is however that they are unsuitable for quantitative measurements [12].

Recently, a new so-called 'nutritional supplement' was introduced on the market, named 'Ultradrol', allegedly containing methylstenbolone. This designer steroid is an oral active variant of stenbolone, since the 17 α -alkylation prevents the first-pass effect in the liver [13]. The human metabolism of stenbolone has been studied since 1991. Its typical structure with 1-ene double

bond in combination with a 2-methyl group makes this steroid stable to reductive metabolism and major metabolites retain either the 1-ene-3-keto or 1-ene group [14, 15]. Limited information is available on the metabolism of methylstenbolone. Only recently, two 16-hydroxylated metabolites were described [16]. The aim of this study was to further identify possible markers of misuse for this steroid product. For this purpose HLM (*in vitro*) as well as the *in vivo* chimeric mouse model were applied.

2 Materials and methods

2.1 Chemicals and reagents

The steroid product named 'Ultradrol' from Antaeus Labs was purchased from the internet. The reference material of methasterone (2 α ,17 α -dimethyl-17 β -hydroxy-5 α -androstane-3-one) was bought from Toronto Research Chemicals (TRC, Toronto, Canada). The internal standard (IS) 17 α -methyltestosterone was a gift from Organon (Oss, the Netherlands). Pooled HLM from 20-30 donors (HLM; 452161), the nicotinamide adenine dinucleotide phosphate (NADPH) regenerating system solutions A (451220) and B (451200) and phosphate buffer pH 7.4 (451201) were purchased from BD Gentest (Erembodegem, Belgium). Ethanol (EtOH) and ammonium acetate (NH₄OAc) were purchased from Biosolve (Valkenswaard, the Netherlands). Diethyl ether and methanol (MeOH) were obtained from Fisher Scientific (Loughborough, UK). Sodium sulfate (Na₂SO₄), sodium hydroxide (NaOH), sodium hydrogen carbonate (NaHCO₃), potassium carbonate (K₂CO₃), disodium hydrogen phosphate dihydrate (Na₂HPO₄·2H₂O), sodium dihydrogen phosphate monohydrate (NaH₂PO₄·H₂O), ammonium iodide (NH₄I), acetic acid (HOAc), LC grade water and LC grade MeOH were from Merck (Darmstadt, Germany). The β -glucuronidase preparation from Escherichia coli (E. coli) K12 was purchased from Roche Diagnostics (Mannheim, Germany). N-methyl-N-trimethylsilyltrifluoroacetamide (MSTFA) was from Karl Bucher (Waldstetten, Germany). Ethanethiol was obtained from Acros (Geel, Belgium). Phosphate Buffered Saline (PBS) was from Invitrogen (Merelbeke, Belgium). The gasses helium (He), nitrogen (N₂) and oxygen free nitrogen (OFN) were delivered by Air Liquide (Bornem, Belgium).

2.2 Instrumentation

2.2.1 HPLC

High performance liquid chromatography (HPLC) fraction collection was performed on a Thermo Scientific Surveyor (Bremen, Germany) with an injection volume of 100 μ L. Separation was achieved using a Phenomenex Gemini C18 (150 mm x 4.6 mm x 5 μ m) column (Torrance, California, USA). For the HPLC fraction collection a MeOH/water mobile phase was used (solvent

A, 10/90 MeOH/H₂O; solvent B, MeOH). The HPLC procedure started with 100% of solvent A until 1 min, then 40% of solvent A until 20 min, then 100% of solvent B till 25 min and finally 100% of solvent A from 25 min and held until 30 min. Two fractions were automatically collected with a Gilson FC 204 (Gilson, Middleton, WI, USA): F1 (11.1-12.1 min) and F2 (12.2-13 min).

2.2.2 GC-MS

An Agilent 6890 gas chromatograph was interfaced to an Agilent 5973 mass spectrometer (Agilent Technologies, Palo Alto, USA). 1 µL of sample was injected into the system using a 7683 series Autosampler with a splitless injector (Agilent Technologies, Palo Alto, USA). The GC separation was performed using a JW Ultra-1 capillary column (17 m x 200 µm i.d., 0.11 µm; Agilent Technologies) and He as mobile phase at a flow rate of 0.6 mL/min at 10.15 psi (constant flow). The temperature program and other instrumental parameters were applied as described in Chapter 3 (2.2.1 GC-MS).

2.2.3 GC-MS/MS

An Agilent 7890 gas chromatograph coupled with an Agilent 7000 B triple quadrupole mass spectrometer (Palo Alto, USA) and an MPS2 autosampler and PTV-injector from Gerstel (Mülheim an der Ruhr, Germany) were used. A retention gap column (1.25 m x 0.2 mm and no film inside) was coupled in front of an HP-1MS (15 m x 320 µm with a film thickness of 0.25 µm) both from J&W Scientific (Agilent Technologies, Palo Alto, USA). The following oven temperature program was used: the initial temperature was 120 °C, increased at 50 °C/min to 185 °C, then at 5 °C/min to 225 °C, next at 25 °C/min to 285 °C and finally increased at 75 °C/min to reach a final temperature of 320 °C (held for 1.8 min). The total run time was 13.97 min. The transfer line was set at 310 °C. He was used as a carrier gas with a pressure program to ensure a constant flow of 1.28 mL/min. In the QqQ collision cell He was used as quench gas at 2.25 mL/min and N₂ as a collision gas at 1.5 mL/min. 6 µL of sample was injected using the solvent vent mode of the PTV-injector. The vent flow was 15 mL/min at 5 psi until 0.01 min with an initial temperature of 80 °C and increased at 12 °C/s to 310 °C. A MRM method was developed for the detection of methylstenbolone misuse, see Table 4.1 for the ion transitions.

2.2.4 LC-MS/MS

All experiments were performed under the same LC conditions using a Thermo Finnigan Surveyor Autosampler Plus and a MS Pump Plus (Thermo Scientific, Bremen, Germany). Electrospray ionization (ESI) was used for the ionization of the steroids. The mobile phase consisted of LC grade water (solvent A) and LC grade MeOH (solvent B) both with 1 mM NH₄OAc and 0.1% HOAc.

The LC separation was performed using a SunFire™ C18 column (50 mm × 2.1 mm i.d., 3.5 μm) from Waters (AH Etten-Leur, the Netherlands), at a flow rate of 250 μL/min. 20 μL of sample was injected into the instrument. The gradient program was adopted from Pozo *et al.* [17], the percentage of solvent B was changed as follows: 0 min, 30%; 1.5 min, 30%; 8 min, 55%; 15 min, 55%; 29.5 min, 95%; 30.5 min, 95%; 31 min, 30%; 34 min, 30%. The methods have a total run time of 34 min.

For the low resolution methods a TSQ Quantum Discovery MAX triple quadrupole mass spectrometer (Thermo Scientific) was used. The other instrumental parameters were adopted from Pozo *et al.* [17]. A precursor ion scan method was used to search for (unknown) metabolites. For the precursor ions scan method the ions with m/z 77, 91 and 105 were selected as product ions. The collision energy (CE) was 45 eV for m/z 105 and 91 and 50 eV for m/z 77. For the structural investigation of metabolites product ion scans were performed for some selected ions and CE of 10, 20, 30 and 50 eV were applied.

The HR-MS(/MS) were performed on an Exactive benchtop Orbitrap-based mass spectrometer (Thermo Scientific). The instrument operated in positive, full scan mode from m/z 100 to 2000 at a resolving power of 50,000 with a data acquisition rate of 2 Hz. All ion fragmentation was performed by higher-collision dissociation (HCD), at a CE of 30 eV.

2.2.5 Analysis and clean-up of the steroid product

The methylstenbolone product was analyzed by GC-MS and LC-MS. Individual steroids, present in this steroid formulation were isolated by the following procedure: extraction of the steroids was performed by adding 12 mL of ethanol to 1200 mg of the product and rolling for 2 h. Subsequently centrifugation was performed (1500 g, 5 min) and 9.5 ml was transferred and evaporated under OFN and redissolved in 1.3 mL MeOH. This solution containing the extracted steroid product was distributed in vials (50 μL in each vial and addition of 50 μL 50/50 MeOH/water) and used for the HPLC fraction collection. The two collected fractions (F1 and F2) were then dried under OFN and quantitatively transferred (3 x 1 mL ethanol) into separate vials and redissolved in 750 μL ethanol.

2.2.6 HLM incubations

Both the steroid product as well as the individual cleaned-up steroids were administered to HLM (final concentration of 40 μg/mL). Before administration, all solutions (reference standard, steroid product and cleaned-up product (F1 and F2)) were analyzed by GC-MS and LC-MS for purity verification.

The *in vitro* HLM incubation studies were performed as described in Chapter 1 (7.2.2.2 *Protocol in vitro metabolism studies*; Table 1.6). Substrate stability samples (blank; without HLM) and

system blank samples (without test compound) control samples were also incubated to verify the enzymatic reactions. Methandienone was incubated as test compound in the positive control samples. At the appropriate time (after 2, 4, and 18 h) the enzymatic reactions were stopped by adding 250 μ L ice-cold MeOH.

In a second experiment with methylstenbolone, higher initial concentrations (2, 5 and 10 x higher) of the test compound were used to see the influence on the detected metabolites. With these experiments the final concentration of the solvent (EtOH) was also kept at 1%, to prevent inhibition of the microsomal enzymes.

2.2.7 Excretion studies with the chimeric mouse model

The protocol of the *in vivo* administration studies was applied as described in Chapter 1 (7.2.3 *In vivo metabolism studies*).

The chimeric mouse model was developed in cooperation with CEVAC of Ghent University Hospital [10]. The *in vivo* metabolism studies were approved by the Animal Ethical Committee of the Faculty of Medicine of Ghent University (ECD 06/09). The dose and route of administration (oral gavage) were similar to previous metabolism studies with the same model [6, 7, 9]. The metabolism studies were performed by administration of 1 mg of the test compound (as supplement or as purified steroid, as indicated in the text) dissolved in ethanol/PBS (20/80) in a single dose to one chimeric and one non-chimeric mouse.

2.3 Sample preparation for HLM and mouse urine

2.3.1 Liquid-liquid extraction (LLE)

For the *in vitro* metabolic assays the samples were first centrifuged at 4 °C (12,000 *g*, 5 min) followed by transfer of 400 μ L into new tubes. All tubes were eventually stored in the refrigerator until all samples were collected. Transferred incubation samples were then evaporated, after which LLE was performed as described below. From the mouse urine 500 μ L was used.

A 50 μ L aliquot of the IS 17 α -methyltestosterone (2 μ g/mL) was added to all samples. For the microsomal incubation samples (unconjugated fraction) LLE was performed as described in Chapter 3 (2.5.1 *Liquid-liquid extraction (LLE)*). To study the total fraction (conjugated and unconjugated steroids) in the chimeric mouse urine samples an enzymatic hydrolysis (β -glucuronidase) was performed prior to the LLE as described in Chapter 3 (2.5.1 *Liquid-liquid extraction (LLE)*).

After evaporation the residues were redissolved in 100 μ L mobile phase (95/5 solvent A and B see 2.2.4 *LC-MS/MS*) for LC-MS analysis. For GC-MS analysis the evaporated samples were

derivatized by adding 100 μL derivatization solution containing MSTFA, NH_4I and ethanethiol (500/4/2) and incubation during 1 h at 80 ± 5 $^\circ\text{C}$.

3 Results and discussion

3.1 Analysis of the steroid product

Analysis of the so-called ‘nutritional supplement’ ‘Ultradrol’ showed the presence of not only methylstenbolone, the steroid claimed on the label, but also methasterone (Figure 4.1). Such contamination is not unique [18, 19] and indicates lack of quality in production or manufacturing which can lead to additional health risks [20]. In 2006 the US Food and Drug Administration warned against the manufacture of unapproved steroids in dietary supplements, such as methasterone. In this way the general public was also made aware of the possible dangerous effects associated with these so-called dietary supplements. Indeed, toxic effects on liver and kidney were already demonstrated after use of ‘Superdrol’, which contains the steroid methasterone [21-23]. Methasterone is also explicitly mentioned on World Anti-Doping Agency’s prohibited list, while methylstenbolone will be prohibited since it has similar biological effects and a similar chemical structure [24]. Methasterone is the 17α -methylated derivative of drostanolone. The metabolism of methasterone has already been extensively investigated with both *in vitro* [25] and *in vivo* human [26-28] and chimeric mouse [8] studies.

To further investigate the metabolism of methylstenbolone, the steroid product was fractionated by HPLC. Analysis of the fraction containing methylstenbolone (F1) by GC-MS after TMS-derivatization, showed a molecular ion with m/z 460 corresponding to double silylation.

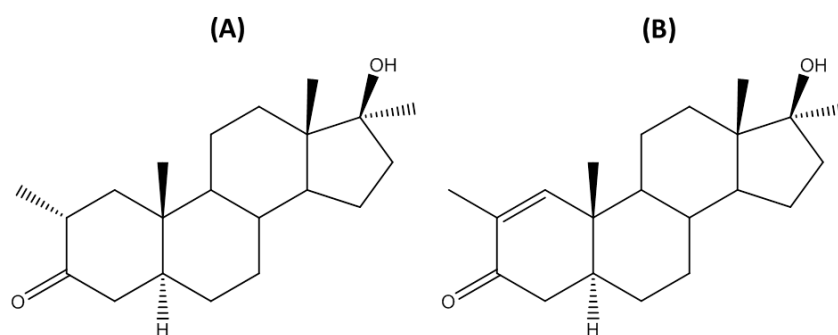


Figure 4.1. Chemical structures of (A) methasterone (marketed as ‘Superdrol’) and (B) methylstenbolone (marketed as ‘Ultradrol’).

Additionally, three characteristic ions: m/z 193, 208 and 221 (Figure 4.2) were present in the structure. These ions were already described for stenbolone [15] and are characteristic for substances with a (2-methyl-1-en-3-one)-A-ring structure. Additional analysis of the fraction by LC-HRMS showed a characteristic $[\text{M}+\text{H}]^+$ with a m/z of 317.2473. This represents a mass

deviation of 0.63 ppm from the theoretical mass of the protonated molecule. Higher energy collision dissociation (HCD) fragmentation of the steroid yielded product ions at m/z 145.1013 and 201.1640. A product ion of m/z 145 (theoretical accurate mass of 145.1017) has also been described by Pozo *et al.* [29] as a typical ion for 1-ene-3-keto anabolic steroids and would originate from the B and C rings. In this study one abundant ion was also observed for the 1-ene-3-keto steroids, which was related to a three ring structure including the B, C and D rings. For methylstenbolone 201.1640 was present as abundant ion, this ion is originating from the B, C and D rings as this ion was also observed for 17-methyl-1-testosterone, 201.1647 [29] and, both steroids have an identical structure at the B, C and D ring. As observed for other 1-ene-3-keto steroids, methylstenbolone also showed consecutive losses of water related to the numbers of oxygen atoms in the molecule. Additionally, a loss of acetone (-58 Da) was observed, as was described by Pozo *et al.* [29] for the steroid 17-methyl-1-testosterone.

To investigate the metabolism of methylstenbolone, this steroid was administered to both the HLM and chimeric mouse model.

3.2 Metabolism of methylstenbolone

3.2.1 HLM experiments

For the isolated and purified methylstenbolone (fraction F1), eleven possible metabolites (U1-U10 and U13) were detected by GC-MS after microsomal incubation (Table 4.1). These metabolites were identified by comparing chromatograms of pre- and post-incubation samples. Mass spectra of the metabolites are presented in Figure 4.2. As the metabolites detected in all microsomal incubation samples were very similar, only the results of the 4 h incubation sample are shown in the figures.

The main detected metabolites are hydroxylated analogues of the parent compound, with an m/z 548 (U1-U4, U6-U8, and U10). The mass spectra show a typical, but non-informative, loss of a methylgroup by presence of m/z 533 after TMS-derivatization.

To further elucidate and confirm the structures of metabolites U1-U10, detected by GC-MS, precursor ion scanning was performed on LC-MS/MS. The selected fragment ions were m/z 105, 91 and 77 (Figure 4.3). These ions can be explained by the complete fragmentation of either the B or the C ring at high CE as described by Pozo *et al.* [17].

Table 4.1. Overview of metabolites detected after incubation of isolated methylstenbolone and reference standard of methasterone to HLM and the chimeric mouse model by GC-MS. Ion transitions of selected compounds in the developed multiple reaction monitoring (MRM) method (GC-MS/MS) for the detection of methylstenbolone and methasterone misuse are listed.

Steroid ^a	RT ^b	Characteristic TMS-ions	MRM transitions	CE ^c (V)	HLM	Chimeric mouse
Methylstenbolone	14.67	460	460->208	5	✓	/
		445/370/355/	460->220	5		
		221/208/193/	460->193	30		
		143	460->143	30		
IS^d	14.82	446	446->301	15	✓	✓
		431/301/143	446->198	20		
U1	15.48	548	445->193	5	✓	/
		533/458/445/	445->149	5		
		353/221/208/	445->219	10		
		193/143	445->245	10		
U2	15.61	548			✓	/
		533/458/445/				
U3	15.66	548			✓	/
		533				
U4	15.75	548	533->281	5	✓	/
		533/458/443	533->149	5		
		/309/295/281/	533->193	30		
		143	533->109	5		
U5	15.81	546			✓	/
		531				
U6	16.10	548	548->195	20	✓	/
		533/458/443/	548->353	20		
		256	548->281	20		
U7	16.25	548	533->281	10	✓	/
		533/309/295/	533->109	20		
		281/143	533->149	20		
U8	16.33	548			✓	/
		533				
U9	16.46	546			✓	/
		531				
U10	16.56	548			✓	/
		533/256				
U11	16.72	634	634->454	10	/	✓
		544/529/454	634->529	10		
			634->323	10		
U12	16.81	636	636->546	10	/	✓
		621/533	636->351	10		
			636->441	10		
U13	16.23	502	502->208	10	✓	/
			502->193	20		

Table 4.1. Continued.

Steroid ^a	RT ^b	Characteristic TMS-ions	MRM transitions	CE ^c (V)	HLM	Chimeric mouse
U-External^e	n.d.	550 218/231	550->143	5	/	/
			550->117	15		
			550->141	15		
Methasterone	15.06	462 447/419/157/ 143	462->143	15	√	√
			462->141	15		
			462->419	15		
			462->216	15		
S1	13.15	464 449/374/359/ 284/269/143	449->269	10	√	/
			449->213	20		
S2	15.67	552 537/462/447/ 420/332/157/ 143	537->283	10	√	/
			537->267	10		
			537->357	10		
			537->227	10		
S3	16.22	550 535/460/445/ 433/420/143	535->405	10	√	± ^f
			535->203	20		
			535->215	20		

^a U = metabolites of methylstenbolone; S = metabolites of methasterone

^b RT = Retention Time (when analyzing with the full scan GC-MS method)

^c CE = Collision Energy

^d IS = 17 α -methyltestosterone

^e U-External = metabolite 'S2' detected in the study of Cavalcanti *et al.*, with as proposed structure 2 α ,17 α -dimethyl-3 α ,16 ξ ,17 β -trihydroxy-5 α -androst-1-ene [16]

^f detection of an isomer of S3 in chimeric mouse urine [8]

By LC-MS/MS analysis in total seven metabolites were detected. These metabolites could be divided into three classes of derivatives (I-III) as can be seen in Figure 4.3.

Categories I and II correspond to metabolites with mass m/z 548 (U1-U4, U6-U8, and U10) and 546 (U5 and U9) by GC-MS after TMS-derivatization, respectively. By GC-MS, three additional metabolites were detected for category I (8 versus 5) and one metabolite more for class II (2 versus 1). The metabolite belonging to class III was not detected by GC-MS.

The GC-MS mass spectra of U1 and U2 exhibit the characteristic ions m/z 193, 208 and 221 (Figure 4.2). These three ions are formed by fragmentation of the intact A and B rings [15], similar to the parent compound. The ion at m/z 445 (loss of m/z 103) is characteristic for steroids bearing a hydroxymethyl group either at C18 or C19 positions and results from the loss of a CH₂-OTMS ion from the molecular ion [14]. Hence, GC-MS indicated that these metabolites are 18-hydroxylated analogs (epimers) of methylstenbolone. Analysis of the microsomal incubation sample (4 h) with the product ion method in LC-MS, resulted in the detection of a metabolite, characterized by a loss of formaldehyde (M+H-H₂O-H₂CO), besides three losses of

water. As described previously, such a loss of formaldehyde is observed for steroids with a hydroxymethyl group [29]. Hence, this finding confirmed the presence of C18 hydroxymethylated analogs of methylstenbolone.

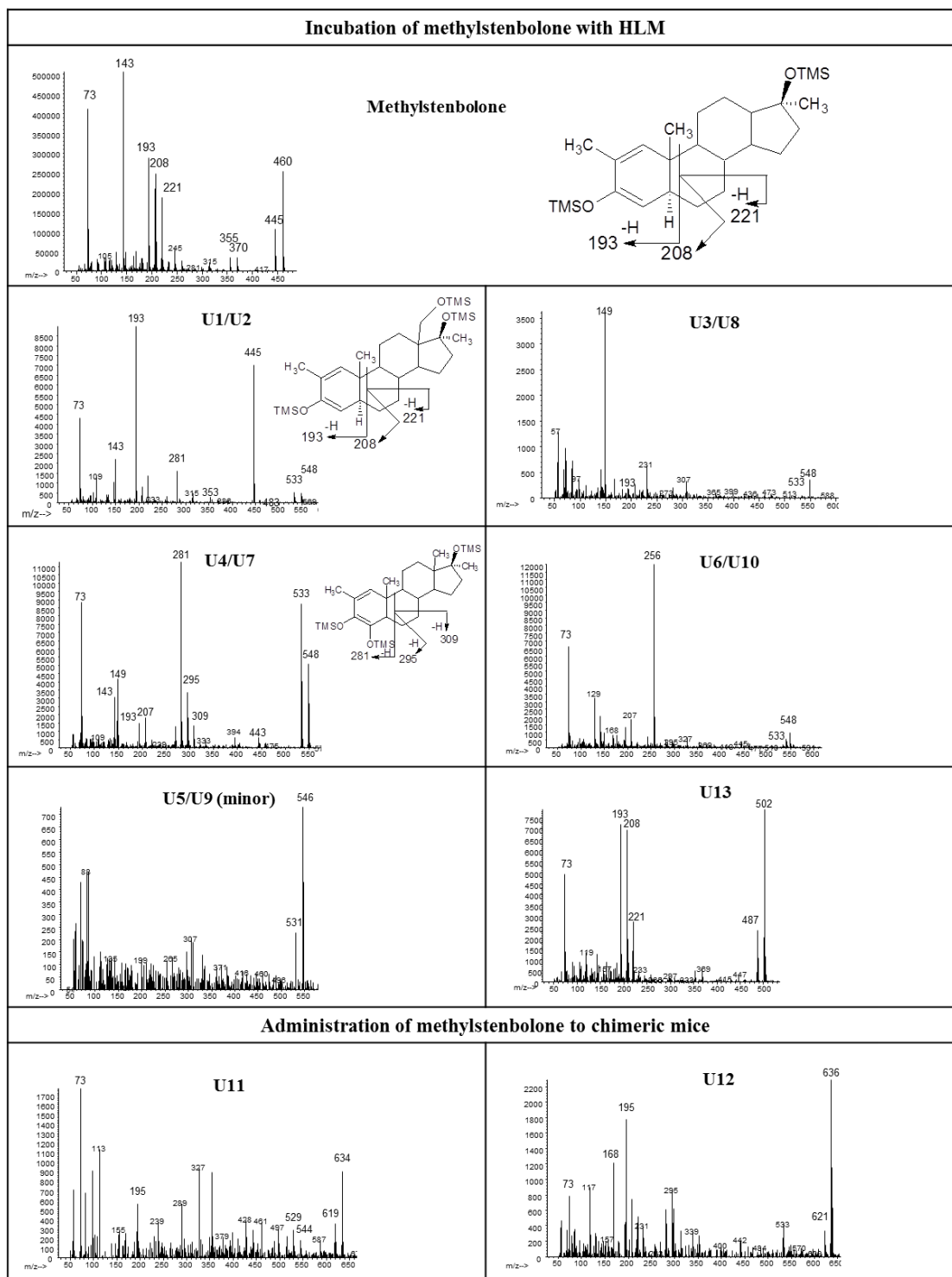


Figure 4.2. GC-MS mass spectra of the detected metabolites of methylstenbolone after HLM incubation or administration to the chimeric mouse model of the purified steroid product.

For metabolites U4 and U7 the ion at m/z 281 is abundantly present in the GC-MS mass spectrum, as well as ions at m/z 295 and 309. The simultaneous occurrence of these three ions is indicative for a hydroxylation of the A ring (C1 or C4) (Figure 4.2). Indeed, these three ions are formed via similar fragmentation patterns to m/z 193, 208 and 221 in the parent compound, but indicate that there is an additional hydroxylfunction in the A ring.

For U3/U8 and U6/U10 similar GC-MS mass spectra were obtained with an apparent molecular weight (MW) of 548. For these monohydroxylated metabolites none of the characteristic ions of the parent compound were present, indicating alterations to the A ring. However, lack of characteristic fragmentation (Figure 4.2) prevented proper elucidation of the structure. Compatible metabolites were detected in class I by LC-MS.

Additionally, minor metabolites formed by a combination of oxidation (dehydrogenation) and hydroxylation of the parent compound were observed (U5 and U9). These substances gave an apparent molecular ion at m/z 546. In LC-MS, this could be compatible with the metabolites belonging to class II.

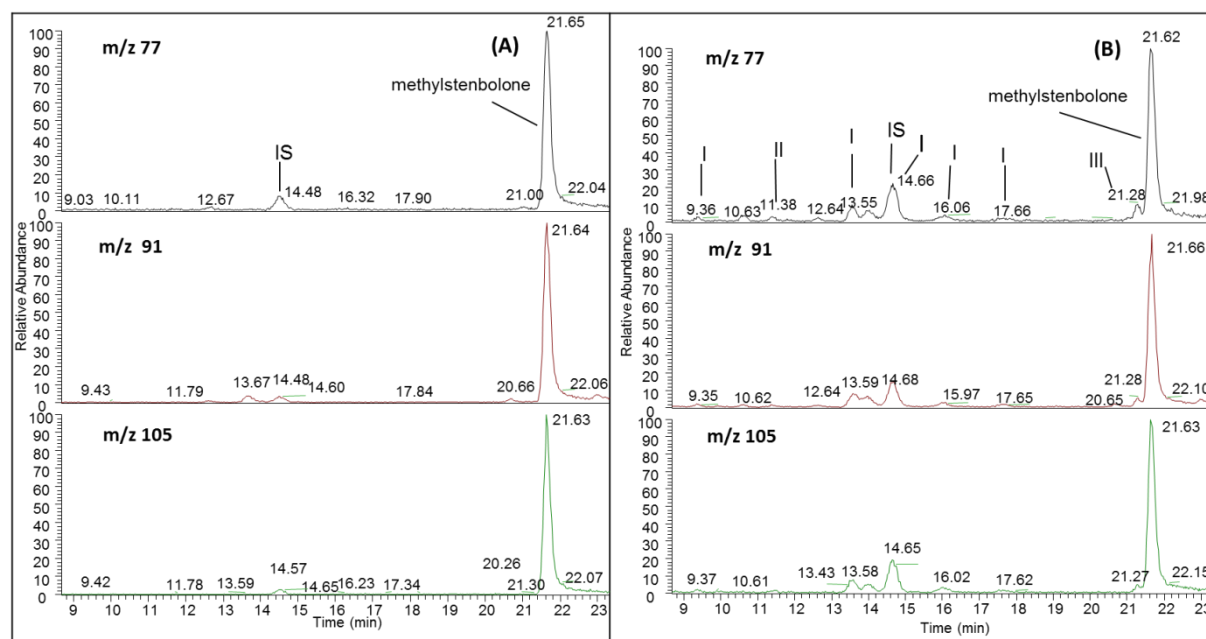


Figure 4.3. LC-MS/MS precursor ion scan chromatograms of (A) blank (substrate stability) sample and (B) 4 h microsomal incubation sample of isolated methylstenbolone (m/z 317). IS = 17α -methyltestosterone (m/z 303).

Based upon the LC-MS/MS data, the metabolite belonging to class III could be a dehydrogenated metabolite of methylstenbolone.

One additional and interesting marker, metabolite U13, was detected by GC-MS and not by LC-MS. U13 has an apparent molecular ion of m/z 502 after TMS derivatization (Table 4.1). The characteristic ions at m/z 193, 208 and 221 are present in its mass spectrum (Figure 4.2). The

presence of these three ions indicates that no modifications occurred at the A or B ring of the parent compound. The detected mass (m/z 502) cannot be explained based on common modifications observed in phase I metabolic reactions (reduction, oxidation, hydroxylation, etc.). Indeed, the difference in mass of metabolite U13 and the parent compound is only m/z 42. Loss of an OTMS-group (m/z 90) could not be detected in the mass spectrum. Therefore, the nature of the modification of this metabolite in the C/D ring is unclear. Moreover, this metabolite was not detected in the LC-MS method. Hence, it cannot be excluded that U13 is an artefact, formed through rearrangement of the C/D ring after derivatization, rather than a metabolite.

3.2.2 Excretion studies with the chimeric mouse model

In vivo studies with the chimeric mouse model were also performed to study the metabolism of methylstenbolone. Methylstenbolone, purified product (F1), was administered to both chimeric as non-chimeric mice to be able to control for interspecies differences.

In the chimeric mouse urine metabolites U1-U10 and U13 could not be confirmed. Also the parent compound could not be detected. However, two other, additional, dihydroxylated metabolites (U11 and U12) were detected (Figure 4.2). These two compounds were also detected in the non-chimeric mouse. Because hydroxylation has been reported as a major metabolic pathway in mice [5-9], it cannot be excluded that these metabolites are murine rather than human.

U11 is formed by a combination of a dehydrogenation and dihydroxylation of the parent compound. The positions of hydroxylations could not be identified for U11, as no informative ions are present in the mass spectrum of this metabolite. The presence of the ion with m/z 533 (M-103) in the mass spectrum of U12 indicates a hydroxylation at the C18 or C19 position [14], as could also be seen in U1 and U2. At the same time m/z 295 is observed, which can indicate 6-hydroxylation [30].

3.3 Comparison of methylstenbolone and methasterone metabolism

In contrast to our findings for methylstenbolone, the article of Cavalcanti *et al.* [16] does not mention the presence of methasterone in 'Ultradol'. Two metabolites were detected in their studies, and the diagnostic ions m/z 218 and 231 in their mass spectra indicate 16-hydroxylated derivatives of methylstenbolone. The proposed structures for their metabolites are 2,17 α -dimethyl-16 ξ ,17 β -dihydroxy-5 α -androst-1-en-3-one and 2,17 α -dimethyl-3 α ,16 ξ ,17 β -trihydroxy-5 α -androst-1-ene [16]. These metabolites were not detected in our metabolism studies of methylstenbolone. Interestingly, however, the mass spectrum of the 3-keto reduced metabolite described by Cavalcanti *et al.* shows strong resemblance with the 16-hydroxylated metabolite of

methasterone, previously described by Gauthier *et al.* [25]. Taking into account the simultaneous presence of methasterone and methylstenbolone in the ‘Ultradrol’ in our study, it cannot be excluded that this metabolite originates from a contamination in the product.

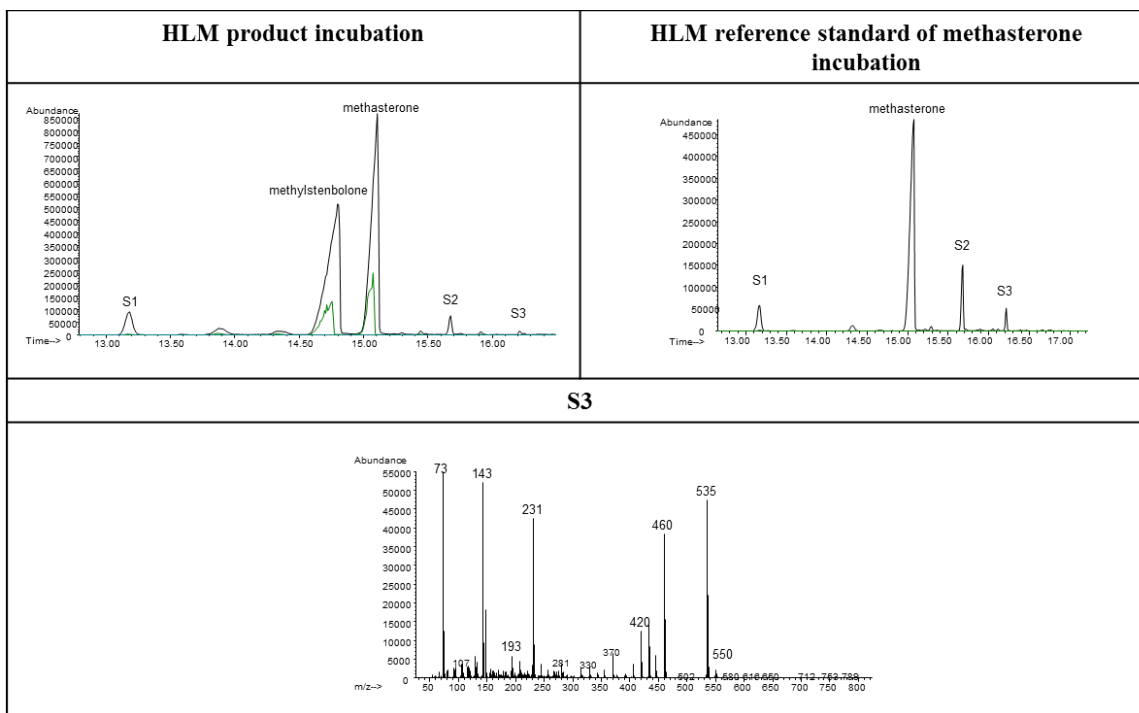


Figure 4.4. EIC (m/z 143) after 4 h incubation of steroid product containing methasterone and methylstenbolone and incubation of the reference standard of methasterone with HLM. Metabolites S1, S2 and S3 of methasterone are indicated. The mass spectrum of S3 is shown.

However, based upon the similar structures of methasterone and methylstenbolone (Figure 4.1), it cannot be excluded that both steroids share - to some extent - the same metabolites. Therefore the methasterone standard was incubated with HLM. Three abundant metabolites (S1-S3) were detected in the microsomal incubation sample. Further identification of these metabolites was based on the correlation of the mass spectra detected in the HLM studies with the metabolites already described in literature. Metabolites S1 and S2 are already described [25-28] as metabolites of methasterone (Figure 4.4). Metabolite S1 was identified in literature as $2\alpha,17\alpha$ -dimethyl- 5α -androstane- $3\alpha,17\beta$ -diol and is the most important metabolite of methasterone in human excretion studies [26-28]. In the studies of Bylina *et al.* [28] and Gauthier *et al.* [25] metabolite S2 was also detected, with as proposed structure $2\alpha,17\alpha$ -dimethyl- 5α -androstane- $2\beta,3\alpha,17\beta$ -triol [25]. S3, a hydroxylated metabolite of methasterone, has not yet been described. The presence of m/z 143 in the mass spectrum of S3 excludes hydroxylation in the D ring. Informative ions for an extra hydroxylation in the A ring like m/z 420 and 421 are present, however the ion m/z 332 was not present [25].

The methasterone metabolism after administration to the chimeric mouse model has already been studied by our laboratory [8]. Unlike with the microsomal incubation samples, metabolites S1 and S2 were not found in the chimeric mouse urine. Dihydroxylated derivatives of methasterone previously reported in the chimeric mouse model could be confirmed with the microsomes (results not shown here).

The results in both models indicate that methasterone does not yield detectable metabolites of methylstenbolone.

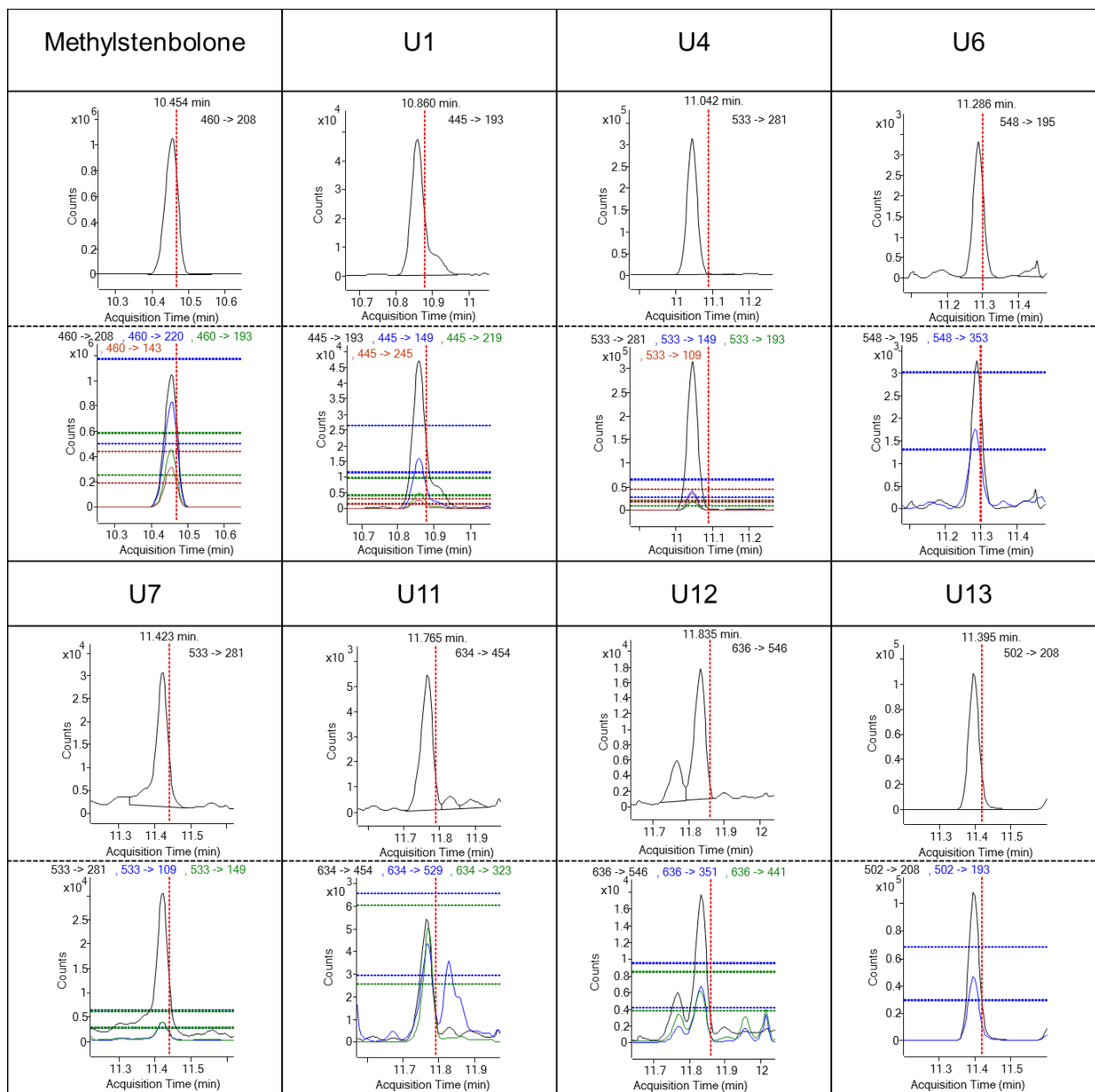


Figure 4.5. Developed MRM method to detect misuse of methylstenbolone via parent compound, U1, U4, U6, U7, U11, U12 and U13. This method was applied to a mix of microsomal incubation samples and chimeric mouse urine after administration of isolated methylstenbolone.

Administration of the raw steroid product, containing both steroids methylstenbolone and methasterone, to HLM (Figure 4.1) and the chimeric mouse model resulted mainly in the detection of methasterone metabolites. The same metabolites were detected as those described above after administration of methasterone standard to both models.

Goudreault *et al.* [15] indicated that stenbolone is relatively stable to reductive metabolism because of the methyl group at C2 and the double bond in C1. Similarly, this could also explain why methylstenbolone compound is not converted to methasterone. In case of stenbolone the major metabolites retained the 1-ene-3-keto or the 1-ene group and hydroxylation of C16 was promoted [15]. This type of metabolites was not confirmed in our study but could be detected in a human excretion study of Cavalcanti *et al.* [16]. In our study 18-hydroxyderivatives of methylstenbolone were detected, which was found to be typical for steroids with C1 or C2 methylgroups [14, 31]. Such metabolites have also been described as metabolites for stenbolone in human urine samples [14].

3.4 Application to real samples

Based upon the results, a multiple reaction monitoring (MRM) detection method on GC-triple quadrupole MS for the misuse of methylstenbolone was developed. This method screens for the parent compound of methylstenbolone and metabolites U1, U4, U6, U7, U11, U12 and U13; since these were selected as most specific markers (Table 4.1).

The method was also applied to a mix of HLM incubation samples and chimeric mouse urine after administration of methylstenbolone. All eight compounds could be detected with this highly specific and sensitive method (Figure 4.5). One of the metabolites found in the study of Cavalcanti *et al.* [16], 2,17 α -dimethyl-3 α ,16 ξ ,17 β -trihydroxy-5 α -androst-1-ene (proposed structure) here named as U-External, was added to the MRM method (Table 4.1). As the product contains both methylstenbolone and methasterone, the parent compound of methasterone and its metabolites (S1-S3) were also included into the developed method (Table 4.1).

Three doping control samples that had previously shown the presence of methasterone were reanalyzed using this method. In all these samples the parent compound of methasterone and its metabolite S1 could be detected (results not shown here). One sample showed the presence of methylstenbolone (parent) and metabolite U13 and was therefore considered as a sample that did not exclusively contain methasterone and its metabolites (Figure 4.6). The significance of the other discovered methylstenbolone metabolites U1-U12 is unclear, as at first sight they were not detected in the studied human urine sample. The metabolite U-External was also not detected in this human urine sample.

These results however do illustrate the applicability of the developed method in this study to adequately detect misuse of methylstenbolone as well as the necessity to screen for the parent drug and not only for the previously identified metabolites [16]. Moreover, metabolite U13 seems to be a useful marker for methylstenbolone misuse in human urine. Unfortunately, the structure of this compound could not be unequivocally determined.

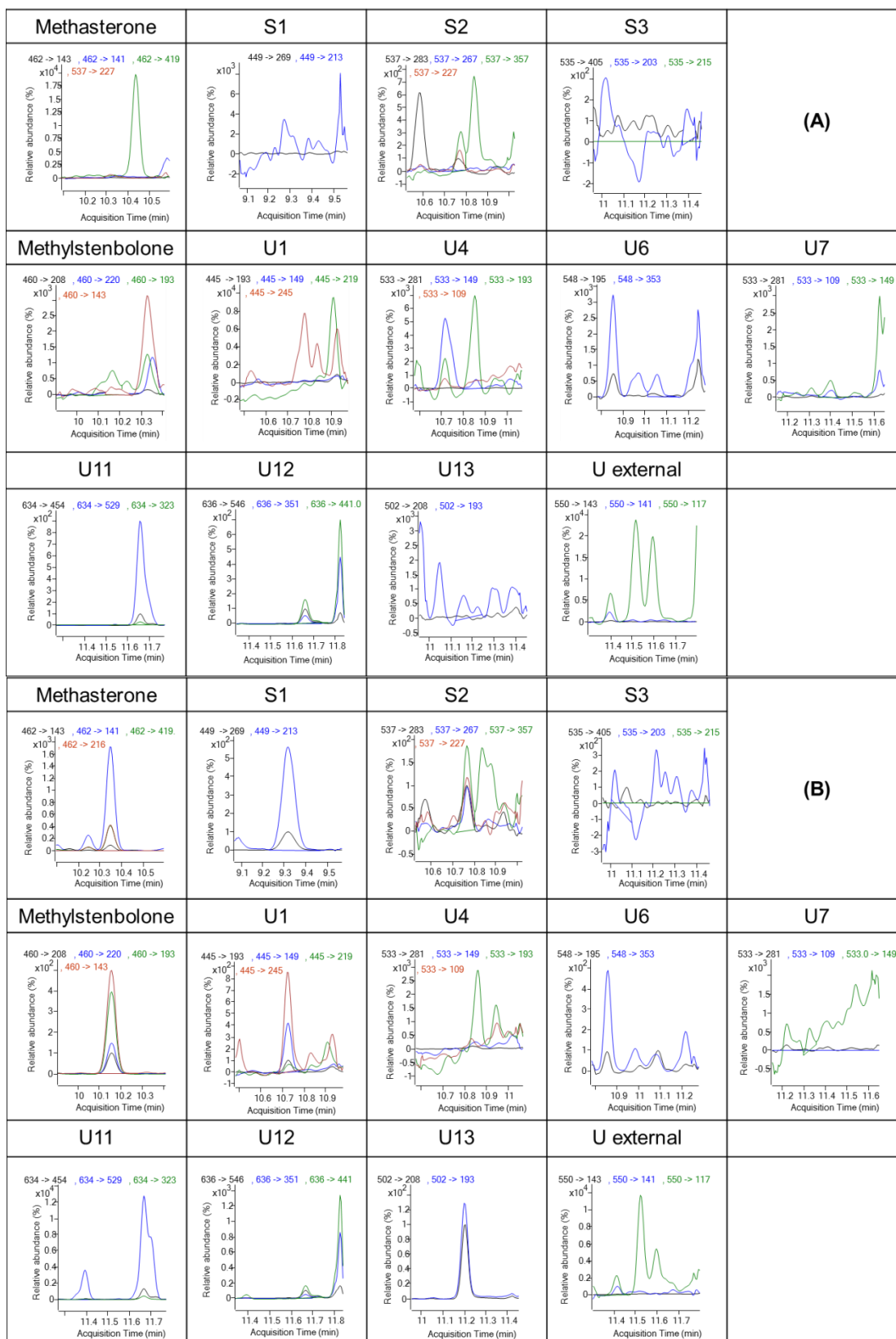


Figure 4.6. GC-MS/MS chromatograms obtained in the application of the developed MRM method to (A) negative human urine sample and (B) human urine sample declared positive for methasterone.

4 Conclusions

HLM and a chimeric mouse model were used to investigate the metabolism of the substance marketed as ‘the nutritional supplement’ ‘Ultradrol’. According to the label this product contains methylstenbolone. However, when analyzing the product a non-declared steroid, methasterone, was also detected. This proves that labels are not always reliable but also shows the dangers for the consumers of these so-called supplements, as use of methasterone has already been associated with some serious adverse health effects [21-23] and no clear information is available on the potential toxicity and adverse effects of the co-administration of methylstenbolone and methasterone.

Incubation of this steroid product containing both steroids methylstenbolone and methasterone with HLM gives rise predominantly to methasterone metabolites; the same could be seen in the chimeric mouse urine. Neither of the metabolites previously described in Cavalcanti *et al.* were detected in the HLM or chimeric mouse experiments.

Further experiments were performed to elucidate the metabolism of methylstenbolone. These experiments, with purified steroid product, showed that methylstenbolone is neither converted into methasterone nor metabolites of this compound. Both models studied indicated that methylstenbolone is metabolized by hydroxylation and/or dehydrogenation. In the HLM incubation samples mainly monohydroxylated compounds were detected, whereas in the chimeric mouse urine only dihydroxylated compounds were found. Metabolites U1 and U2 were 18-hydroxy metabolites of methylstenbolone and the hydroxyl group of U4 and U7 is proposed to be located in the A ring.

The 16-hydroxylated metabolites previously described by Cavalcanti *et al.* were not detected, neither in the two models nor in the analyzed urine samples. However, an excellent correlation with previous human administration studies was found for the metabolism of methasterone.

Based upon the current results, it is suggested that, for the effective control of the misuse of the steroid product (methasterone and methylstenbolone), a detection method should at least contain transitions for methasterone, S1 and methylstenbolone. Metabolite U13 could also be a useful marker for methylstenbolone misuse. However, the structure of this metabolite could not be unequivocally established. The relevance of the hydroxylated derivatives of methylstenbolone should also be further investigated.

Acknowledgements

This study was financially supported by the Partnership for Clean Competition (PCC). The authors want to thank Wim Van Gansbeke and Lieven Verhoye for technical assistance.

References

1. Scarth JP, Clarke AD, Teale P, and Pearce CM (2010). Comparative in vitro metabolism of the 'designer' steroid estra-4,9-diene-3,17-dione between the equine, canine and human: Identification of target metabolites for use in sports doping control. *Steroids* 75, 643-652.
2. Tingle MD, and Helsby NA (2006). Can in vitro drug metabolism studies with human tissue replace in vivo animal studies? *Environ. Toxicol. Pharmacol.* 21, 184-190.
3. Scarth JP, Spencer HA, Hudson SC, Teale P, Gray BP, and Hillyer LL (2010). The application of in vitro technologies to study the metabolism of the androgenic/anabolic steroid stanozolol in the equine. *Steroids* 75, 57-69.
4. Levesque JF, Gaudreault M, Aubin Y, and Chauret N (2005). Discovery, biosynthesis, and structure elucidation of new metabolites of norandrostenedione using in vitro systems. *Steroids* 70, 305-317.
5. Lootens L, Van Eenoo P, Meuleman P, Leroux-Roels G, and Delbeke FT (2009). The uPA(+/-)-SCID Mouse with Humanized Liver as a Model for in Vivo Metabolism of 4-Androstene-3,17-dione. *Drug Metab. Dispos.* 37, 2367-2374.
6. Lootens L, Meuleman P, Pozo OJ, Van Eenoo P, Leroux-Roels G, and Delbeke FT (2009). uPA(+/-)-SCID Mouse with Humanized Liver as a Model for In Vivo Metabolism of Exogenous Steroids: Methandienone as a Case Study. *Clin. Chem.* 55, 1783-1793.
7. Pozo OJ, Lootens L, Van Eenoo P, Deventer K, Meuleman P, Leroux-Roels G, Parr MK, Schänzer W, and Delbeke FT (2009). Combination of liquid-chromatography tandem mass spectrometry in different scan modes with human and chimeric mouse urine for the study of steroid metabolism. *Drug Test. Anal.* 1, 554-567.
8. Lootens L, Meuleman P, Leroux-Roels G, and Van Eenoo P (2011). Metabolic studies with promagnon, methylclostebol and methasterone in the uPA(+/-)-SCID chimeric mice. *J. Steroid Biochem. Mol. Biol.* 127, 374-381.
9. Lootens L, Van Eenoo P, Meuleman P, Pozo OJ, Van Renterghem P, Leroux-Roels G, and Delbeke FT (2009). Steroid metabolism in chimeric mice with humanized liver. *Drug Test. Anal.* 1, 531-537.
10. Meuleman P, Libbrecht L, De Vos R, de Hemptinne B, Gevaert K, Vandekerckhove J, Roskams T, and Leroux-Roels G (2005). Morphological and biochemical characterization of a human liver in a uPA-SCID mouse chimera. *Hepatology* 41, 847-856.
11. Jia L, and Liu X (2007). The conduct of drug metabolism studies considered good practice (II): in vitro experiments. *Curr. Drug Metab.* 8, 822-829.
12. Brandon EFA, Raap CD, Meijerman I, Beijnen JH, and Schellens JHM (2003). An update on in vitro test methods in human hepatic drug biotransformation research: pros and cons. *Toxicol. Appl. Pharmacol.* 189, 233-246.
13. Kicman AT, and Gower DB (2003). Anabolic steroids in sport: biochemical, clinical and analytical perspectives. *Ann. Clin. Biochem.* 40, 321-356.

14. Masse R, and Goudreault D (1992). Studies on anabolic-steroids. 11. 18-hydroxylated metabolites of mesterolone, methenolone and stenbolone - New steroids isolated from human urine. *J. Steroid Biochem. Mol. Biol.* 42, 399-410.
15. Goudreault D, and Masse R (1991). Studies on anabolic-steroids. 6. Identification of urinary metabolites of stenbolone acetate (17-beta-acetoxy-2-methyl-5-alpha-androst-1-en-3-one) in human by gas-chromatography mass-spectrometry. *J. Steroid Biochem. Mol. Biol.* 38, 639-655.
16. Cavalcanti GD, Leal FD, Garrido BC, Padilha MC, and Neto FR (2012). Detection of designer steroid methylstenbolone in "nutritional supplement" using gas chromatography and tandem mass spectrometry: elucidation of its urinary metabolites. *Steroids* 78, 228-233.
17. Pozo OJ, Deventer K, Eenoo PV, and Delbeke FT (2008). Efficient approach for the comprehensive detection of unknown anabolic steroids and metabolites in human urine by liquid chromatography-electrospray-tandem mass spectrometry. *Anal. Chem.* 80, 1709-1720.
18. Van Thuyne W, Van Eenoo P, and Delbeke FT (2006). Nutritional supplements: prevalence of use and contamination with doping agents. *Nutr. Res. Rev.* 19, 147-158.
19. Geyer H, Parr MK, Koehler K, Mareck U, Schänzer W, and Thevis M (2008). Nutritional supplements cross-contaminated and faked with doping substances. *J. Mass Spectrom.* 43, 892-902.
20. Van Eenoo P, and Delbeke FT (2006). Metabolism and excretion of anabolic steroids in doping control - New steroids and new insights. *J. Steroid Biochem. Mol. Biol.* 101, 161-178.
21. Nasr J, and Ahmad J (2009). Severe Cholestasis and Renal Failure Associated with the Use of the Designer Steroid Superdrol (TM) (Methasteron (TM)): A Case Report and Literature Review. *Dig. Dis. Sci.* 54, 1144-1146.
22. Singh V, Rudraraju M, Carey EJ, Byrne TJ, Vargas HE, Williams JE, Balan V, Douglas DD, and Rakela J (2009). Severe Hepatotoxicity Caused by a Methasteron-containing Performance-enhancing Supplement. *J. Clin. Gastroenterol.* 43, 287-287.
23. Jasiurkowski B, Raj J, Wisinger D, Carlson R, Zou LX, and Nadir A (2006). Cholestatic jaundice and IgA nephropathy induced by OTC muscle building agent superdrol. *Am. J. Gastroenterol.* 101, 2659-2662.
24. WADA. The 2016 Prohibited List, International Standard. Montreal (2016) <https://wada-main-prod.s3.amazonaws.com/resources/files/wada-2016-prohibited-list-en.pdf> (access date 04.01.16).
25. Gauthier J, Goudreault D, Poirier D, and Ayotte C (2009). Identification of drostanolone and 17-methyldrostanolone metabolites produced by cryopreserved human hepatocytes. *Steroids* 74, 306-314.
26. Parr MK, Opfermann G, and Schänzer W (2006). Detection of new 17-alkylated anabolic steroids on WADA 2006 list, In *Recent Advances in Doping Analysis (14)*, Proceedings of the 24th Cologne Workshop on dope analysis (Schänzer W, Geyer H, Gotzmann A, and Mareck-Engelke U, Eds.), pp 249-258, Sport & Buch Strauss, Cologne, Germany.
27. Rodchenkov G, Sobolevsky T, and Sizoi V (2006). New designer anabolic steroids from internet, In *Recent Advances in Doping Analysis (14)*, Proceedings of the 24th Cologne Workshop on dope analysis (Schänzer W, Geyer H, Gotzmann A, and Mareck-Engelke U, Eds.), pp 141-150, Sport & Buch Strauss, Cologne, Germany.

28. Bylina DV, Gryn SV, and Tkachuk AA (2012). Detection of the methasterone and its metabolite in human urine by the gas chromatography/high resolution mass spectrometry (HRMS) method. *Methods and objects of chemical analysis* 7, 87-93.
29. Pozo OJ, Van Eenoo P, Deventer K, Grimalt S, Sancho JV, Hernandez F, and Delbeke FT (2008). Collision-induced dissociation of 3-keto anabolic steroids and related compounds after electrospray ionization. Considerations for structural elucidation. *Rapid Commun. Mass Spectrom.* 22, 4009-4024.
30. Goudreault D, and Masse R (1990). Studies on anabolic-steroids. 4. Identification of new urinary metabolites of methenolone acetate (Primobolan) in human by gas-chromatography mass-spectrometry. *J. Steroid Biochem. Mol. Biol.* 37, 137-154.
31. Fragkaki AG, Angelis YS, Tsantili-Kakoulidou A, Koupparis M, and Georgakopoulos C (2009). Schemes of metabolic patterns of anabolic androgenic steroids for the estimation of metabolites of designer steroids in human urine. *J. Steroid Biochem. Mol. Biol.* 115, 44-61.

Chapter 5

***In vitro* and *in vivo* metabolism studies of dimethazine**

Adapted from:

Geldof L, Tudela E, Lootens L, Van Lysebeth J, Meuleman P, Leroux-Roels G, Van Eenoo P and Deventer K (2015). *In vitro* and *in vivo* metabolism studies of dimethazine. Biomedical Chromatography (In press; DOI: 10.1002/bmc.3668).

Abstract

The use of anabolic steroids is prohibited in sports. Effective control is done by monitoring their metabolites in urine samples collected from athletes. Ethical objections however restrict the use of designer steroids in human administration studies. To overcome these problems alternative *in vitro* and *in vivo* models were developed to identify metabolites and to assure a fast response by anti-doping laboratories to evolutions on the steroid market.

In this study human liver microsomes and an uPA^{+/+}-SCID chimeric mouse model were used to elucidate the metabolism of a steroid product called 'Xtreme DMZ'. This product contains the designer steroid dimethazine (DMZ), which consists of two methasterone molecules linked by an azine group. In the performed stability study, degradation from DMZ to methasterone was observed.

By a combination of liquid chromatography-high resolution mass spectrometry (LC-HRMS) and gas chromatography-(tandem) mass spectrometry (GC-MS(/MS)) analysis methasterone and six other DMZ metabolites (M1-M6), which are all methasterone metabolites, could be detected besides the parent compound in both models. The phase II metabolism of DMZ was also investigated in the mouse urine samples. Only metabolites M1 and M2 were exclusively detected in the glucuro-conjugated fraction, all other compounds were also found in the free fraction. For an effective control of DMZ misuse in doping control samples the screening for methasterone and methasterone metabolites should be sufficient.

1 Introduction

Since the turn of the millennium designer steroids have appeared on the market to circumvent legal and sport ethical prohibitions, leading to the sales of these steroids in so-called dietary supplements via the internet. Methasterone was such a steroid and was added to the ‘Designer anabolic steroid control act of 2012’ of the United States government [1]. To circumvent the prohibition of the sales of anabolic steroids included in the law, ‘supplement’ companies tend to be creative, as shown with the designer steroid dimethazine (DMZ), which consists of two methasterone molecules linked by an azine group (Figure 5.1).

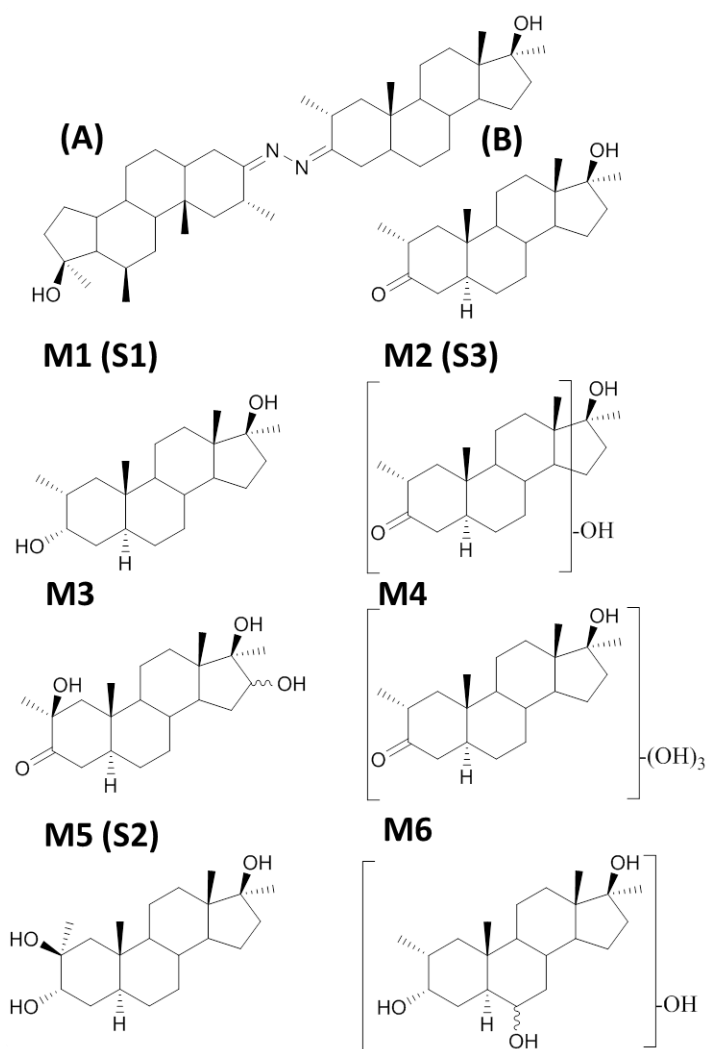


Figure 5.1. Chemical structures of dimethazine (A), methasterone (B), M1 (S1) and tentative structures for metabolites M2 till M6.

In animal experiments a good anabolic-androgenic dissociation was observed [2], therefore therapeutic indications for DMZ were to stimulate weight gain and protein anabolism [3]. DMZ

or mebolazine is no longer sold as prescribed drug (Roxilon®) [3], but is still available on the black market (e.g. Dymethazine, Xtreme DMZ, Powerdrol-10, etc.).

The metabolism of methasterone has already been extensively investigated with both *in vitro* [4-6] and *in vivo* human [7-9] and chimeric mouse [10] models. Owing to the structural relationship between DMZ and methasterone and the reported toxic effects on liver and kidney after administration of methasterone [11-13] the use of human excretion studies is ethically limited. Moreover, a case of liver injury was linked to combined administration of DMZ and methylstenbolone [14]. Therefore, the aim of this study was to elucidate the metabolism of DMZ with human liver microsomes (HLM) and an uPA^{+/+}-SCID chimeric mouse model to target the best DMZ metabolites for doping control purposes.

2 Materials and methods

2.1 Chemicals and reagents

Reference materials of DMZ (17 β -hydroxy-2 α ,17 α -dimethyl-5 α -androstan-3-one-(3,3')-azine) and methasterone (17 β -hydroxy-2 α ,17 α -dimethyl-5 α -androstan-3-one) were purchased from Toronto Research Chemicals (TRC, North York, Canada). 2 α ,17 α -dimethyl-5 α -androstan-3 α ,17 β -diol (S1) was acquired from WAADS. 'Xtreme DMZ' from Anabolic Technologies was purchased over the internet. Hydrochloric acid was from Merck (Darmstadt, Germany). The internal standard (IS) 17 α -methyltestosterone was purchased from Organon (Oss, the Netherlands). Pooled HLM from 20-30 donors, phosphate buffer pH 7.4, the NADPH regenerating system solutions A and B were purchased from BD Gentest (Erembodegem, Belgium). Ethanol (EtOH) was purchased from Biosolve (Valkenswaard, the Netherlands). Diethyl ether and methanol (MeOH) were obtained from Fisher Scientific (Loughborough, UK). Na₂SO₄, NaOH, NaHCO₃, K₂CO₃, Na₂HPO₄·2H₂O, NaH₂PO₄·H₂O, NH₄I, LC grade water and LC grade MeOH were from Merck (Darmstadt, Germany). The β -glucuronidase preparation from *Escherichia coli* (E. coli) K12 was purchased from Roche Diagnostics (Mannheim, Germany). MSTFA was from Karl Bucher (Waldstetten, Germany). Ethanethiol was obtained from Acros (Geel, Belgium). Phosphate Buffered Saline (PBS) was from Invitrogen (Merelbeke, Belgium). The gasses helium (He) and oxygen free nitrogen (OFN) were delivered by Air Liquide (Bornem, Belgium).

2.2 Instrumentation

2.2.1 GC-MS(/MS)

The GC-MS analyses were performed with an Agilent 6890 gas chromatograph interfaced to an Agilent 5973 mass spectrometer and for the GC-MS/MS analysis with an Agilent 7890 gas

chromatograph coupled with an Agilent 7000 B triple quadrupole mass (all from Agilent Technologies, Palo Alto, USA).

Full scan GC-MS analysis was performed at a mass range of m/z 50–800 and 2 cycles/s. A 1 μL aliquot of sample was injected into the GC-MS system using a 7683 series autosampler with a splitless injector (Agilent Technologies). The GC separation was performed using a JW Ultra-1 capillary column (17 m \times 200 μm i.d., 0.11 μm ; Agilent Technologies) and He as mobile phase at a flow rate of 0.6 mL/min at 10.15 psi (constant flow). The temperature program and other instrumental parameters were applied as described in Chapter 3 (2.2.1 GC-MS). The GC-triple quadrupole MS MRM method for the detection of methasterone and its metabolites (S1, S2 and S3) was applied as described previously [6] (Chapter 4).

2.2.2 LC-MS/MS

All experiments (low and high resolution) were performed under the same LC conditions as described below. A Finnigan Surveyor Autosampler Plus and a MS Pump Plus (Thermo Scientific, Bremen, Germany) were used for the low resolution experiments. For the high resolution (HR) experiments an Accela autosampler and 1250 pump (Thermo Scientific, Bremen, Germany) were used. The LC separation was performed using a Varian Omnispher C18 column (100 mm \times 2 mm I.D., 3 μm) (Varian, Sint-Katelijne-Waver, Belgium) at a flow rate of 250 $\mu\text{L}/\text{min}$. 25 μL of sample was injected into the instrument. The mobile phase consisted of LC grade water and MeOH both with 1 mM NH_4COOH and 0.001% HCOOH . In the used gradient program the percentage of the methanolic mobile phase changed as follows: 0 min, 45%; 0.5 min, 45%; 3 min, 75%; 3.5 min 75%; 3.6 min, 85%; 5 min, 85%; 5.1 min, 95%; 10.0 min, 95%; 10.10 min, 100%; 10.5 min, 100%; 10.6 min, 45% and 15 min, 45%.

The LC-HRMS instrument (Exactive from Thermo Scientific) operated in full scan (both positive and negative ionization) mode from m/z 100-2000 at a resolving power of 50,000 and acquisition rate of 2 Hz. Additionally, a precursor ion scan method, with selected product ions m/z 77, 91 and 105 was applied to search for (unknown) metabolites [15] (Chapter 4 – 2.2.4 LC-MS/MS) by a (low resolution) TSQ Quantum Discovery MAX triple quadrupole mass spectrometer MS (Thermo Scientific). Product ion scans with $[\text{M}+\text{H}]^+$ or $[\text{M}+\text{NH}_4]^+$ as selected precursor ion were also performed by a LC-HRMS instrument (Q-Exactive from Thermo Scientific) with collision energies (CE) of 25, 35, 45 and 55 eV at a resolving power of 70,000. Using this method also five fractions (Fr1: 2.0-3.5 min; Fr2: 3.5-4.2 min; Fr3: 4.2-4.7 min; Fr4: 5.2-5.8 min and Fr5: 5.8-7.5 min) were collected by switching the valve from the detector to the 'waste' to collect these fractions into separate tubes.

Relative abundances of the detected metabolites were calculated from the basis of the absolute peak height from an extracted ion chromatogram, of the most abundant ions, of the metabolites relative to the absolute peak height of the IS in the samples.

2.3 Extraction of the steroid from the steroid product

The steroid was isolated from the steroid product by adding 5 mL of EtOH to the content of 3 capsules (each containing according to the label 16 mg DMZ) and homogenization by rolling for 2 h and followed by centrifugation (1500 *g*, 5 min). 100 μ L of the upper layer, after a tenfold dilution, was then used for LC-HRMS analysis.

2.4 Stability study of dimethazine

DMZ was spiked at 20 μ g/mL in 7.5 mL of three different storage solutions: two aqueous (acetate buffer pH 5.2 and hydrochloric acid 0.1 N pH 0.5) and MeOH. The spiked samples were incubated at 37 °C during 8 h. 100 μ L aliquots were taken in triplicate at 0 min and every 30 min, after which these were stored at -20 °C until analysis. For the stability test in 0.1 N HCl, the $t = 0$ min was taken first, before adding HCl. Before analysis the samples (aqueous solutions) were diluted with 100 μ L of MeOH/(25% NH₃ in H₂O) (95/5) or 100 μ L H₂O (for the methanolic solution) and 20 ng of the IS (17 α -methyltestosterone) was added to all samples. A reference standard of DMZ (20 μ g/mL) was also analyzed in triplicate.

Linear curves were fitted through the logarithmic areas according to $\log(A_t) = \log(A_0) - 0,43 k \cdot t$. The half-life ($t_{1/2}$) was also calculated and provides a measure of the degradation reaction rate.

2.5 In vitro and in vivo metabolism studies

The *in vitro* HLM incubation studies were performed as described in Chapter 1 (7.2.2.2 *Protocol in vitro metabolism studies*; Table 1.6). In short, the reference standard of DMZ (final concentration of 40 μ g/mL) was incubated with HLM as test compound. Substrate stability samples (blank; without HLM) and system blank samples (without test compound) control samples were used to verify the enzymatic reactions. Methasterone was used as test compound in the positive control samples. At the appropriate time (after 2, 4, and 18 h) the enzymatic reactions were stopped by adding 250 μ L ice-cold MeOH.

The *in vivo* metabolism studies were performed as described in Chapter 1 (7.2.3 *In vivo metabolism studies*). The project was approved by the Animal Ethics Committee of the Faculty of Medicine of Ghent University (ECD 06/09). 200 μ L of a 20 mg/mL solution (4 mg) of the DMZ reference standard dissolved in ethanol/PBS (20/80) was administered by oral gavage to two non-chimeric and four chimeric mice.

2.6 Sample preparation for *in vitro* and *in vivo* samples

The sample preparation procedure, for 400 μL of the *in vitro* and 500 μL of *in vivo* samples, has been described in Chapter 3 (2.5.1 *Liquid-liquid extraction (LLE)*). In short, a 50 μL aliquot of the IS 17 α -methyltestosterone (2 $\mu\text{g}/\text{mL}$) was added to all samples. For the *in vitro* samples (unconjugated fraction) LLE was performed at pH 9.5 (carbonate buffer) with diethylether. To study the total (unconjugated and glucuro-conjugated) fraction in the *in vivo* samples an enzymatic hydrolysis (β -glucuronidase) was performed prior to the LLE as described in Chapter 3 (2.5.1 *Liquid-liquid extraction (LLE)*).

To study the phase II metabolism of DMZ (*in vivo*) the separated free and glucuro-conjugated fractions were also investigated of a blank sample and a urine sample collected 24 h after administration. Therefore the free fraction of the *in vivo* samples was first studied in these samples by performing LLE without hydrolysis. After separation of the organic fraction hydrolysis with β -glucuronidase from *E. coli* and subsequent LLE (glucuronidated fraction) was performed on the same samples.

Finally, the residues of the dried organic layers were dissolved in 200 μL MeOH/H₂O (50/50) for LC-MS analysis or TMS-derivatized for GC-MS analysis by adding 100 μL derivatization solution containing MSTFA, NH₄I and ethanethiol (500/4/2) and incubation for 1 h at 80 \pm 5 $^{\circ}\text{C}$.

3 Results and discussion

3.1 Analysis of the steroid product

In the 'supplement' both DMZ and methasterone (31.5% relative to DMZ in the total ion chromatogram) were detected by LC-HRMS, with mass deviations of <2 ppm ($[\text{M}+\text{H}]^+$ experimental masses were 633.5357 (0.51 ppm) and 319.2634 (0.90 ppm) respectively). The presence of methasterone could be due to instability of DMZ as methasterone was also detected as trace amounts (1.8% relative to DMZ) in the methanolic solution of the DMZ reference standard. Therefore a small stability study was performed.

3.2 Stability study of dimethazine

The stability of DMZ was tested in two aqueous conditions and in MeOH (results not shown here). In the methanolic solution of the DMZ reference standard, methasterone was observed, but the stability study showed that DMZ is relatively stable in MeOH (half-life of 24.8 h at 37 $^{\circ}\text{C}$). In both aqueous conditions a decrease of DMZ was observed, which was accelerated at the lower pH ($t_{1/2}$ of 223 min at pH 5.2 versus $t_{1/2}$ of 23.7 min at pH 0.5). The hydrolysis of

hydrazones at acidic conditions has also been described before [16]. The high degradation speed at low pH indicates that after ingestion of the product, conversion in the stomach of DMZ into methasterone will be substantial. The exact *in vivo* conversion rate is however difficult to predict based upon the performed experiments as the pH *in vivo* will range between the two tested conditions (pH 0.5 and 5.2). The decreasing DMZ is correlated with the formation of methasterone. No other DMZ degradation products were observed by LC-HRMS and GC-MS analysis.

3.3 *In vitro* and *in vivo* metabolism studies

The reference standard of DMZ was used for all the *in vitro* and *in vivo* metabolism studies, as this standard did only contain trace amounts of methasterone (1.8% relative to DMZ) as an impurity in comparison with the amount of methasterone detected in the steroid product.

3.3.1 HLM incubations

The HLM incubation samples were analyzed with a full scan HRMS acquisition method. Based upon general steroid metabolic pathways, exact masses for the parent and possible metabolites were extracted from the chromatograms with a mass window of 10 ppm. If a signal for a theoretical metabolite was detected, the metabolic nature was established by comparing the extracted chromatogram of the samples with those in negative (without DMZ) and blank (without HLM) control samples. The metabolites detected in all microsomal incubation samples were very similar, independent of incubation time. The results of the 4 h incubation sample are shown in Figure 5.2. In all samples incubated with DMZ, methasterone and six previously reported metabolites of methasterone [4-10] were detected (Table 5.1). These compounds were also detected in the positive control sample (methasterone incubation) but not in blank and negative control samples. The main metabolic pathway observed in the microsomal incubation samples was the hydrolysis of the azine group leading to methasterone, followed by hydroxylation (mono- (M2), di- (M3a/b) and trihydroxylations (M4)) and combination of a reduction and dihydroxylation (M6a/b) of methasterone. Metabolites M1 and M5 could not be detected by LC-HRMS analysis, as the proposed structure of these metabolites presents ionization difficulties in LC-MS. In these cases GC-MS(/MS) analysis was used to identify these substances. For metabolite M6 two isomers were detected of which only the sodium and ammonium adducts could be observed. For the other metabolites (M2, M3 and M4) also the protonated molecules could be detected. It is postulated that the additional hydroxyl group(s) of M6 (dihydroxylated 3-keto reduced methasterone metabolite) in comparison to saturated metabolites M1 and M5 could possibly lead to a better stabilization of sodium and ammonium adducts as was observed for other polyhydroxylated steroids, i.e. 9-fluoro-17 α -methyl-androst-4-ene-3 α ,6 β ,11 β ,17 β -tetrol [17, 18].

In addition to the target processing method (based upon theoretical metabolic pathways), an untargeted precursor ion scan method was also used [15], which did not lead to the detection of additional metabolites.

To obtain more structural information, the samples were also analyzed by GC-MS(/MS). Therefore, five LC-MS fractions (Fr1-Fr5) were collected from a 4 h HLM sample and a negative control. Methasterone was collected in Fr5 and used as a control compound. The other fractions were collected in such way that they only contained some selected metabolites (Fr1: M4 and M6a; Fr2: M6b and M3a; Fr3: M3b; Fr4: M2).

Analysis of the collected fractions by GC-MS(/MS) confirmed the presence of methasterone in Fr5. However, no metabolites were observed in the first three fractions (Fr1-Fr3). It is assumed that the concentration of the metabolites in these first three fractions was too low for GC-MS detection. This assumption is supported by the fact that the collected metabolites in these fractions were di- or trihydroxylated methasterone metabolites and as observed in previous *in vitro* experiments by our research group these have in general lower abundance than monohydroxylated metabolites. In Fr4 a monohydroxylated methasterone metabolite was detected. Comparison with data from previous HLM incubations with methasterone shows that M2 corresponds to the previously described metabolite S3 (Table 5.1) [6].

The previously developed MRM method [6] (Chapter 4) for the detection of methasterone and its metabolites (S1, S2 and S3) was also applied to the microsomal incubation samples. All previously described metabolites (S1, S2 and S3) [6] could be detected after incubation of DMZ. M1 corresponds to S1, the main methasterone metabolite in human excretion studies [7-9], and M5 to S2 (Table 5.1). In the case of M1, the structure was unequivocally confirmed since its reference standard is commercially available. As no reference material is available for metabolite M5 structural characterization was based on correlation of the mass spectrum with a methasterone metabolite earlier described by Gauthier *et al.* and Geldof *et al.* [4, 6] (Chapter 4). The same characteristic fragment ions m/z 143, 130, 157, 332, 420 and 421 were observed in the GC-MS mass spectrum after TMS derivatization of M5. Gauthier *et al.* identified this metabolite as $2\alpha,17\alpha$ -dimethyl- 5α -androstane- $2\beta,3\alpha,17\beta$ -triol by direct comparison with a synthesized compound [4].

3.3.2 Administration to the chimeric mouse model

The *in vivo* results after administration of a single oral dose of 4 mg DMZ are mentioned in Table 5.1. The *in vivo* results were consistent within each type of mouse (chimeric and non-chimeric) used in this DMZ administration study. With this dose, the parent drug could be detected in the chimeric and non-chimeric mouse urine however, methasterone was only detectable in the chimeric mouse urine (until 24 h after administration of DMZ). In both non-chimeric and

chimeric mouse urine the same four types of metabolites (M2, M3, M4 and M6) were detected as in the HLM incubation samples by full scan LC-HRMS analysis (Table 5.1). These metabolites were previously described as methasterone metabolites in chimeric mice administration studies with methasterone [10].

Using the previously developed MRM method [6] metabolites M1 and M2 could be detected in the chimeric mouse urine samples after administration of DMZ, M5 was not detected. This is in accordance with previously performed *in vivo* methasterone administration studies [6, 10], in which M5 was also not found. M1 was only detected in the chimeric mouse urine indicating an exclusive human origin of this metabolite, whereas metabolite M2 was detected in both the non- and the chimeric mouse urine samples.

Full scan GC-MS analysis of the mouse urine samples after derivatization led to the detection of two isomeric M3 and M6 metabolites (M3c and M6c, Table 5.1). The presence of fragment ions m/z 218 and 231 in their GC mass spectra indicate 16-hydroxylated methasterone metabolites. Based on their mass spectra these 16-hydroxylated methasterone metabolites could be linked to methasterone metabolites S2 (M6c) and S4 (M3c) reported by Lootens *et al.* [10]. M6c was also described as 2,16-dihydroxy and 3-keto reduced metabolite (5H) in the *in vitro* metabolism studies with methasterone by Gauthier *et al.* [4]. Typical ions for 16-hydroxylation (m/z 218 and 231) and small fragment ions specific for 2-hydroxylation (m/z 508, 420 and 157) are present in the GC mass spectrum of M6c.

To verify the presence of these metabolites in the *in vitro* samples full scan GC-MS analysis after TMS-derivatization was also applied. The fragment ions indicating 16-hydroxylation (m/z 218 and 231) were not found in the GC-MS mass spectra of the *in vitro* produced metabolites (both after incubation of DMZ and methasterone (positive control)). These results are in agreement with the previous metabolism studies of methasterone by Geldof *et al.*, where also no 16-hydroxylated methasterone derivatives were found in the *in vitro* samples [6].

In addition to M3a/b and M6a/b isomeric M3 and M6 metabolites were also detected in the *in vivo* samples by LC-HRMS. These isomeric metabolites were not detected in the *in vitro* samples. Although no unequivocal link of GC and LC metabolites was established, it is postulated that these isomeric metabolites (LC) correspond to the 16-hydroxylated metabolites M3c and M6c detected by GC-MS. Metabolites M3c and M6c were previously reported as typical human metabolites [10]. The results from the current study however indicate that these metabolites can be both human and murine. The absence of M3c and M6c in the non-chimeric mouse samples in the previous study might be due to the fact that in the previous study both dose (0.8 mg versus 4 mg) and volume of urine (100 μ l versus 500 μ l) were considerably lower [10].

The relative abundances of the *in vivo* detected metabolites are reported in Table 5.1. All detected metabolites (M2, M3, M4 and M6) have higher relative abundances than DMZ and methasterone in the *in vivo* samples. In both the non-chimeric as well as in the chimeric mouse urine samples dihydroxylated metabolites (M3b and M6c) have the highest relative abundances by LC-MS. Based on these relative abundances DMZ metabolites M3b, M6 (a/b/c) and M2 might be incorporated into existing screening methods to anticipate DMZ misuse. However, extrapolation of these chimeric mouse results to the human situation is difficult. Therefore, the relevance of these described metabolites in real doping control samples should also be determined. Nevertheless, monitoring methasterone and its metabolites seems sufficient to screen for DMZ misuse.

The chimeric mouse model was also used to investigate the phase II metabolism (glucuronidation) of DMZ (Table 5.1). Therefore the free and glucuro-conjugated fractions were compared after enzymatic hydrolysis (β -glucuronidase, *E. coli* K12) of the conjugated fraction. M1 and M2 were only detected in the glucuronidated fraction, whereas methasterone and all other metabolites could be detected in both fractions. The lower concentration of metabolites in the previously described study can explain why methasterone was then only detected in the glucuronidated fraction and metabolite M6c (S2) only in the free fraction [10].

3.4 Structure elucidation by performing LC-HRMS product ion scans

To obtain more structural information of the metabolites M2, M3, M4 and M6 product ion scans were performed by LC-HRMS. Therefore product ion scans of DMZ and methasterone reference standards were also performed. All described product ions below were detected with <5 ppm mass deviation.

The most abundant ion in the product ion scan mass spectrum of DMZ (m/z 318.2789) could be linked to the chemical formula $C_{21}H_{36}ON$ with a mass deviation of 0.21 ppm (Figure 5.3). Although this fragment was formed in the product ion scan experiments it was not detected as degradation product and no DMZ metabolites with this fragment as core structure could be detected. In addition to the precursor ion (m/z 319.2631) also two losses of water were observed in the product ion scan mass spectrum of methasterone: m/z 301.2520 and 283.2415 (Figure 5.3). Similar to what was observed for unconjugated-3-keto-anabolic steroids by Pozo *et al.* [19] the number of losses of water is identical to the number of oxygens in the molecule.

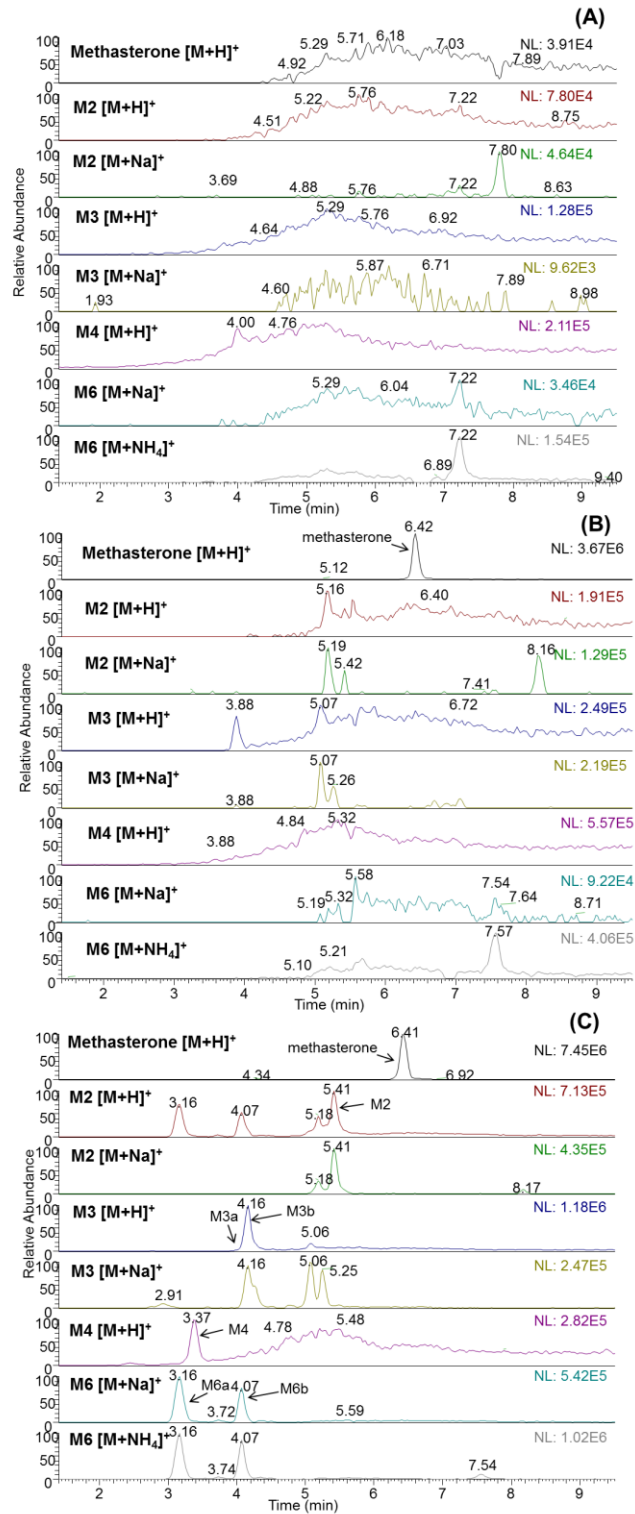


Figure 5.2. Extracted ion LC-HRMS chromatograms of methasterone and metabolites M2, M3, M4 and M6 in a negative control sample (without DMZ) (A), a blank control sample (without HLM) (B) and a 4 h HLM incubation sample of DMZ (C).

Additionally, a loss of 58 Da (acetone) was also observed for methasterone (m/z 243.2103 ($-H_2O-58$)), which would originate from the A-ring according to Pozo *et al.* [19]. Moreover, the B/C ring ions m/z 121.1013 and 107.0858, corresponding to C_9H_{13} and C_8H_{11} respectively, indicated in the paper of Pozo *et al.* for unconjugated 3-keto steroids were also detected.

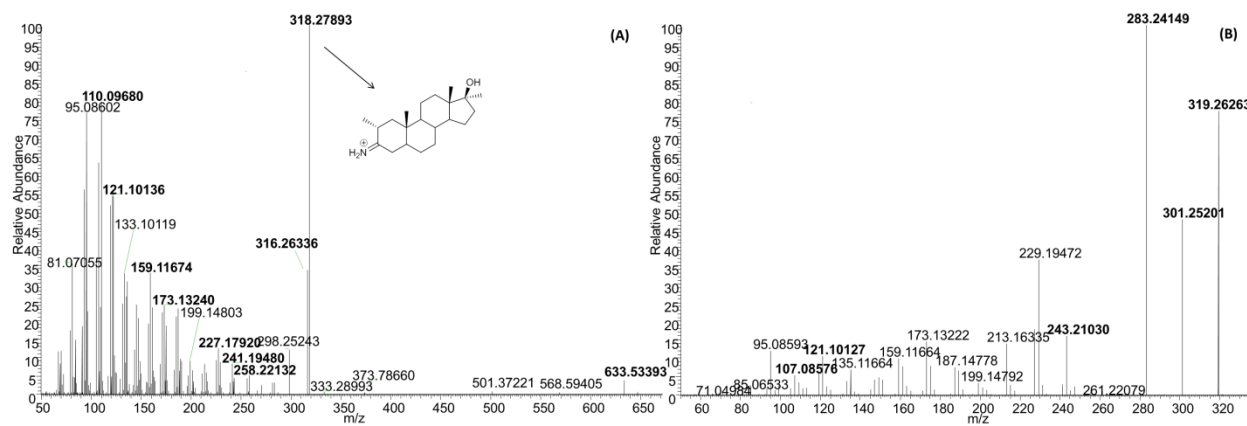


Figure 5.3. Product ion scan mass spectra (LC-HRMS) of DMZ (A) and methasterone (B) obtained from their reference standard with as selected precursor ion m/z 633.5354 (CE of 55eV) and 319.2632 (CE of 25eV) respectively.

Similar to methasterone the number of water losses for metabolite M2 was identical to the number of oxygen atoms present in the molecule. As metabolite M2 is a hydroxylated methasterone derivative three losses of water were observed: m/z 317.2473, 299.2368 and 281.2262 (Figure 5.4). The typical loss of acetone was also observed at m/z 259.2054 ($-H_2O-58$) and 241.1945 ($-2H_2O-58$). For M2 typical B/C ring fragments were also observed: m/z 133.1012 ($C_{10}H_{13}$), 121.1013 (C_9H_{13}), 109.1015 (C_8H_{13}) and 107.0859 (C_8H_{11}). In addition a fragment ion m/z 191.1428 ($C_{13}H_{19}O$) was observed, which indicates a hydroxylation of the ion m/z 175.1478 ($C_{13}H_{19}$) detected for methasterone. These fragments could originate from the A/B/C rings. The GC-MS mass spectrum of M2 also excludes hydroxylation in the D-ring by the presence of m/z 143. However, the exact position of hydroxylation could not be determined by both techniques (LC-MS and GC-MS). The number of water losses for metabolite M3a/b/c (Figure 5.4) was also identical to the number of oxygen atoms present in the molecule, four losses of water were observed: m/z 333.2419, 315.2315, 297.2209 and 279.2105. The typical loss of acetone was also observed (m/z 257.1896 ($-2H_2O-58$)). Besides the above described ions, some B/C-rings fragments were found: m/z 161.1323, 135.1167, 121.1014, 109.1014, 107.0858 (for M3a/b/c). These fragment ions correspond to $C_{12}H_{17}$, $C_{10}H_{15}$, C_9H_{13} , C_8H_{13} , C_8H_{11} respectively. This data could indicate that no modifications occurred in the B/C-rings for M3 (a/b/c).

Table 5.1. Overview of dimethazine metabolites detected in metabolism studies with HLM and the chimeric mouse model by LC-HRMS. See Figure 5.1 for tentative structures of the metabolites.

Metabolites	Metabolic reaction	Chemical Formula	Ion species	Experimental m/z (Δ ppm)	HLM RRT ^c	Non-chimeric mouse	Chimeric mouse RRT ^c	Relative abundance (%) ^d	Fraction (in chimeric mouse urine) ^e	Reference
Dimethazine	parent compound	C ₄₂ H ₆₈ N ₂ O ₂	[M+H] ⁺	633.5327 (4.25)	1.84	√	√	0.46	free + gluc	/
Methasterone	cleavage of the azine bound	C ₂₁ H ₃₄ O ₂	[M+H] ⁺	319.2622 (3.13)	1.23	×	√	0.73	free + gluc	[6-8]
IS	17 α -methyl-testosterone	C ₂₀ H ₃₀ O ₂	[M+H] ⁺	303.2305 (4.48)	1	√	√	100	×	/
M1 (S1)^a	reduction	C ₂₁ H ₃₆ O ₂	×	×	√ (GC)	×	√	/	gluc	[4-9]
M2 (S3)^a	hydroxylation	C ₂₁ H ₃₄ O ₃	[M+H] ⁺	335.2565 (4.57)	1.04	√	√	39.75	gluc	[4, 6, 10]
M3 (a/b)	dihydroxylation	C ₂₁ H ₃₄ O ₄	[M+H] ⁺	351.2514 (4.59)	0.76/0.82	√/√	√/√	35.09/59.01	free + gluc	[10]
M3c^b	dihydroxylation	C ₂₁ H ₃₄ O ₄	[M+H] ⁺	351.2520 (2.69)	×	√ (GC)	0.52 √ (GC)	13.47	free + gluc	[10]
M4	trihydroxylation	C ₂₁ H ₃₄ O ₅	[M+H] ⁺	367.2462 (4.76)	0.65	√	√	6.61	free + gluc	[10]
M5 (S2)^a	3-keto reduction + hydroxylation	C ₂₁ H ₃₆ O ₃	×	×	√ (GC)	×	×	×	×	[4-6, 9]
M6 (a/b)	3-keto reduction + dihydroxylation	C ₂₁ H ₃₆ O ₄	[M+NH ₄] ⁺	370.2936 (4.28)	0.61/0.78	√/√	√/√	40.75/43.45	free + gluc	[4, 5, 10]
M6c^b	3-keto reduction + dihydroxylation	C ₂₁ H ₃₆ O ₄	[M+NH ₄] ⁺	370.2949 (0.30)	×	√ (GC)	0.40 √ (GC)	98.87	×	[9, 10]

^a S1-S3 refer to metabolites described in [6]

M1 (S1) = 2 α ,17 α -dimethyl-5 α -androstane-3 α ,17 β -diol;

proposed structure of M5 (S2): 2 α ,17 α -dimethyl-5 α -androstane-2 β ,3 α ,17 β -triol [4, 6, 9],

^b Isomeric M3 and M6 metabolites were detected in the chimeric mouse model by both LC-MS and GC-MS. The ions m/z 218 and 231 in their GC-MS mass spectrum after TMS-derivatization indicate 16-hydroxylated metabolites.

^c RRT= relative retention time (to IS, 5.21 min)

^d relative abundances for each peak were calculated, relative to the IS, in chimeric mouse urine samples

^e study of glucuro-conjugation in chimeric mouse urine samples: free or gluc= glucuronidated fraction

×: not detected; √: detected ; √ (GC) detected by GC-MS(/MS) analysis.

M3c was described as x,16-dihydroxylated methasterone metabolite by Lootens *et al.* [10]. In analogy with M5 and M6c also fragment ion m/z 157 was detected by GC-MS, indicating a second hydroxylation at C2. Therefore, the proposed tentative structure of M3c is 2,16-dihydroxylated methasterone. However, in contrast to the GC-MS mass spectra, no diagnostic fragment ions indicating 16-hydroxylation were found in the obtained LC-HRMS product ion scan mass spectrum of M3c.

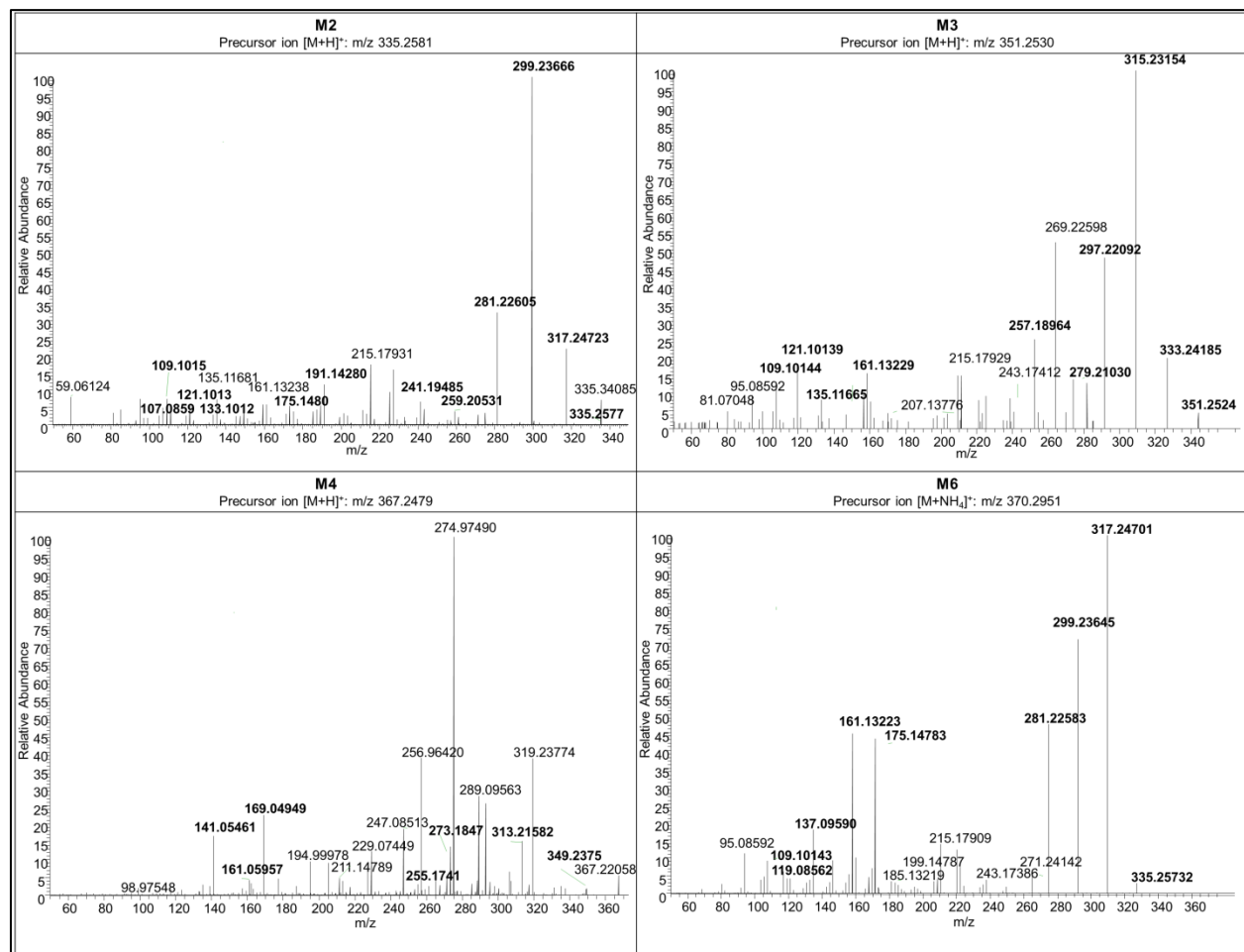


Figure 5.4 Product ion scan mass spectra (LC-HRMS) of metabolites M2, M3 (b) and M6 (a) obtained from *in vitro* samples and M4 from *in vivo* sample at a CE of 25eV (M2, M3 (b) and M4) or 35 eV (M6 (a)).

In the product ion scan mass spectrum of M4 four losses of water were observed (m/z 349.2375, 331.2268, 313.2160 and 295.2056) and three fragment ions indicating loss of acetone (m/z 291.1952 ($-\text{H}_2\text{O}-58$), 273.1847 ($-2\text{H}_2\text{O}-58$) and 255.1741 ($-3\text{H}_2\text{O}-58$)) (Figure 5.4). Although, five oxygen atoms are present in M4 no fifth loss of water was observed. However, this could be related to the lower abundance of this metabolite (Table 5.1) and therefore lower abundances of the fragment ions. In contrast to what was observed for methasterone and other metabolites no typical B/C ring fragment ions were found in the M4 product ion scan data. On the other hand fragment ions m/z 141.0546 and 169.0495 were detected which could be linked to $\text{C}_7\text{H}_9\text{O}_3$

and $C_8H_9O_4$ respectively. These fragment ions probably originate from the A/B/C rings and indicates modifications in these rings rather than in the D-ring. The exact position of the three hydroxylations could not be determined for M4.

For metabolite M6 the number of losses of water is also identical to the number of oxygens present in the molecule (Figure 5.4). As it is a dihydroxylated methasterone metabolite, four losses of water were observed: m/z 335.2573, 317.2470, 299.2365 and 281.2258. In contrast to methasterone and M3, the loss of acetone typical for unconjugated 3-keto steroids was not found for metabolite M6. This observation might be due to the 3-keto reduced structure of M6. Similar to methasterone and M3, some B/C-ring fragments were found comparable to those described by Pozo *et al.* [19] m/z 161.1322 ($C_{12}H_{17}$), 119.0856 (C_9H_{11}), 109.1014 (C_8H_{13}), 107.0858 (C_8H_{11}). Additionally the ions with m/z 175.1478 and m/z 137.0959 could be linked to $C_{13}H_{19}$ and $C_9H_{13}O$ respectively. This latter ion indicates a hydroxylation of the B/C fragment C_9H_{13} (121.1013) observed for methasterone, which suggests a hydroxylation in the B/C-ring. Based on common hydroxylation positions described in literature, a 6-hydroxylation is suggested for metabolite M6. No definitive answer for the position of the second hydroxylation could be derived from the product ion scan data. The position of the second hydroxyl-group could therefore for example be C2 or C12. M6c was identified as 2,16-hydroxylated 3-keto reduced methasterone structure, based on its GC-MS mass spectrum [4, 10]. Similar to M3c no diagnostic fragment ions indicating 16-hydroxylation were found in the LC product ion scan mass spectrum of M6c.

4 Conclusions

The metabolism of the steroid product 'Xtreme DMZ' containing the anabolic agent dimethazine was studied for the first time using *in vitro* (HLM) and *in vivo* (chimeric mouse) models. In the metabolism studies of both models methasterone and methasterone metabolites (M1-M6) were detected. These metabolites are in good agreement with earlier reported methasterone metabolism studies [4-10]. A stability study of DMZ shows that this compound degrades to methasterone at pH 0.5 ($t_{1/2}$ of 23.7 min). Therefore an oral administration of DMZ would probably lead to a substantial degradation of DMZ to methasterone in the stomach.

Hence, screening for methasterone and its metabolites is adequate for detection of DMZ misuse by GC-MS/MS and LC-HRMS.

Acknowledgements

This study was financially supported by the Partnership for Clean Competition (PCC). The authors want to thank Lieven Verhoye for technical assistance.

References

1. Government of the United States U. Designer anabolic steroid control act of 2012. (2012) <https://www.govtrack.us/congress/bills/112/s3431/text> (access date 04/04/2014).
2. Matscher R, Lupo C, and De Ruggieri P (1962). Biological activity of dimethazine in the protein anabolic sense. *Bollettino della Società italiana di biologia sperimentale* 38, 988-990.
3. Shakoori AR, Kausar N, and Lone KP (2003). Effect of single dose of dimethazine on regeneration of partially hepatectomized rabbit liver, In *Proceedings of Pakistan congress of zoology* (Ahmad M, and Shakoori AR, Eds.), pp 243-270, Rawalpindi, Pakistan.
4. Gauthier J, Goudreault D, Poirier D, and Ayotte C (2009). Identification of drostanolone and 17-methylandrostanolone metabolites produced by cryopreserved human hepatocytes. *Steroids* 74, 306-314.
5. Ayotte C, Goudreault D, Cyr D, Gauthier J, Ayotte P, Larochelle C, and Poirier D (2006). Characterisation of chemical and pharmacological properties of new steroids related to doping of athletes, In *Recent Advances in Doping Analysis (14)* , *Proceedings of the 24th Cologne Workshop on dope analysis* (Schänzer W, Geyer H, Gotzmann A, and Mareck-Engelke U, Eds.), pp 151-160, Sport & Buch Strauss, Cologne, Germany.
6. Geldof L, Lootens L, Polet M, Eichner D, Campbell T, Nair V, Botre F, Meuleman P, Leroux-Roels G, Deventer K, and Van Eenoo P (2014). Metabolism of methylstenbolone studied with human liver microsomes and the uPA -SCID chimeric mouse model. *Biomed. Chromatogr.* 28, 974-985.
7. Parr MK, Opfermann G, and Schänzer W (2006). Detection of new 17-alkylated anabolic steroids on WADA 2006 list, In *Recent Advances in Doping Analysis (14)* , *Proceedings of the 24th Cologne Workshop on dope analysis* (Schänzer W, Geyer H, Gotzmann A, and Mareck-Engelke U, Eds.), pp 249-258, Sport & Buch Strauss, Cologne, Germany.
8. Rodchenkov G, Sobolevsky T, and Sizoi V (2006). New designer anabolic steroids from internet, In *Recent Advances in Doping Analysis (14)* , *Proceedings of the 24th Cologne Workshop on dope analysis* (Schänzer W, Geyer H, Gotzmann A, and Mareck-Engelke U, Eds.), pp 141-150, Sport & Buch Strauss, Cologne, Germany.
9. Bylina DV, Gryn SV, and Tkachuk AA (2012). Detection of the methasterone and its metabolite in human urine by the gas chromatography/high resolution mass spectrometry (HRMS) method. *Methods and objects of chemical analysis* 7, 87-93.
10. Lootens L, Meuleman P, Leroux-Roels G, and Van Eenoo P (2011). Metabolic studies with promagnon, methylclostebol and methasterone in the uPA(+/-)-SCID chimeric mice. *J. Steroid Biochem. Mol. Biol.* 127, 374-381.
11. Nasr J, and Ahmad J (2009). Severe Cholestasis and Renal Failure Associated with the Use of the Designer Steroid Superdrol (TM) (Methasteron (TM)): A Case Report and Literature Review. *Dig. Dis. Sci.* 54, 1144-1146.
12. Singh V, Rudraraju M, Carey EJ, Byrne TJ, Vargas HE, Williams JE, Balan V, Douglas DD, and Rakela J (2009). Severe Hepatotoxicity Caused by a Methasteron-containing Performance-enhancing Supplement. *J. Clin. Gastroenterol.* 43, 287-287.

13. Jasiurkowski B, Raj J, Wisinger D, Carlson R, Zou LX, and Nadir A (2006). Cholestatic jaundice and IgA nephropathy induced by OTC muscle building agent superdrol. *Am. J. Gastroenterol.* 101, 2659-2662.
14. Agbenyefia P, Arnold C, and Kirkpatrick III R (2014). Cholestatic jaundice with the use of methylestenbolone and dymethazine, designer steroids found in super DMZ rx 2.0 "nutritional supplement": a case report. *Journal of Investigative Medicine High Impact Case Reports* 2, DOI: 10.1177/2324709614532800.
15. Pozo OJ, Deventer K, Eenoo PV, and Delbeke FT (2008). Efficient approach for the comprehensive detection of unknown anabolic steroids and metabolites in human urine by liquid chromatography-electrospray-tandem mass spectrometry. *Anal. Chem.* 80, 1709-1720.
16. Kalia J, and Raines RT (2008). Hydrolytic stability of hydrazones and oximes. *Angew. Chem.-Int. Edit.* 47, 7523-7526.
17. Leinonen A, Kuuranne T, Kotiaho T, and Kostianen R (2004). Screening of free 17-alkyl-substituted anabolic steroids in human urine by liquid chromatography-electrospray ionization tandem mass spectrometry. *Steroids* 69, 101-109.
18. Pozo OJ, Van Eenoo P, Deventer K, and Delbeke FT (2007). Ionization of anabolic steroids by adduct formation in liquid chromatography electrospray mass spectrometry. *J. Mass Spectrom.* 42, 497-516.
19. Pozo OJ, Van Eenoo P, Deventer K, Grimalt S, Sancho JV, Hernandez F, and Delbeke FT (2008). Collision-induced dissociation of 3-keto anabolic steroids and related compounds after electrospray ionization. Considerations for structural elucidation. *Rapid Commun. Mass Spectrom.* 22, 4009-4024.

Chapter 6

***In vitro* and *in vivo* metabolism studies of estra-4,9-diene-3,17-dione**

Authors:

Geldof L, Lootens L, Van Lysebeth J, Meuleman P, Leroux-Roels G, Deventer K and Van Eenoo P. (To be submitted)

Abstract

Ethical and safety aspects limit the use of human volunteers to perform metabolism studies for doping control purposes, especially in the case of designer steroids. To ensure effective detection of non-pharmaceutical grade substances there is a quest for alternative models for these human excretion studies.

In this study human liver microsomes and the chimeric mouse model were applied for metabolism studies with the steroid product 'Tren X' which contains estra-4,9-diene-3,17-dione. Analysis of the *in vitro* and *in vivo* samples was performed by LC-MS/MS (precursor ion scan), LC-HRMS and GC-MS. In the *in vitro* incubation samples four estra-4,9-diene-3,17-dione metabolites (M1-M4) were found by LC-MS and two of these metabolites could be confirmed (M1 and M2) by GC-MS. From these *in vitro* metabolites, three metabolites (M1, M2 and M3) were also detected in the chimeric mouse urine samples.

M2 was the main metabolite in both models and was unequivocally identified as 17 β -hydroxyestra-4,9-diene-3-one. This metabolite has also been reported in literature as major human metabolite of estra-4,9-diene-3,17-dione. These results indicate that both the *in vitro* and the *in vivo* model are valuable alternatives for human metabolism studies with designer steroids. Moreover, human liver microsomes can be useful to reduce the number of *in vivo* excretion studies.

1 Introduction

In vitro models are increasingly used for metabolism studies as alternative for human administration studies since *in vitro* studies have several advantages. *In vitro* studies are associated with less ethical objections in comparison to human excretion studies. This is particularly true in case of designer compounds or non-approved pharmaceutical drugs without predefined toxicological profiles. Application of *in vitro* models can also reduce the number of animal experiments needed. Moreover, these *in vitro* metabolism studies can accelerate the determination of metabolic profiles, since more concentrated and cleaner extracts for analysis can be obtained and the time needed for planning and execution of the *in vitro* studies is much shorter than for administration studies to humans. In this way a short response time to new threats in the doping field can be assured [1]. *In vitro* studies can therefore be useful for anti-doping laboratories to anticipate new evolutions on the steroid market, such as the appearance of new designer steroids. These compounds are often sold as so-called dietary supplements, sometimes with no or only limited knowledge about their side effects [2]. Furthermore, due to the illicit production process the purity of these products is not guaranteed and labelling is often incorrect [2-5]. Therefore safety and ethical concerns limit the use of human volunteers.

The steroid product TREN-X was purchased over the internet. This product is marketed as so-called ‘supplement’ to increase muscle size and strength with the anabolic steroid estra-4,9-diene-3,17-dione as active ingredient. Estra-4,9-diene-3,17-dione, or in short dienedione, is the precursor of dienolone (17 β -hydroxy-estra-4,9-diene-3-one) and is sometimes mistakenly sold as prohormone of trenbolone (17 β -hydroxy-estra-4,9,11-triene-3-one) because of the structural similarity (Figure 6.1) [6]. Although estra-4,9-diene-3,17-dione is not explicitly mentioned on WADA’s prohibited list, its misuse will be prohibited since it is structurally related to trenbolone, 19-norandrostenedione (estra-4-ene-3,17-dione) and methyldienolone (17 β -hydroxy-17 α -methyl-estra-4,9-diene-3-one) and similar biological, anabolic, effects might be expected [7].

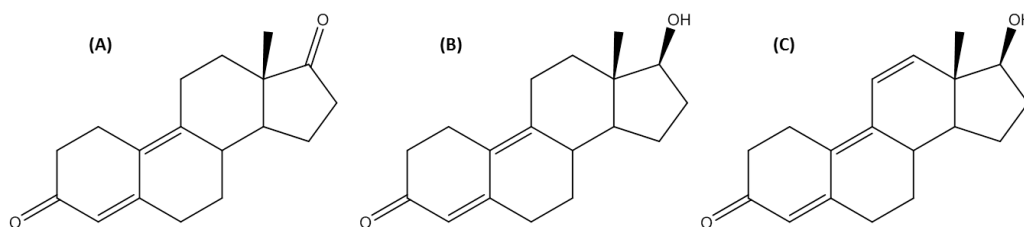


Figure 6.1. Chemical structures of (A) estradienedione, (B) dienolone and (C) trenbolone.

In the current study the metabolism of estra-4,9-diene-3,17-dione was investigated by human liver microsomes (HLM) and the uPA^{+/+}-SCID chimeric mouse model. Both models are based on

the liver, as this is the principal organ for steroid metabolism. HLM are derived from liver tissue by differential centrifugation steps and provide an enriched source of membrane-bound drug metabolizing enzymes, such as the CYP450 superfamily [8]. For the mouse model a transplantation of primary human hepatocytes is required to restore the normal liver function of the mice, which are suffering from a liver disease induced by a liver specific over-expression of the mouse urokinase plasminogen activator (uPA) gene. Graft rejection is limited in these immunodeficient (SCID: severe combined immunodeficient disorder) mice. This mouse model with humanized liver has already proven to be a good alternative for human excretion studies based on steroid research in the past [9-13].

The metabolism of estra-4,9-diene-3,17-dione has been studied before in a human excretion study [14] and equine, canine and human *in vitro* studies using S9 liver fractions [6]. To verify if HLM incubations can also be a valuable tool as alternative for human administration studies, the *in vitro* generated metabolites will be compared with those obtained in the chimeric mouse model and the human metabolites described in literature.

2 Materials and methods

2.1 Chemicals and reagents

A steroid product called Tren-X was purchased over the internet. The reference material of estra-4,9-diene-3,17-dione and dienolone (17 β -hydroxy-estra-4,9-diene-3-one) was bought from Toronto Research Chemicals (TRC, Toronto, Canada). Methandienone was obtained from the National Measurement Institute (NMI, North Ryde, Australia). The internal standard 17 α -methyltestosterone was a gift from Organon (Oss, the Netherlands).

Pooled HLM from 20-30 donors (HLM; 452161), the nicotinamide adenine dinucleotide phosphate (NADPH) regenerating system solutions A (451220) and B (451200) and phosphate buffer pH 7.4 (451201) were purchased from BD Gentest (Erembodegem, Belgium).

Ethanol and ammonium acetate (NH₄OAc) were purchased from Biosolve (Valkenswaard, the Netherlands). Diethyl ether and methanol (MeOH) were obtained from Fisher Scientific (Loughborough, UK). Sodium sulfate (Na₂SO₄), sodium hydroxide (NaOH), sodium hydrogen carbonate (NaHCO₃), potassium carbonate (K₂CO₃), disodium hydrogen phosphate dihydrate (Na₂HPO₄·2H₂O), sodium dihydrogen phosphate monohydrate (NaH₂PO₄·H₂O), and ammonium iodide (NH₄I), acetic acid (HOAc), LC grade water and LC grade MeOH were from Merck (Darmstadt, Germany). The β -glucuronidase preparation from Escherichia coli (E. coli) K12 was purchased from Roche Diagnostics (Mannheim, Germany). N-methyl-N-trimethylsilyltrifluoroacetamide (MSTFA) was from Karl Bucher (Waldstetten, Germany).

Ethanethiol was obtained from Acros (Geel, Belgium). Phosphate Buffered Saline (PBS) was from Invitrogen (Merelbeke, Belgium). The gasses helium (He) and oxygen free nitrogen (OFN) were delivered by Air Liquide (Bornem, Belgium).

2.2 Instrumentation

2.2.1 GC-MS

An Agilent 6890 gas chromatograph was interfaced to an Agilent 5973 mass spectrometer (Agilent Technologies, Palo Alto, USA). 1 μ L of sample was injected into the system using a 7683 series Autosampler with a splitless injector (Agilent Technologies, Palo Alto, USA). The GC separation was performed using a JW Ultra-1 capillary column (17 m x 200 μ m i.d., 0.11 μ m; Agilent Technologies) and He as mobile phase at a flow rate of 0.6 mL/min at 10.15 psi (constant flow). The temperature program and other instrumental parameters were applied as described in Chapter 3 (2.2.1 GC-MS).

2.2.2 LC-MS/MS

All experiments were performed under the same LC conditions using a Thermo Finnigan Surveyor Autosampler Plus and a MS Pump Plus (Thermo Scientific, Bremen, Germany). Electrospray ionization (ESI) was used for the ionization of the steroids. The mobile phase consisted of LC grade water (solvent A) and LC grade MeOH (solvent B) both with 1 mM NH_4OAc and 0.1% HOAc. The LC separation was performed using a SunFire™ C18 column (50 mm x 2.1 mm i.d., 3.5 μ m) from Waters (AH Etten-Leur, the Netherlands), at a flow rate of 250 μ L/min. 20 μ L of sample was injected into the instrument. In the gradient program the percentage of the methanolic mobile phase changed as follows: 0 min, 5%; 1.5 min, 5%; 29.5 min, 95%; 30.5 min 95%; 31 min, 5%; 35 min, 5%.

For the low resolution methods a TSQ Quantum Discovery MAX triple quadrupole mass spectrometer (Thermo Scientific) was used. The other instrumental parameters were adopted from Pozo *et al.* [15]. A precursor ion scan method was used to search for (unknown) metabolites. For the precursor ion scan method the ions m/z 77, 91 and 105 were selected as product ions. The collision energy (CE) was 45 eV for m/z 105 and 91 and 50 eV for m/z 77. For the structural investigation of metabolites, product ions scans were performed for some selected ions and CE of 15, 25, 35 and 50 eV were applied.

The high resolution (HR) analyses were performed on an Exactive benchtop Orbitrap-based mass spectrometer (Thermo Scientific). The instrument operated in positive, full scan mode from m/z 100 to 2000 at a resolving power of 50,000 with a data acquisition rate of 2 Hz. All ion fragmentation was performed by higher-collision dissociation (HCD), at a CE of 30 eV.

2.3 Extraction of the steroid from the steroid product

Estra-4,9-diene-3,17-dione was first isolated from the Tren-X steroid product for purity verification. Therefore an extraction step was performed by adding 5 mL of ethanol to the content of 3 homogenized capsules and rolling during 2 h. Then a centrifugation step was performed (1500 g, 5 min). 100 µL of the upper layer was then used for both LC-HRMS and GC-MS analyses.

2.4 In vitro metabolism studies

Before administration, all solutions (reference standard and steroid product) were analyzed by GC-MS and LC-(HR)MS for purity verification. Finally, the reference standard of estra-4,9-diene-3,17-dione was administered to HLM and the chimeric mouse model.

The *in vitro* HLM incubation assays were performed as described in Chapter 1 (7.2.2.2 *Protocol in vitro metabolism studies*; Table 1.6). Briefly, HLM incubations with estra-4,9-diene-3,17-dione at a final concentration of 40 µg/mL were performed. Substrate stability (blank; without HLM) and system blank (without test compound) control samples were used to verify the enzymatic reactions. Methandienone was incubated as test compound in the positive control samples. At the appropriate time (after 2, 4 and 18 h) the enzymatic reactions were stopped by adding 250 µL of ice-cold MeOH.

2.5 In vivo metabolism studies

The protocol of the *in vivo* administration studies was applied as described in Chapter 1 (7.2.3 *In vivo metabolism studies*). The chimeric mouse model was developed in cooperation with CEVAC of Ghent University Hospital [16]. The *in vivo* metabolism studies were approved by the Animal Ethical Committee of the Faculty of Medicine of Ghent University (ECD 06/09).

The dose and route of administration were similar to previous metabolism studies with the same model [10, 11, 13]. Before administration of the test compound to the chimeric mice, dose testing was performed with the non-chimeric mice with a test dose of 0.5 mg. The final administration dose for the *in vivo* metabolism studies was 1 mg of the test compound dissolved in 200 µL ethanol–PBS (20:80). The test compound (extracted from the Tren-X steroid product) was administered in a single dose to one chimeric and one non-chimeric mouse by oral gavage.

2.6 Sample preparation for in vitro and in vivo samples

For the *in vitro* metabolic assays the samples were first centrifuged at 4 °C (12,000 g, 5 min) followed by transfer of 400 µL into new tubes. All tubes were eventually stored in the

refrigerator until all samples were collected to enable sample preparation and analysis at the same time. Transferred incubation samples were then evaporated after which liquid–liquid extraction (LLE) was performed as described below. From the mouse urine 500 μL was used.

A 50 μL aliquot of the internal standard (IS) 17 α -methyltestosterone (2 $\mu\text{g}/\text{mL}$) was added to all samples. For the microsomal incubation samples (unconjugated fraction) LLE was performed as described in Chapter 3 (2.5.1 *Liquid-liquid extraction (LLE)*). To study the total fraction (conjugated and unconjugated steroids) in the chimeric mouse urine an enzymatic hydrolysis (β -glucuronidase) was performed prior to the LLE as described in Chapter 3 (2.5.1 *Liquid-liquid extraction (LLE)*).

After evaporation the residues were reconstituted in 100 μL mobile phase (95/5 solvent A and B) for LC-MS analysis. For GC-MS analysis the evaporated samples were derivatized by adding 100 μL derivatization solution containing MSTFA, NH_4I and ethanethiol (500/4/2) and incubation for 1 h at $80 \pm 5^\circ\text{C}$.

3 Results and discussion

3.1 Analysis of the steroid product

Analysis of the Tren-X steroid product by GC-MS and LC-MS/MS and comparison with the reference standard confirmed the presence of estra-4,9-diene-3,17-dione (estimated amount of 20 mg per g steroid product). No other steroid compounds were detected in the steroid product. However, two peaks (m/z 414 and 412) could be detected by GC-MS analysis after TMS-derivatization. This was also observed by Parr *et al.* [14] for estra-4,9-diene-3,17-dione and has been described for trenbolone [17, 18]. This can be explained by artefact formation after derivatization of the parent compound (m/z 414), due to the formation of enol derivatives at the C3-position in several tautomeric forms which are not stable and can lose two (m/z 412) or four (m/z 410) hydrogens [17, 19].

The presence of the conjugated double bond system results in good proton affinities for ESI LC-MS analysis. In this way also the artefact formation can be circumvented. Analysis of estra-4,9-diene-3,17-dione in the steroid product by LC-HRMS (Figure 6.2) showed a characteristic protonated molecule ($[\text{M}+\text{H}]^+$) at m/z 271.1693. This represents a mass deviation of only 0.18 ppm from the theoretical mass of the protonated molecule.

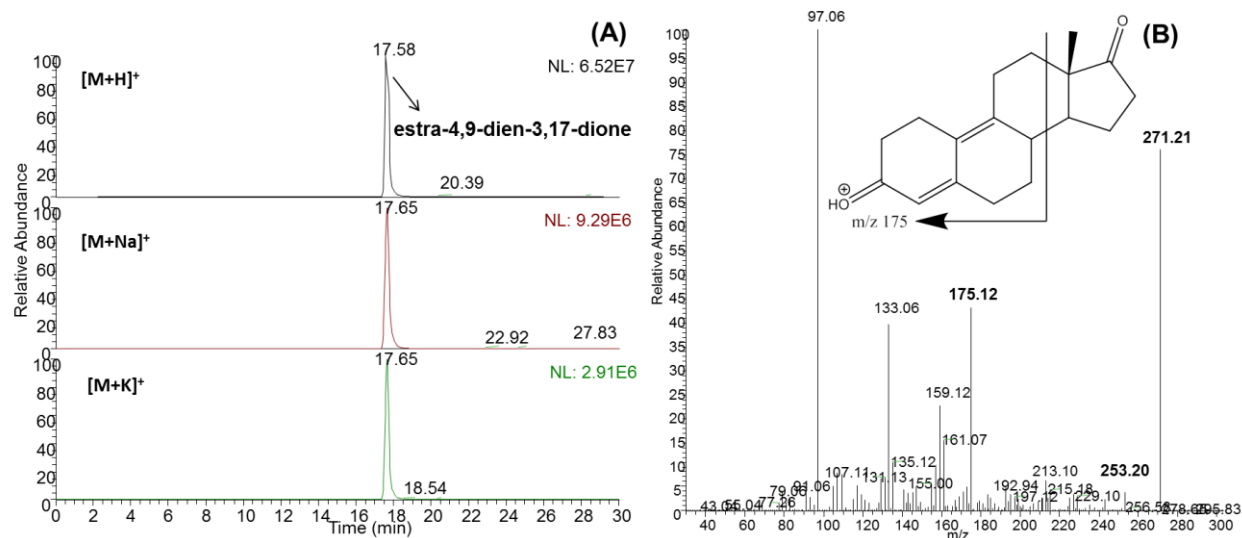


Figure 6.2. LC-HRMS extracted ion chromatogram of estradienedione in the steroid product (A) and LC-MS/MS product ion scan mass spectrum at 25 eV (B).

3.2 *In vitro* metabolism studies

The HLM incubation samples with estradienedione were first analyzed by a LC-MS/MS precursor ion scan method with as selected product ions m/z 77, 91 and 105. The application of the precursor ion scan method led to the detection of two metabolites (M1 and M2). Two additional metabolites (M3 and M4) were detected in the *in vitro* metabolism samples by LC-HRMS (Figure 6.3). The results of the 4 h incubation sample are presented in Figure 6.3, however similar results were obtained in the other incubations samples (2 and 18 h).

The proposed metabolic modifications, based on the observed m/z difference in comparison with the parent compound, are indicated in Table 6.1 and could be linked to the metabolites with less than 2 ppm mass deviation by LC-HRMS.

Product ion scans were performed to obtain more structural information of the metabolites. Therefore, fragmentation patterns of the parent compound were studied first to identify characteristic fragment ions (Figure 6.2). The fragmentation behavior of estradienedione was similar to that of trenbolone [20]. As for trenbolone, only one loss of water (m/z 253) was observed for estradienedione, despite the presence of two oxygen atoms. In addition, a typical fragment ion m/z 175 derived from the A-, B- and C-rings was detected (Figure 6.2). This fragment ion was also described by Scarth *et al.* [6].

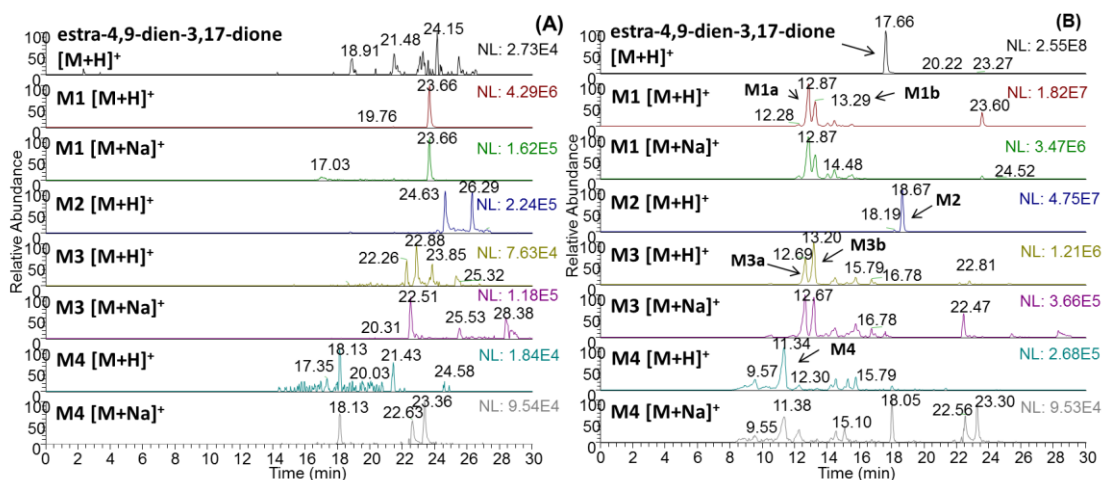


Figure 6.3. Extracted LC-HRMS ion chromatograms of the parent compound and metabolites M1-M4 in a (A) negative control sample and a (B) 4 h HLM incubation sample of estradienedione.

In the product ion scan mass spectrum of M1 (a/b) fragment ions related to the loss of water, m/z 269 ($-H_2O$) and m/z 251 ($-2H_2O$), were observed (Figure 6.4). The lack of fragment ion m/z 175 for M1 (a/b) suggests that a hydroxylation occurred in the A-, B-, or C-ring [6]. The ion m/z 141 indicates a hydroxylation in the A- or B-ring rather than the C-ring. A similar metabolite was detected by Scarth *et al.* [6], for which a hydroxylation was proposed at C6. However, the exact position of the hydroxylation could not be established unequivocally. As suggested by Fragkaki *et al.* for other steroids with conjugated double bonds ($\Delta 4,9$ or $\Delta 4,9,11$) a hydroxylation at position 2 would also be feasible [21].

The product ion scan mass spectrum of metabolite M2 is identical to the mass spectrum of the metabolite described by Scarth *et al.* with as suggested structure 17β -hydroxy-estra-4,9-diene-3-one [6]. In contrast to Scarth *et al.*, this metabolite could be confirmed unequivocally in our study by comparison with reference material. This metabolite was also described as main metabolite in a human excretion study with estradienedione [14]. Although 3-keto reduced and 3,17-keto reduced metabolites were also described in that study, these metabolites were not detected in ours and in the *in vitro* (human S9 liver fractions) metabolism studies performed by Scarth *et al.* [6]. Moreover, for closely related steroids, e.g. trenbolone, it was observed that the presence of the conjugated double bond system inhibits reductive metabolism of the A-ring [6]. Therefore it might also be expected that reduction at position 17 would be more significant [6]. However, the double reduced metabolite was also described as minor equine pathway [6].

For metabolite M3 (a/b) two losses of water molecules were observed (m/z 271 and 253) but no additional information could be obtained for the positions of reduction and hydroxylation from the product ion scan data.

No further information was obtained for the positions of hydroxylations for the dihydroxylated metabolite M4.

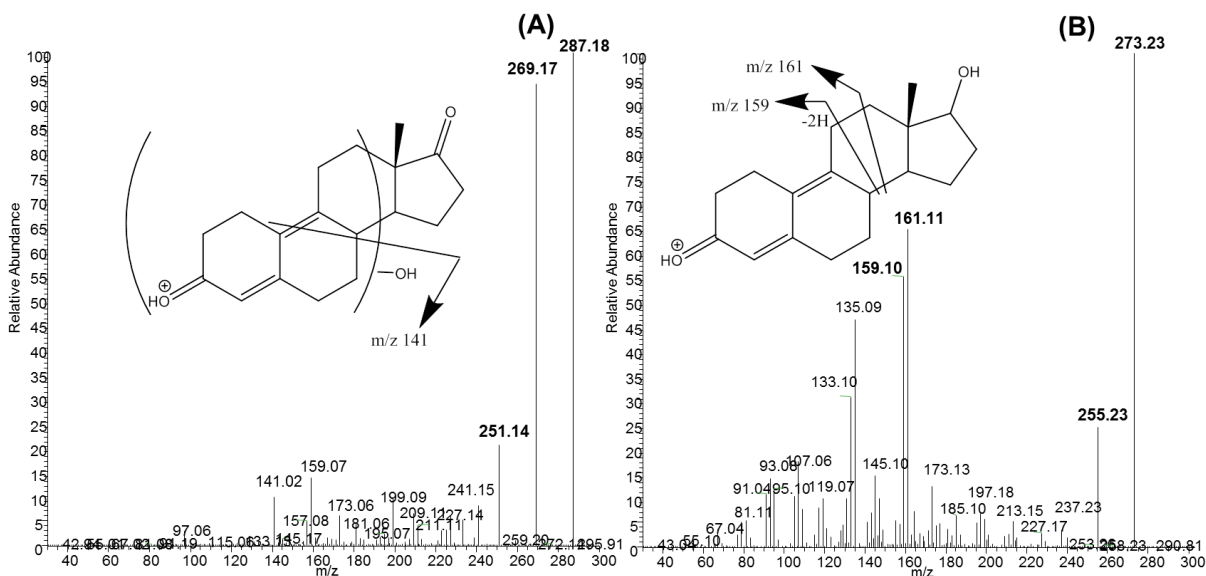


Figure 6.4. Product ion scan mass spectrum of (A) M1a (m/z 287) at 15 eV and (B) M2 (m/z 273) at 25eV and proposed fragmentation pathways.

To allow a proper detection of compounds with lower proton affinities GC-MS analysis was also performed. However, due to the conjugated double bond systems in the structure some problems were observed for the detection of the derivatized compounds and only metabolites M1 and M2 could be detected in the *in vitro* metabolism samples by full scan GC-MS analysis.

3.3 *In vivo* metabolism studies

The metabolism of *estra-4,6-diene-3,17-dione* was also studied in both non-chimeric and chimeric mice, which allows determination of interspecies differences. The relative abundances of the metabolites relative to M2 observed in the chimeric mouse urine samples are indicated in Table 6.1.

Table 6.1. Overview of estradiol-4,9-diene-3,17-dione metabolites detected in metabolism studies with HLM and the chimeric mouse model by LC-HRMS and GC-MS.

Compound	Metabolic reaction ^a	Chemical Formula	Experimental m/z [M+H] ⁺	Δ ppm	HLM RRT ^b		Chimeric mice	
					LC	GC	LC	Relative abundance (%) ^d
Estra-4,9-diene-3,17-dione	Parent compound	C ₁₈ H ₂₂ O ₂	271.1693	0.19	0.83	0.87	√	3.82
IS^c	17 α -methyl-testosterone	C ₂₁ H ₃₀ O ₂	303.2319	0.23	1.00	1.00	√	4.45
M1 (a/b)	Hydroxylation	C ₁₈ H ₂₂ O ₃	287.1640	0.70	0.61/0.63	0.98	√/√	12.62/18.17
M2	Reduction	C ₁₈ H ₂₄ O ₂	273.1849	0.11	0.89	0.90	√	100
M3 (a/b)	Reduction + hydroxylation	C ₁₈ H ₂₄ O ₃	289.1798	0.07	0.60/0.64	/	√/√	52.40/9.01
M4	Dihydroxylation	C ₁₈ H ₂₂ O ₄	303.1590	0.20	0.54	/	/	/

^a metabolic reaction to the parent compound

^b RRT= relative retention time, relative to retention time of the IS (LC RT:21.06 min; GC RT:8.20 min)

^c IS = 17 α -methyltestosterone

^d Relative abundances were calculated in the chimeric mouse urine samples, relative to the most abundant metabolite (M2).

Metabolites M1, M2 and M3 were detected in the murine urine samples by LC-MS (Table 6.1). Similar to what was observed in the HLM assays and was reported before, metabolite M2 was the main metabolite of estra-4,9-diene-3,17-dione in the chimeric mouse model. The dihydroxylated metabolite M4 was only detected in the non-chimeric mouse urine samples. As M4 is not detected in the chimeric mouse urine samples, this rather indicates a production by mouse hepatocytes and suggests M4 is not a typical human metabolite.

4 Conclusions

Human liver microsomes and a chimeric uPA^{+/+}-SCID mouse model were applied to investigate the metabolism of the steroid product ‘Tren-X’ containing the steroid estra-4,9-diene-3,17-dione.

In both models metabolite M2 could be detected as main metabolite. M2 was unequivocally identified with commercially available reference material as 17 β -hydroxy-estra-4,9-diene-3-one. M2 has previously been described as major human metabolite of estra-4,9-diene-3,17-dione, confirming our results [14]. In addition hydroxylated (M1 a/b) and hydroxylated 17-keto reduced (M3 a/b) metabolites were detected in our study via both the *in vitro* and the *in vivo* model.

In the *in vitro* incubation and non-chimeric mouse urine samples also a dihydroxylated metabolite (M4) could be detected. As metabolite M4 has never been reported before, the relevance as marker for human administration of estra-4,9-diene-3,17-dione is unknown. However, the presence of this metabolite could also be related to the higher hydroxylation rates generally observed in the HLM model.

The results obtained in the HLM model are similar to the chimeric mouse model. Moreover, the metabolites observed in this study are confirmed by previously reported studies [6, 14]. Therefore, these results indicate that HLM metabolism studies can be a valuable alternative for *in vivo* excretion studies with designer steroids. In the future this offers a lot of opportunities to improve screening methods in the framework of doping control worldwide.

Acknowledgements

This study was financially supported by the Partnership for Clean Competition (PCC). The authors want to thank Daniel Eichner, Thane Campbell and Vinod Nair from the Sports Medicine Research and Testing Laboratory (SMRTL) and Lieven Verhoye from CEVAC for their technical assistance.

References

1. Scarth JP, Spencer HA, Hudson SC, Teale P, Gray BP, and Hillyer LL (2010). The application of in vitro technologies to study the metabolism of the androgenic/anabolic steroid stanozolol in the equine. *Steroids* 75, 57-69.
2. Kazlauskas R (2010). Designer steroids. In *Handb Exp Pharmacol* (Thieme, D., and Hemmersbach, P., Eds.) 195, 155-185.
3. Kohler M, Thomas A, Geyer H, Petrou M, Schänzer W, and Thevis M (2010). Confiscated black market products and nutritional supplements with non-approved ingredients analyzed in the Cologne Doping Control Laboratory 2009. *Drug Test. Anal.* 2, 533-537.
4. Geyer H, Parr MK, Koehler K, Mareck U, Schänzer W, and Thevis M (2008). Nutritional supplements cross-contaminated and faked with doping substances. *J. Mass Spectrom.* 43, 892-902.
5. Van Thuyne W, Van Eenoo P, and Delbeke FT (2006). Nutritional supplements: prevalence of use and contamination with doping agents. *Nutr. Res. Rev.* 19, 147-158.
6. Scarth JP, Clarke AD, Teale P, and Pearce CM (2010). Comparative in vitro metabolism of the 'designer' steroid estra-4,9-diene-3,17-dione between the equine, canine and human: Identification of target metabolites for use in sports doping control. *Steroids* 75, 643-652.
7. WADA. The 2016 Prohibited List, International Standard. Montreal (2016) <https://wada-main-prod.s3.amazonaws.com/resources/files/wada-2016-prohibited-list-en.pdf> (access date 04.01.16).
8. Jia L, and Liu X (2007). The conduct of drug metabolism studies considered good practice (II): in vitro experiments. *Curr. Drug Metab.* 8, 822-829.
9. Lootens L, Van Eenoo P, Meuleman P, Leroux-Roels G, and Delbeke FT (2009). The uPA(+/-)-SCID Mouse with Humanized Liver as a Model for in Vivo Metabolism of 4-Androstene-3,17-dione. *Drug Metab. Dispos.* 37, 2367-2374.
10. Lootens L, Meuleman P, Pozo OJ, Van Eenoo P, Leroux-Roels G, and Delbeke FT (2009). uPA(+/-)-SCID Mouse with Humanized Liver as a Model for In Vivo Metabolism of Exogenous Steroids: Methandienone as a Case Study. *Clin. Chem.* 55, 1783-1793.
11. Pozo OJ, Lootens L, Van Eenoo P, Deventer K, Meuleman P, Leroux-Roels G, Parr MK, Schänzer W, and Delbeke FT (2009). Combination of liquid-chromatography tandem mass spectrometry in different scan modes with human and chimeric mouse urine for the study of steroid metabolism. *Drug Test. Anal.* 1, 554-567.
12. Lootens L, Meuleman P, Leroux-Roels G, and Van Eenoo P (2011). Metabolic studies with promagnon, methylclostebol and methasterone in the uPA(+/-)-SCID chimeric mice. *J. Steroid Biochem. Mol. Biol.* 127, 374-381.
13. Lootens L, Van Eenoo P, Meuleman P, Pozo OJ, Van Renterghem P, Leroux-Roels G, and Delbeke FT (2009). Steroid metabolism in chimeric mice with humanized liver. *Drug Test. Anal.* 1, 531-537.
14. Parr MK, Geyer H, Gütschow M, Haenelt N, Opfermann G, Thevis M, and Schänzer W (2008). New steroids on the "supplement" market, In *Recent Advances in Doping Analysis* (16) ,

- Proceedings of the 26th Cologne Workshop on dope analysis (Schänzer W, Geyer H, Gotzmann A, and Mareck-Engelke U, Eds.), pp 73-82, Sport & Buch Strauss, Cologne, Germany.
15. Pozo OJ, Deventer K, Eenoo PV, and Delbeke FT (2008). Efficient approach for the comprehensive detection of unknown anabolic steroids and metabolites in human urine by liquid chromatography-electrospray-tandem mass spectrometry. *Anal. Chem.* 80, 1709-1720.
 16. Meuleman P, Libbrecht L, De Vos R, de Hemptinne B, Gevaert K, Vandekerckhove J, Roskams T, and Leroux-Roels G (2005). Morphological and biochemical characterization of a human liver in a uPA-SCID mouse chimera. *Hepatology* 41, 847-856.
 17. Deboer D, Bernal MEG, Vanoooyen RD, and Maes RAA (1991). The analysis of trenbolone and the human urinary metabolites of trenbolone acetate by gas-chromatography mass-spectrometry and gas-chromatography tandem mass-spectrometry. *Biol. Mass Spectrom.* 20, 459-466.
 18. Marques MAS, Pereira HMG, Padilha MC, and Neto FRD (2007). Analysis of synthetic 19-norsteroids trenbolone, tetrahydrogestrinone and gestrinone by gas chromatography-mass spectrometry. *J. Chromatogr. A* 1150, 215-225.
 19. Marcos J, and Pozo OJ (2015). Derivatization of steroids in biological samples for GC-MS and LC-MS analyses. *Bioanalysis* 7, 2515-2536.
 20. Pozo OJ, Van Eenoo P, Deventer K, Grimalt S, Sancho JV, Hernandez F, and Delbeke FT (2008). Collision-induced dissociation of 3-keto anabolic steroids and related compounds after electrospray ionization. Considerations for structural elucidation. *Rapid Commun. Mass Spectrom.* 22, 4009-4024.
 21. Fragkaki AG, Angelis YS, Tsantili-Kakoulidou A, Koupparis M, and Georgakopoulos C (2009). Schemes of metabolic patterns of anabolic androgenic steroids for the estimation of metabolites of designer steroids in human urine. *J. Steroid Biochem. Mol. Biol.* 115, 44-61.

Chapter 7

Dilute-and-shoot LC-HRMS method for the detection of (un)conjugated AAS

In vitro application: synthesis of glucuronide conjugates

Adapted from:

Tudela E, Deventer K, Geldof L and Van Eenoo P (2015). Urinary detection of conjugated and unconjugated anabolic steroids by dilute-and-shoot liquid chromatography-high resolution mass spectrometry. *Drug Testing and Analysis* 7, 95-108.

Abstract

Anabolic androgenic steroids (AAS) are an important class of doping agents. The metabolism of these substances is generally very extensive and includes phase I and phase II pathways. In this work a comprehensive detection of these metabolites is described using a 2-fold dilution of urine and subsequent analysis by liquid chromatography - high resolution mass spectrometry (LC-HRMS). The method was applied to study 32 different metabolites, excreted free or conjugated (glucuronide or sulfate), which permit the detection of misuse of at least 21 anabolic steroids. The method has been fully validated for 21 target compounds (8 glucuronide, 1 sulfate and 12 free steroids) and 18 out of 21 compounds had detection limits in the range of 1-10 ng/mL in urine. For the conjugated compounds for which no reference standards are available, metabolites were synthesized *in vitro* or excretion studies were investigated. The detection limits for these compounds ranged between 0.5 and 18 ng/mL in urine.

The simple and straightforward methodology complements the traditional methods based on hydrolysis, liquid-liquid extraction, derivatization and analysis by gas chromatography-mass spectrometry (GC-MS) and liquid chromatography-mass spectrometry (LC-MS).

1 Introduction

Anabolic-androgenic steroids (AAS) are an important group of synthetic compounds derived from testosterone and are commonly used by athletes and non-athletes to enhance physical performance. The effects and the side effects of these compounds are well known [1], for these reasons they are classified as prohibited substances by the World Anti-Doping Agency (WADA) [2]. The category of AAS represents the most detected banned compounds by WADA accredited laboratories [3], and therefore investigations on development of analytical methods for anabolic steroids is still of great importance in doping control.

AAS are transformed within the human body following both phase I and phase II metabolic pathways facilitating their elimination. Phase I reactions include i.a. oxidation and reduction, whereas phase II transformations imply the conjugation of the compound with glucuronic acid, sulfate, acyl or methyl groups, amino acids or glutathione. Among these phase II reactions, the most common reactions in humans are the formation of the corresponding glucuronide or sulfate [4].

In general, analytical methods to detect AAS include hydrolysis, extraction and detection by liquid chromatography-mass spectrometry (LC-MS) [5] or by gas chromatography-mass spectrometry (GC-MS) (after a derivatization step) [6, 7]. Both GC-MS and LC-MS present advantages and disadvantages for some steroids and currently, a combination of both needs to be applied in anti-doping laboratories to successfully detect all prohibited steroids. The detection of the intact conjugated anabolic steroid presents the advantage of simplified sample preparation, as the hydrolysis is not mandatory. Additionally, problems in relation with enzymatic hydrolysis have been reported. For example, the enzymatic hydrolysis can be incomplete due to a complex urinary matrix [8] or due to the presence of certain drugs in the urine [9]. Furthermore, the detection can be hampered due to elevated background or by interferences [10]. Normally, for the cleavage of both glucuronide and sulfate conjugates hydrolysis using digestive juice of *Helix pomatia* (Hp) which contains both β -glucuronidase and arylsulfatase activities, is useful. However, problems associated with the production of artifacts [11] and conversion between steroids [12] have also been described.

It has been reported that in some situations the detection of the corresponding conjugate can present advantages compared to the aglycone. For example, the detection of stanozolol misuse improves when 3'-hydroxystanozolol glucuronide is monitored instead of the corresponding aglycone [13]. Furthermore, the detection of glucuronide metabolites of stanozolol gives the opportunity to discriminate between metabolites which differ in the location of the glucuronide moiety improving the knowledge on the metabolism [14]. Moreover, several steroidal structures are currently difficult to detect by LC-MS due to lack of an ionizable moiety [15]. In such cases, it should be investigated if the conjugated steroid

might offer better ionization properties. Indeed, some anabolic steroids, like 5 α - and 5 β -methyltestosterone metabolites, typically monitored by GC-MS, have been detected as glucuronide by LC-MS highlighting the importance of this approach [16].

Normally the analysis of glucuronidated AAS from biological matrices like urine starts with an extraction based on liquid-liquid [17-19] or solid phase extraction [14, 16, 18, 20-22] followed by LC-MS [8, 17-19, 21-24] or GC-MS [20]. LC-MS is a more suitable technique as no derivatization is required and the ionization in both positive and negative mode for the detection of glucuronidated AAS is possible. On the other hand, because faster screening methods are highly desirable in order to face the increasing number of doping-control samples and to decrease reporting times, minimization of sample preparation is of high interest. In this sense application of dilute-and-shoot liquid chromatography mass spectrometry (DS-LC-MS) in urine can reduce significantly turnaround time and reagent costs. Hence, this approach has been successfully applied for other classes of prohibited substances [25]. Only a few examples with selected glucuronidated anabolic steroids have been reported using this technique [14, 19].

Therefore the aim of this paper was to investigate and evaluate the applicability of DS-LC-MS approach in routine doping control analysis, for the direct detection of AAS. More than thirty compounds excreted as conjugates (glucuronides and sulfates) and as free steroids in diluted urine were tested. It should be noted that throughout this manuscript concentrations of conjugated steroids are expressed as aglycone equivalents to allow a direct interpretation of the MRPL criteria with the one described by WADA [26].

2 Materials and Methods

2.1 Chemical and Reagents

9 α -fluoro-17 α -methyl-4-androsten-3 α ,6 β ,11 β ,17 β -tetrol (FLUm1), 9 α -fluoro-17,17-dimethyl-18-norandrosta-4,13-dien-11 β -ol-3-one (FLUm2), 4-chloro-methandienone (CMD), 6 β -hydroxy-4-chloro-methandienone (CMDm), 6 β -hydroxymethandienone (MEDm1), epioxandrolone (OXAm), 2-hydroxymethyl-17 α -methyl-androstan-1,4-dien-11 α ,17 β -diol-3-one (FMBm1), 17 α -epimethandienone (MEDm2), Boldenone glucuronide (BOLDG; potassium salt), Boldenone sulfate (BOLDS; triethylamine salt), 5 β -androst-1-en-17 β -ol-3-one glucuronide (BOLDmG), 2 α -methyl-5 α -androstan-3 α -ol-17-one glucuronide (DROmG; sodium salt), 1 α -methyl-5 α -androstan-3 α -ol-17-one glucuronide (MESm1G; sodium salt), 1 α -methyl-5 α -androstan-3 α ,17 β -diol glucuronide (MESm2G), 1-methylene-5 α -androstan-3 α -ol-17-one glucuronide (MTNmG; sodium salt), 7 β ,17 α -dimethyl-5 β -androstane-3 α ,17 β -diol glucuronide (CALmG; sodium salt), 7 α ,17 α -dimethyl-5 β -androstane-3 α ,17 β -diol glucuronide (BOLmG; sodium salt), 3'-hydroxy-stanozolol glucuronide (3STANG), 19-Norandrosterone glucuronide (NANGm1; sodium salt), 19-Norethiocholanolone glucuronide

(NANGm2; sodium salt) and the internal standard d3-epitestosterone glucuronide (EGd3) were purchased from the National Measurement Institute (North Ryde, Australia). 17-epimethyltestosterone (METm3) was obtained from TRC (Toronto, Canada). 17 α -methyl-11 α ,17 β -diol-4-androsten-3-one (FMBm2) was purchased from Steraloids (Newport, R.I, U.S.A). Ethisterone (DANm) and oxandrolone (OXA) were kind gifts from Winthrop, Laboratório de Análises e Dopagem (Instituto do Desporto, Lisbon, Portugal) and Searle & Co (Chicago, IL, USA), respectively.

LC grade methanol (MeOH) and LC grade water were purchased from Biosolve (Valkenswaard, Netherlands). Ammonium acetate (NH₄OAc) was obtained from Sigma (St. Louis, MO, USA). Ammonium formate p.a. and formic acid Optima[®] LC-MS were purchased from Fischer Scientific (Loughborough, UK). Hydrochloric acid (HCl), ammonium hydroxide (NH₄OH), acetic acid (HOAc) p.a., sodium acetate p.a., potassium carbonate (K₂CO₃), sodium hydrogencarbonate (NaHCO₃) were of analytical grade and were purchased from Merck (Darmstadt, Germany). Stock solutions were prepared by dissolving the reference material in MeOH and stored at -15 °C. Working solutions were prepared by diluting adequate amounts of stock solutions in MeOH and stored at -15 °C.

For the *in vitro* synthesis of glucuronide-conjugated anabolic steroids, pooled human liver microsomes (HLM) from 20-30 donors (452161) and uridine diphosphate-glucuronosyltransferase (UGT) reaction mix solutions A (25 mM Uridine 5'-Diphospho-Glucuronic Acid, UDPGA, in water; catalog number 451300) and B (250 mM Tris-HCl, 40 mM MgCl₂, 0.125 mg/mL Alamethicin in water; catalog number 451320) were obtained from BD Gentest (Erembodegem, Belgium). The ethanol was purchased from Biosolve (Valkenswaard, the Netherlands).

2.2 Instrumentation

The liquid chromatographic system was an Accela LC (Thermo Scientific, Bremen, Germany) equipped with degasser, Accela 1250 pump, autosampler thermostated at 10 °C and a heated column compartment at 35 °C. The LC separation was performed on a Varian Omnispher C18 column (100mm×2mm I.D., 3 μ m) (Varian, Sint-Katelijne-Waver, Belgium) at a flow rate of 250 μ L/min using a ChromSep guard column (10mm×2mm I.D., 5 μ m) (Varian, Sint-Katelijne-Waver, Belgium). The LC effluent was pumped to an Exactive benchtop Orbitrap-based high resolution mass spectrometer (Thermo Scientific, Bremen, Germany) operated in the positive–negative polarity switching modes and equipped with an electrospray ionization (ESI) source. Nitrogen sheath gas flow rate and auxiliary gas were set at 60 and 30 (arbitrary units), respectively. The capillary temperature was 250 °C, the spray voltage 4 kV or -4 kV and the capillary voltage 30 V in positive or negative ion modes. The instrument operated in full scan mode from m/z 100 to 2000 at 50,000 resolving power. The

automatic gain control (AGC) was $10e^6$. The Orbitrap performance in both positive and negative ionization modes was evaluated daily and external calibration of the mass spectrometer was done with Exactive Calibration Kit solutions (Sigma–Aldrich, St. Louis, USA and ABCR GmbH & Co. KG, Karlsruhe, Germany). A tolerance window of 5 ppm was applied to process the data.

The aqueous and methanolic mobile phases consisted both of 1mM NH_4OAc and 0.1% HOAc. The percentage of organic and aqueous solvent in the gradient is presented in Figure 7.1.

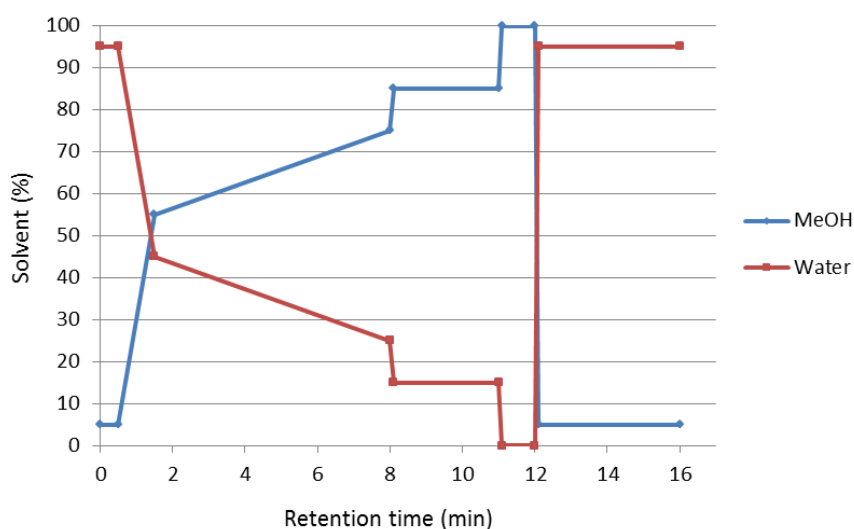


Figure 7.1. Optimized gradient.

2.3 Sample preparation

An aliquot of 200 μ L of urine was transferred to an Eppendorf type vial, containing 200 μ L of methanolic internal standard solution (IS, EGd3 40 ng/mL). After centrifugation of the samples (5 min at $14,000 \times g$) 25 μ L of supernatant were injected into the chromatographic system.

2.4 Assay Validation

The qualitative detection of several exogenous anabolic steroids excreted as conjugates or free in human urine was validated regarding specificity, selectivity, limit of detection (LOD) and matrix effects in compliance with the WADA International Standards for Laboratories (ISL) [27] and according to Eurachem guidelines [28].

Ten different blank human urine samples (five male and five female; pH-range from 5.6 to 8.0; specific gravity between 1.003 and 1.026 g/L) were spiked at 1, 2, 5, 10, 20, 50 and 100 ng/mL respectively with a standard solution containing all commercially available

compounds (compounds present in Table 7.1). Blank urine samples and a distilled water sample, spiked only with the IS, were also included. The samples were analyzed according to the described protocol. The LOD was defined as the lowest level at which an analyte can be detected in all ten urine samples using one diagnostic ion (Table 7.1) with a signal to noise (S/N) ratio higher than 3 and a retention time difference no higher than 2% or ± 0.1 min (whichever is smaller) compared with a reference material analyzed in the same analytical batch, as is described in the WADA technical document TD2010IDCR [29]. Only one diagnostic ion was used to monitor each compound (present in Table 7.1), which requires high selectivity and specificity of the ion.

Specificity was tested during the validation procedure by probing for interfering peaks in the selected ion chromatograms at the expected retention times for the target compounds. Selectivity was tested by analyzing several other doping compounds and drugs, including a wide range of beta-blockers, beta-agonists, narcotics, corticosteroids, stimulants and NSAIDs, all of them as 1:1 MeOH-H₂O solutions at 1 $\mu\text{g/mL}$. Matrix effects (M.E.) were studied only for compounds present in Table 7.1, according to Matuszewski *et al.* [30]. Ten urine samples and a water sample were spiked equally at 20 or 100 ng/mL (at 20 ng/mL for those compounds with limit of detection lower than or equal to 20 ng/mL and at 100 ng/mL for compounds with a LOD higher than 20 ng/mL), the areas (A) of each diagnostic ion were compared in both matrices and the mean value of the ten urines was calculated. The formula used was: $\text{M.E. (\%)} = \frac{(A(\text{urine}) - A(\text{standard solution}))}{A(\text{standard solution})} \times 100$.

2.5 *In vitro* synthesis

For the synthesis of (non-commercially available) anabolic steroid glucuronides, the phase II metabolism was simulated using human liver microsomes (HLM). The phase II microsomal incubations were performed using 10 μg of the parent compound as described in Chapter 1 (7.2.2.2 *Protocol in vitro* metabolism studies; Table 1.6).

System blank samples, without the substrate, were also added to study the matrix background. The obtained supernatants, after removal of the HLM, were directly injected into the LC-HRMS system. *In vitro* synthesis was performed for gestrinone, tetrahydrogestrinone, trenbolone, 4 β -hydroxystanozolol and 16 β -hydroxystanozolol.

2.6 Excretion samples/administration samples

Positive samples from earlier approved excretion studies with human participants and quality assessment samples from WADA were used for the study of non-commercially available phase II metabolites of several AAS (compounds present in Table 7.2). These urine samples were analyzed by the current routine methods of our laboratory [7], using a

hydrolysis step. The concentration of the different metabolites was estimated by direct comparison to a quality control sample spiked at the minimum required performance limit (MRPL) of WADA. When necessary, the excretion urines were diluted with blank urine and re-quantified to match these MRPL-levels in order to study if the corresponding compounds can be detected at that concentration or not.

3 Results and discussion

3.1 Mass spectrometry

The study of the full scan spectra of the reference standards of the selected conjugated anabolic steroids (glucuronides and sulfates present in Table 7.1) showed that all these compounds were ionizable in both polarities, which was not possible with all the steroid aglycones due to the lack of ionizable groups.

In negative ion mode the deprotonated molecule ($[M-H]^-$) presents the most abundant species due to the delocalization of the negative charge at the carboxylic acid or sulfate group [17, 19]. In positive ionization the protonated molecule ($[M+H]^+$) constitutes the base peak for those compounds with high proton affinity groups like conjugated 3-keto function (boldenone metabolites, METm3) or a pyrazol group (stanozolol metabolites). For the other unconjugated anabolic steroids, the ammonium adduct ($[M+NH_4]^+$) constitutes the base peak in positive ionization [15, 18].

Due to the presence of the sulfate group in BOLDS it was expected that the negative ion mode would yield a more intense deprotonated molecule than the protonated molecule in positive ion mode. However, a comparable peak intensity was obtained in both polarities.

In general terms, the deprotonated molecular ions in negative ionization were more abundant than the ions in positive ionization, except for the stanozolol metabolites. However the specificity in negative ionization is sometimes lower due to the increased incidence of endogenous interference [18]. Taking into account these parameters, the most abundant and specific ion selected for every compound is shown in Tables 7.1 and 7.2.

Despite the importance of phase II metabolism for exogenous and endogenous anabolic steroids, some metabolites are nevertheless excreted unconjugated [4, 31]. Therefore the detection of metabolites of seven steroids which are excreted unconjugated, including fluoxymesterone, 4-chloro-methandienone, methyltestosterone, methandienone, danazol, oxandrolone and formebolone, were also included in the study. For all substances full scan mass spectra in both positive and negative ionization were studied.

In positive mode, the observed ions were in agreement with previous works, e.g. the sodium adduct ($[M+Na]^+$) and the protonated molecule ($[M+H]^+$) [15]. In negative polarity the

ionization of unconjugated steroids is generally weak, due to the lack of suitable structures, but an abundant acetate adduct ($[M+OAc]^-$) was found for FLUm1 and MEDm1.

Heated Electrospray Ionization Source (HESI) at 250 °C was tested in order to improve the ionization of the target compounds. The abundance of ions like $[M+H]^+$ or $[M-H]^-$ was comparable or higher when a HESI source was used. However, the abundance of adducts like $[M+Na]^+$ or $[M+OAc]^-$ was significantly lower with HESI. For this reason, no HESI source was used in the final method.

Table 7.1. Structure, chemical formula, detected ion and theoretical mass, retention time and standard deviation (n=10) and matrix effects for the commercially available investigated compounds.

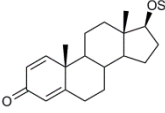
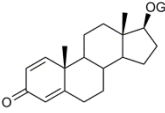
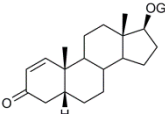
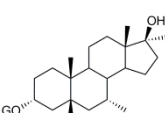
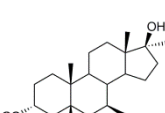
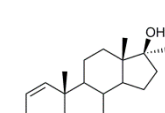
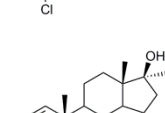
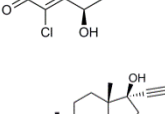
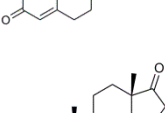
Parent Compound	Target Compound	Structure	Chemical Formula	Adduct ions	<i>m/z</i>	RT ± std (min)	Matrix Effects (%)
Boldenone	BOLDS		C ₁₉ H ₂₆ O ₅ S	[M+Na] ⁺	389.1393	4,43±0.01	-76
	BOLDG		C ₂₅ H ₃₄ O ₈	[M+Na] ⁺	485.2146	4,40±0.02	
	BOLDmG		C ₂₅ H ₃₆ O ₈	[M+Na] ⁺	487.2302	5,90±0.02	
Bolasterone	BOLmG		C ₂₇ H ₄₄ O ₈	[M+NH ₄] ⁺	514.3374	6,58±0.02	-38
Calusterone	CALmG		C ₂₇ H ₄₄ O ₈	[M-H] ⁻	495.2963	7,29±0.01	-26
4-chloro-methandienone	CMD		C ₂₀ H ₂₇ ClO ₂	[M+Na] ⁺	357.1592	8,25±0.01	-6
	CMDm		C ₂₀ H ₂₇ ClO ₃	[M+Na] ⁺	373.1541	5,46±0.01	-70
Danazol	DANm		C ₂₁ H ₂₈ O ₂	[M+H] ⁺	313.2162	7,26±0.02	6
Drostanolone	DROmG		C ₂₆ H ₄₀ O ₈	[M+NH ₄] ⁺	498.3061	8,55±0.02	-20

Table 7.1 Continued.

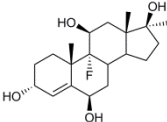
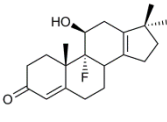
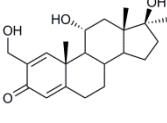
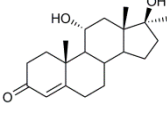
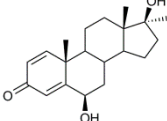
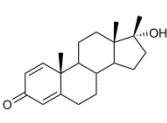
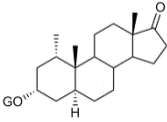
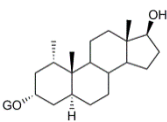
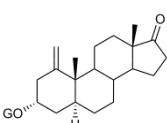
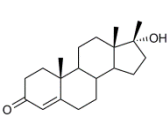
Parent Compound	Target Compound	Structure	Chemical Formula	Adduct ions	<i>m/z</i>	RT ± std (min)	Matrix Effects (%)
Fluoxymesterone	FLUm1		C ₂₀ H ₃₁ FO ₄	[M+OAc] ⁻	413.2345	3,20±0.01	-77
	FLUm2		C ₂₀ H ₂₇ FO ₂	[M+H] ⁺	319.2068	9,60±0.01	8
Formebolone	FMBm1		C ₂₁ H ₃₀ O ₄	[M+Na] ⁺	369.20363	4,72±0.02	-48
	FMBm2		C ₂₀ H ₃₀ O ₃	[M+Na] ⁺	341.2087	5,52±0.01	-65
Methandienone	MEDm1		C ₂₀ H ₂₈ O ₃	[M+OAc] ⁻	375.2177	4,49±0.02	-50
	MEDm2		C ₂₀ H ₂₈ O ₂	[M+Na] ⁺	323.1981	8,56±0.02	-3
Mesterolone	MESm1G		C ₂₆ H ₄₂ O ₈	[M-H] ⁻	479.2650	7,44±0.01	-8
	MESm2G		C ₂₆ H ₄₀ O ₈	[M+NH ₄] ⁺	500.3218	6,52±0.02	-34
Methenolone	MTNmG		C ₂₆ H ₃₈ O ₈	[M-H] ⁻	477.2494	6,63±0.02	-29
Methyltestosterone	METm3		C ₂₀ H ₃₀ O ₂	[M+H] ⁺	303.2319	9,64±0.01	23

Table 7.1 Continued.

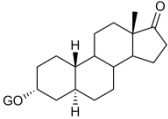
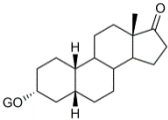
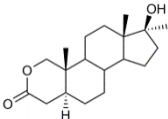
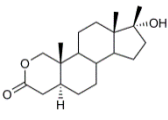
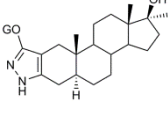
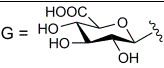
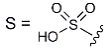
Parent Compound	Target Compound	Structure	Chemical Formula	Adduct ions	<i>m/z</i>	RT ± std (min)	Matrix Effects (%)
Nandrolone	NANm1G		C ₂₄ H ₃₆ O ₈	[M-H] ⁻	451.2337	6,35±0.02	
	NANm2G		C ₂₄ H ₃₆ O ₈	[M-H] ⁻	451.2337	6,03±0.01	-24
Oxandrolone	OXA		C ₁₉ H ₃₀ O ₃	[M+Na] ⁺	329.2087	6,52±0.01	-32
	OXAm		C ₁₉ H ₃₀ O ₃	[M+Na] ⁺	329.2087	8,51±0.02	-13
Stanozolol	3STANG		C ₂₇ H ₄₀ N ₂ O ₈	[M-H] ⁻	519.2712	5,97±0.01	-37
 							

Table 7.2. Structure, chemical formula, detected ions, theoretical and experimental masses and retention time for the non-commercially available investigated compounds.

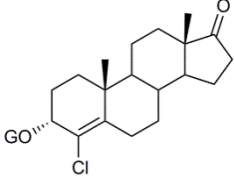
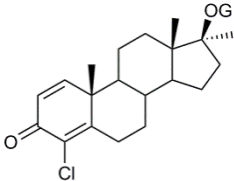
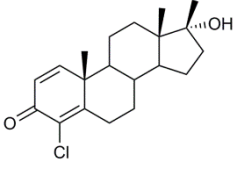
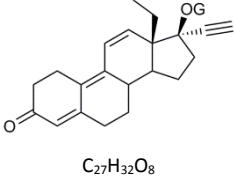
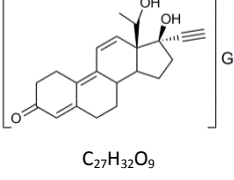
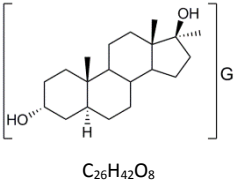
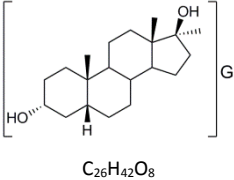
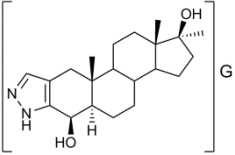
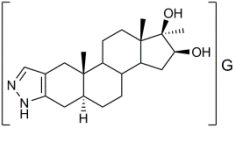
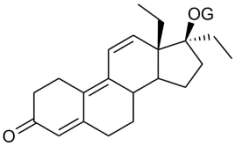
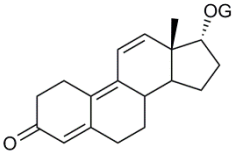
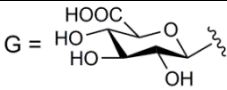
Parent Compound	Target Compound	Structure and Chemical Formula	Adduct ions	Theoretical m/z	Experimental m/z (Δ ppm)	RT (min)
Clostebol	CLOSmG	 $C_{25}H_{35}ClO_8$	$[M-H]^-$	497.1948	497.1945 (0.60)	6.94
			$[M+NH_4]^+$	516.2359	516.2357 (0.39)	
4-chloro-methandienone	CMDG	 $C_{26}H_{35}ClO_8$	$[M-H]^-$	509.1948	509.1955 (1.40)	5.76
			$[M+H]^+$	511.2093	511.2093 (0.00)	
	Epi-CMD	 $C_{20}H_{27}ClO_2$	$[M+H]^+$	335.1772	335.1775 (0.90)	9.74
$[M+H-H_2O]^+$	317.1667	317.1669 (0.63)				
Gestrinone	GESG	 $C_{27}H_{32}O_8$	$[M-H]^-$	483.2024	483.2026 (0.41)	4.49
			$[M+H]^+$	485.2170	485.2157 (2.70)	
	GESmG	 $C_{27}H_{32}O_9$	$[M-H]^-$	499.1974	499.1970 (0.80)	3.85
			$[M+H]^+$	501.2119	501.2123 (0.80)	
Oxymetholone/Methyltestosterone	METm1G	 $C_{26}H_{42}O_8$	$[M-H]^-$	481.2807	481.2800 (1.50)	6.37
			$[M+NH_4]^+$	500.3218	500.3207 (2.20)	
Methandriol/Methyltestosterone	METm2G	 $C_{26}H_{42}O_8$	$[M-H]^-$	481.2807	481.2810 (0.62)	6.30
			$[M+NH_4]^+$	500.3218	500.3208 (2.00)	

Table 7.2. Continued.

Parent Compound	Target Compound	Structure and Chemical Formula	Adduct ions	Theoretical m/z	Experimental m/z (Δ ppm)	RT (min)
Stanozolol	4STANG	 $C_{27}H_{40}N_2O_8$	$[M-H]^-$	519.2712	519.2711 (0.19)	5.54
			$[M+H]^+$	521.2857	521.2857 (0.00)	
	16STANG	 $C_{27}H_{40}N_2O_8$	$[M-H]^-$	519.2712	519.2715 (0.58)	4.94
			$[M+H]^+$	521.2857	521.2846 (2.10)	
Tetrahydrogestrinone	THGG	 $C_{27}H_{36}O_8$	$[M-H]^-$	487.2337	487.2332 (1.00)	5.61
			$[M+H]^+$	489.2483	489.2479 (0.82)	
Trenbolone	TRENmG	 $C_{24}H_{30}O_8$	$[M-H]^-$	445.1868	445.1868 (0.00)	4.60
			$[M+H]^+$	447.2013	447.1999 (1.30)	
 $G =$						

3.2 Chromatography

An Omnisphere C18 column was selected according to previous research, exhibiting good retention and peak shape for steroid glucuronides [17].

Methanol was preferred as organic modifier, because better resolution for conjugated steroids can be achieved compared to acetonitrile [8]. Due to the acidic character of the glucuronides, acidic conditions were necessary in order to improve their chromatographic retention [17]. For these reasons, different percentages of HOAc were evaluated, i.e. 0.1%, 0.01% and 0.001%.

The main difference observed, was that the retention of the anabolic steroid glucuronides increases with decreasing pH. The non-glucuronidated AAS and BOLDS were less affected, which is consistent with their differences in pKa values. Intensity of the signals was comparable independent from the amount of acid used.

Finally attending to the retention of the glucuronidated compounds, the aqueous and methanolic mobile phases consisted both of 1mM ammonium acetate and 0.1% of HOAc.

In order to analyze multiple compounds with great differences in polarity, like glucuronides and neutral compounds, it is important to optimize the gradient of the mobile phase. The two extreme compounds, early-eluting FLUm1 and highly retained FLUm2, were selected to adjust the gradient run.

With the optimized gradient, all the isomeric compounds were baseline separated with a resolution higher than 2 except for NANm1G and NANm2G, which are not completely baseline separated ($R_s = 1.3$). The corresponding retention time for every compound is shown in Table 7.1. A simulated chromatogram of a spiked urine with all the anabolic steroids included in the method is presented in Figure 7.2, presenting the distribution of all compounds along the chromatogram in positive and negative ionization.

3.3 Sample preparation

Since a profound dilution (at least 10-fold) allows to reduce matrix effects [32, 33], a 10-fold dilution of urine with mobile phase was initially applied. Unfortunately pilot tests showed that this dilution did not allow to detect almost any substance at the corresponding MRPL [26]. For this reason, sample dilution was limited to a 2-fold dilution of urine with MeOH.

Due to the limited volume of urine available to anti-doping laboratories, methods requiring small volumes of urine are preferred, especially for screening purposes, in order to leave enough urine if further experiments are necessary. Here, a volume of only 200 μ L of urine was enough for the sample preparation.

3.4 Method validation

The determined LODs for every compound are shown in Table 7.3. All selected parent compounds were detected at concentrations equal or lower than the current MRPL [26] with the exception of boldenone and stanozolol. Previously described screening methods for selected anabolic steroid glucuronides after solid-phase extraction (SPE) [16] or liquid-phase microextraction (LPME) [18] of the urinary samples, show LODs higher than those herein reported with the exception of 3STANG and MTNmG, where the described LOD were as low as 2 ng/mL instead of 5 ng/mL.

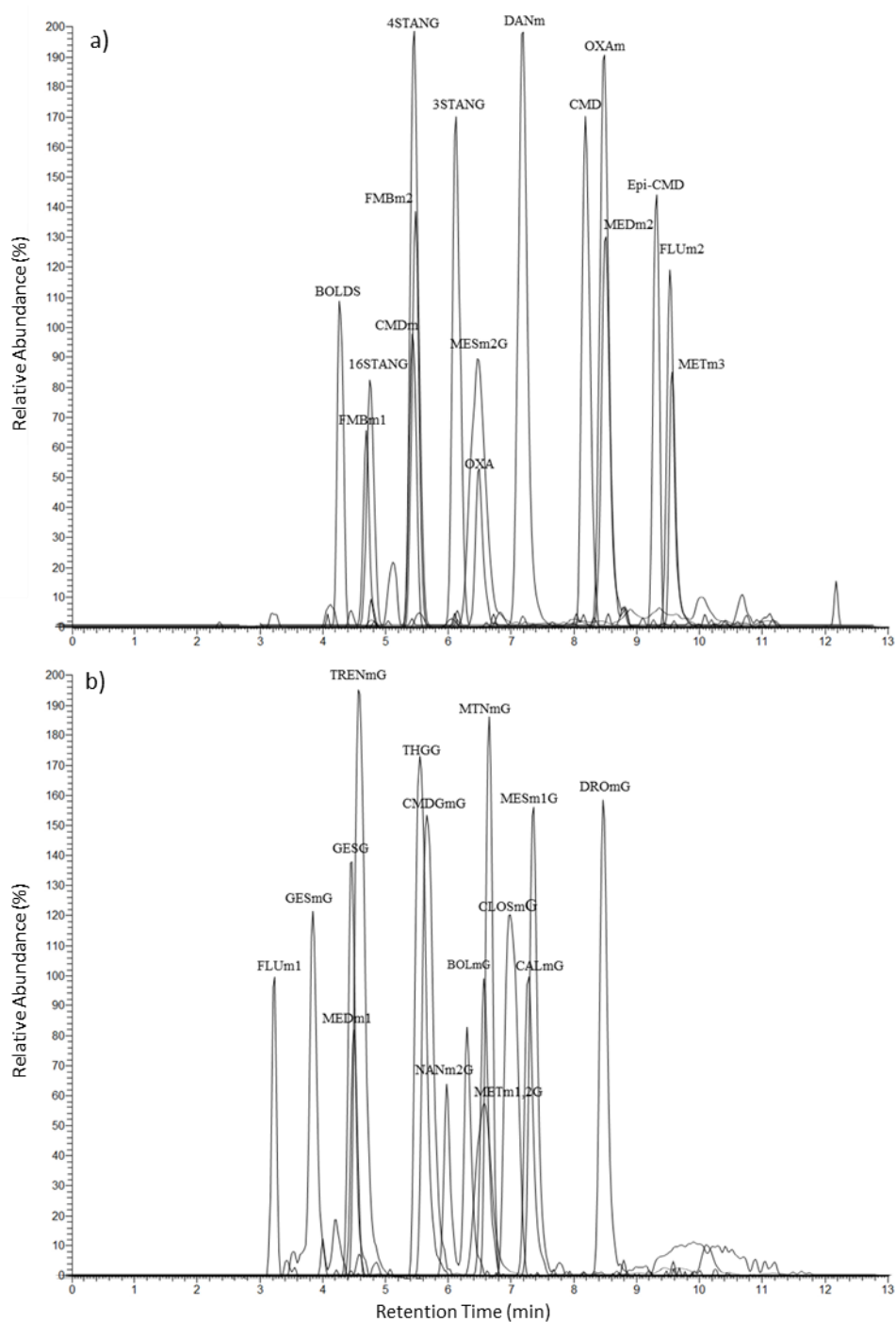


Figure 7.2. Simulated chromatogram of a spiked urine at 50 ng/mL with the compounds included in the DS-LC-HRMS method in positive (A) and negative (B) ionization mode. (The scale was adjusted to visualize all compounds. LOD's are presented in Table 7.3).

BOLDG, BOLDs and BOLDmG co-elute with endogenous compounds, which complicates the detection of boldenone misuse. In the case of BOLDs the most abundant diagnostic ions $[M+H]^+$ and $[M-H]^-$ co-elute with an unknown interference present in all the studied urines. However, the interference is not present in urine from children younger than three years

old, which present lower concentrations of endogenous steroids [34], indicating that the interference is probably an endogenous steroid. The sodium adduct ($[M+Na]^+$) seems to be specific and no interferences were detected and can therefore be used to detect BOLDs without any interference. Unfortunately, its abundance is very small and therefore LOD for BOLDs was very high (100 ng/mL).

For the detection of nandrolone misuse, the main metabolites NANm1G and NANm2G^[35] were monitored. Small interferences were found for NANm1G in negative control urines. Therefore NANm1G could not be included in the validation. However, NANm2G can be used for the detection of nandrolone abuse and a limit of detection of 2 ng/mL is described. The origin of the interference could not be elucidated, but it should be noted that previous studies have indicated that NANm1 is also endogenous [36, 37].

In the case of 3STANG, the target compound was detected in 9 of the 10 urines used for the validation at 2 ng/mL. In one urine however, it was only detected at 5 ng/mL and therefore the LOD was set at this latter level.


All the investigated compounds which are excreted non-conjugated could be detected by the parent compound and/or one metabolite at the corresponding MRPL. Some of the metabolites presented a LOD higher than the corresponding MRPL but at least one target metabolite per parent compound was detectable at the MRPL. Therefore compliance with WADA's technical requirements for misuse of these compounds can still be guaranteed. Indeed, it has been described that the most appropriate way to detect fluoxymesterone misuse is monitoring FLUm2 [38]. In the case of formebolone, FMBm2 is excreted in higher concentration compared with FMBm1 [39] and both MEDm1 and MEDm2 constitute two of the most important metabolites for the detection of methandienone misuse [40]. The compounds FLUm2, CMD, METm3, MEDm2, DANm and OXAm could be detected at 1 ng/mL which constitutes the lowest studied level. For the detection of 4-chloro-methandienone misuse, the parent compound CMD and the main metabolite CMDm are monitored, however only CMD can be detected fulfilling MRPL criteria [26].

The retention times, shown in Table 7.1, seem to be very stable with standard deviations between 0.01 and 0.02 min.

The method is selective when other doping products were analyzed with the described method. One interference was found for METm3, due to the presence in the solution of stebolone which is an isomeric compound. In addition, analysis of ten blank urines did not result in the detection of interfering substances, demonstrating the specificity of the method.

Table 7.3. Obtained LOD (ng/mL) for the investigated compounds.

	Boldenone	Bolasterone	Calusterone	Clostebol	4-chloro-methandienone	Danazol	Drostanolone	Fluoxymesterone	Formebolone	Gestrinone	Methandienone	Mesterolone	Oxymetholone	Methandiol	Methyltestosterone	Methenolone	Nandrolone	Oxandrolone	Stanozolol	Tetrahydrogestrinone	Trenbolone	
BOLDS	100																					
BOLmG		2																				
CALmG			2																			
CLOSmG				5																		
CMD					1																	
CMDG					*																	
CMDm					5																	
Epi-CMD					*																	
DANm						1																
DROmG							2															
FLUm1								50														
FLUm2								1														
FMBm1									20													
FMBm2									5													
GESG										1												
GESmG										*												
MEDm1											10											
MEDm2											1											
MESm1G												5										
MESm2G												2										
METm1G													5									
METm2G														2	2							
METm3															1							
MTNmG																5						
NANm2G																	2					
OXA																		2				
OXAm																		1				
3STANG																						
4STANG																			5			
16STANG																			0.5			
THGG																					1	
TRENmG																						4

 Excretion urines

* The LOD could not be estimated due to the lack of reference material

The matrix effects could only be identified in those cases where a certified reference material is available. The obtained results are shown in Table 7.1. Most of the compounds present small to moderate matrix effects, either ion enhancement or ion suppression. The matrix effects values range from +23% corresponding to METm3 to -77% of FLUMm1. It is important to note that those compounds with the highest values of ion suppression, like FLUm1 (77%) and BOLDS (76%), are the same compounds with the highest values of LOD, 50 and 100 ng/mL, respectively.

3.5 Excretion urines and *in vitro* synthesis

Only for a limited number of steroids, glucuronidated standards are commercially available (compounds present in Table 7.1). For this reason, several excretion urines were analyzed and exact masses for the parent and/or the main metabolites [31, 41] were extracted from the chromatograms with a mass window of 5 ppm. To verify the correct assignment of the metabolites without reference standard, multiple blank and excretion study urine samples were analyzed and two diagnostic ions were selected for monitoring of these target compounds. The obtained results are shown in Table 7.2.

In order to estimate if these compounds can be detected at the corresponding MRPL [26], the excretion urines were analyzed using the current routine analysis methods [7] of our laboratory and diluted with negative urine to the corresponding MRPL.

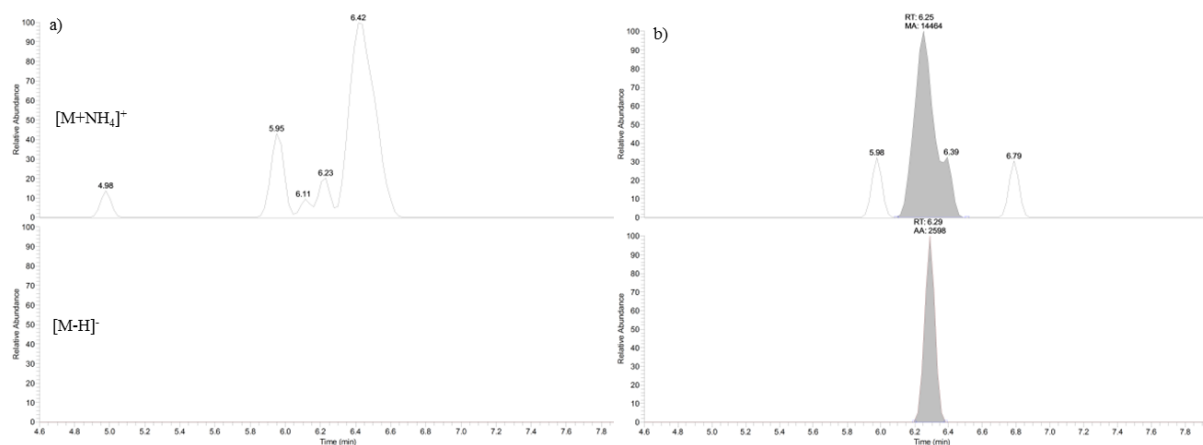


Figure 7.3. Detection of methyltestosterone: (A) Negative urine. (B) METm2G detected in a methyltestosterone excretion urine where only METm2 at 2 ng/mL was detected by GC-MS.

For the isomeric compounds METm1G and METm2G co-elution was observed yielding only one peak. Different anabolic steroids yield at least one of these 2 metabolites (oxymetholone and mestanolone give only METm1G and, methandriol and methandienone give only METm2G) or both in the case of methyltestosterone [31, 41]. Hence, during confirmation analysis both substances should be chromatographically separated to determine which parent AAS was administered. These two metabolites are therefore among the most important metabolites to detect the misuse of a wide-range of compounds and present ionization difficulties in LC-MS, if analyzed as aglycone. In Figure 7.3, a representative chromatogram of METm2G at 2 ng/mL in an excretion urine of methyltestosterone is shown. In those cases, where only a limited number of excretion urines were available, e.g. tetrahydrogestrinone, gestrinone and trenbolone, additional *in vitro* experiments were performed to unequivocally establish the metabolic nature of the identified target peaks, whose mass spectrometric characteristics were compatible with the

expected metabolites. Therefore the corresponding glucuronide conjugates of the parent compound or the metabolites in the excretion urines were confirmed with the corresponding glucuronides synthesized by an earlier-described method by Kuuranne *et al.* [42].

Studying excretion urines of stanozolol, two other isomeric peaks, alongside 3STANG, were observed in the chromatograms, considering two diagnostic ions: the protonated ($[M+H]^+$) and the deprotonated ($[M-H]^-$) molecules. These peaks were assigned to 4 β -hydroxystanozolol glucuronide (4STANG) and 16 β -hydroxystanozolol glucuronide (16STANG). In order to associate every signal to the corresponding isomer, the respective hydroxystanozolol glucuronides were also synthesized *in vitro* and analyzed in the DS-LC-MS method. As described in the method validation section, 3STANG could not be detected at the current MRPL for stanozolol. However in an excretion sample, where the concentration of 3STAN, 4STAN and 16STAN were estimated at 0.3, 0.5 and 1 ng/mL, respectively, only 4STANG was detectable with the DS-LC-MS method. Hence monitoring 4STANG metabolite allows for the control of stanozolol at MRPL-level.

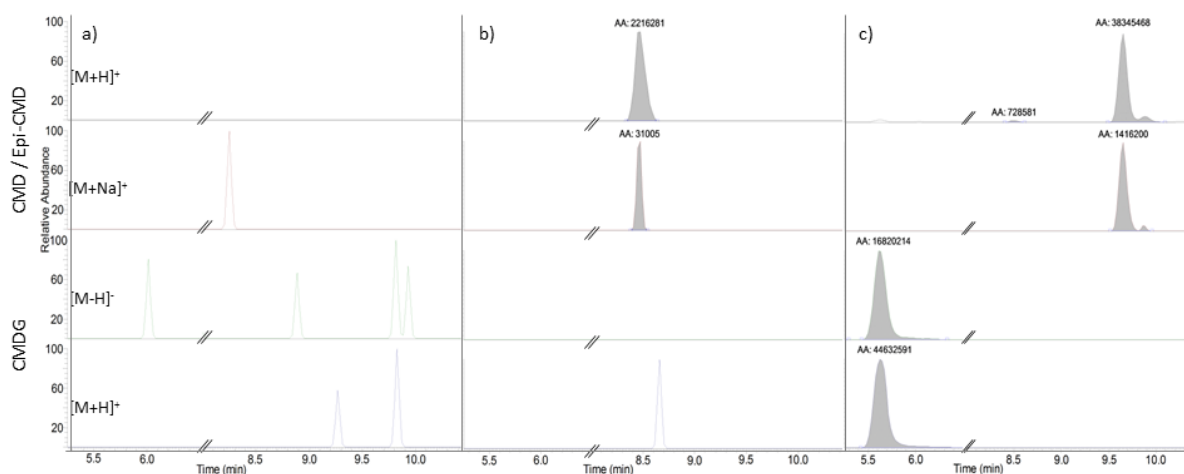


Figure 7.4. Detection of CMD misuse. (A) Negative urine. (B) Spiked urine with CMD (100 ng/mL). (C) CMD excretion urine.

Despite the fact that CMD was compliant with the MRPL of 2 ng/mL, using spiked urines, the investigation of excretion urine samples not only yielded the detection of CMD in some urine samples but also an isomeric compound which was baseline separated and present at a higher abundance and increased retention (Figure 7.4). Furthermore, an abundant signal corresponding to a glucuronide conjugate of CMD or the isomeric compound was also detected (Figure 7.4). The collection of a fraction containing the glucuronide species and further hydrolysis revealed that this substance corresponds to the parent compound CMD. The presence of CMDG in human urine is also in agreement with one of the first investigations of the metabolism of CMD [43] but is in contrast with others where no parent

compound was detected [44, 45]. Product ion scan spectra of these two analytes showed similar fragments but in different relative abundances. This fact suggests that the isomeric compound is most probably the 17-epi-chloro-methandienone (epi-CMD) which is excreted unconjugated because it is formed through the corresponding 17 β -sulfate conjugate [4]. This 17-epimer has been described as a minor metabolite by GC-MS [45], however the abundance observed by LC-HRMS is higher than the parent compound (Figure 7.4).

Obviously, due to the lack of reference material, the validation of the method for compounds present in Table 7.2 was limited to establishing selectivity and specificity and an estimation of the LOD. No matrix effect however could be established. Therefore, they were not considered as fully validated although the method is clearly suited for their detection.

4 Conclusions

For the first time a validated DS-LC-HRMS method for the detection of 32 AAS in urine has been described (Figure 7.2). The method includes both conjugated and unconjugated substances. The direct detection of the intact phase II metabolites offers the possibility to detect by LC-MS several steroids which are not ionizable as aglycones.

The lack of hydrolysis and extraction procedures allows very rapid analyses that have the required sensitivity and consumes only a small amount of urine.

For 21 AAS reference standards were available and for these steroids the method could be fully validated. Fifteen steroids were fully compliant with WADA's MRPL requirements and LODs were ranging between 1 and 20 ng/mL and the method seems to be specific and selective. For eleven steroids, another approach, using *in vitro* experiments and/or use of excretion urines needed to be developed.

The use of excretion urines allowed for the identification of conjugated species which are not commercially available. Furthermore, the study of the metabolism and the detection of new species give the opportunity to improve the current method by monitoring other substances with higher sensitivity. Including the species detected in excretion urines, the developed method can be used for the detection of 32 compounds, which are baseline separated with the exception of the diastereoisomeric metabolites of methyltestosterone METm1 and METm2. The *in vitro* synthesis of different glucuronides allows the confirmation of the presence of these species in excretion urines.

Because the mass spectrometer operates in full scan mode, a retrospective analysis of the samples can be applied and more compounds can be included without the need to modify the method. The open detection of compounds gives flexibility to the method with the

possibility to detect unknown steroids, improving the knowledge in the metabolism and improving the scope of the method as has been previously demonstrated [19].

Acknowledgements

The authors wish to thank WADA for financial support (grant 11A17PV).

Authors also gratefully acknowledge the technical assistance of Fiona Hooghe, Wim Van Gansbeke, Dominique Dhaenens and Kris Roels.

References

1. Maravelias C, Dona A, Stefanidou M, and Spiliopoulou C (2005). Adverse effects of anabolic steroids in athletes - A constant threat. *Toxicol. Lett.* 158, 167-175.
2. WADA (2013). The 2013 Prohibited List, International Standard, World Anti-Doping Agency (WADA), Montreal.
3. WADA (2011). 2011 Adverse Analytical Findings and Atypical Findings Reported by Accredited Laboratories, World Anti-Doping Agency (WADA), Montreal.
4. Schänzer W (1996). Metabolism of anabolic androgenic steroids. *Clin. Chem.* 42, 1001-1020.
5. Jeon BW, Yoo HH, Jeong ES, Kim HJ, Jin C, Kim DH, and Lee J (2011). LC-ESI/MS/MS method for rapid screening and confirmation of 44 exogenous anabolic steroids in human urine. *Anal. Bioanal. Chem.* 401, 1353-1363.
6. Mazzarino M, Oreggia M, and Botre F (2007). Application of fast gas chromatography/mass spectrometry for the rapid screening of synthetic anabolic steroids and other drugs in anti-doping analysis. *Rapid Commun. Mass Spectrom.* 21, 4117-4124.
7. Van Eenoo P, Van Gansbeke W, De Brabanter N, Deventer K, and Delbeke FT (2011). A fast, comprehensive screening method for doping agents in urine by gas chromatography-triple quadrupole mass spectrometry. *Journal of Chromatography A* 1218, 3306-3316.
8. Bowers LD, and Sanallah (1996). Direct measurement of steroid sulfate and glucuronide conjugates with high-performance liquid chromatography mass spectrometry. *Journal of Chromatography B* 687, 61-68.
9. Mareck U, Geyer H, Opfermann G, Thevis M, and Schanzer W (2008). Factors influencing the steroid profile in doping control analysis. *J. Mass Spectrom.* 43, 877-891.
10. Pozo OJ, Deventer K, Van Eenoo P, and Delbeke FT (2008). Efficient approach for the comprehensive detection of unknown anabolic steroids and metabolites in human urine by liquid chromatography - Electrospray-tandem mass spectrometry. *Analytical Chemistry* 80, 1709-1720.
11. Houghton E, Grainger L, Dumasia MC, and Teale P (1992). Application of gas-chromatography mass-spectrometry to steroid analysis in equine sports - Problems with enzyme hydrolysis. *Org. Mass Spectrom.* 27, 1061-1070.
12. Hauser B, Schulz D, Boesch C, and Deschner T (2008). Measuring urinary testosterone levels of the great apes - Problems with enzymatic hydrolysis using *Helix pomatia* juice. *Gen. Comp. Endocrinol.* 158, 77-86.
13. Tudela E, Deventer K, and Van Eenoo P (2013). Sensitive detection of 3'-hydroxy-stanozolol glucuronide by liquid chromatography-tandem mass spectrometry. *J. Chromatogr., A* 1292, 195-200.
14. Schänzer W, Guddat S, Thomas A, Opfermann G, Geyer H, and Thevis M (2013). Expanding analytical possibilities concerning the detection of stanozolol misuse by means of high resolution/high accuracy mass spectrometric detection of stanozolol glucuronides in human sports drug testing. *Drug Test. Anal.* 5, 810-818.

15. Pozo OJ, Van Eenoo P, Deventer K, and Delbeke FT (2007). Ionization of anabolic steroids by adduct formation in liquid chromatography electrospray mass spectrometry. *J. Mass Spectrom.* 42, 497-516.
16. Hintikka L, Kuuranne T, Leinonen A, Thevis M, Schänzer W, Halket J, Cowan D, Grosse J, Hemmersbach P, Nielen MWF, and Kostianen R (2008). Liquid chromatographic-mass spectrometric analysis of glucuronide-conjugated anabolic steroid metabolites: method validation and interlaboratory comparison. *J. Mass Spectrom.* 43, 965-973.
17. Pozo OJ, Van Eenoo P, Van Thuyne W, Deventer K, and Delbeke FT (2008). Direct quantification of steroid glucuronides in human urine by liquid chromatography-electrospray tandem mass spectrometry. *Journal of Chromatography A* 1183, 108-118.
18. Kuuranne T, Kotiaho T, Pedersen-Bjergaard S, Rasmussen KE, Leinonen A, Westwood S, and Kostianen R (2003). Feasibility of a liquid-phase microextraction sample clean-up and liquid chromatographic/mass spectrometric screening method for selected anabolic steroid glucuronides in biological samples. *J. Mass Spectrom.* 38, 16-26.
19. Fabregat A, Pozo OJ, Marcos J, Segura J, and Ventura R (2013). Use of LC-MS/MS for the Open Detection of Steroid Metabolites Conjugated with Glucuronic Acid. *Anal. Chem.* 85, 5005-5014.
20. Choi MH, Kim KR, and Chung BC (2000). Simultaneous determination of urinary androgen glucuronides by high temperature gas chromatography-mass spectrometry with selected ion monitoring. *Steroids* 65, 54-59.
21. Antignac JP, Brosseau A, Gaudin-Hirret I, Andre F, and Le Bizec B (2005). Analytical strategies for the direct mass spectrometric analysis of steroid and corticosteroid phase II metabolites. *Steroids* 70, 205-216.
22. Badoud F, Grata E, Boccard J, Guillarme D, Veuthey J-L, Rudaz S, and Saugy M (2011). Quantification of glucuronidated and sulfated steroids in human urine by ultra-high pressure liquid chromatography quadrupole time-of-flight mass spectrometry. *Analytical and Bioanalytical Chemistry* 400, 503-516.
23. Bean KA, and Henion JD (1997). Direct determination of anabolic steroid conjugates in human urine by combined high-performance liquid chromatography and tandem mass spectrometry. *Journal of Chromatography B* 690, 65-75.
24. Schulze JJ, Thorngren JO, Garle M, Ekstrom L, and Rane A (2011). Androgen Sulfation in Healthy UDP-Glucuronosyl Transferase 2B17 Enzyme-Deficient Men. *Journal of Clinical Endocrinology & Metabolism* 96, 3440-3447.
25. Deventer K, Pozo OJ, Verstraetec AG, and Eenoo PV (2014). Dilute-and-shoot-liquid chromatography-mass spectrometry for urine analysis in doping control and analytical toxicology. *TrAC*, <http://dx.doi.org/10.1016/j.trac.2013.1010.1012>.
26. WADA (2013). Technical Document – TD2013MRPL, Minimum Required Performance Levels for Detection of Prohibited Substances, World Anti-Doping Agency (WADA), Montreal.
27. WADA (2012). International Standard for Laboratories, version 7.0, World Anti-Doping Agency (WADA), Montreal.
28. Eurachem (1998). The fitness for purpose of analytical methods. A laboratory guide to method validation and related topics, Eurachem, Teddington.

29. WADA (2010). Technical Document – TD2010IDCR, Identification criteria for qualitative assays incorporating column chromatography and mass spectrometry, World Anti-Doping Agency (WADA), Montreal.
30. Matuszewski BK, Constanzer ML, and Chavez-Eng CM (2003). Strategies for the assessment of matrix effect in quantitative bioanalytical methods based on HPLC-MS/MS. *Anal. Chem.* 75, 3019-3030.
31. Schänzer W, and Donike M (1993). Metabolism of Anabolic-Steroids in Man - Synthesis and Use of Reference Substances for Identification of Anabolic-Steroid Metabolites. *Anal. Chim. Acta* 275, 23-48.
32. Pozo OJ, Van Eenoo P, Deventer K, Lootens L, Grimalt S, Sancho JV, Hernandez F, Meuleman P, Leroux-Roels G, and Delbeke FT (2009). Detection and structural investigation of metabolites of stanozolol in human urine by liquid chromatography tandem mass spectrometry. *Steroids* 74, 837-852.
33. Deventer K, Pozo OJ, Van Eenoo P, and Delbeke FT (2009). Development and validation of an LC-MS/MS method for the quantification of ephedrines in urine. *Journal of Chromatography B-Analytical Technologies in the Biomedical and Life Sciences* 877, 369-374.
34. Weykamp CW, Penders TJ, Schmidt NA, Borburgh AJ, Vandecalseyde JF, and Wolthers BJ (1989). Steroid profile for urine - Reference values. *Clin. Chem.* 35, 2281-2284.
35. Engel LL, Alexander J, and Wheeler M (1958). Urinary metabolites of administered 19-Nortestosterone. *J. Biol. Chem.* 231, 159-164.
36. Le Bizec B, Monteau F, Gaudin I, and Andre F (1999). Evidence for the presence of endogenous 19-norandrosterone in human urine. *J. Chromatogr. B: Biomed. Sci. Appl.* 723, 157-172.
37. Van Eenoo P, Delbeke FT, de Jong FH, and De Backer P (2001). Endogenous origin of norandrosterone in female urine: indirect evidence for the production of 19-norsteroids as by-products in the conversion from androgen to estrogen. *J. Steroid Biochem. Mol. Biol.* 78, 351-357.
38. Pozo OJ, Van Thuyne W, Deventer K, Van Eenoo P, and Delbeke FT (2008). Elucidation of urinary metabolites of fluoxymesterone by liquid chromatography-tandem mass spectrometry and gas chromatography-mass spectrometry. *J. Mass Spectrom.* 43, 394-408.
39. Masse R, Bi H, and Du P (1991). Studies on anabolic steroids. VII. Analysis of urinary metabolites of formebolone in man by gas chromatography-mass spectrometry. *Anal. Chim. Acta* 247, 211-221.
40. Macdonald BS, Sykes PJ, Adhikary PM, and Harkness RA (1971). Identification of 17 α -hydroxy-17 β -methylandrosta-1,4-dien-3-one as a metabolite of 17 β -hydroxy-17 α -methylandrosta-1,4-dien-3-one in man. *Biochem. J.* 122, 26P.
41. Fragkaki AG, Angelis YS, Tsantili-Kakoulidou A, Koupparis M, and Georgakopoulos C (2009). Schemes of metabolic patterns of anabolic androgenic steroids for the estimation of metabolites of designer steroids in human urine. *J. Steroid Biochem. Mol. Biol.* 115, 44-61.
42. Kuuranne T, Pystynen KH, Thevis M, Leinonen A, Schänzer W, and Kostianen R (2008). Screening of *in vitro* synthesised metabolites of 4,9,11-trien-3-one steroids by liquid chromatography-mass spectrometry. *Eur. J. Mass Spectrom.* 14, 181-189.

43. Schubert K, and Wehrberg K (1970). Metabolism of steroid drugs. II. Isolation and characterization of metabolites of 4-chloro-17 α -methy-17 β -hydroxy-1,4-androstadien-3-one. *Endokrinologie* 55, 257-269.
44. Duerbeck HW, Bueker I, Scheulen B, and Telin B (1983). GC and capillary column GC/MS determination of synthetic anabolic steroids. II. 4-Chloro-methandienone (oral turinabol) and its metabolites. *J. Chromatogr. Sci.* 21, 405-410.
45. Sobolevsky T, and Rodchenkov G (2012). Detection and mass spectrometric characterization of novel long-term dehydrochloromethyltestosterone metabolites in human urine. *J. Steroid Biochem. Mol. Biol.* 128, 121-127.

PART 3

Metabolism studies with other performance enhancing substances

Chapter 8

***In vitro* metabolism studies of SARM LGD-4033**

Adapted from:

Geldof L, Pozo OJ, Lootens L, Morthier W, Van Eenoo P and Deventer K (2016). *In vitro* metabolism study of a black market product containing SARM LGD-4033. Drug Testing and Analysis (In press; DOI: 10.1002/dta.1930).

Abstract

Anabolic agents are often used by athletes to enhance their performances. However, use of steroids leads to considerable side effects. Non-steroidal selective androgen receptor modulators (SARMs) are a novel class of substances that have not been approved so far but seem to have a more favorable anabolic/androgenic ratio than steroids and produce fewer side effects. Therefore the use of SARMs is prohibited since 2008 by the World Anti-Doping Agency. Several of these SARMs have been detected on the black market.

Metabolism studies are essential to identify the best urinary markers to ensure effective control of emerging substances by doping control laboratories. As black market products often contain non-pharmaceutical grade substances, alternatives for human excretion studies are needed to elucidate the metabolism.

A black market product labeled to contain the SARM LGD-4033 was purchased over the internet. Purity verification of the black market product led to the detection of LGD-4033, without other contaminants. Human liver microsomes and S9 liver fractions were used to perform phase I and phase II (glucuronidation) metabolism studies. The samples of the *in vitro* metabolism studies were analyzed by gas chromatography-(tandem) mass spectrometry (GC-MS(/MS)) and liquid chromatography-(high resolution) tandem mass spectrometry (LC-(HR)MS/MS). LC-HRMS product ion scans allowed to identify typical fragment ions for the parent compound and to further determine metabolite structures.

In total five metabolites were detected, all modified in the pyrrolidine ring of LGD-4033. The metabolic modifications ranged from hydroxylation combined with keto-formation (M1) or cleavage of the pyrrolidine ring (M2), hydroxylation and methylation (M3/M4) and dihydroxylation (M5). The parent compound and M2 were also detected as glucuronide-conjugates.

1 Introduction

A wide-range of potential performance enhancing substances is currently available over the internet. While in the 1990s and early 2000s, these products were almost exclusively anabolic androgenic steroids (AAS) and designer steroids, these days a diverse range of compounds is available, including peptides [1-6] and non-steroidal selective androgen receptor modulators (SARMs) [7-9].

SARMs interact selectively with the androgen receptor, stimulating the anabolic effects with fewer androgenic side effects compared to AAS [7, 10-12]. Besides improving the anabolic/androgenic dissociation these SARMs exhibit better oral bioavailability and represent more metabolically stable compounds with reduced liver toxicity [13].

To discourage the use of potentially harmful substances and to protect fair play in sports the World Anti-Doping Agency (WADA) publishes each year the Prohibited List [14]. Since January 2008 SARMs have also been included in this list under the class of anabolic agents [10].

SARMs have diverse chemical pharmacophore structures including arylpropionamides, bicyclic hydantoin, quinolines and tetrahydroquinolines [10-12]. However, this group is continuously expanding with new substances and other pharmacophores. LGD-4033 (4-(2-((S)-2,2,2-trifluoro-1-hydroxyethyl)pyrrolidin-1-yl)-2-(trifluoromethyl)-benzonitrile) [15-17] for example is a new class of SARMs with a pyrrolidin-benzonitrile structure (Table 8.1).

The therapeutic indications for SARMs are muscle wasting disorders, sarcopenia, osteoporosis, breast cancer and as hormone replacement therapy [7, 12, 18, 19]. Currently no SARMs are available as pharmaceutical preparations as they are all still undergoing clinical evaluation. Even though there is no clinical approval, LGD-4033 is already available as a performance-enhancing substance in black market products [15-17]. This bears considerable potential danger as knowledge of its toxicological profile is missing. Moreover, lack of quality control and often incorrect labeling of these black market products implies additional health risks [8, 15].

Since the promising anabolic effects of LGD-4033 [18] and its presence in black market products, sold over the internet [15-17], there is a potential risk for misuse by athletes. As observed by Grata *et al.* [20] absence of pharmaceutical grade products is not preventing misuse of SARMs. Furthermore, two cases of andarine misuse were reported in 2010 [20, 21] and in 2013 thirteen cases of SARMs misuse were reported during doping control sample analysis [22]. Therefore it is essential that misuse of LGD-4033 is screened for in doping control samples. To improve the detection window of prohibited substances, metabolism studies should be performed to identify the best target metabolites. As LGD-4033 is a non-approved pharmaceutical drug, ethical objections and safety aspects limit the use of human volunteers.

Table 8.1. Detected metabolites after HLM incubation with LGD-4033. Both LC-HRMS as GC-MS results are indicated.

LC-HRMS							
Compound	Metabolic transformation	Ion species	Exp. ^a (error (ppm))	m/z	RT ^b (min)	Glucuro- conjugate ^c	(Proposed) chemical structure ^d
LGD-4033	parent compound	[M-H] ⁻	337.0771 (2.77)		19.26	√	
$C_{14}H_{12}F_6N_2O$		[M+OAc] ⁻	397.0999 (1.88)				
		[M+H] ⁺	339.0917 (3.81)				
M1	hydroxylation and double bond	[M-H] ⁻	351.0573 (0.09)		9.55	×	
$C_{14}H_{10}F_6N_2O_2$		[M+ OAc] ⁻	411.0783 (0.39)				
		[M+H] ⁺	353.0718 (0.24)				
M2	hydroxylation and cleavage pyrrolidine ring	[M-H] ⁻	355.0887 (0.03)		10.44	√	
$C_{14}H_{14}F_6N_2O_2$		[M+ OAc] ⁻	415.1101 (0.60)				
		[M+H] ⁺	357.1031 (0.37)				
M3/M4	hydroxylation and methylation	[M-H] ⁻	367.0884 (0.74)		17.22	×	
$C_{15}H_{14}F_6N_2O_2$		[M+ OAc] ⁻	427.1091 (1.41)		17.77		
		[M+H] ⁺	369.1030 (0.60)				
M5	dihydroxylation	[M-H] ⁻	369.0677 (0.66)		10.67	×	
$C_{14}H_{12}F_6N_2O_3$		[M+H] ⁺	371.0820 (1.40)				
GC-MS							
Compound	Metabolic transformation	Chemical formula	Characteristic TMS-ions m/z		RT ^a (min)		
LGD-4033	parent compound	$C_{14}H_{12}F_6N_2O$	410 - 395 - 239 - 197 - 170		5.11		
M1	hydroxylation and double bond	$C_{14}H_{10}F_6N_2O_2$	253 - 197 - 170		5.34		

^a Exp.: experimental^b RT: Retention Time^c √: detected; ×: not detected^d Proposed structures are indicated for the LGD-4033 metabolites, only one possible configuration is shown.

For this purpose alternative *in vitro* models are often applied for metabolism studies of non-pharmaceutical grade substances. Therefore a similar study was conducted by Thevis *et al.* [16] to elucidate the metabolism of LGD-4033. Our *in vitro* LGD-4033 metabolism study further investigates and complements their study [16]. As the hepatic enzyme activity plays an important role in the metabolism, pooled human liver microsomes (HLM) and S9 liver fractions were used in this study. A black market product advertised to contain the SARM LGD-4033 was purchased over the internet and analyzed.

2 Materials and Methods

2.1 Chemicals and reagents

The black market product (powder) containing LGD-4033 was purchased over the internet. The internal standard (IS) 17 α -methyltestosterone was a gift from Organon (Oss, the Netherlands). The reference standard of methandienone was obtained from 'National Measurement Institute' (NMI, North Ryde, Australia). Pooled HLM from 20–30 donors, S9 liver fractions, the nicotinamide adenine dinucleotide phosphate (NADPH) regenerating system solutions A and B, the UGT reaction mix solutions A and B and phosphate buffer pH 7.4 all from Gentest were purchased by Corning (Amsterdam, the Netherlands). Ethanol and ammonium acetate (NH₄OAc) were purchased from Biosolve (Valkenswaard, the Netherlands). Diethyl ether and methanol (MeOH) were obtained from Fisher Scientific (Loughborough, UK). Sodium sulfate (Na₂SO₄), sodium hydrogen carbonate (NaHCO₃), potassium carbonate (K₂CO₃), ammonium iodide (NH₄I) and acetic acid (HOAc) were from Merck (Darmstadt, Germany). LC grade water and LC grade MeOH were purchased from J.T. Baker (Deventer, the Netherlands). N-Methyl-N-trimethylsilyltrifluoroacetamide (MSTFA) was from Karl Bucher (Waldstetten, Germany). Ethanethiol was obtained from Acros (Geel, Belgium). The gases helium, ammonia, hydrogen and oxygen-free nitrogen (OFN) were delivered by Air Liquide (Bornem, Belgium).

2.2 Instrumentation

2.2.1 GC-MS

An Agilent 6890 gas chromatograph was interfaced to an Agilent 5973 mass spectrometer (Agilent Technologies, Palo Alto, USA). 1 μ L of sample was injected into the system using a 7683 series Autosampler with a splitless injector (Agilent Technologies, Palo Alto, USA). The GC separation was performed using a JW Ultra-1 capillary column (17 m x 200 μ m i.d., 0.11 μ m; Agilent Technologies) and helium as mobile phase at a flow rate of 0.6 mL/min at 10.15 psi (constant flow). The temperature program and other instrumental parameters were applied as described in Chapter 3 (2.2.1 GC-MS).

Also full scan (m/z 50-800) GC-chemical ionization (CI)-MS analysis was performed by an Agilent 7890 gas chromatograph coupled with an Agilent 7000 B triple quadrupole mass spectrometer (Palo Alto, USA) and a MPS2 autosampler and PTV-injector from Gerstel (Mülheim an der Ruhr, Germany). 6 μ L of sample was injected using the solvent vent mode of the PTV-injector. The vent flow was 15 mL/min at 5 psi until 0.01 min with an initial temperature of 80 °C and increased at 12 °C/s to 310 °C. A retention gap column (1.25 m \times 0.2 mm and no film inside) was coupled in front of an HP-1MS (15 m \times 320 μ m with a film thickness of 0.25 μ m) both from J&W Scientific (Agilent Technologies, Palo Alto, USA). Helium was used as a carrier gas with a pressure program to ensure a constant flow of 1.28 mL/min. The following oven temperature program was used: the initial temperature was 90 °C, increased at 70 °C/min to 125 °C, then at 35 °C/min to 194 °C, next at 10 °C/min to 215 °C, at 20 °C/min to 250 °C, at 30 °C/min to 275 °C and finally increased at 75 °C/min to reach a final temperature of 320 °C (held for 1.3 min). The total run time was 9.35 min. The transfer line was set at 310 °C. For the ionization CI was applied using ammonia as reagent gas.

2.2.2 Gas chromatography-nitrogen phosphorous detector (GC-NPD)

2 μ L of sample was injected into a 6890 gas chromatograph equipped with a NPD detector using a 7683 series Autosampler with a splitless injector (all from Agilent Technologies) at 250 °C. The GC separation was performed using a RTX5-amine column (15 m \times 250 μ m i.d., 1.0 μ m; Restek, Middelburg, the Netherlands) and helium as mobile phase at a flow rate of 1.2 mL/min and 4 psi. The temperature program was as follows: initial temperature was 70 °C and increased at a rate of 5 °C/min until 100 °C is reached. Temperature was then further increased with 10 °C/min to 140 °C, with 20 °C/min to 200 °C, 30 °C/min to 250 °C and finally the temperature raised with 50 °C/min to 315 °C. This final temperature was held during 5 min. The total run time was 21.97 min. The temperature of the NPD detector was set at 300 °C, a hydrogen flow of 2.0 mL/min and air flow of 60 mL/min were applied.

2.2.3 Nuclear magnetic resonance spectroscopy (NMR)

The NMR experiments were performed by dissolving the black market product into deuterated methanol (CD_3OD) and transferring to the NMR probe. Both 1H NMR and diffusion ordered spectroscopy (DOSY) were performed by a 500 MHz Avance III ascend instrument (Bruker, Karlsruhe, Germany).

2.2.4 LC-(HR)MS

All experiments were performed under the same LC conditions using a Thermo Finnigan Surveyor Autosampler Plus and a MS Pump Plus (Thermo Scientific, Bremen, Germany). The mobile phase consisted of LC grade water and LC grade MeOH both with 1 mM NH_4OAc and 0.1% HOAc.

LC separation was performed using a SunFire™ C18 column (50 mm × 2.1 mm i.d., 3.5 μm) from Waters (AH Etten-Leur, the Netherlands), at a flow rate of 250 μL/min. 20 μL of sample was injected into the instrument. The applied gradient program is described in chapter 4 (2.2.4 LC-MS/MS). The methods have a total run time of 35 min.

For the low resolution methods a TSQ Quantum Discovery MAX triple quadrupole mass spectrometer (Thermo Scientific) was used. A full scan method was applied in a range of m/z 30-1500 in both positive and negative mode. The other MS conditions were: interface: electrospray ionization (ESI), capillary voltage: 3.5 kV, source temperature: 350 °C, sheath gas pressure: 50 (arbitrary units), auxiliary gas pressure: 20 (arbitrary units), tube lens offset: 100 V, scan time: 0.5 s.

Using the full scan method also eight fractions (Fr1: 7-8.5 min; Fr2: 8.5-9.8 min; Fr3: 9.8-11 min; Fr4: 11-14 min, Fr5: 14-15.3 min, Fr6: 15.3-17.2 min, Fr7: 17.2-19.5 and Fr8: 19.5-25 min) were collected into separate tubes in triplicate by switching the valve from the detector to the 'waste' to collect these fractions.

The high resolution (HRMS) experiments were performed on an Exactive benchtop Orbitrap-based mass spectrometer (Thermo Scientific). The instrument operated in both positive and negative full scan mode from m/z 100 to 2000 at a resolving power of 50,000 with a data acquisition rate of 2 Hz. For the structural investigation of metabolites LC-HRMS product ions scans were performed by a Q-Exactive benchtop Orbitrap-based mass spectrometer (Thermo Scientific) for the protonated and deprotonated molecules as selected ions with an isolation window of m/z 1.0 at a resolving power of 70,000 and CE of 15, 25, 35 and 55 eV. The other MS parameter settings for both LC-HRMS instruments were identical to the low resolution LC instruments except for spray voltage: 4 kV, source temperature of 250 °C and heated ESI (HESI) (probe heater at 300 °C).

2.3 *In vitro* incubation studies

Prior to the *in vitro* metabolism studies, the purity of the black market product containing LGD-4033 was verified. The purity verification was performed by full scan GC-MS, GC-MS/MS(CI) and LC-MS (both low as high resolution) analysis. Additionally, the black market product was analyzed by GC-NPD (underivatized product) and by NMR.

Phase I, phase II and combined phase I and phase II *in vitro* metabolism assays (HLM and S9 liver fractions) were applied as described in Chapter 1 (7.2.2.2 *Protocol in vitro metabolism studies*; Table 1.6). Substrate stability (blank; without HLM) and system blank (without test compound) control samples were used to verify the enzymatic reactions. Methandienone was used as test compound in the positive control samples. The phase I samples were incubated during 2, 4 or 18

h, the phase II samples during 2 h. The combined phase I and phase II samples were first 2 h incubated for the phase I and an additional 2 h for the phase II enzymatic reactions.

2.4 Sample preparation

The samples of the *in vitro* metabolic assays were first centrifuged at 4 °C (12,000 g, 5 min) followed by transferring 400 µL into new tubes. 50 µL of the internal standard (IS) 17 α -methyltestosterone (2 µg/mL) was added to all samples. The phase II (UGT) and combined phase I and II HLM incubation samples were analyzed by direct injection on LC-HRMS, after removal of the enzymatic proteins. For the phase I *in vitro* incubation samples (unconjugated fraction) liquid-liquid extraction (LLE), as described in Chapter 3 (2.5.1 *Liquid-liquid extraction (LLE)*), was performed after evaporation of the samples under oxygen free nitrogen (OFN). After evaporation the residues were dissolved in 100 µL H₂O/MeOH (50/50) for LC-(HR)MS/MS analysis. For GC-MS analysis the evaporated samples were derivatized by adding 100 µL derivatization solution containing MSTFA, NH₄I and ethanethiol (500:4:2) and incubation during 1 h at 80 ± 5 °C.

3 Results and Discussion

3.1 Analysis of black market product

Prior to the metabolism studies the presence of LGD-4033 in the black market product and its purity was verified. LC-HRMS analysis confirmed the presence of LGD-4033 with a mass deviation of 2.77 ppm in negative and 3.81 ppm in positive polarity mode (Figure 8.1). LGD-4033 could also be detected in the black market product by GC-MS analysis (Figure 8.1). The molecular ion of LGD-4033 after TMS-derivatization m/z 410 and a typical loss of methyl (- m/z 15) was observed in the GC-MS mass spectrum. However, the fragment ions with m/z 239, 197 and 170 are more abundant. The proposed origin of these fragment ions is indicated in the structure of LGD-4033 in Figure 8.1.

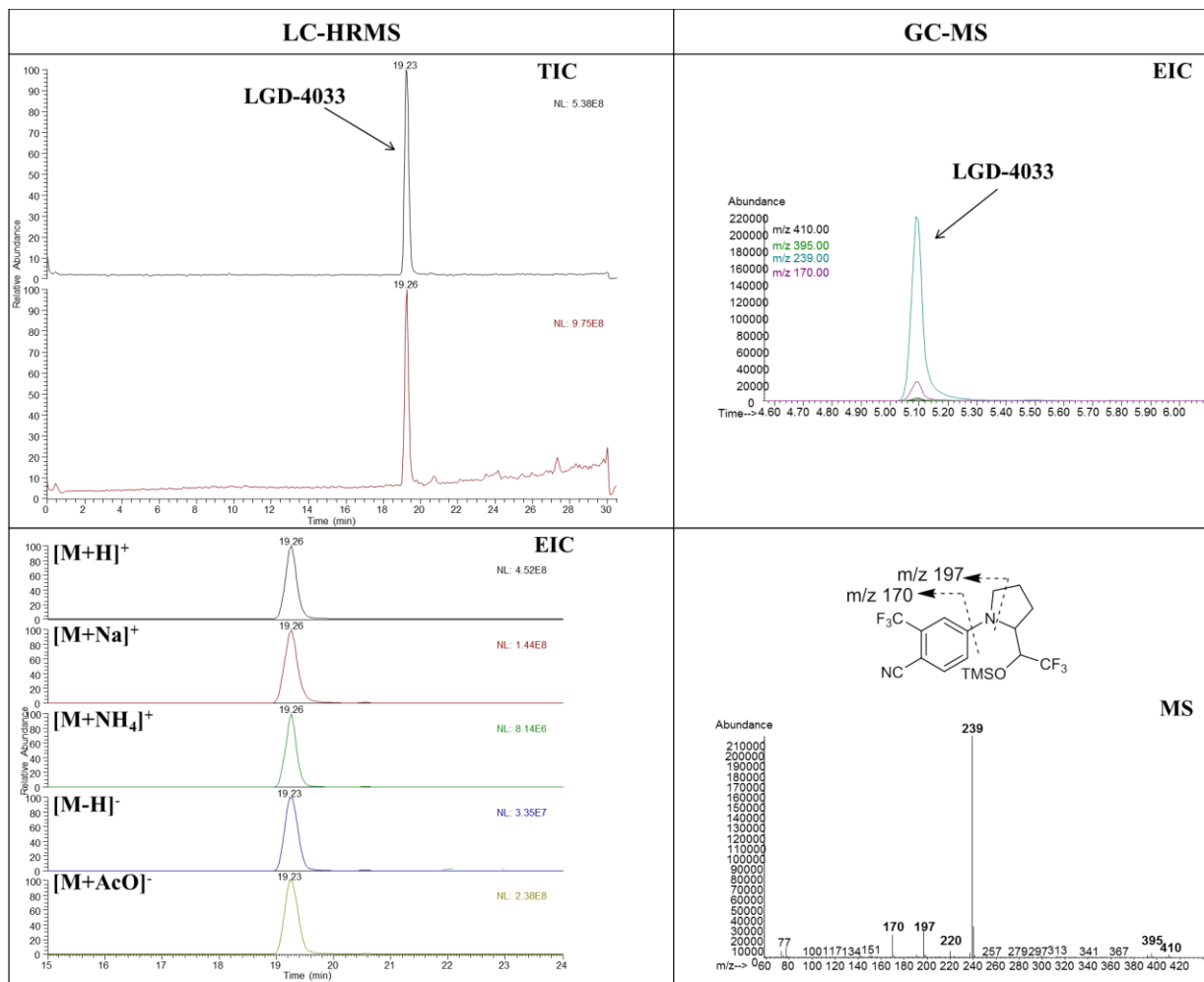


Figure 8.1. LC-HRMS and GC-MS analysis of black market product containing LGD-4033. LC-HRMS: both the TIC and EIC are shown. GC-MS: EIC, electron ionization (EI) mass spectrum of LGD-4033 and proposed fragmentation pattern after TMS-derivatization is also presented.

However, as no reference material is available additional ^1H NMR analyzes were performed to further characterize the detected compound in the black market product. The obtained NMR data confirm 4-(2-((S)-2,2,2-trifluoro-1-hydroxyethyl)pyrrolidin-1-yl)-2-(trifluoromethyl)-benzotrile as chemical structure for the detected compound in the black market product: ^1H -NMR (500 MHz, CD_3OD) δ = 7.7 (1H, H-11), 7.2 (1H, H-8), 7.05 (1H, H-9), 4.8 (1H, H-15), 4.3 (1H, H-3), 4.0 (1H, H-2), 3.6 (1H, H-6), 3.3 (1H, H-6), 2.2 (4H, H-4/H-5).

So, in agreement with what was reported before [15, 17] the presence of this non-approved drug was observed in a black market product circulating over the internet. The investigated black market product seems to have a good quality as no major contaminants were detected by GC-MS(/MS), LC-(HR)MS, GC-NPD and DOSY analyzes.

3.2 *In vitro* metabolism studies

Metabolites were searched for by comparing both total ion chromatograms (TIC) and extracted ion chromatograms (EIC) of incubated samples with control samples. The extracted ions were based on theoretically possible metabolic pathways including oxidations ((di)hydroxylations, -H₂) and reductions (+H₂) and combinations of these metabolic pathways.

LC-(HR)MS analysis of the *in vitro* metabolism studies of LGD-4033 led to the detection of five (M1-M5) metabolites (Figure 8.2 and Table 8.1). No additional metabolites were detected by incubation with S9 liver fractions compared to the HLM incubation samples. Therefore only the results of the HLM metabolism studies are presented in the figures below.

The number of the *in vitro* produced LGD-4033 metabolites is comparatively low to what is observed for other SARMs [10, 23-29], which indicates that LGD-4033 is metabolically relatively stable. This is reasonable since the purpose for the development of new SARMs is not only to obtain a better anabolic/androgenic dissociation but also to improve pharmacokinetic properties. The presence of a cyano group in LGD-4033 instead of a nitro group in the phenyl group of other SARMs can lead to metabolically more stable compounds, which improves the half-life of the compound [24]. In addition, the presence of only one phenyl group in the structure of LGD-4033 could also decrease the clearance and consequently improve the half-life as described for nilutamide, for example [13, 30].

The possible metabolic transformations, based on the observed mass differences of the metabolites M1, M2 and M5 in comparison to the parent compound, are indicated in Table 8.1. A study of the LC-HRMS results confirmed these suggested modifications with less than 1 ppm mass deviation. The structures shown in Table 8.1 are proposals that fulfil the MS behaviour observed for the metabolites (both in positive and negative ionization modes) described below (3.3 *Structure characterization of the detected metabolites by HRMS/MS*). Metabolite M5 was also reported by Thevis *et al.* [16] and in a poster at a conference by Sobolevsky *et al.* [31].

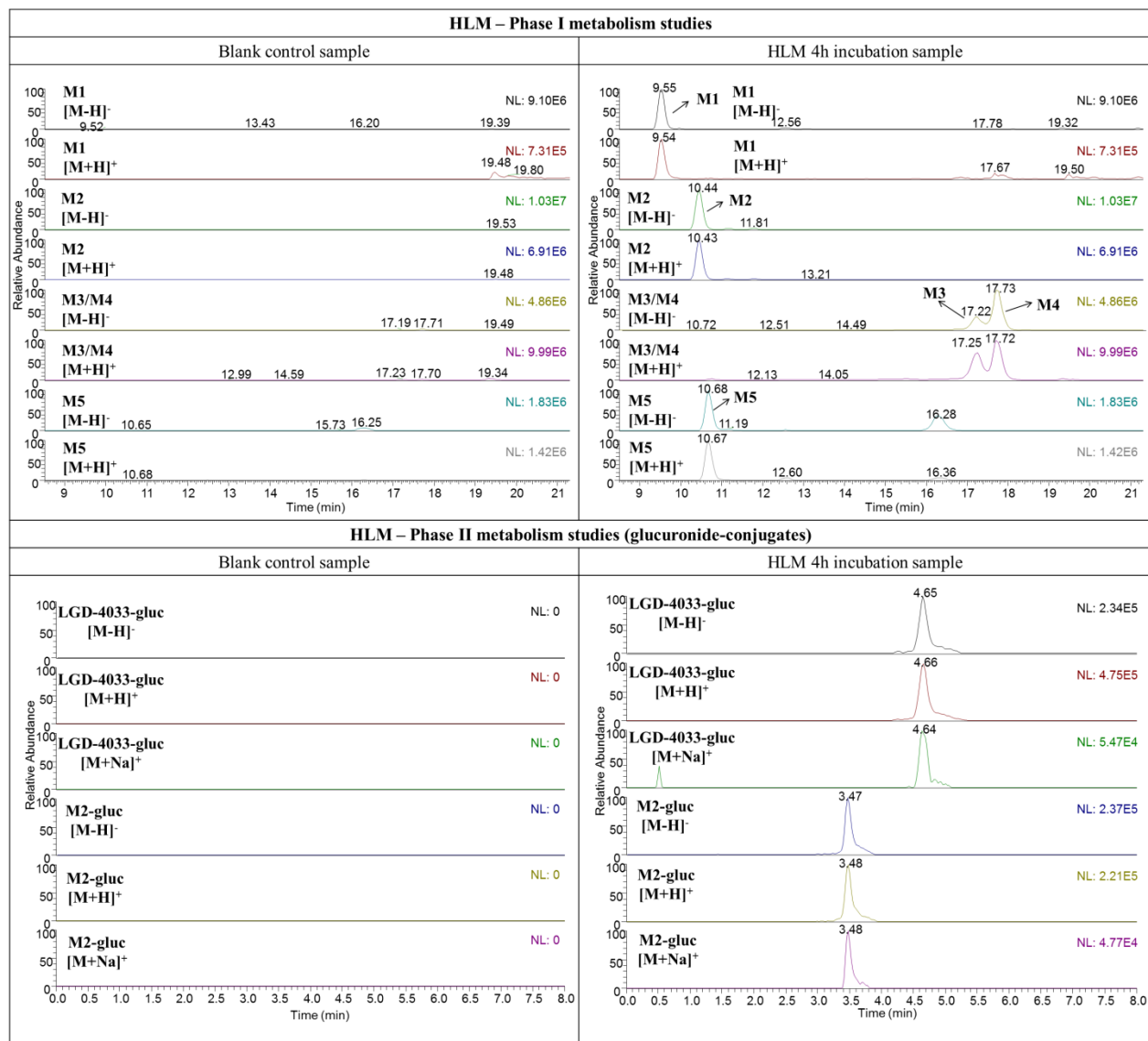


Figure 8.2. Phase I and phase II (UGT) LGD-4033 metabolism studies with HLM. The 4 h HLM incubation samples are presented in comparison with the blank control samples.

Based on the relative abundances of the metabolites detected in the current study, metabolites M1 and M2 might be incorporated besides the parent compound into existing screening methods to anticipate LGD-4033 misuse. However, extrapolation of these *in vitro* results to the more complex *in vivo* human situation is difficult. Sobolevsky *et al.* [31] observed that screening for a dihydroxylated metabolite, comparable to M5, in positive ionization mode could prolong the detection window of LGD-4033 misuse in human urine samples. Sobolevsky *et al.* [31] only used the LC-MS in positive ionization mode, whereas only negative ionization mode was applied by Thevis *et al.* [16]. Because negative ionization mode generally gives less background than positive ionization mode and the target molecules yielded abundant acetate adducts these metabolites (M1-M4) were readily detectable in TIC in our study. While, in positive ionization

mode all metabolites were only detectable in EIC. Therefore, the relevance of these described metabolites for screening in real human doping control samples should also be determined (in negative ionization mode).

For the isomeric metabolites M3 and M4 an elemental composition of $C_{15}H_{14}F_6N_2O_2$ was determined by the LC-HRMS data with 0.74 ppm mass deviation in negative polarity mode. This indicates the addition of CH_2O which could correlate to a hydroxylation in combination with a methylation, a rare metabolic pathway that has however been previously described for other compounds like estrogens [32]. Methylation of hydroxy-groups was also observed for SARMS as phase II metabolic pathway in rats [13].

GC-MS analysis was performed on LC-fractions of both the HLM incubation and control samples to obtain more structural information about the detected metabolites. Although reanalysis of the collected fractions by LC-MS proved the presence of the metabolites in their respective fractions only the parent compound and M1 could be detected by GC-MS (Table 8.1), both with and without TMS-derivatization. GC-MS/MS analysis did not lead to improved detection of metabolites, neither in EI nor in CI mode.

Subsequent phase I and phase II (glucuronidation) metabolic reactions in a combined HLM incubation assay were also performed. Only the parent compound and metabolite M2 could be detected as glucuronidated derivatives (Figure 8.2). Similar results were also observed for the glucuronidated conjugates by Sobolevsky *et al.* [31].

3.3 Structure characterization of the detected metabolites by HRMS/MS

To further characterize the structures of the metabolites detected by the full scan LC-HRMS and GC-MS analyses structure-specific product ions of the detected metabolites were monitored by LC-HRMS/MS (Table 8.2). The fragmentation patterns of the parent compound were studied first in both positive and negative ionization mode (Figure 8.3 and Table 8.2). In the LC-HRMS product ion scan of LGD-4033 fragment ion m/z 267 (Figure 8.3) was observed in negative ionization mode together with the typical fragment ions m/z 239 and 170 which were also found in the GC-MS mass spectrum. The fragment ions m/z 170 and 267 could be linked to the structure of the parent compound with less than 5 ppm mass deviation similar to Thevis *et al.* and Krug *et al.* [15-17]. However, for fragment ion m/z 239.0436 a mass deviation of 185 ppm was observed for the chemical formula $C_{12}H_{10}F_3N_2$ suggested by Krug *et al.* [15]. An alternative fragmentation pattern is proposed in Figure 8.3. In addition to the typical fragment ions (m/z 240, 220, 213, and 199) derived from fragmentation of the pyrrolidine ring, also losses of water

(m/z 321) and hydrogen fluoride (HF; m/z 319) were observed for LGD-4033 in positive ionization mode.

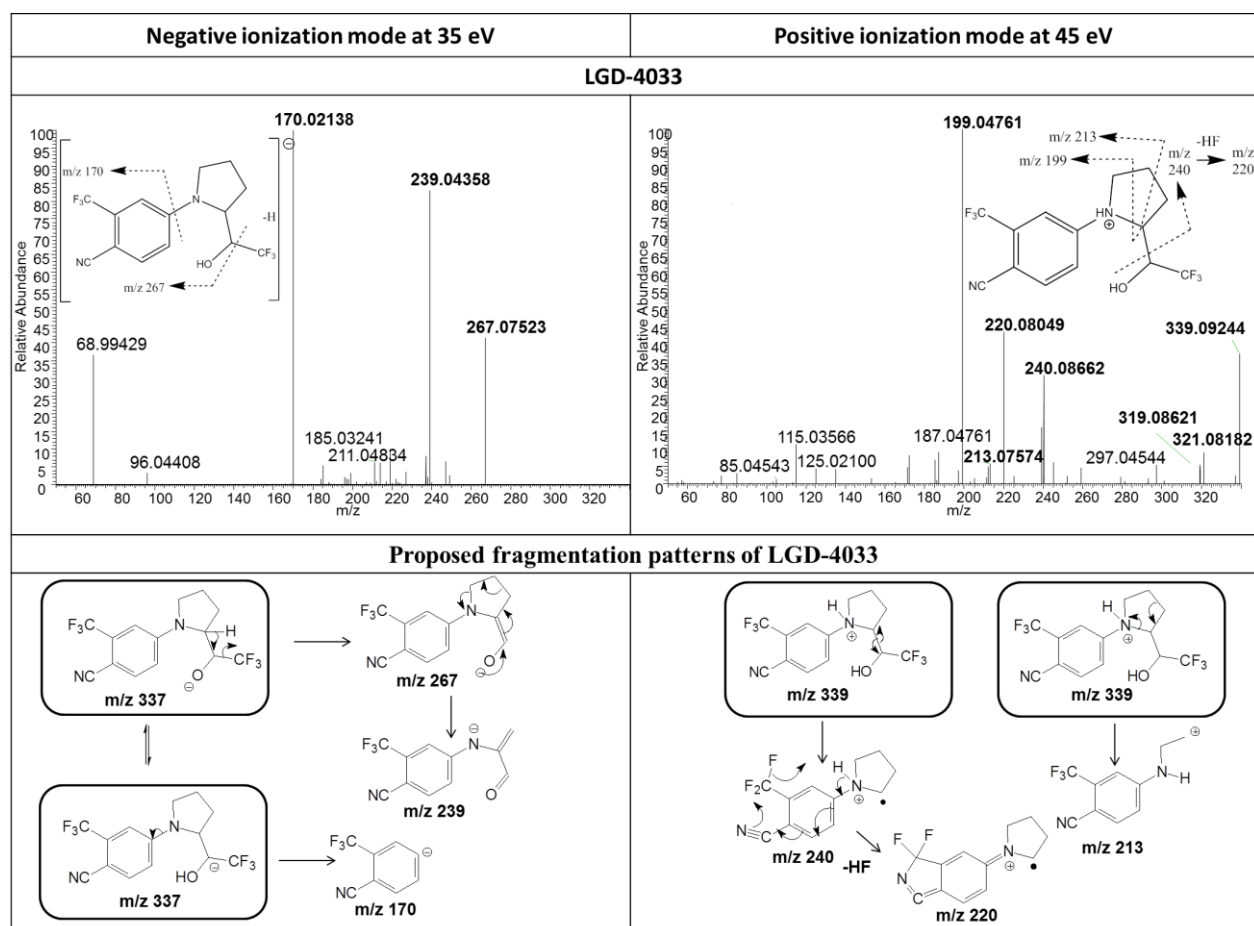


Figure 8.3. LC-HRMS/MS mass spectra of LGD-4033 are shown in both negative and positive ionization mode at a CE of 35 eV and 45 eV respectively. The tentative fragmentation patterns are also presented.

The fragment ions m/z 170 and m/z 185, indicating an unmodified benzonitrile ring (Figure 8.3), could be detected for all the LGD-4033 metabolites (M1-M5) in negative ionization mode. This unmodified benzonitrile ring was confirmed in positive ionization mode by the detection of ions with m/z 199 or m/z 197 and eventually m/z 187 in the LGD-4033 metabolites (Table 8.2). These findings indicate that all metabolites are formed by modifications of the pyrrolidine ring of the parent compound. This is in contrast to the studies of Thevis *et al.* [16] and Sobolevsky *et al.* [31] where also hydroxylation into the benzonitrile ring was observed for some metabolites. The fragment ions m/z 253 (negative ionization mode) and 234 (positive ionization mode) detected in the LC-HRMS product scans of M1 also suggest a hydroxylation and subsequent oxidation to a carbonyl in the pyrrolidine ring (Table 8.1 and Table 8.2). In analogy to the LC-HRMS data typical fragment ions m/z 170 and m/z 253 were detected in the GC-MS mass spectrum (results not shown here). The presence of an unaltered benzonitrile ring was further supported by the

presence of the fragment ion at m/z 197 in the GC-MS mass spectrum of M1. This latter ion was also found in the GC-MS spectrum of the parent compound and is comparable to the ion m/z 199 detected by LC-HRMS in positive ionization mode (Table 8.2).

Table 8.2. Results derived from LC-HRMS/MS (ESI) product ion scans in negative and positive ionization mode of LGD-4033 and its metabolites.

Compound	Negative mode (deprotonated ions)				Positive mode (protonated ions)			
	Product ions	Chemical formula	Error (ppm)	origin	Product ions	Chemical formula	Error (ppm)	origin
LGD-4033	267.0752	C ₁₃ H ₁₀ F ₃ N ₂ O	0.48	-CHF ₃	321.0819	C ₁₄ H ₁₁ F ₆ N ₂	0.61	-H ₂ O
	239.0436	C ₁₁ H ₆ F ₃ N ₂ O	0.79	-CHF ₃ -C ₂ H ₄	319.0862	C ₁₄ H ₁₂ F ₅ N ₂ O	0.79	-HF
	185.0324	C ₈ H ₄ F ₃ N ₂	4.36	-C ₆ H ₇ F ₃ O	240.0866	C ₁₂ H ₁₁ F ₃ N ₂	1.10	-CHOH-CF ₃
	170.0214	C ₈ H ₃ F ₃ N	5.45	-C ₆ H ₈ F ₃ NO	220.0805	C ₁₂ H ₁₀ F ₂ N ₂	0.76	-CHOH-CF ₃ -HF
M1	281.0541	C ₁₃ H ₈ F ₃ N ₂ O 2	0.80	-CHF ₃	213.0633	C ₁₀ H ₈ F ₃ N ₂	0.42	-CHOH-CF ₃ -C ₂ H ₃
	263.0436	C ₁₃ H ₆ F ₃ N ₂ O	0.84	-CHF ₃ -H ₂ O	199.0476	C ₉ H ₆ F ₃ N ₂	0.70	-CHOH-CF ₃ -C ₃ H ₅
	253.0227	C ₁₁ H ₄ F ₃ N ₂ O ₂	1.33	-CHF ₃ -C ₂ H ₄	335.0610	C ₁₄ H ₉ F ₆ N ₂ O	0.95	-H ₂ O
	237.0640	C ₁₂ H ₈ F ₃ N ₂	2.28	-CHF ₃ -CO ₂	333.0653	C ₁₄ H ₁₀ F ₅ N ₂ O ₂	1.25	-HF
	185.0322	C ₈ H ₄ F ₃ N ₂	5.43	-C ₆ H ₅ F ₃ O ₂	317.0507	C ₁₄ H ₇ F ₆ N ₂	0.42	-2H ₂ O
	170.0212	C ₈ H ₃ F ₃ N	6.81	-C ₆ H ₆ F ₃ NO ₂	234.0598	C ₁₂ H ₈ F ₂ N ₂ O	0.73	- [•] CHOHCF ₃ -HF
M2	285.0855	C ₁₃ H ₁₂ F ₃ N ₂ O ₂	0.44	-CHF ₃	199.0477	C ₉ H ₆ F ₃ N ₂	0.60	-CHOHCF ₃ -C ₃ H ₃ O
	257.0905	C ₁₂ H ₁₂ F ₃ N ₂ O	0.94	-CHF ₃ -CO	339.0925	C ₁₄ H ₁₃ F ₆ N ₂ O	0.47	-H ₂ O
	239.0789	C ₁₂ H ₁₀ F ₃ N ₂	1.60	-CHF ₃ -CO-H ₂ O	321.0819	C ₁₄ H ₁₁ F ₆ N ₂	0.29	-2H ₂ O
	237.0641	C ₁₂ H ₈ F ₃ N ₂	1.63	-CHF ₃ -CHOH-H ₂ O	297.0455	C ₁₁ H ₇ F ₆ N ₂ O	0.60	-C ₃ H ₇ OH
	226.0354	C ₁₀ H ₅ F ₃ N ₂ O	2.54	- [•] CH ₃ CH ₂ CHOH-HCF ₃	279.0349	C ₁₁ H ₅ F ₆ N ₂	0.95	-C ₃ H ₇ OH-H ₂ O
	199.0480	C ₉ H ₆ F ₃ N ₂	4.05	-C ₅ H ₇ F ₃ O ₂	259.0289	C ₁₁ H ₄ F ₅ N ₂	0.64	-C ₃ H ₇ OH-H ₂ O-HF
M3/M4	185.0323	C ₈ H ₄ F ₃ N ₂	4.90	-C ₆ H ₉ F ₃ O ₂	199.0476	C ₉ H ₆ F ₃ N ₂	0.70	-CHOHCF ₃ - C ₃ H ₆ OH
	170.0212	C ₈ H ₃ F ₃ N	6.10	-C ₆ H ₁₀ F ₃ NO ₂	187.0476	C ₈ H ₆ F ₃ N ₂	0.75	-CHOHCF ₃ - C ₄ H ₆ OH
	297.0853	C ₁₄ H ₁₂ F ₃ N ₂ O ₂	1.03	-CHF ₃	135.0416	C ₆ H ₆ F ₃	0.14	-C ₈ H ₅ F ₃ N ₂ -2H ₂ O
	265.0591	C ₁₃ H ₈ F ₃ N ₂ O	0.83	-CHF ₃ -CH ₃ OH	115.0357	C ₆ H ₅ F ₂	2.75	-C ₈ H ₅ F ₃ N ₂ -2H ₂ O- HF
	237.0640	C ₁₂ H ₈ F ₃ N ₂	2.09	-COCHF ₃ -CH ₃ OH	349.0966	C ₁₅ H ₁₄ F ₅ N ₂ O ₂	1.25	-HF
	185.0321	C ₈ H ₄ F ₃ N ₂	5.76	-C ₇ H ₉ F ₃ O ₂	337.0768	C ₁₄ H ₁₁ F ₆ N ₂ O	0.77	-CH ₃ OH
M5	170.0212	C ₈ H ₃ F ₃ N	6.81	-C ₇ H ₁₀ F ₃ NO ₂	319.0663	C ₁₄ H ₉ F ₆ N ₂	0.51	-CH ₃ OH-H ₂ O
	297.0853	C ₁₄ H ₁₂ F ₃ N ₂ O ₂	1.03	-CHF ₃	299.0601	C ₁₄ H ₈ F ₅ N ₂	0.32	-CH ₃ OH-H ₂ O-HF
	265.0591	C ₁₃ H ₈ F ₃ N ₂ O	0.83	-CHF ₃ -CH ₃ OH	213.0632	C ₁₀ H ₈ F ₃ N ₂	0.89	-CHOHCF ₃ -C ₂ H ₂ - CH ₂ OH
	237.0640	C ₁₂ H ₈ F ₃ N ₂	2.09	-COCHF ₃ -CH ₃ OH	197.0315	C ₉ H ₄ F ₃ N ₂	0.66	-CHOHCF ₃ -C ₃ H ₆ - CH ₂ OH
	185.0321	C ₈ H ₄ F ₃ N ₂	5.76	-C ₇ H ₉ F ₃ O ₂	353.0719	C ₁₄ H ₁₁ F ₆ N ₂ O ₂	0.32	-H ₂ O
	170.0212	C ₈ H ₃ F ₃ N	6.81	-C ₇ H ₁₀ F ₃ NO ₂	351.0762	C ₁₄ H ₁₂ F ₅ N ₂ O ₃	0.17	-HF
	351.0570	C ₁₄ H ₉ F ₆ N ₂ O ₂	1.20	-H ₂ O	335.0613	C ₁₄ H ₉ F ₆ N ₂ O	0.06	-2H ₂ O
	299.0645	C ₁₃ H ₁₀ F ₃ N ₂ O ₃	1.51	-CHF ₃	333.0657	C ₁₄ H ₁₀ F ₅ N ₂ O ₂	0.11	-H ₂ O-HF
	281.0539	C ₁₃ H ₈ F ₃ N ₂ O ₂	1.59	-H ₂ O-CHF ₃	317.0508	C ₁₄ H ₇ F ₆ N ₂	0.05	-3H ₂ O
	263.0434	C ₁₃ H ₆ F ₃ N ₂ O	1.41	-2H ₂ O-CHF ₃	234.0598	C ₁₂ H ₈ F ₂ N ₂ O	0.13	-CHOHCF ₃ -H ₂ O-HF
255.0746	C ₁₂ H ₁₀ F ₃ N ₂ O	1.96	-CHF ₃ -CO ₂	199.0477	C ₉ H ₆ F ₃ N ₂	0.15	-CHOHCF ₃ -C ₃ H ₃ - H ₂ O	
253.0589	C ₁₂ H ₈ F ₃ N ₂ O	2.18	-CHOHCF ₃ -H ₂ O	187.0476	C ₈ H ₆ F ₃ N ₂	0.32		
253.0225	C ₁₁ H ₄ F ₃ N ₂ O ₂	2.04	-CHF ₃ -C ₂ H ₄ -H ₂ O	167.0315	C ₆ H ₆ F ₃ O ₂	0.06		
237.0638	C ₁₂ H ₈ F ₃ N ₂	2.81	-CO ₂ -CHF ₃ -H ₂ O	167.0414	C ₈ H ₅ F ₂ N ₂	0.97	m/z 187-HF	
185.0301	C ₈ H ₄ F ₃ N ₂	6.46	-C ₆ H ₇ F ₃ O ₂	139.0366	C ₅ H ₆ F ₃ O	0.39		
170.0211	C ₈ H ₃ F ₃ N	0.88	-C ₆ H ₈ F ₃ NO ₃	125.0211	C ₄ H ₄ F ₃ O	1.74		

Based on the LC-HRMS analysis hydroxylation and cleavage of the pyrrolidine ring was assumed as modification for M2 (Table 8.1). In negative ionization mode this modification was supported by the detection of ions m/z 257 and m/z 285, indicating modified ions at m/z 239 and m/z 267 respectively (Table 8.2). A similar metabolite was observed by Sobolevsky *et al.* [31] but our product ion scan data suggest another structure for our detected metabolite.

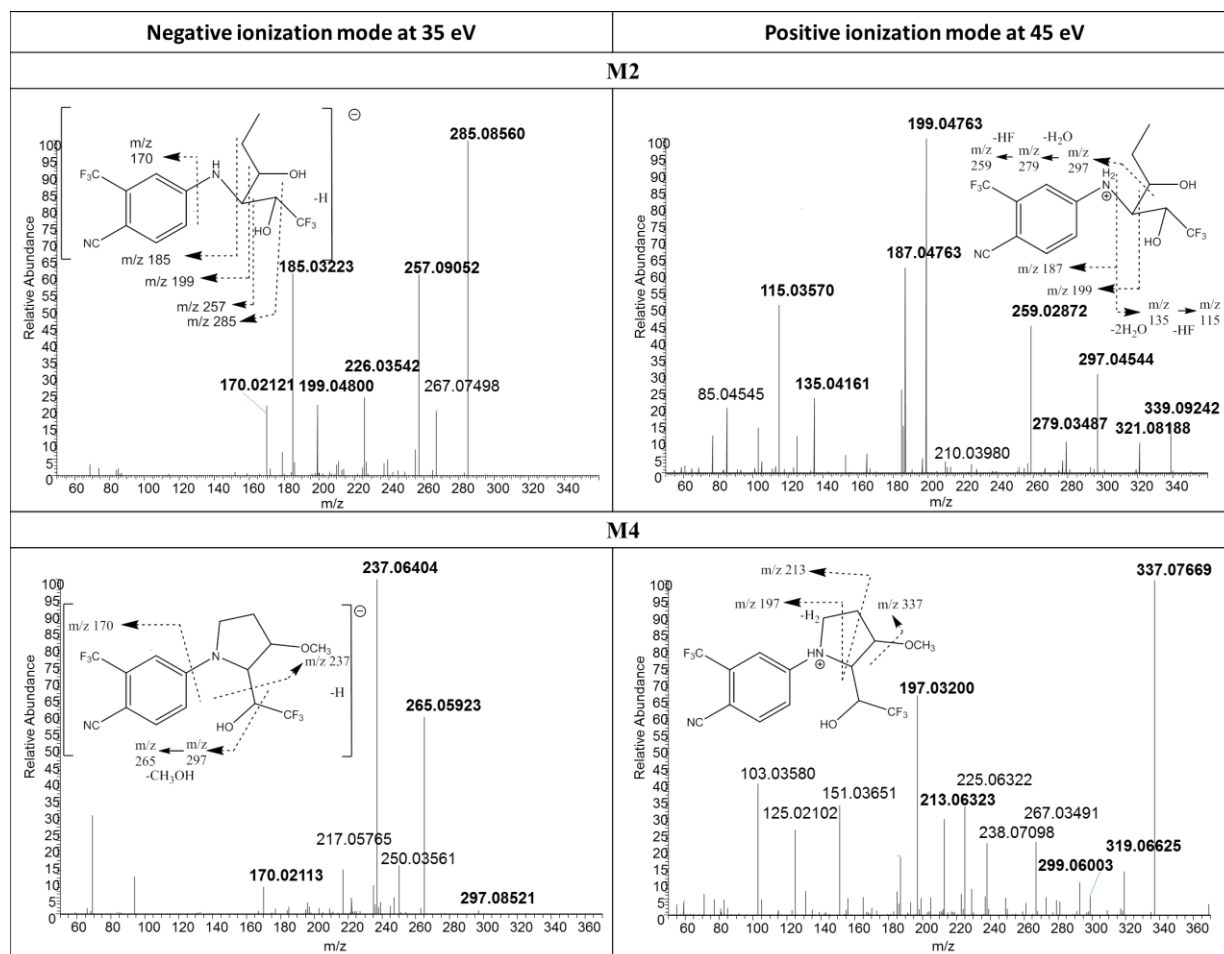


Figure 8.4. LC-HRMS/MS mass spectra of LGD-4033 metabolites M2 and M4 are shown in both negative and positive ionization mode at a CE of 35 eV and 45 eV respectively. The tentative fragmentation patterns are also presented.

In negative ionization mode, the ions at m/z 170, m/z 185 and m/z 199 indicated that the phenyl ring was unaltered (m/z 170), with a nitrogen bonded (m/z 185) and with an alkylic C bonded to the nitrogen (m/z 199). Similar ions (m/z 199 and m/z 187) were observed in positive ionization mode. Other product ions suggested the proposed structure for M2 with a cleavage of the pyrrolidine ring at carbon C6 (Figure 8.4). The ion at m/z 226 can only be explained by the neutral loss of CHF_3 and $\text{C}_3\text{H}_7\text{O}$ suggesting the presence of a hydroxypropyl group in M2. The presence of the hydroxypropyl group was also supported by the ions at m/z 297, m/z 279 and

m/z 259 observed in positive ionization mode. All of these could be explained after the neutral loss of $\text{CH}_3\text{CH}_2\text{CH}_2\text{OH}$ (Table 8.2).

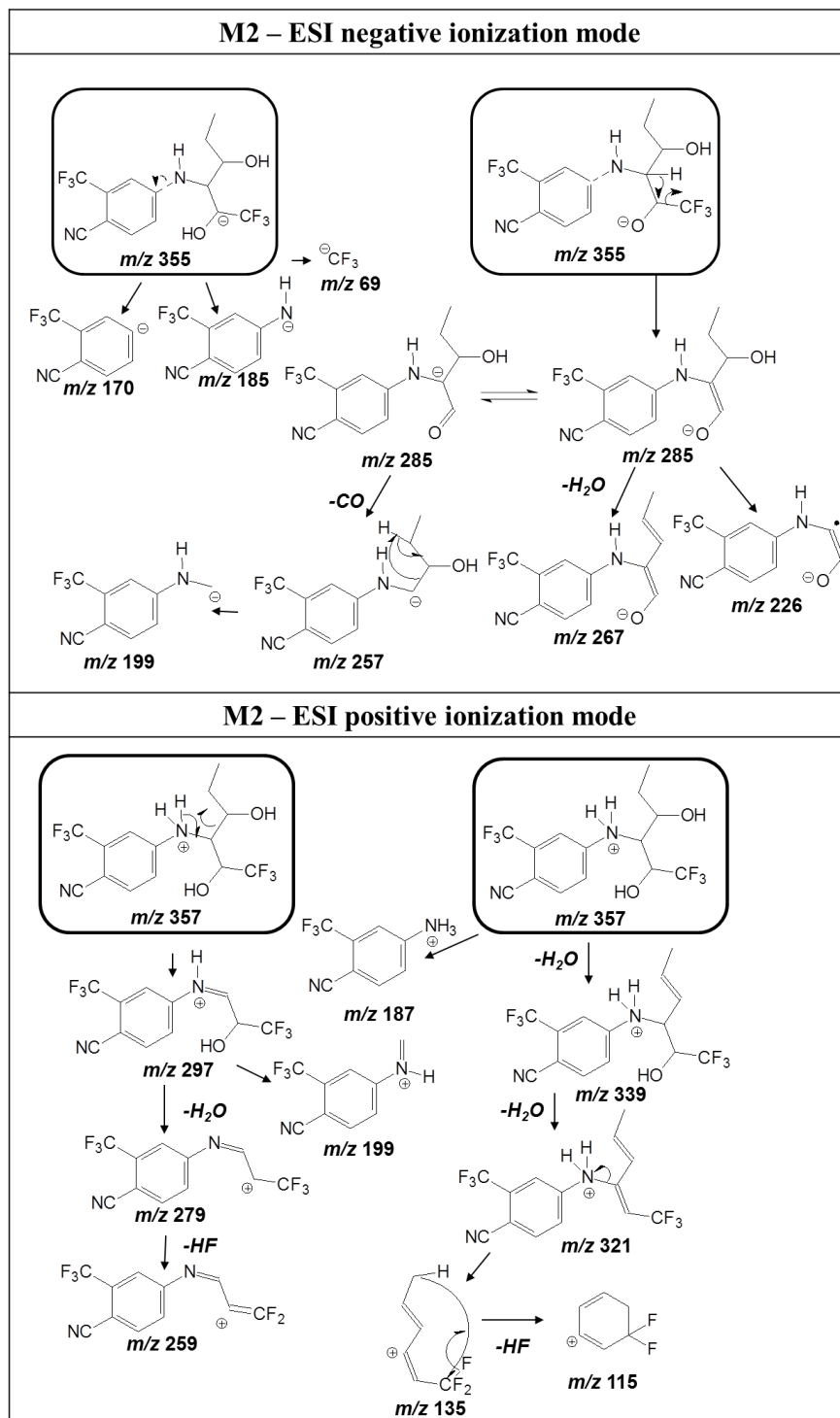


Figure 8.5. Tentative fragmentation pathways of LGD-4033 metabolite M2 in both negative and positive ionization mode. Only one possible configuration of metabolite M2 is presented here.

Additionally, m/z 185 is shown in all compounds but is more important in M2 probably due to the opening of the ring supporting the assignment. The proposed fragmentation pathways leading to the detected fragment ions by LC-HRMS in negative and positive ionization mode are indicated in Figure 8.5.

The earlier mentioned LC-HRMS data suggest a hydroxylation and methylation of LGD-4033 for M3 and M4, rather than hydroxylated M1 metabolites (Table 8.1). The LC-HRMS product ion scan experiments further underpinned this hypothesis (Figure 8.4 and Table 8.2). Whereas metabolites M1 and M2 exhibited an identical number of losses of water as the number of oxygen atoms present in the molecule, only one loss of water was observed in positive ionization mode for M3 and M4. Moreover, a loss of methanol was found for M3 and M4 in both positive and negative ionization mode. The presence of fragment ion m/z 213 in the LC-HRMS/MS experiments in positive ionization mode of M3 and M4 indicate a hydroxylated methylgroup at carbon C4 in the pyrrolidine ring (Figure 8.4 and Table 8.2). In Figure 8.6 the proposed fragmentation pathways for M3/M4 are shown.

The dihydroxylated LGD-4033 structure for M5 was also indicated by three losses of water molecules (Table 8.2). Similar to M1 and M2 the number of losses of water equals the number of oxygen atoms in the molecule. The observed fragment ions for M5 were identical to those for a metabolite described by Thevis *et al.* [16]. Thevis *et al.* were able to identify the structure of this metabolite by NMR and therefore this structure is also shown for M5 in Table 8.1.

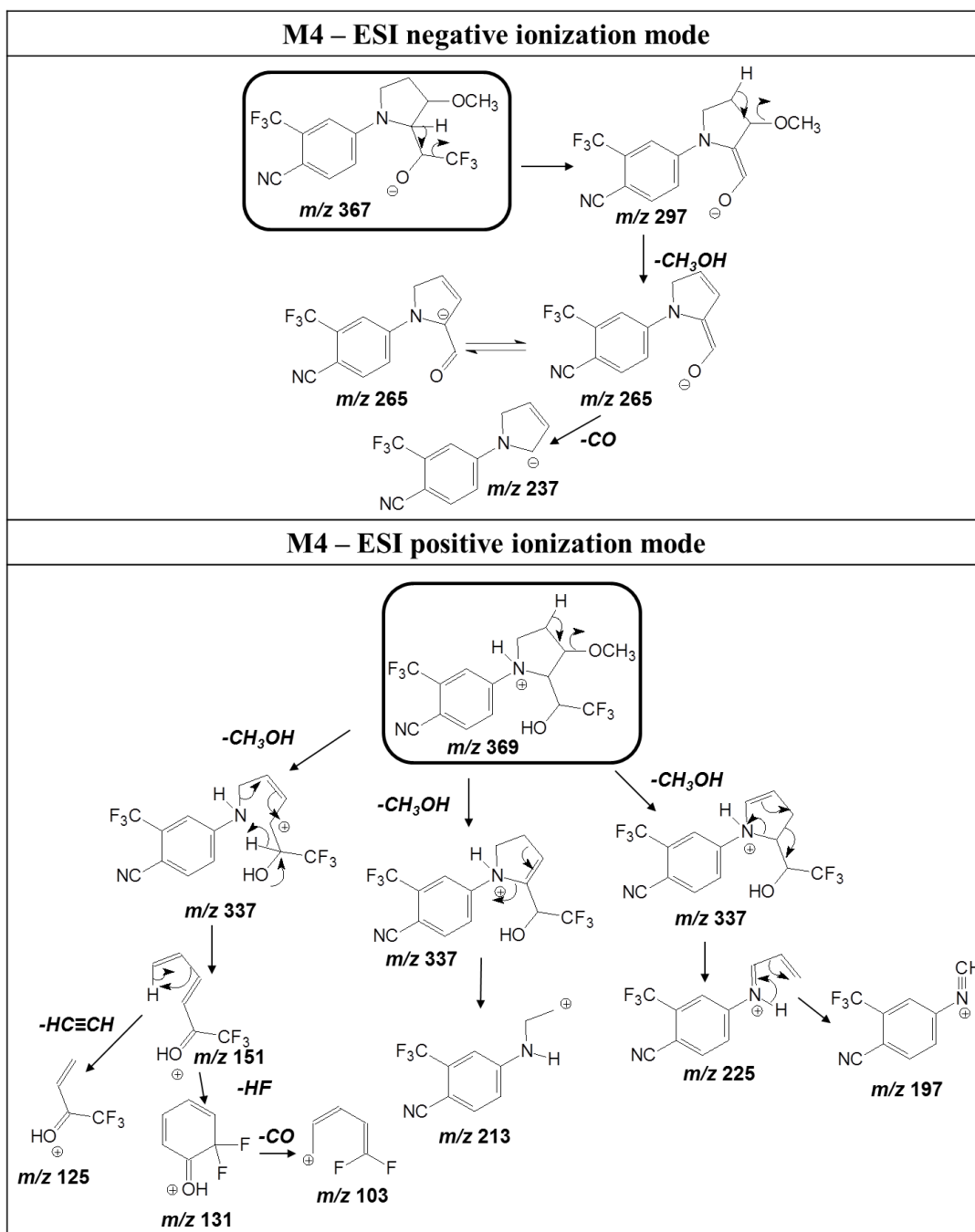


Figure 8.6. Tentative fragmentation pathways of LGD-4033 metabolite M4 in both negative and positive ionization mode. Only one possible configuration of metabolite M4 is presented here.

4 Conclusions

The SARM LGD-4033 is present as black market product and available via the internet to athletes. The metabolic fate of LGD-4033 was elucidated to improve its detection by doping control laboratories.

LGD-4033 seems relatively stable as only five phase I metabolites were identified in this *in vitro* study. Negative ionization mode is preferred for screening of these metabolites. The *in vitro* observed metabolic modifications of LGD-4033 were hydroxylation combined with keto-formation or cleavage of the pyrrolidine ring, dihydroxylation and hydroxylation combined with methylation. Identification of LGD-4033 metabolites was based on knowledge of fragmentation pathways of the parent compound. The LC-HRMS/MS product ion scans indicate that all above mentioned metabolic modifications are situated in the pyrrolidine ring of LGD-4033. Only for the parent compound and M2 glucuronide conjugates were detected. Even though further research is needed to determine the best target compounds in real human samples, implementing these metabolites could improve detection windows of LGD-4033.

Acknowledgements

The authors want to thank all the colleagues for the technical support. We are grateful to Prof. dr. José Martins and Tim Courtin (Ghent University, Department of organic and macromolecular chemistry - NMR and Structural analysis unit) for the excellent technical assistance with the NMR experiments. OJP was supported by contract MS10/00576.

References

1. Thevis M, Kuuranne T, Geyer H, and Schänzer W (2013). Annual banned-substance review: analytical approaches in human sports drug testing. *Drug Test. Anal.* 5, 1-19.
2. Esposito S, Deventer K, Goeman J, Van der Eycken J, and Van Eenoo P (2012). Synthesis and characterization of the N-terminal acetylated 17-23 fragment of thymosin beta 4 identified in TB-500, a product suspected to possess doping potential. *Drug Test. Anal.* 4, 733-738.
3. Esposito S, Deventer K, and Van Eenoo P (2012). Characterization and identification of a C-terminal amidated mechano growth factor (MGF) analogue in black market products. *Rapid Commun. Mass Spectrom.* 26, 686-692.
4. Henninge J, Pepaj M, Hullstein I, and Hemmersbach P (2010). Identification of CJC-1295, a growth-hormone-releasing peptide, in an unknown pharmaceutical preparation. *Drug Test. Anal.* 2, 647-650.
5. Kohler M, Thomas A, Walpurgis K, Terlouw K, Schänzer W, and Thevis M (2010). Detection of His-tagged Long-R-3-IGF-I in a black market product. *Growth Horm. IGF Res.* 20, 386-390.
6. Thomas A, Kohler M, Mester J, Geyer H, Schänzer W, Petrou M, and Thevis M (2010). Identification of the growth-hormone-releasing peptide-2 (GHRP-2) in a nutritional supplement. *Drug Test. Anal.* 2, 144-148.
7. Thevis M, and Schänzer W (2010). Synthetic anabolic agents: steroids and nonsteroidal selective androgen receptor modulators. In *Handb Exp Pharmacol* (Thieme D, and Hemmersbach P, Eds.) 195, 99-126, Heidelberg Germany.
8. Kohler M, Thomas A, Geyer H, Petrou M, Schänzer W, and Thevis M (2010). Confiscated black market products and nutritional supplements with non-approved ingredients analyzed in the Cologne Doping Control Laboratory 2009. *Drug Test. Anal.* 2, 533-537.
9. Thevis M, Thomas A, Kohler M, Beuck S, and Schänzer W (2009). Emerging drugs: mechanism of action, mass spectrometry and doping control analysis. *J. Mass Spectrom.* 44, 442-460.
10. Thevis M, and Schänzer W (2008). Mass spectrometry of selective androgen receptor modulators. *J. Mass Spectrom.* 43, 865-876.
11. Fragkaki AG, Angelis YS, Koupparis M, Tsantili-Kakoulidou A, Kokotos G, and Georgakopoulos C (2009). Structural characteristics of anabolic androgenic steroids contributing to binding to the androgen receptor and to their anabolic and androgenic activities Applied modifications in the steroidal structure. *Steroids* 74, 172-197.
12. Chen JY, Kim J, and Dalton JT (2005). Discovery and therapeutic promise of selective androgen receptor modulators. *Mol. Interv.* 5, 173-188.
13. Wu D, Wu ZR, Yang J, Nair VA, Miller DD, and Dalton JT (2006). Pharmacokinetics and metabolism of a selective androgen receptor modulator in rats: Implication of molecular properties and intensive metabolic profile to investigate ideal pharmacokinetic characteristics of a propanamide in preclinical study. *Drug Metab. Dispos.* 34, 483-494.
14. WADA. The 2016 Prohibited List, International Standard. Montreal (2016) <https://wada-main-prod.s3.amazonaws.com/resources/files/wada-2016-prohibited-list-en.pdf> (access date 04.01.16).

15. Krug O, Thomas A, Walpurgis K, Piper T, Sigmund G, Schänzer W, Laussmann T, and Thevis M (2014). Identification of black market products and potential doping agents in Germany 2010-2013. *Eur. J. Clin. Pharmacol.* 70, 1303-1311.
16. Thevis M, Lagojda A, Kuehne D, Thomas A, Dib J, Hansson A, Hedeland M, Bondesson U, Wigger T, Karst U, and Schänzer W (2015). Characterization of a non-approved selective androgen receptor modulator drug candidate sold via the Internet and identification of in vitro generated phase-I metabolites for human sports drug testing. *Rapid Commun. Mass Spectrom.* 29, 991-999.
17. Thevis M, and Schänzer W (2014). Analytical approaches for the detection of emerging therapeutics and non-approved drugs in human doping controls. *J Pharm Biomed Anal* 101, 66-83.
18. Basaria S, Collins L, Dillon EL, Orwoll K, Storer TW, Miciek R, Ulloor J, Zhang AQ, Eder R, Zientek H, Gordon G, Kazmi S, Sheffied-Moore M, and Bhasin S (2013). The Safety, Pharmacokinetics, and Effects of LGD-4033, a Novel Nonsteroidal Oral, Selective Androgen Receptor Modulator, in Healthy Young Men. *J. Gerontol. Ser. A-Biol. Sci. Med. Sci.* 68, 87-95.
19. Gao WQ, and Dalton JT (2007). Expanding the therapeutic use of androgens via selective androgen receptor modulators (SARMs). *Drug Discov. Today* 12, 241-248.
20. Grata E, Perrenoud L, Saugy M, and Baume N (2011). SARM-S4 and metabolites detection in sports drug testing: A case report. *Forensic Sci.Int.* 213, 104-108.
21. WADA. 2010 Anti-Doping Testing Figures - Laboratory report. Montreal (2011) https://wada-main-prod.s3.amazonaws.com/resources/files/WADA_2010_Laboratory_Statistics_Report.pdf (access date 17/07/2015).
22. WADA. 2013 Anti-Doping Testing Figures - Laboratory report. Montreal (2014) <https://wada-main-prod.s3.amazonaws.com/resources/files/WADA-2013-Anti-Doping-Testing-Figures-LABORATORY-REPORT.pdf> (access date 08/01/2015).
23. Thevis M, Thomas A, Fussholler G, Beuck S, Geyer H, and Schänzer W (2010). Mass spectrometric characterization of urinary metabolites of the selective androgen receptor modulator andarine (S-4) for routine doping control purposes. *Rapid Commun. Mass Spectrom.* 24, 2245-2254.
24. Kuuranne T, Leinonen A, Schänzer W, Kamber M, Kostianen R, and Thevis M (2008). Aryl-propionamide-derived selective androgen receptor modulators: Liquid chromatography-tandem mass spectrometry characterization of the in vitro synthesized metabolites for doping control purposes. *Drug Metab. Dispos.* 36, 571-581.
25. Gao WQ, Wu ZR, Bohl CE, Yang J, Miller DD, and Dalton JT (2006). Characterization of the in vitro metabolism of selective androgen receptor modulator using human, rat, and dog liver enzyme preparations. *Drug Metab. Dispos.* 34, 243-253.
26. Thevis M, Geyer H, Thomas A, and Schänzer W (2011). Trafficking of drug candidates relevant for sports drug testing: detection of non-approved therapeutics categorized as anabolic and gene doping agents in products distributed via the Internet. *Drug Test. Anal.* 3, 331-336.
27. Thevis M, Gerace E, Thomas A, Beuck S, Geyer H, Schlorer N, Kearbey JD, Dalton JT, and Schänzer W (2010). Characterization of in vitro generated metabolites of the selective androgen receptor modulators S-22 and S-23 and in vivo comparison to post-administration canine urine specimens. *Drug Test. Anal.* 2, 589-598.

28. Thevis M, Thomas A, Moller I, Geyer H, Dalton JT, and Schänzer W (2011). Mass spectrometric characterization of urinary metabolites of the selective androgen receptor modulator S-22 to identify potential targets for routine doping controls. *Rapid Commun. Mass Spectrom.* 25, 2187-2195.
29. Thevis M, Kamber M, and Schänzer W (2006). Screening for metabolically stable aryl-propionamide-derived selective androgen receptor modulators for doping control purposes. *Rapid Commun. Mass Spectrom.* 20, 870-876.
30. Creaven PJ, Pendyala L, and Tremblay D (1991). PHARMACOKINETICS AND METABOLISM OF NILUTAMIDE. *Urology* 37, 13-19.
31. Sobolevsky T, Dikunets M, Dudko G, and Rodchenkov G (2015). Metabolism study of selective androgen receptor modulator LGD-4033, In Poster presented at Manfred Donike Workshop - 33rd Cologne workshop on dope analysis (01/03/2015-06/03/2015).
32. Zhu BT, and Lee AJ (2005). NADPH-dependent metabolism of 17 beta-estradiol and estrone to polar and nonpolar metabolites by human tissues and cytochrome P450 isoforms. *Steroids* 70, 225-244.

Chapter 9

***In vitro* metabolism studies of REV-ERB α agonists SR9009 and SR9011**

Authors:

Geldof L, Deventer K, Tudela E and Van Eenoo P. (To be submitted)

Abstract

SR9009 and SR9011 are promising drug candidates for several metabolic disorders due to their REV-ERB modulation activity. The nuclear REV-ERB α and REV-ERB β receptors play an important role in maintaining circadian rhythm and energy homeostasis. The increase in exercise endurance observed in animal experiments makes these substances also attractive as performance enhancing substances. Although no pharmaceutical preparations are available yet, illicit use of SR9009 and SR9011 for doping purposes can be anticipated, especially since SR9009 is marketed in illicit products. Therefore, methods need to be developed to effectively control the use of these substances. *In vitro* metabolism studies can assist preventive doping research leading to the incorporation of diagnostic metabolites into screening methods.

In this study the presence of SR9009 could be demonstrated in a black market product purchased over the internet. The metabolic fate of SR9009 and SR9011 was studied using human liver microsomes. In total eight metabolites were detected for SR9009 and fourteen metabolites for SR9011 by LC-(HR)MS analysis. Structure elucidation was performed for all metabolites by LC-HRMS product ion scans in both positive and negative ionization mode.

The research method used for the detection of the parent compounds and their metabolites was qualitatively validated. The limit of detection of the parent compounds was 2 ng/mL for SR9009 and 5 ng/mL for SR9011. Retrospective data analysis was applied to 1511 doping control samples previously analyzed by a full scan LC-HRMS screening method to verify the presence of SR9009, SR9011 and their metabolites. So far, the presence of neither the parent compound nor the metabolites could be detected in routine urine samples.

1 Introduction

Physiological processes as metabolism and behavior e.g. activity/rest, are generally organized on a cycle of approximately 24 h driven by a circadian rhythm [1-3]. The nuclear receptors REV-ERB α and REV-ERB β regulate the expression of core clock proteins and therefore help to modulate the circadian rhythm [1, 2, 4, 5].

Modulation of the REV-ERB activity by synthetic agonists e.g. SR9009 and SR9011 (Figure 9.1) alters the expression of genes involved in lipid and glucose metabolism and plays therefore an important role in maintaining the energy homeostasis [1, 4, 6]. Effects of SR9009 and SR9011 observed via *in vitro* and *in vivo* animal studies were increased basal oxygen consumption, decreased lipogenesis, cholesterol and bile acid synthesis in the liver, increased mitochondrial content, glucose and fatty acids oxidation in the skeletal muscle and decreased lipid storage in the white adipose tissue [1, 2, 4, 6, 7].

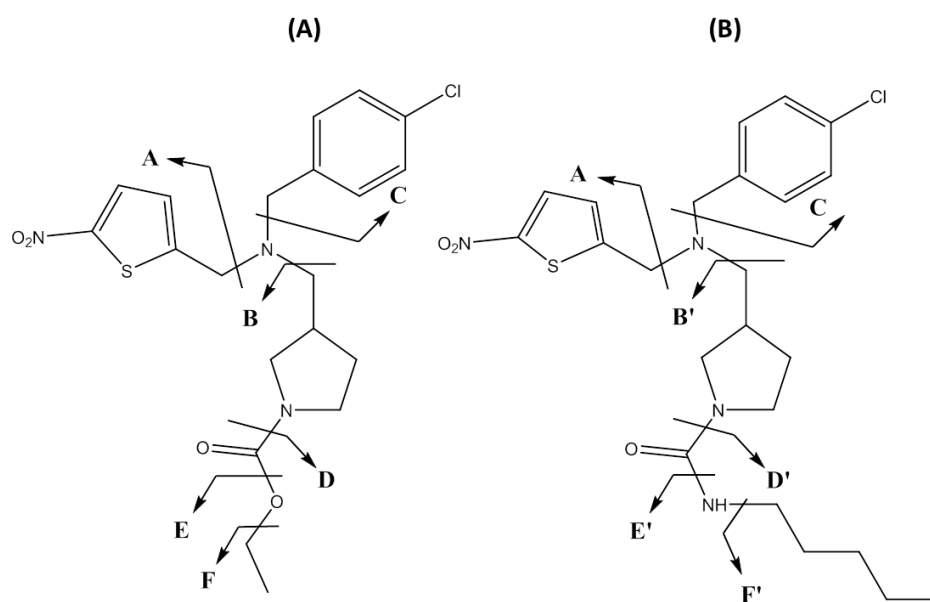


Figure 9.1. Chemical structures of REV-ERB α agonists SR9009 (A) and SR9011 (B). The tentative fragmentation patterns are also indicated.

The observed increase in energy expenditure and decrease in fat mass make the REV-ERB agonists SR9009 and SR9011 promising drug candidates for treatment of several metabolic disorders [3, 4, 6]. At the same time the increase in exercise capacity observed via *in vivo* animal studies [6, 8] makes these compounds also attractive for performance enhancement by athletes, although such use can be classified as doping. The potential interest as doping agents is clearly shown by their popularity in discussion fora on the internet, where they are mentioned

as the ultimate ‘exercise in a pill’ compounds [8-14]. Although these REV-ERB agonists are currently still undergoing clinical evaluation and are therefore not approved for therapeutic use, distribution in black market products might be expected as observed before for designer steroids [15-17], peptides [18-23], several SARMs [24-26] and GW501516 [26].

Even though not explicitly mentioned on the Prohibited List published by the World Anti-Doping Agency (WADA) they are indirectly prohibited as non-approved substances (Class S0), but could potentially also be classified as metabolic modulators (Class S4) [27].

As illicit use of SR9009 and SR9011 can be anticipated, monitoring of their presence on the market and use by doping control laboratories is recommended. These preventive investigations not only help to close the gap between anti-doping laboratories and the appearance of new doping agents but also contribute to deter the use of these compounds and therefore protect fair play and the health of athletes, as athletes are deterred from use when a substance is detectable.

To allow a fast response to the appearance of new non-approved performance enhancing substances, *in vitro* metabolism studies are frequently applied. As the liver is the principal organ for drug metabolism *in vitro* models are often based on human liver fractions (e.g. human liver microsomes (HLM)) [28]. These *in vitro* studies not only circumvent the ethical objections related to the use of human volunteers for excretion studies, they are more affordable and can be applied rapidly. Moreover, analytically, the clean extracts improve the characterization of metabolites [29]. However, careful extrapolation of these *in vitro* studies to real human metabolism should be performed as some metabolic pathways may be over or under expressed [28]. Nevertheless, *in vitro* metabolism studies allow to incorporate metabolites into existing screening methods which could improve the detection window compared to the parent compound and they can provide reference material to improve identification of suspicious doping control samples [29].

In the current study, a black market product sold as performance enhancing product and labeled to contain SR9009 was purchased over the internet to verify its content. The analysis resulted in the identification of the mentioned compound. Consecutively, HLM were applied to perform metabolism studies of SR9009 and SR9011.

2 Materials and Methods

2.1 Chemicals and reagents

A black market gross sales product, claiming to contain SR9009, was purchased over the internet (to prevent athletes of purchasing this product, further details remain confidential). The internal standard (IS) 17 α -methyltestosterone was obtained from Organon (Oss, the Netherlands). 4-hydroxytamoxifen-d5 was purchased from Toronto Research Chemicals (TRC, Toronto, Canada). The reference standard of methandienone was obtained from the 'National Measurement Institute' (NMI, North Ryde, Australia). Reference material of SR9009 and SR9011 was purchased from Calbiochem (Merck Chemicals, Nottingham, UK) and Xcess Bio (San Diego, US), respectively. Pooled HLM from 20–30 donors, the nicotinamide adenine dinucleotide phosphate (NADPH) regenerating system solutions A and B and phosphate buffer pH 7.4 all from Gentest were purchased by Corning (Amsterdam, the Netherlands). Ethanol and ammonium acetate (NH₄OAc) were purchased from Biosolve (Valkenswaard, the Netherlands). Diethyl ether and methanol (MeOH) were obtained from Fisher Scientific (Loughborough, UK). Sodium sulfate (Na₂SO₄), sodium hydrogen carbonate (NaHCO₃), potassium carbonate (K₂CO₃), ammonium iodide (NH₄I) and acetic acid (HOAc) were from Merck (Darmstadt, Germany). LC grade water and LC grade MeOH were purchased from J.T. Baker (Deventer, the Netherlands). Nitrogen (N₂) and oxygen-free nitrogen (OFN) was delivered by Air Liquide (Bornem, Belgium).

2.2 Instrumentation

2.2.1 LC-(HR)MS

All experiments were performed under the same LC conditions using a Thermo Finnigan Surveyor Autosampler Plus and a MS Pump Plus (Thermo Scientific, Bremen, Germany). The LC separation was performed using a SunFire™ C18 column (50 mm × 2.1 mm i.d., 3.5 μ m) from Waters (AH Etten-Leur, the Netherlands), at a flow rate of 250 μ L/min. The injection volume was 25 μ L in the no waste injection mode. The mobile phase consisted of LC grade water (solvent A) and LC grade MeOH (solvent B) both with 1 mM NH₄OAc and 0.1% HOAc. The percentage of the organic solvent in the applied gradient program was linearly changed as follows: 0 min, 15%; 1 min, 15%; 6.5 min, 70%; 14 min, 75%; 16.0 min, 100%; 16.9 min, 100%; 17 min, 15% and 20 min, 15%. The methods have a total run time of 20 min.

For the low resolution methods a TSQ Quantum Discovery MAX triple quadrupole mass spectrometer (Thermo Scientific) was used. Therefore a full scan method was applied in a range of m/z 100-500 in both positive and negative mode. The other MS conditions were interface: electrospray ionization (ESI), capillary voltage: 3.5 kV, source temperature: 350 °C, sheath gas

(N₂) pressure: 50 (arbitrary units), auxiliary gas (N₂) pressure: 20 (arbitrary units), tube lens offset: 100 V, scan time: 0.5 s.

The HR-MS(/MS) experiments were performed on an Exactive mass spectrometer (Thermo Scientific). The instrument operated in both positive and negative full scan mode from m/z 100 to 2000 at a resolving power of 50,000 with a data acquisition rate of 2 Hz. For the structural investigation of metabolites LC-HRMS product ions scans were performed by a Q-Exactive mass spectrometer (Thermo Scientific) for the protonated and deprotonated molecules as selected ions with an isolation window of 1.0 m/z at a resolving power of 70,000 at collision energies of 15, 25, 35 and 45 eV. The other MS parameters for both LC-HRMS instruments were identical to the low resolution instruments except for spray voltage: 4 kV, source temperature of 250 °C and heated ESI (HESI) (probe heater at 300 °C). A LC-HRMS screening method as indicated in [30] was also applied for the assay validation.

2.3 *In vitro* incubation studies

Prior to the *in vitro* metabolism studies, the black market product containing SR9009 and available reference material of SR9011 and SR9009 were analyzed by LC-(HR)MS for purity verification.

Phase I *in vitro* metabolic assays (HLM) were applied as described in Chapter 1 (7.2.2.2 *Protocol in vitro metabolism studies*; Table 1.6). The final concentration of SR9009 and SR9009 in the *in vitro* incubation samples was 40 µg/mL. Substrate stability samples (blank; without HLM) and system blank samples (without test compound) control samples were used to verify the enzymatic reactions. Methandienone was used as test compound in the positive control samples. At the appropriate time (after 2, 4 and 18 h) the enzymatic reactions were terminated by adding 250 µL of ice-cold MeOH.

2.4 Assay validation

The qualitative determination of SR9009 and SR9011 was validated in human urine regarding specificity, extraction recovery and limit of detection (LOD) according to the Eurachem guidelines [31] and in compliance with the WADA International Standards for Laboratories (ISL) [32].

Specificity was tested during the validation procedure by checking for possible interfering peaks in the extracted ion chromatograms (EIC) at the expected retention times for SR9009 and SR9011.

The LOD was defined as the lowest concentration that can be detected in ten human urine samples with a signal to noise ratio (S/N) higher than three. Ten different blank human urine samples (seven male and three female; pH-range from 4.72 to 6.89; specific gravity between 1.006 and 1.035 g/L) were spiked at 2, 5, 10 and 20 ng/mL for SR9009 and at 5, 10, 20 and 50 ng/mL for SR9011. For the assay validation 4-hydroxytamoxifen-d5 was used as internal standard. Blank urines and distilled water samples spiked only with this IS were also included. Sample preparation was performed as described in the following section (2.5 *Sample preparation*). The samples were analyzed according to an existing LC-HRMS screening method [30] providing the data necessary to determine the LOD.

The extraction recovery of SR9009 and SR9011 during sample preparation was determined at 20 ng/mL and at 50 ng/mL respectively. Recovery was calculated by comparison of the mean peak area of the analytes for urine samples spiked before and after sample preparation. Therefore, the results of the ten blank urines applied for determination of the LOD spiked with SR9009 and SR9011 before sample preparation were used. Another batch of the same blank urines was spiked with SR9009 and SR9011 after sample preparation.

Additionally, matrix effects were studied at 20 ng/mL for SR9009 and at 50 ng/mL for SR9011. Matrix effects were measured by comparing the peak area (A) of the analytes spiked in 10 extracted urines and in a neat standard solution following the formula:

$$\text{M.E. (\%)} = \frac{(A(\text{urine}) - A(\text{standard solution}))}{A(\text{standard solution})} \times 100.$$

2.5 *Sample preparation*

The samples of the *in vitro* metabolic assays were analyzed by direct injection on LC-HRMS, after removal of the enzymatic proteins. Therefore, the HLM incubation samples were first centrifuged at 4 °C (12,000 g, 5 min) followed by transferring 400 µL into new tubes. 50 µL of the internal standard (IS) 17α-methyltestosterone (2 µg/mL) was added to all samples.

The samples for the assay validation were first enzymatically hydrolyzed by β-glucuronidase and then a liquid-liquid extraction (LLE) was performed as described in Chapter 3 (2.5.1 *Liquid-liquid extraction (LLE)*). The residues were dissolved in 100 µL H₂O/MeOH (50/50) for LC-(HR)MS/MS analysis.

3 Results and Discussion

3.1 Analysis of black market product

Reference standards of SR9009 and SR9011 were analyzed by both low resolution and high resolution LC-MS instruments. The presence of SR9009 in the black market product was also verified by comparison with commercially available reference material by LC-(HR)MS. Mass deviations smaller than 1 ppm were observed for SR9009 and SR9011 in the reference material and black market product (LC-HRMS). Identification criteria in chromatography and mass spectrometry, as stipulated in the WADA Technical Document [33] were also met for the black market product. LC-(HR)MS analysis did not result in the detection of major impurities (<5% total peak height in the total ion chromatogram) in the black market product. These results indicate that the use of SR9009 is no longer a potential threat, but a real doping threat. Shortly after the purchase of the substance from the gross sale internet market, the product also appeared for purchase in individual quantities from several internet suppliers of performance enhancing substances. This indicates that the substance has now become readily available to athletes and that detection methods need to be developed for the product.

3.2 In vitro metabolism studies

In the current study the metabolic fate of SR9009 and SR9011 was determined by HLM incubations with commercially available reference standards. The HLM incubation samples were analyzed by full scan LC-HRMS analysis in both positive and negative ionization mode. The search for potential metabolites was complemented with the extraction of specific exact mass ions for “expected” metabolites, based upon knowledge of HLM transformations and theoretically possible metabolic pathways including oxidations (e.g. hydroxylations, double bond formation), reductions (e.g. ring opening), cleavage of the structure and combinations of these pathways [34, 35].

Eight metabolites (SR09-1 till SR09-8) and fourteen metabolites (SR11-1 till SR11-14) were detected in the HLM incubation samples for SR9009 and SR9011, respectively (Figure 9.2 and Figure 9.3). All metabolites were detected with less than 5 ppm mass deviation from their proposed structures (Figure 9.4). To facilitate further discussion the different parts of the molecules of both parent compounds were assigned to a letter (Figure 9.1 and Table 9.1).

Table 9.1. LC-HRMS product ion scans of SR9009 and SR9011. Common product ions of the parent compounds and metabolites are also indicated.

Compound	Fragment ^a	Chemical formula	Polarity mode	Theoretic mass (m/z)	Δ ppm	Detected in metabolites
SR9009 / SR9011	A	C ₅ H ₃ NO ₂ S	+	141.9957	2.58	SR09-: 1; 5-8 SR11-: 1-4; 7a/b/c; 8a/b; 9-11; 14
SR9009	B	C ₈ H ₁₁ NO ₂	+	154.0863	0.94	SR09-: 1; 2; 6
SR9011	B'	C ₁₁ H ₂₀ N ₂ O	+	197.1648	0.41	/
SR9009 / SR9011	C	C ₇ H ₅ Cl	+	125.0153	3.96	SR09-: 1; 2; 3(a/b/c); 4(a/b); 5; 7; 8 SR11-: 1-6; 9-13
SR9009	-C	C ₁₃ H ₁₇ N ₃ O ₄ S	+	312.1013	1.78	SR09-1
			-	311.0945	1.30	/
	-C-NO ₂	C ₁₃ H ₁₈ N ₂ O ₂ S	-	265.1016	1.25	/
SR9011	-C	C ₁₆ H ₂₄ N ₄ O ₃ S	+	353.1642	1.99	SR11-: 1; 7
	-C-D'	C ₁₀ H ₁₃ N ₃ OS	-	239.0734	1.86	SR11-: 1; 3; 9
	-C-D'-NO ₂	C ₁₀ H ₁₄ N ₂ S	-	193.0805	4.83	SR11-: 1; 9
	-D'+2H	C ₁₇ H ₂₀ N ₃ O ₂ ClS	+	366.1038	2.18	SR11-: 1-4; 9
SR9009 / SR9011	-E/E'	C ₁₈ H ₁₈ N ₃ O ₃ ClS	+	392.0830	2.08	SR11-: 1-4
SR9009 / SR9011	C+CNH ₄	C ₈ H ₈ NCl	+	154.0418	1.06	SR09-: 3(b/c); 4b; 8 SR11-: 1-6; 9-11; 13
SR9009	B-CH ₂	C ₇ H ₁₁ NO ₂	+	142.0863	0.18	SR09-: 2; 3(b/c); 4b
	-B+CH ₂	C ₁₃ H ₁₁ N ₂ O ₂ ClS	+	295.0303	0.96	SR09-: 1; 8 SR11-: 10; 11
	-A	C ₁₅ H ₁₉ N ₂ O ₂ Cl	+	295.1208	0.72	SR09-: 1; 3a/b/c
SR9011	B'-CH ₂	C ₁₀ H ₁₈ N ₂ O	+	183.1492	0.49	SR11-: 8b
SR9009 / SR9011	-C-E/E'	C ₁₁ H ₁₃ N ₃ O ₃ S	+	268.0750	0.12	SR11-: 1, 2; 4; 7a/b; 8a; 9; 14

^a See Figure 9.1 for structures of fragments A, B, B', C, D, D', E and E'; – symbolizes loss of the indicated fragment.

The highest relative abundances in the HLM incubation samples with SR9009 were observed for metabolites SR09-1, SR09-2, SR09-4(a), SR09-5 and SR09-7. For SR9011 metabolites SR11-1, SR11-3, SR11-5 and SR11-9 have the highest relative abundances. Metabolite SR09-5 and similar metabolites as SR11-5, SR11-6 and SR11-13 were also described by Sobolevsky *et al.* as major human metabolites of SR9009 and SR9011, respectively [36].

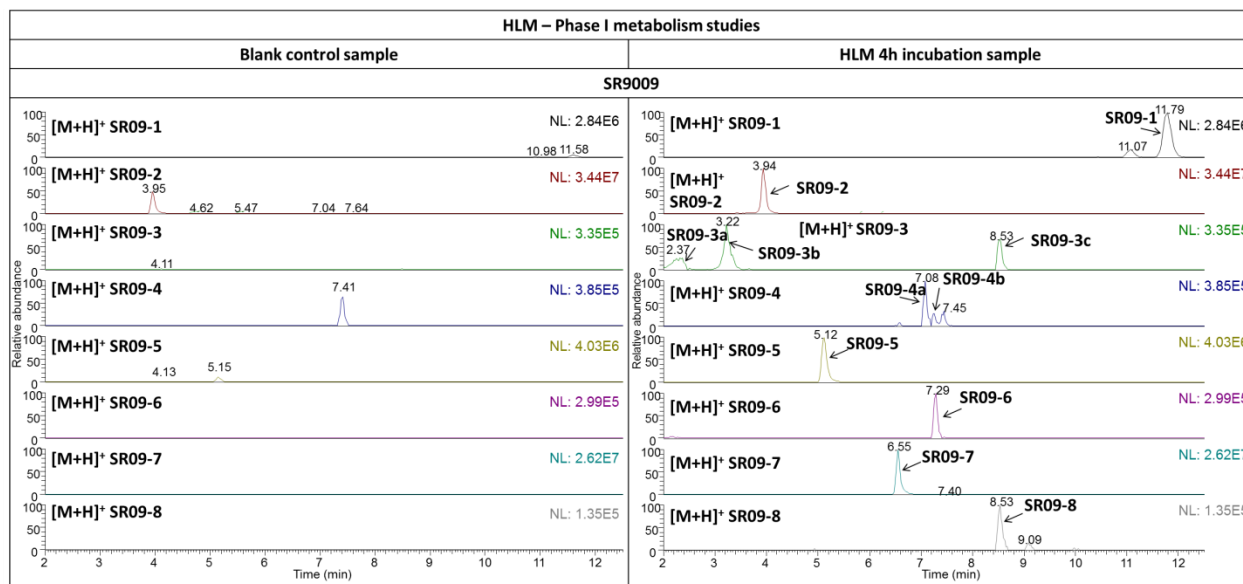


Figure 9.2. *In vitro* metabolism studies with SR9009. The extracted ion LC-HRMS chromatograms of the 4 h HLM incubation samples (right column) are presented in comparison with blank (without HLM) control samples (left column).

3.3 Structure characterization by LC-HRMS/MS

Initially, the fragmentation patterns of the parent compounds were studied in both positive and negative ionization mode to identify diagnostic product ions (Figure 9.1 and Table 9.1). Similar fragmentation patterns were observed for SR9009 and SR9011 leading to diagnostic fragments A, B/B' and C. As indicated in Figure 9.1 fragment B/B' was further fragmented for both SR9009 and SR9011, respectively. Structure elucidation of the SR9009 and SR9011 metabolites was based on the detection of structure-specific product ions by LC-HRMS (Table 9.2 and Table 9.3).

3.3.1 SR9009

For all hydroxylated SR9009 metabolites product ions related to a loss of water were observed (Table 9.2).

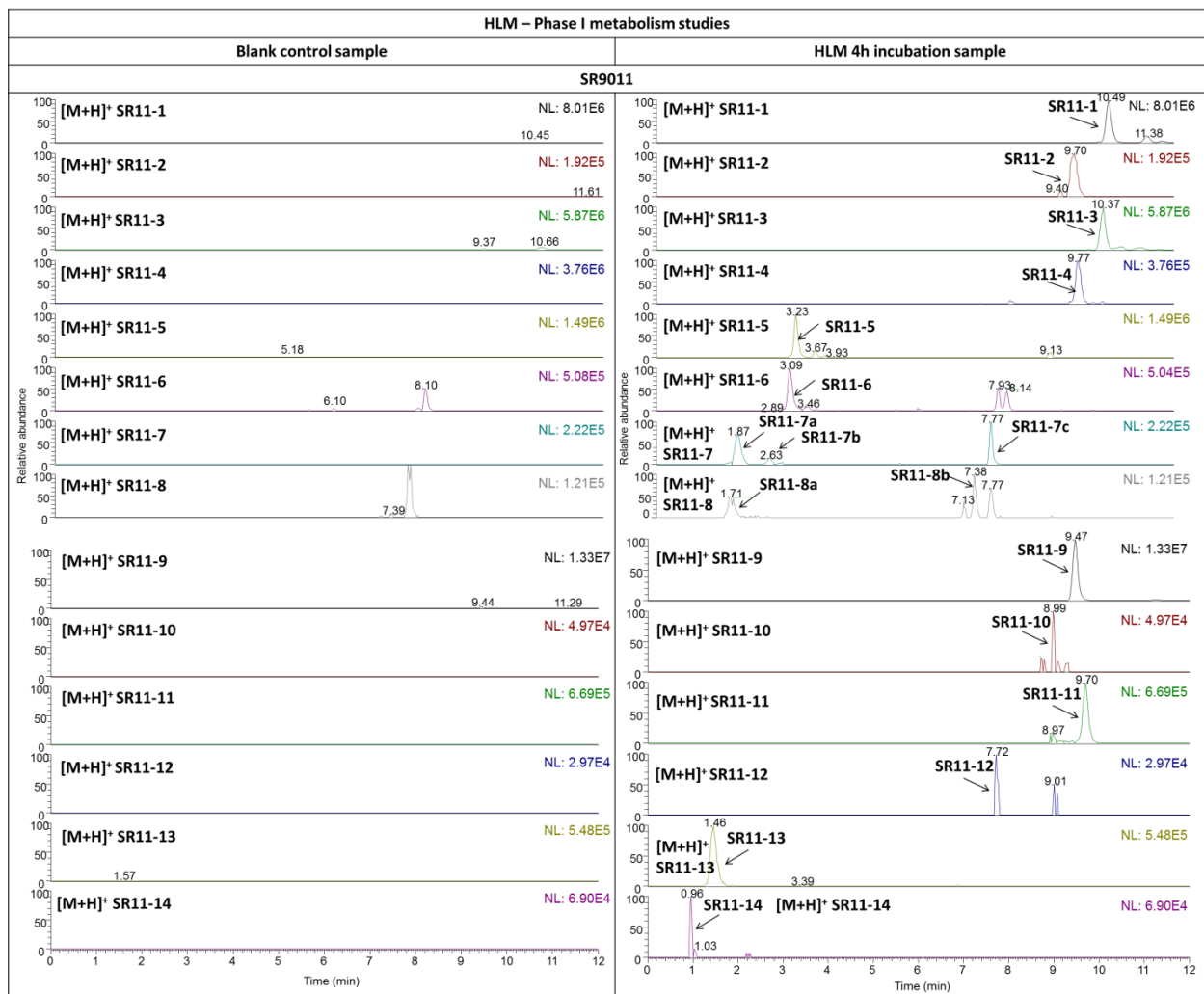


Figure 9.3. *In vitro* metabolism studies with SR9011. The extracted ion LC-HRMS chromatograms of the 4 h HLM incubation samples (right column) are presented in comparison with blank (without HLM) control samples (left column).

In the product ion scan mass spectra of SR09-1 a base peak was observed at m/z 295.0298 in positive ionization mode. This ion was also found for SR9009 and could be linked to $C_{13}H_{12}O_2N_2ClS$ by HRMS (Table 9.1). Fragments A, B and C were also observed for SR09-1 (Table 9.1). In negative ionization mode ions m/z 327.0895 and 251.0494 indicate a hydroxylation of the parent compound outside C and F (Table 9.2). In positive ionization mode a fragment ion m/z 172.0965 was found, which indicates a hydroxylation in B (Table 9.2).

The structure of metabolite SR09-2 corresponds to a loss of A of the parent compound. The product ion data were also consistent with this structure as only fragments B and C were observed (Table 9.1 and Table 9.2). For metabolites SR09-5 and SR09-7, with structures corresponding to loss of B and D respectively, only product ions related to A and C were observed (Table 9.1).

Metabolites SR09-3 and SR09-4 correspond to hydroxylated derivatives of SR09-2 after loss of A (Table 9.2). For all isomeric SR09-3 and SR09-4 metabolites fragment C was observed. In the product ion scan mass spectrum of SR09-3a m/z 158.0811 was observed, which indicates a hydroxylation in B (m/z 142.0863) as this fragment corresponds to $C_7H_{12}NO_3$ with 0.63 ppm mass deviation (Table 9.2). In contrast to what was observed in the product ion scan mass spectra of all other metabolites, product ion m/z 154.0418 corresponding to C_8H_9NCl was more abundant than product ion m/z 125.0153 (fragment C) for SR09-3b. For SR09-3b m/z 141.0100 was also observed which corresponds to C_7H_6OCl with 1.12 ppm mass deviation and is indicative for a hydroxylation at C of the parent compound. For metabolite SR09-3c and SR09-4a no indicative ions for the position of hydroxylation (and further oxidation (-H₂)) were found. The ion m/z 170.0364 observed for SR09-4b would indicate a hydroxylation and subsequent keto-formation in C of the parent compound, as this corresponds to C_8H_9NOCl with 1.75 ppm mass deviation (Table 9.2).

The ion m/z 157.9904 in the product ion scan mass spectrum of SR09-6 indicates a hydroxylation in A (m/z 141.9957) for this metabolite (Table 9.2).

Fragments A and C were observed in the product ion scan mass spectrum of SR09-8. Similar to metabolite SR09-1 an abundant fragment ion m/z 295.0299 was observed. Although no indicative ions for the position of hydroxylation were found, this base peak (m/z 295.0299) could also indicate a modification (hydroxylation and keto-formation) in B(-D) (Table 9.2).

Similar metabolites for SR9009 were also described in the HLM incubation and human excretion urine samples by Sobolevsky *et al.* [36]. Metabolites SR09-1 and SR09-6 were not reported in their study. However, two additional metabolites were detected in their study; one metabolite characterized by a loss of D and hydroxylation and another by as loss of C [36]. This latter metabolite was also described as a major human metabolite [36]. Considering the structures of SR09-6 (-C+OH) and SR09-7 (-D), these metabolic modifications observed by Sobolevsky *et al.* seem possible in our *in vitro* incubation samples [36].

Table 9.2. Characterization of metabolites detected in HLM incubation samples with SR9009 by LC-HRMS analysis.

Compound	Metabolic modification ^a	Chemical formula	[M+H] ⁺ (Δ ppm)	Product ion				
				Polarity mode	Exp m/z ^b	Chemical formula	Δ ppm	Origin ^a
SR09-1	+OH	C ₂₀ H ₂₄ N ₃ O ₅ ClS	454.1192 (0.94)	+	172.0965	C ₈ H ₁₄ NO ₃	1.68	B+H ₂ O
				-	327.0895	C ₁₃ H ₁₇ N ₃ O ₅ S	0.31	-C+OH
					281.0476	C ₁₁ H ₁₁ N ₃ O ₄ S	0.09	-C-F+OH
SR09-2	-A	C ₁₅ H ₂₁ N ₂ O ₂ Cl	297.1361 (1.08)	+	251.0942	C ₁₃ H ₁₆ N ₂ OCl	1.42	-A-E
SR09-3 a	-A+OH	C ₁₅ H ₂₁ N ₂ O ₃ Cl	313.1309 (1.36)	+	251.0942	C ₁₃ H ₁₆ N ₂ OCl	1.38	-A-E-H ₂ O
					225.1150	C ₁₂ H ₁₈ N ₂ Cl	1.30	-A-D-H ₂ O
					158.0811	C ₇ H ₁₂ NO ₃	0.63	B+CH ₂ +OH
SR09-3 b					141.0100	C ₇ H ₆ OCl	1.12	C+OH
SR09-3 c					267.0890	C ₁₃ H ₁₆ N ₂ O ₂ Cl	1.95	-A-F-H ₂ O
SR09-4 a	-A+OH-H ₂	C ₁₅ H ₁₉ N ₂ O ₃ Cl	311.1148 (1.19)	+	265.0731	C ₁₃ H ₁₄ N ₂ O ₂ Cl	0.85	-F-H ₂ O
				293.1046	C ₁₅ H ₁₈ N ₂ O ₂ Cl	1.88	-H ₂ O	
				265.0734	C ₁₃ H ₁₄ N ₂ O ₂ Cl	1.78	-A-F-H ₂ -H ₂ O	
				170.0364	C ₈ H ₉ NOCl	1.75	A+CH ₃ NO	
SR09-5	-B	C ₁₂ H ₁₁ N ₂ O ₂ SCl	283.0297 (1.88)	+	*			
SR09-6	-C+OH	C ₁₃ H ₁₉ N ₃ O ₅ S	330.1112 (1.84)	+	284.0694	C ₁₁ H ₁₄ N ₃ O ₄ S	2.05	-C-F-H ₂ O
					157.9904	C ₅ H ₄ NO ₃ S	1.33	A+OH
SR09-7	-D	C ₁₇ H ₂₀ N ₃ O ₂ ClS	366.1031 (1.81)	+	*			
SR09-8	-D+OH-H ₂	C ₁₇ H ₁₈ N ₃ O ₃ ClS	380.0826 (1.15)	+	362.07120	C ₁₇ H ₁₇ N ₃ O ₂ ClS	1.36	-H ₂ O

^a The structures of A, B, C, D and F' are indicated in Figure 9.1 and Table 9.1 ; – symbolizes loss of the indicated fragment

^b Exp m/z = experimental m/z

*: see product ion scan data of the parent compounds presented in Table 9.1 for typical fragment ions of the compound(s).

Table 9.3. Characterization of metabolites detected in HLM incubation samples with SR9011 by LC-HRMS analysis.

Compound	Metabolic modification ^a	Chemical formula	[M+H] ⁺ (Δ ppm)	Product ion				
				Polarity mode	Exp m/z ^b	Chemical formula	Δ ppm	Origin ^a
SR11-1	+OH	C ₂₃ H ₃₁ N ₄ O ₄ ClS	495.1818 (1.84)	+	181.1333	C ₁₀ H ₁₇ N ₂ O	1.49	B'-CH ₂ -H ₂
				-	368.1523	C ₁₆ H ₂₄ N ₄ O ₄ S	0.34	-C+OH
SR11-2	+2OH	C ₂₃ H ₃₁ N ₄ O ₅ Cl	511.1771 (1.09)	+	242.0954	C ₁₀ H ₁₆ N ₃ O ₂ S	1.67	-C-D'-2H ₂ O
					215.1387	C ₁₀ H ₁₉ N ₂ O ₃	1.53	B'-CH ₂ -H ₂ +2OH
SR11-3	-H ₂ +OH	C ₂₃ H ₂₉ N ₄ O ₄ ClS	493.1665 (1.24)	+	475.1562	C ₂₃ H ₂₈ N ₄ O ₃ ClS	0.62	-H ₂ O
				-	366.1365	C ₁₆ H ₂₂ N ₄ O ₄ S	0.69	-C+OH-H ₂
SR11-4	-H ₂ +2OH	C ₂₃ H ₂₉ N ₄ O ₅ ClS	509.1616 (0.80)	+	409.1091	C ₁₈ H ₂₂ N ₄ O ₃ ClS	1.06	-F'-2H ₂ O
					242.0952	C ₁₀ H ₁₆ N ₃ O ₂ S	2.33	-C-D'-2H ₂ O
					227.1387	C ₁₁ H ₁₉ N ₂ O ₃	1.45	B'+2OH-H ₂
					213.1230	C ₁₀ H ₁₇ N ₂ O ₃	1.59	B'-CH ₂ +2OH
SR11-5	-A+OH	C ₁₈ H ₂₈ N ₃ O ₂ Cl	354.1932 (3.11)	+	225.1147	C ₁₂ H ₁₈ N ₂ Cl	2.81	-A-D'-H ₂ O
					197.1489	C ₁₁ H ₁₉ N ₂ O	1.28	B'
					144.1130	C ₆ H ₁₄ N ₃ O	1.24	B'-F'
					225.1149	C ₁₂ H ₁₈ N ₂ Cl	1.61	-A-D'-H ₂ O
SR11-6	-A+OH-H ₂	C ₁₈ H ₂₆ N ₃ O ₂ Cl	352.1781 (1.59)	+	211.1436	C ₁₁ H ₁₉ N ₂ O ₂	2.29	B'+OH-H ₂
					197.1280	C ₁₀ H ₁₇ N ₂ O ₂	2.20	B'-CH ₂ +OH-H ₂
					242.0953	C ₁₀ H ₁₆ N ₃ O ₂ S	2.00	-C-D'-H ₂ O
SR11-7 a/b	-C+OH	C ₁₆ H ₂₆ N ₄ O ₄ S	371.1742 (1.52)	+	199.1438	C ₁₀ H ₁₉ O ₂ N ₂	1.63	B'-CH ₂ +OH
					258.0903	C ₁₀ H ₁₆ N ₃ O ₃ S	1.51	-C-D'+OH
					229.1782	C ₁₁ H ₂₃ N ₃ O ₂	1.30	B'+OH
SR11-8 a	-C+OH-H ₂	C ₁₆ H ₂₄ N ₄ O ₄ S	369.1587 (1.20)	+	285.1011	C ₁₁ H ₁₇ N ₄ O ₃ S	1.47	-C-F'-H ₂ O
					242.0953	C ₁₀ H ₁₆ N ₃ O ₂ S	1.67	-C-D'-H ₂ O
SR11-8 b					282.0538	C ₁₁ H ₁₂ N ₃ O ₄ S	1.89	-C-E'+OH
					256.0745	C ₁₀ H ₁₄ N ₃ O ₃ S	2.26	-C-D'+OH
SR11-9	-F'	C ₁₈ H ₂₁ N ₄ O ₃ ClS	409.1088 (1.97)	+	283.0853	C ₁₁ H ₁₅ N ₄ O ₃ S	2.15	-F'-C
					251.0940	C ₁₃ H ₁₆ N ₂ OCl	2.90	-A-E'
SR11-10	-F'+OH	C ₁₈ H ₂₁ N ₄ O ₄ ClS	425.1051 (1.39)	+	364.0876	C ₁₇ H ₁₈ N ₃ O ₂ ClS	1.41	-D'-H ₂ O
					237.0786	C ₁₂ H ₁₄ N ₂ OCl	1.17	-A-D'+OH
					194.0729	C ₆ H ₁₄ N ₂ O ₃ S	4.92	A+CH ₂ +OH

Table 9.3. Continued.

Compound	Metabolic modification ^a	Chemical formula	[M+H] ⁺ (Δ ppm)	Product ion				
				Polarity mode	Exp m/z ^b	Chemical formula	Δ ppm	Origin ^a
SR11-11	-F'-H ₂	C ₁₈ H ₁₉ N ₄ O ₃ ClS	407.0932 (1.83)	+	266.0588	C ₁₁ H ₁₂ N ₃ O ₃ S	2.06	-C-E'-H ₂
					249.0784	C ₁₃ H ₁₄ N ₂ OCl	2.20	-A-E'-H ₂
SR11-12	-F'-H ₂ +OH	C ₁₈ H ₁₉ N ₄ O ₄ ClS	423.1621 (1.94)	+	380.0823	C ₁₇ H ₁₉ N ₃ O ₃ ClS	1.86	-D'+OH
					282.0537	C ₁₁ H ₁₂ N ₃ O ₄ S	2.21	-C-E'+OH
					256.0746	C ₁₀ H ₁₄ N ₃ O ₃ S	2.03	-C-D'+OH
SR11-13	-F'-A	C ₁₃ H ₁₈ N ₃ OCl	268.1205 (2.15)	+	225.1149	C ₁₂ H ₁₈ N ₂ Cl	1.66	-A-D'
SR11-14	-F'-C	C ₁₁ H ₁₆ N ₄ O ₃ S	285.1011 (1.57)	+	*			

^a The structures of A, B, C, D and F' are indicated in Figure 9.1 and Table 9.1; – symbolizes loss of the indicated fragment

^b Exp m/z = experimental m/z

*: see product ion scan data of the parent compounds presented in Table 9.1 for typical fragment ions of the compound.

3.3.2 SR9011

For all SR9011 metabolites, except for SR11-12, the number of losses of water was identical to the proposed number of hydroxylations (Table 9.3).

Typical product ions of fragment A, B', C were observed for SR11-1 but no indicative ions for the position of hydroxylation were found in positive ionization mode (Table 9.1 and Table 9.3). However, in negative ionization mode ion m/z 368.1522 indicates a modification outside fragment C (Table 9.3).

The presence of ion m/z 215.1387 in the product ion mass spectrum of metabolite SR11-2 could indicate a dihydroxylation at B' (m/z 183.1492) (Table 9.1 and Table 9.3).

For SR11-3 no diagnostic product ions for the position of hydroxylation were found in positive ionization mode. However, in negative ionization mode a product ion m/z 366.1365 was observed for SR11-3, which is similar to ion m/z 368.1522 found for SR11-1 (Table 9.3). This ion indicates a hydroxylation and subsequent keto-formation outside C.

Two product ions (m/z 227.1387 and 213.1230) were found for SR11-4 which could be indicative for a dihydroxylation, and subsequent keto-formation of one of these hydroxylgroups, in B'.

Besides a loss of water no diagnostic fragment ions indicating the site of hydroxylation were observed for SR11-5.

Based on the presence of fragment ions m/z 211.1436 and 197.1280, the proposed site of hydroxylation and subsequent keto-formation of SR11-6 is B' (Table 9.3). These product ions correspond to modified fragment ions m/z 197.1648 and 183.1492 respectively, which were observed for SR9011 (Table 9.1).

Three isomeric compounds were detected for SR11-7(a/b/c). For both SR11-7a and SR11-7b a fragment ion m/z 199.1438 was detected, which is similar to the ion m/z 197.1280 observed for SR11-6, and indicates also a hydroxylation in B'. For SR11-7c fragment ions m/z 229.1782 and 258.0903 indicate a hydroxylation in B', outside D'.

For SR11-8b fragment ions m/z 282.0538 and 256.0745 were observed. This first ion corresponds to a modified ion m/z 268.0750 which was observed for SR9011. For SR11-12 similar fragment ions (m/z 282.0537 and 256.0746) and an additional fragment ion m/z 380.0523 were observed. These fragment ions indicate a similar site of modification (hydroxylation and subsequent keto-formation) for SR-8b and SR11-12, in particular in A or B' (outside D'). For SR11-8a no indicative ions for the site of hydroxylation could be identified.

The observed fragment ions for SR11-9, SR11-11, SR11-13 and SR11-14 were consistent with the proposed structure for these metabolites (Table 9.3). By comparing the product ion scan mass spectra of metabolites SR11-9 and SR11-11 two indicative ions (m/z 266.0588 and 249.4784) for the position of the additional modification of SR11-11 could be identified. These indicative ions correspond to fragment ions m/z 268.0744 and 251.0940 observed for SR11-09 (Table 9.1). Therefore the proposed site of double bond formation for SR11-11 is in B'-E'.

The fragment ions m/z 237.0786 and 194.0729 observed in the product ion scan mass spectrum of SR11-10 in positive ionization mode indicate a hydroxylation at a carbon alpha (of B' or C) to the central nitrogen.

Similar metabolites for SR9011 were reported by Sobolevsky *et al.*, but metabolites SR11-2, SR11-3 and SR11-12 were not reported in their study [36]. However, two additional metabolites were detected in their study, characterized by loss of C or A [36]. This latter was also described as major metabolite in the human excretion study [36]. Since hydroxylated metabolites (SR11-5 and SR11-7), after loss of A or C, were detected, these metabolic modifications observed by Sobolevsky *et al.* seem also possible in our *in vitro* incubation samples [36].

3.4 Assay validation

The LOD of SR9009 and SR9011 was determined by an existing screening method applied by our laboratory for doping control purposes [30] and was 2 ng/mL and 5 ng/mL respectively. The extraction recoveries were 63% for SR9009 and 56% for SR9011 using a non-optimized, regularly applied extraction protocol for initial testing of doping control samples [37]. The matrix effects were determined as ion enhancement of 21% and 20% for SR9009 and SR9011 respectively.

3.5 Retrospective analysis

As SR9009 was purchased via the internet from a gross sales company which sells to internet providers of performance enhancing drugs, it was clear that the substance may already have been misused by athletes in the period between its introduction on the gross sales market and the completion of our studies. To verify the presence of SR9009, SR9011 and their metabolites in routine doping control samples from that period, retrospective data analysis (data reprocessing) was performed for a three month period (June 2015 – September 2015). Furthermore, the presence of the parent compounds was monitored in our routine screening method for another three months (September 2015 - December 2015). For the retrospective data analysis 1511 samples previously analyzed by our routine full scan LC-HRMS screening method [30] were reprocessed. This retrospective data analysis of routine doping control

samples analyzed in our laboratory contained the parent compounds and metabolites of SR9009 and SR9011 in these samples. Although misuse of SR9009 and SR9011 could not be demonstrated in our study, it is hoped that laboratories around the world will perform a similar retrospective analysis.

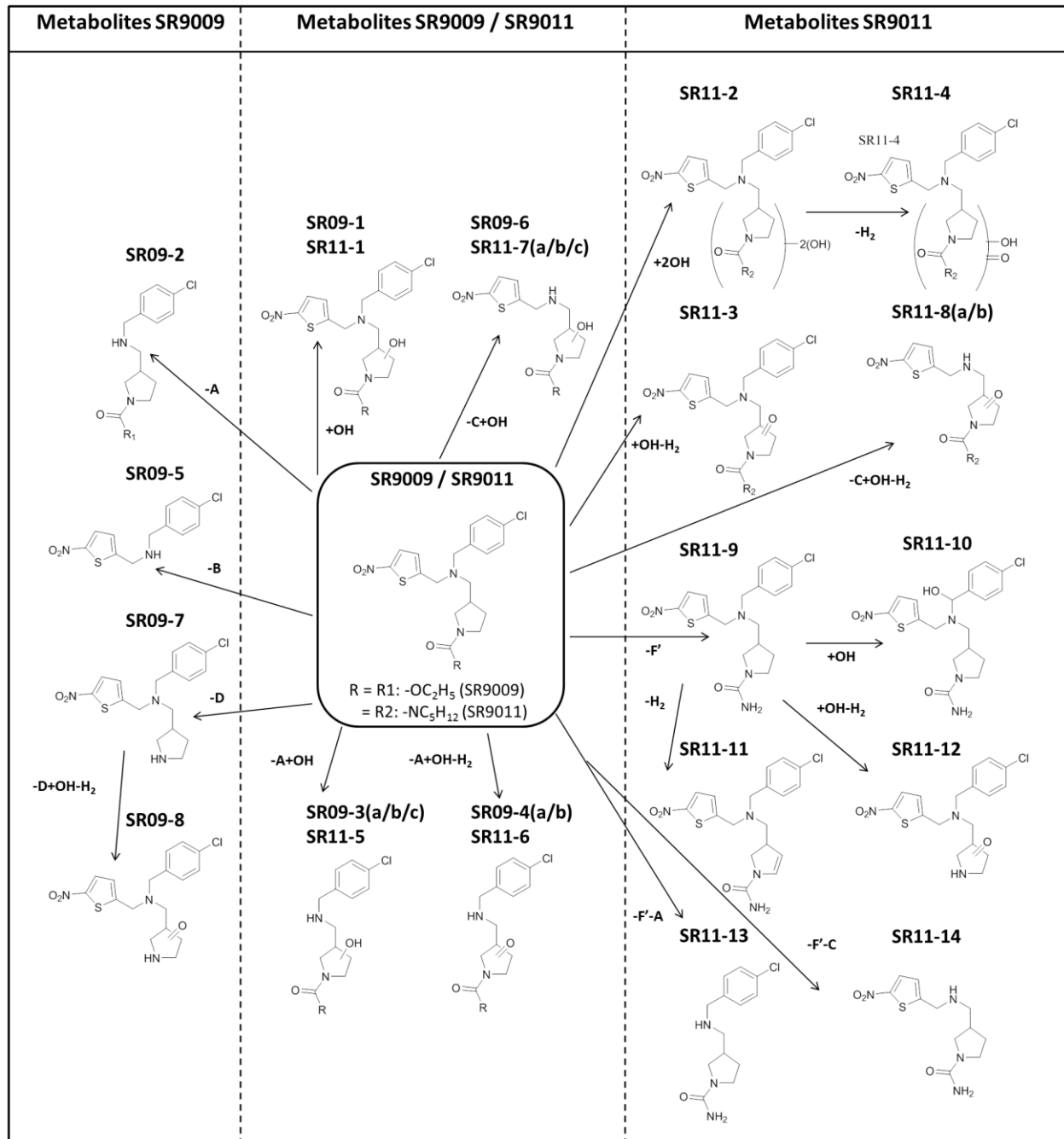


Figure 9.4. Overview of *in vitro* metabolism studies with SR9009 and SR9011. The proposed metabolic modifications are also presented, the structures of A, B, C, D and F' are indicated in Figure 9.1 and Table 9.1. For the position of hydroxylations only one possible configuration is shown.

4 Conclusions

The presence of SR9009 was demonstrated in a black market product obtained via the internet. This finding highlights the high threat for misuse of these potentially performance enhancing substances and the importance of doping control laboratories to anticipate illicit use of SR9009 and SR9011. In this study HLM incubations led to the detection of eight metabolites for SR9009 and fourteen metabolites for SR9011 by LC-(HR)MS analysis. Although modifications were observed in all fragments (A, B, B' and C), most modifications occurred in the B/B' fragment of the parent compounds.

Incorporation of metabolites SR09-1, SR09-2, SR09-4(a), SR09-5, SR09-7 and SR11-1, SR11-3, SR11-5 and SR11-9 might improve screening for misuse of SR9009 and SR9011. However, it should be noted that this assumption is only based on the relative abundances of the metabolites detected in the HLM incubation samples and that extrapolation from these *in vitro* studies to the more complex human situation is difficult. Nevertheless, in the human excretion studies with SR9009 and SR9011 of Sobolevsky *et al.* metabolites SR09-5 and SR11-5 were indeed described as major metabolites of SR9009 and SR9011 respectively [36]. In addition also metabolites SR11-6 and SR11-13 were described as major human metabolites of SR9011 [36].

Therefore, HLM can be considered as a valuable ethically acceptable alternative for human metabolism studies of non-pharmaceutical grade substances.

The LOD was 2 ng/mL for SR9009 and 5 ng/mL for SR9011. To circumvent the low extraction recoveries observed when applying a regularly used sample preparation procedure (hydrolysis and LLE at pH 7) combination with a dilute-and-shoot method is recommended. The presence of SR9009 and SR9011 and their metabolites was verified by retrospective data analysis in 1511 doping control samples. Although misuse of SR9009 and SR9011 could not be demonstrated, incorporation of these substances into screening methods for doping control purposes can help discourage the use of these potentially harmful compounds by both amateur and professional athletes.

Acknowledgements

The Partnership for Clean Competition (PCC) is gratefully acknowledged for financial support. The authors thank Kris Roels for the technical support.

References

1. Shea SA (2012). Obesity and Pharmacologic Control of the Body Clock. *N. Engl. J. Med.* 367, 175-178.
2. Duez H, and Staels B (2008). Rev-erb alpha gives a time cue to metabolism. *FEBS Lett.* 582, 19-25.
3. Bass J (2012). DRUG DISCOVERY Time in a bottle. *Nature* 485, 45-46.
4. Solt LA, Wang YJ, Banerjee S, Hughes T, Kojetin DJ, Lundasen T, Shin Y, Liu J, Cameron MD, Noel R, Yoo SH, Takahashi JS, Butler AA, Kamenecka TM, and Burris TP (2012). Regulation of circadian behaviour and metabolism by synthetic REV-ERB agonists. *Nature* 485, 62-68.
5. Ramakrishnan SN, and Muscat GE (2006). The orphan Rev-erb nuclear receptors: a link between metabolism, circadian rhythm and inflammation? *Nucl. Recept. Signal.* 4, 1-5.
6. Woldt E, Sebti Y, Solt LA, Duhem C, Lancel S, Eeckhoutte J, Hesselink MKC, Paquet C, Delhaye S, Shin YS, Kamenecka TM, Schaart G, Lefebvre P, Neviere R, Burris TP, Schrauwen P, Staels B, and Duez H (2013). Rev-erb-alpha modulates skeletal muscle oxidative capacity by regulating mitochondrial biogenesis and autophagy. *Nat. Med.* 19, 1039-1046.
7. Shin Y, Noel R, Banerjee S, Kojetin D, Song XY, He YJ, Lin L, Cameron MD, Burris TP, and Kamenecka TM (2012). Small molecule tertiary amines as agonists of the nuclear hormone receptor Rev-erb alpha. *Bioorg. Med. Chem. Lett.* 22, 4413-4417.
8. Li S, and Laher I (2015). Exercise Pills: At the Starting Line. *Trends Pharmacol Sci* 36, 906-917.
9. The Huffington Post. 'Exercise Pill' may build muscle, boost athletic performance and lower cholesterol levels (2013). http://www.huffingtonpost.com/2013/08/23/exercise-pill-muscles-athletic-performance-health_n_3797332.html (access date 04.12.15).
10. The Huffington Post. An 'Exercise Pill' may soon exist (2015). http://www.huffingtonpost.com/entry/exercise-pill_us_56128c64e4b0768127028b16 (access date 04.12.2015).
11. ISarms. Stenabolic (SR9009) (2016). <https://www.isarms.com/stenabolic-sr9009> (access date 25.01.16).
12. Elitefitness.com. SARMS RAD140 and SR9009 (2015). <http://www.elitefitness.com/forum/bodybuilding-chemistry-sarms-serms-peptides/sarms-rad140-sr9009-log-1422363.html> (access date 25.01.16).
13. Handschin C (2016). Caloric restriction and exercise "mimetics": Ready for prime time? *Pharmacol Res* 103, 158-166.
14. Fan W, Atkins AR, Yu RT, Downes M, and Evans RM (2013). Road to exercise mimetics: targeting nuclear receptors in skeletal muscle. *J Mol Endocrinol* 51, T87-T100.
15. Geyer H, Parr MK, Koehler K, Mareck U, Schänzer W, and Thevis M (2008). Nutritional supplements cross-contaminated and faked with doping substances. *J. Mass Spectrom.* 43, 892-902.
16. Van Thuyne W, Van Eenoo P, and Delbeke FT (2006). Nutritional supplements: prevalence of use and contamination with doping agents. *Nutr. Res. Rev.* 19, 147-158.

17. Van Eenoo P, and Delbeke FT (2006). Metabolism and excretion of anabolic steroids in doping control - New steroids and new insights. *J. Steroid Biochem. Mol. Biol.* 101, 161-178.
18. Thevis M, Kuuranne T, Geyer H, and Schänzer W (2013). Annual banned-substance review: analytical approaches in human sports drug testing. *Drug Test. Anal.* 5, 1-19.
19. Esposito S, Deventer K, Goeman J, Van der Eycken J, and Van Eenoo P (2012). Synthesis and characterization of the N-terminal acetylated 17-23 fragment of thymosin beta 4 identified in TB-500, a product suspected to possess doping potential. *Drug Test. Anal.* 4, 733-738.
20. Esposito S, Deventer K, and Van Eenoo P (2012). Characterization and identification of a C-terminal amidated mechano growth factor (MGF) analogue in black market products. *Rapid Commun. Mass Spectrom.* 26, 686-692.
21. Henninge J, Pepaj M, Hullstein I, and Hemmersbach P (2010). Identification of CJC-1295, a growth-hormone-releasing peptide, in an unknown pharmaceutical preparation. *Drug Test. Anal.* 2, 647-650.
22. Kohler M, Thomas A, Walpurgis K, Terlouw K, Schänzer W, and Thevis M (2010). Detection of His-tagged Long-R-3-IGF-I in a black market product. *Growth Horm. IGF Res.* 20, 386-390.
23. Thomas A, Kohler M, Mester J, Geyer H, Schänzer W, Petrou M, and Thevis M (2010). Identification of the growth-hormone-releasing peptide-2 (GHRP-2) in a nutritional supplement. *Drug Test. Anal.* 2, 144-148.
24. Thevis M, and Schänzer W (2010). Synthetic anabolic agents: steroids and nonsteroidal selective androgen receptor modulators. In *Handb Exp Pharmacol* (Thieme, D., and Hemmersbach, P., Eds.) 195, 99-126, Heidelberg Germany.
25. Kohler M, Thomas A, Geyer H, Petrou M, Schänzer W, and Thevis M (2010). Confiscated black market products and nutritional supplements with non-approved ingredients analyzed in the Cologne Doping Control Laboratory 2009. *Drug Test. Anal.* 2, 533-537.
26. Thevis M, Thomas A, Kohler M, Beuck S, and Schänzer W (2009). Emerging drugs: mechanism of action, mass spectrometry and doping control analysis. *J. Mass Spectrom.* 44, 442-460.
27. WADA. The 2016 Prohibited List, International Standard. Montreal (2016) <https://wada-main-prod.s3.amazonaws.com/resources/files/wada-2016-prohibited-list-en.pdf> (access date 04.01.16).
28. Brandon EFA, Raap CD, Meijerman I, Beijnen JH, and Schellens JHM (2003). An update on in vitro test methods in human hepatic drug biotransformation research: pros and cons. *Toxicol. Appl. Pharmacol.* 189, 233-246.
29. Scarth JP, Spencer HA, Timbers SE, Hudson SC, and Hillyer LL (2010). The use of in vitro technologies coupled with high resolution accurate mass LC-MS for studying drug metabolism in equine drug surveillance. *Drug Test. Anal.* 2, 1-10.
30. Deventer K, and Van Eenoo P (2015). Screening and confirmation of a glycerol-positive case. *Drug Test Anal* 7, 1009-1013.
31. Eurachem (1998). The fitness for purpose of analytical methods. A laboratory guide to method validation and related topics. Eurachem, Teddington.

32. WADA (2012). International Standard for Laboratories, version 7.0, World Anti-Doping Agency (WADA), Montreal.
33. WADA. Minimum criteria for chromatographic-mass spectrometric confirmation of the identity of analytes for doping control purposes. Montreal (2015) https://wada-main-prod.s3.amazonaws.com/resources/files/wada_td2015idcr_minimum_criteria_chromato-mass_spectro_conf_en.pdf (access date 20.10.15).
34. Timbrell J (2002). Metabolism of foreign compounds. In Introduction to toxicology 3, 39-56, London.
35. Dominguez-Romero JC, Garcia-Reyes JF, Martinez-Romero R, Berton P, Martinez-Lara E, Del Moral-Leal ML, and Molina-Diaz A (2013). Combined data mining strategy for the systematic identification of sport drug metabolites in urine by liquid chromatography time-of-flight mass spectrometry. *Anal. Chim. Acta* 761, 1-10.
36. Sobolevsky T, Dikunets M, and Rodchenkov G (2015). Metabolism study of GSK4122, SR9009 and SR9011, new "exercise-in-a-pill" drug candidates, In Poster presented at Manfred Donike Workshop - 33rd Cologne workshop on dope analysis (01/03/2015-06/03/2015).
37. De Brabanter N, Van Gansbeke W, Geldof L, and Van Eenoo P (2012). An improved gas chromatography screening method for doping substances using triple quadrupole mass spectrometry, with an emphasis on quality assurance. *Biomed. Chromatogr.* 26, 1416-1435.

PART 4

Epilogue





Chapter 10

General discussion

1 Metabolism studies of (designer) steroids

Black market steroid products were purchased over the internet including Orastan-E, Ultradrol, Xtreme DMZ and Tren-X. In all of these steroid products the active ingredients indicated on their labels (prostanazol(-THP), methylstenbolone, dimethazine and estradienedione respectively) could be detected (Table 10.1). However, in the case of the steroid product Ultradrol that was supposed to contain only methylstenbolone, the structural analogue methasterone was also detected. Methasterone was also detected in the steroid product Xtreme DMZ, due to degradation of dimethazine. These findings emphasize the importance to verify the content of black market products.

Table 10.1. Overview of black market products examined in this study.

	Steroid product	Steroids indicated on label	Detected steroids	More information in paragraph
	Orastan-E	Prostanazol-THP	Prostanazol-THP Prostanazol	1.1
	Ultradrol	Methylstenbolone	Methylstenbolone Methasterone	1.2
	Xtreme DMZ	Dimethazine	Dimethazine Methasterone	1.3
	Tren-X	Estradienedione	Estradienedione	1.4

The presence of these (designer) steroids in the black market products available over the internet makes them easily accessible for both recreational and professional athletes and they can therefore be considered as real doping threats. This does not only endanger the ethics of sports but also the health of the athletes as toxicological profiles are often missing. Especially in the case of recreational athletes which tend to self-administer these products without any

medical supervision. Moreover, incorrect labeling and/or contamination issues as observed for Ultradrol bears additional health risks.

Consequently, *in vitro* and *in vivo* metabolism studies were performed to allow efficient detection of these (designer) steroids, which has a deterrent effect on potential misuse.

1.1 Prostanazol

Both prostanazol-THP and prostanazol were detected in the steroid product (Table 10.1 and Chapter 3). Hydrolysis of prostanazol-THP to prostanazol was observed (Figure 10.1). The metabolism of prostanazol was studied *in vitro* (HLM) and *in vivo* (uPA^{+/+}-SCID chimeric mouse model) (Chapter 3). Human administration and excretion studies with prostanazol have been previously performed and allow comparison with the obtained results from the *in vitro* and *in vivo* model.

The prostanazol metabolic pathways described in the human urine samples were similar to those detected in both models (Figure 10.1). C16, C4 and C3' are characteristic positions for hydroxylation of prostanazol in human administration studies, while hydroxylations at C6 and C12 (indicated with question marks in Figure 10.1) were proposed based on common hydroxylation positions of AAS reported in literature.

Monohydroxylated prostanazol metabolites were more abundant than monohydroxylated 17-ketoprostanazol metabolites in the *in vitro* and *in vivo* models, whereas these latter metabolites were more abundant in the human urine samples. However, both 3'-hydroxy- and 16 β -hydroxy-17-ketoprostanazol could be unequivocally identified in the *in vitro* and *in vivo* model by comparison with commercially available reference material. 4-hydroxy-17-ketoprostanazol could not be detected in both models. In the study of Rodchenkov *et al.* this metabolite was also not reported in human samples [1]. In the other human excretion studies [2, 3] and in our reanalyzed positive routine sample 16 β -hydroxy- and 3'-hydroxy-17-ketoprostanazol metabolites were more abundant than 4-hydroxy-17-ketoprostanazol.

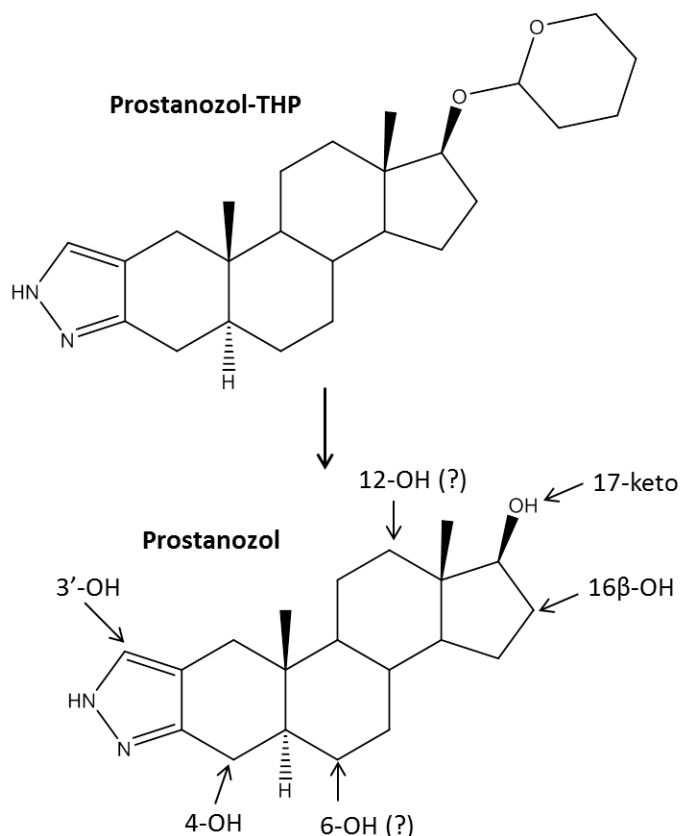


Figure 10.1. Overview of prostanazol metabolic pathways observed via *in vitro* and *in vivo* metabolism studies. The question marks indicate proposed positions for hydroxylations based on common AAS hydroxylation pathways described in literature.

17-ketoprostanazol was described before in a human excretion study of prostanazol [3]. 17-ketoprostanazol itself could only be detected in the *in vitro* model. The absence of this metabolite in the chimeric mouse model is probably due to the faster metabolic rate observed in mice, as several additional hydroxylated 17-ketoprostanazol metabolites could be detected.

In both models several dihydroxylated prostanazol and 17-ketoprostanazol metabolites were detected. Some of these were also reported before in human excretion studies, but not as abundant as the mono-hydroxylated 17-ketoprostanazol metabolites.

Comparison of chimeric and non-chimeric mouse urine samples allowed us to evaluate interspecies differences. Therefore, 3'/4-hydroxy-17-keto prostanazol and 3'/4,x-dihydroxyprostanazol metabolites, which were not detected in the non-chimeric mouse urine samples, could be considered as typical human metabolites. Both categories of metabolites were indeed reported in human excretion studies [1-3]. Hence, the comparison between chimeric and non-chimeric mouse urine samples can be helpful to identify typical human metabolites. This does, however, not exclude that metabolites detected in both models can be human. Indeed, careful

interpretation of the results is recommended. For example 16 β -hydroxy-17-ketoprostanazol was detected in the non-chimeric mouse urine samples as well as in human urine samples [1-3]. This indicates that murine and human metabolites sometimes overlap.

1.2 Methylstenbolone and methasterone

In a black market product (Ultradrol) claiming to contain methylstenbolone however also the exogenous AAS methasterone or methyldrostanolone (or 'Superdrol') was detected (Chapter 4). This fact raises additional concerns about the potential adverse health effects of misuse of this steroid product. Indeed, administration of methasterone has been related to severe side effects [4-7]. In 2012 methasterone was also added to the 'Designer anabolic steroid control act' of the Government of the United States [8].

Since both methylstenbolone and methasterone were detected in the steroid product, *in vitro* and *in vivo* metabolism studies of the two substances (independently and together) were performed. For both substances human excretion studies are described in literature, allowing the verification of the human nature of the observed metabolites. However, further research also indicated that for the administration of methylstenbolone to the human volunteer in the published research, no purity verification had been performed. Later research showed that the ingested capsule was also contaminated with methyldrostanolone in this study.

The observed metabolic pathways for methylstenbolone and methasterone are presented in Figure 10.2. In the *in vitro* and *in vivo* models no conversion of methylstenbolone to methasterone or vice versa was detected. Although structurally closely related, no common metabolites were found for both substances.

1.2.1 Methylstenbolone

For methylstenbolone the observed metabolic pathways were different for the *in vitro* and *in vivo* metabolism studies. Whereas only monohydroxylated methylstenbolone metabolites were detected *in vitro*, only dihydroxylated metabolites were detected in the chimeric mouse urine samples. The presence of the dihydroxylated metabolites in both the chimeric and non-chimeric mouse urine samples might indicate a murine origin of these metabolites. In both models however (mono/di)hydroxylated methylstenbolone metabolites with an additional oxidation (-H₂) were observed. The main proposed positions of hydroxylations of the *in vitro* metabolites are at the A-ring or C18. Hydroxylation at C18 was also proposed for an *in vivo* (mouse) metabolite and has also previously been reported for stenbolone in human urine samples [9]. This position of hydroxylation would be typical for steroids with C1 or C2 methyl groups [9, 10]. The typical structure of stenbolone (double bond at C1 and C2-methyl group) makes it relatively stable to reductive metabolism. Therefore, major stenbolone metabolites retain either the 1-

ene-3-keto or 1-ene structure and hydroxylation at C16 is promoted [11]. In our metabolism studies with (17 α -)methylstenbolone all metabolites retained the 1-ene-3-keto structure and 16-hydroxylation was not observed. In the human excretion study of Cavalcanti *et al.* also 16-hydroxylated and 3-keto reduced methylstenbolone metabolites were reported [12]. This stable A-ring structure could also explain why methylstenbolone is not converted to methasterone (Figure 10.2).

In a routine urine sample positive for methylstenbolone (and methasterone) only the parent compound and an unfortunately still unidentified methylstenbolone metabolite could be detected with the developed MRM method. However, in these samples no relevant information (such as purity of the product, dose and time interval) is available.

1.2.2 Methasterone

In the HLM incubation samples the main metabolites for methasterone were 3-keto reduced (M1), hydroxylated (M2) and combined hydroxylated 3-keto reduced (M5) metabolites.

The latter metabolite was not found in the chimeric mouse model. However, metabolites M1 and M2 were also detected in the chimeric mouse urine samples.

Metabolite M1 could be unequivocally identified as 3 α -hydroxymethasterone by comparison to a reference standard. This metabolite was also observed as main methasterone metabolite in human excretion studies [1, 13, 14] and in a doping control urine samples positive for methasterone in our study. Identification of M5 as 2 α ,17 α -dimethyl-5 α -androstane-2 β ,3 α ,17 β -triol was based on correlation with the mass spectrum of an earlier reported methasterone metabolite by Gauthier *et al.* [15]. This metabolite was also a major methasterone metabolite in a human excretion study [14].

In both models several dihydroxylated metabolites and a trihydroxylated metabolite were observed. Only in the mouse model indications for 16-hydroxylated metabolites of methasterone were found. These were also reported in metabolism studies of methasterone in literature [14-16]. Other proposed positions for hydroxylation of methasterone are presented in Figure 10.2.

1.3 Dimethazine (DMZ) or mebolazine

The supplement Xtreme DMZ contained dimethazine (Chapter 5). The structure of dimethazine can be described as two methasterone molecules coupled by an azine group (Figure 10.2). As methasterone was detected in the steroid product Xtreme DMZ, while this was not mentioned on the label, a stability study was performed. It was observed that dimethazine degrades to methasterone, which could explain the presence of methasterone in the steroid product. Based

upon the structural relation, it was also expected that oral administration of DMZ might lead to a substantial conversion of DMZ to methasterone in the stomach.

Not surprisingly, only methasterone and methasterone metabolites were detected in the *in vitro* and *in vivo* metabolism studies with DMZ (Figure 10.2 and 1.2.2 *Methasterone*).

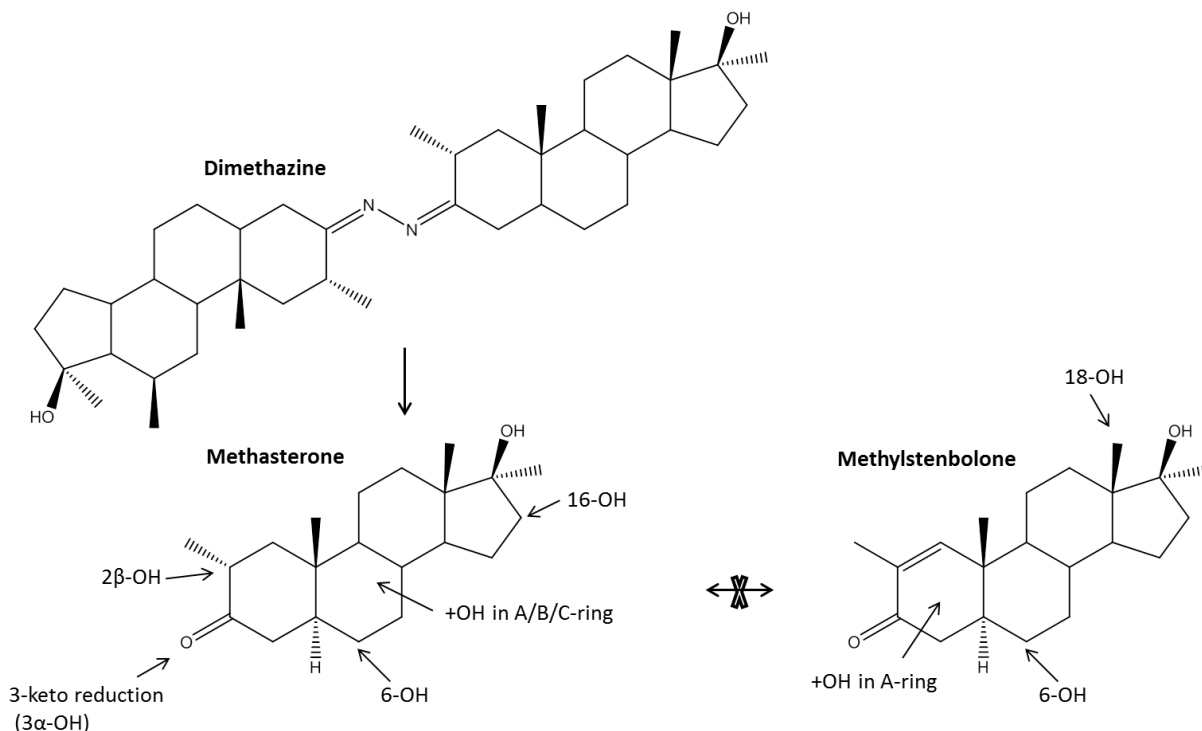


Figure 10.2. Overview of metabolic pathways observed for dimethazine, methasterone and methylstenbolone via *in vitro* and *in vivo* metabolism studies.

1.4 *Estra-4,9-diene-3,17-dione*

Estra-4,9-diene-3,17-dione was detected in the steroid product (Tren-X). Four metabolites were observed in the HLM incubation samples, of which three metabolites were also detected via the chimeric mouse model (Chapter 6). The main metabolite in both models was unequivocally identified as 17β -hydroxyestra-4,9-diene-3-one by comparison with commercially available reference material. This metabolite is also described as major human metabolite of *estra-4,9-diene-3,17-dione* in literature. Other metabolic modifications included (mono/di)hydroxylation of the parent compound and additional hydroxylation of 17β -hydroxyestra-4,9-diene-3-one (Figure 10.3). The dihydroxylated metabolite was however only detected via *in vitro* and non-chimeric mouse experiments, which implies careful extrapolation as human metabolite. In contrast to the other metabolic pathways, dihydroxylation was also not described in previously reported studies with *estra-4,9-diene-3,17-dione* [17, 18].

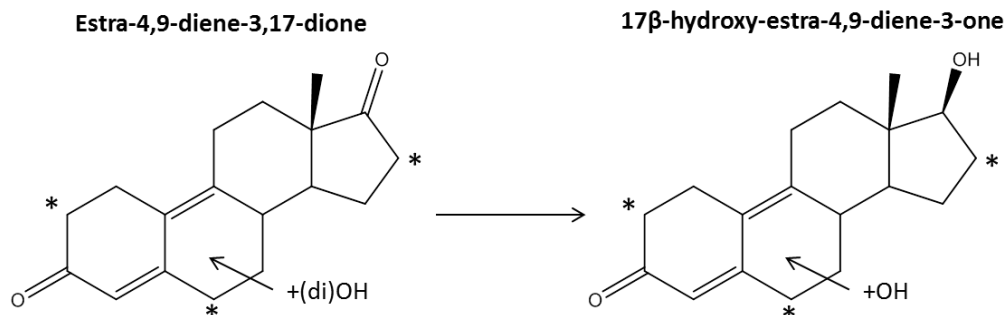


Figure 10.3. Overview of metabolic pathways observed for estra-4,9-diene-3,17-dione via *in vitro* and *in vivo* metabolism studies. The proposed positions for hydroxylations are at C2, C6 or C16 (indicated with a *).

1.5 General considerations about metabolism studies with (designer) steroids

The *in vitro* and *in vivo* metabolism studies with (designer steroids) indicated that both models are valuable alternatives for human administration studies. The models can complement each other to obtain an extensive overview of phase I and phase II metabolic pathways of (designer) steroids to identify multiple markers for detection. Therefore, an integrated approach can be applied as alternative for metabolism studies of performance enhancing substances, for which ethical and safety aspects limit the use of human volunteers (Figure 10.4).

In this approach preliminary metabolism studies can be performed using HLM and S9 liver fractions to obtain an initial overview of metabolic pathways. HLM and S9 liver fractions are fit for this purpose as they can be applied with a straightforward protocol and produce metabolites in a fast way.

In a second step the *in vitro* metabolic pathways can be verified by administration to both chimeric and non-chimeric mice. The chimeric mouse model complements the *in vitro* experiments with a more complete overview of phase I and phase II metabolic pathways in an *in vivo* environment. The application of *in vitro* models in the initial metabolism studies can also help to refine the number of animal experiments for example by optimizing the detection methods.

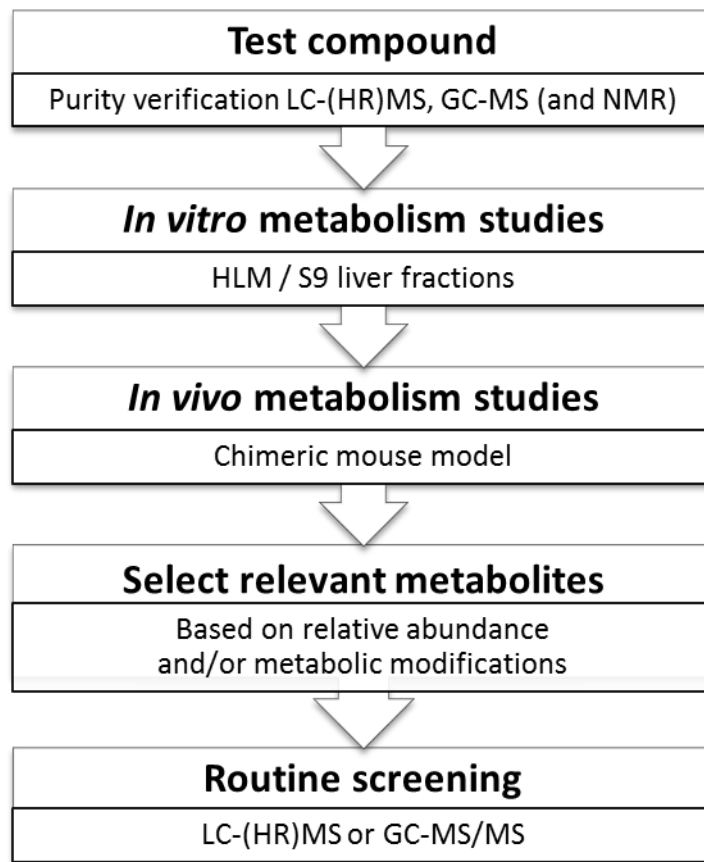


Figure 10.4. Integrated approach for metabolism studies.

The determination of typical human metabolites in both models can sometimes be difficult. (Poly)hydroxylated metabolites have in general the highest relative abundances in both models. However, cautious extrapolation of these metabolites, especially polyhydroxylated metabolites, to the more complex human situation is suggested. For example in human excretion studies hydroxylated 17-ketoprostanazol metabolites are more abundant than hydroxylated prostanazol metabolites, while in our models the opposite was observed.

Therefore, the following consideration can be helpful to predict *in vivo* human metabolism. Combined metabolic modifications (e.g. hydroxylation and additional oxidation or reduction) might be more easily interpreted as typical human metabolites. Furthermore, knowledge of metabolism of structurally related AAS can assist in the determination of possible human metabolic pathways.

For the chimeric mouse model comparison with results from non-chimeric mice facilitates the assessment of interspecies (mouse versus human) differences. However, careful interpretation of these observed differences is still recommended (cfr. above for prostanazol (1.1 Prostanazol)).

The phase II metabolism of the designer steroids prostanazol and dimethazine was also studied in the chimeric mouse model. An indirect detection strategy was applied including LLE without and with hydrolysis. However, application of direct detection of intact glucuronide and sulfate conjugates by LC-MS in the future should facilitate the interpretation of the phase II metabolism studies [19, 20].

1.6 *In vitro* application: synthesis of glucuronide conjugates

In chapter 7 *in vitro* (HLM) incubations were successfully applied to produce glucuronide conjugates of gestrinone, tetrahydrogestrinone, trenbolone, 4 β -hydroxystanozolol and 16 β -hydroxystanozolol. Since commercially available reference standards of glucuronide conjugates of these substances are missing, the *in vitro* produced glucuronide conjugates were used for comparative purposes to establish the metabolic nature and to further characterize substances observed in excretion urine samples.

Although the *in vitro* model was successfully applied for the production of glucuronide conjugates, a disadvantage of this *in vitro* production is the generally low yield of metabolites. This finding limits the use of *in vitro* techniques based on HLM or S9 liver fractions, to biologically synthesize metabolites as reference standards. However, this yield can be sufficient for comparative purposes to establish the metabolic nature of compounds.

2 Metabolism studies of other performance enhancing substances

2.1 SARMs: LGD-4033

The presence of LGD-4033 could be detected in a black market product purchased over the internet (Chapter 8). Since no reference material is commercially available and no detailed structural information is present, NMR analysis was applied to confirm the structure of LGD-4033 (Figure 10.5).

Consecutively, this black market product was used for the phase I and phase II *in vitro* (HLM and S9 liver fractions) metabolism studies of LGD-4033. The observed metabolic pathways are indicated in Figure 10.5.

The phase I metabolic pathways observed via *in vitro* (HLM) incubation studies by other research groups included (di)hydroxylations [21, 22] and ring opening combined with hydroxylation [21]. A common metabolite observed in all the *in vitro* metabolism studies is a dihydroxylated metabolite of LGD-4033. Furthermore, in the human excretion study of LGD-

4033 performed by Sobolevsky *et al.* the dihydroxylated LGD-4033 metabolite was a major human metabolite [21]. The human urine samples were, however, only analyzed in positive ionization mode. Based on our results, also re-evaluation of the relevance of observed metabolites for routine human urine samples in negative ionization mode is recommended. The combined phase I and phase II (UGT) metabolism studies led to similar glucuronide-conjugates as observed by Sobolevsky *et al.* [21].

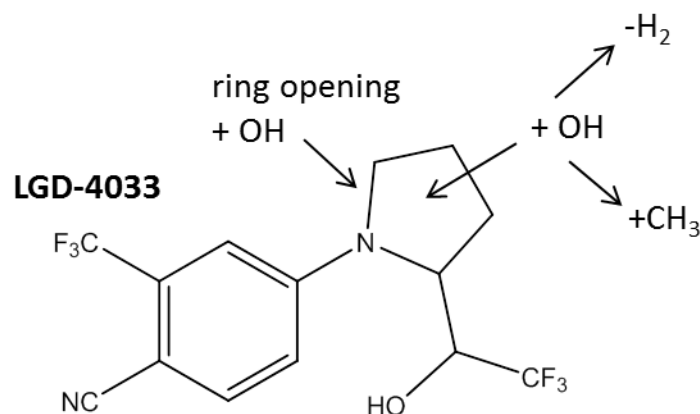


Figure 10.5. Overview of metabolic pathways observed for LGD-4033 via *in vitro* metabolism studies.

2.2 REV-ERB agonists: SR9009 and SR9011

SR9009 is available as black market product over the internet. Taking into account the similar structures and potential performance enhancing effects of SR9009 and SR9011 *in vitro* (HLM) metabolism studies of both substances were performed (Chapter 9). An overview of the metabolic pathways observed for SR9009 and SR9011 is shown in Figure 10.6. Besides hydroxylation of the parent compounds also losses of A, B, C, D and F', as indicated in Figure 10.6, were observed. The structures of A, B, C, D and F' are described in Chapter 9 (Figure 9.1 and Table 9.1). For the hydroxylations only one possible position of hydroxylation is indicated and also combinations of the presented pathways were observed.

Similar metabolic pathways were observed in the metabolism studies with HLM and human subjects of SR9009 and SR9011 by another research group [23].

To verify the presence of SR9009, SR9011 and their metabolites in doping control samples retrospective data analysis (reprocessing) and monitoring in our routine screening method, for a six month period (June 2015 – December 2015), were performed. The misuse of SR9009 and SR9011, during this period, could not be demonstrated. However, to further discourage the use

of these potential harmful compounds by both amateur and professional athletes incorporation of these substances into screening methods is highly recommended.

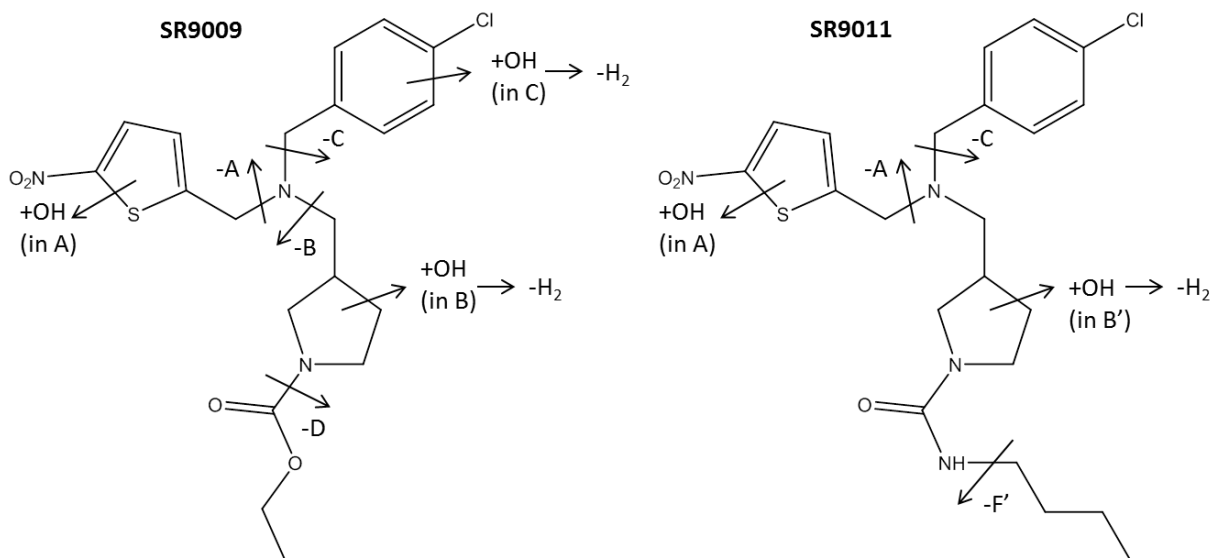


Figure 10.6. Overview of metabolic pathways observed for SR9009 and SR9011 via *in vitro* metabolism studies. The structures of A, B, C, D and F' are indicated in Chapter 9 (Figure 9.1 and Table 9.4).

2.3 Other applications: synthetic cannabinoids and peptides

Furthermore, the range of test compounds for the metabolism studies was extended with other emerging performance enhancing substances including synthetic cannabinoids and small peptide hormones in order to update the doping control screening methods.

The metabolism of the synthetic cannabinoids JWH-200 and JWH-122 was studied using HLM and the chimeric mouse model by De Brabanter *et al.* [19, 20]. Most of the *in vitro* detected metabolites were also confirmed in the chimeric mouse model. The *in vivo* mouse model also allowed to study the phase II metabolism of these synthetic cannabinoids [19, 20]. HLM incubations with synthetic cannabinoids were also performed to *in vitro* generate synthetic cannabinoid-metabolites as an alternative for excretion urines [24]. The metabolism of the following synthetic cannabinoids was studied: JWH-015, JWH-019, JWH-081, JWH-122, JWH-210, AM-2201 and AM-2233. These *in vitro* incubation samples were successfully applied in the quality control samples of the LC-HRMS screening method by spiking to negative urine samples, as at least one metabolite could be detected for each substance. Therefore, HLM incubations could be a valuable tool to use as alternative for excretion urines if no metabolite standard is available. However, as described above, the yield of the produced metabolites is rather low.

The *in vitro* model was also applied to study the metabolism of small peptide hormones by Esposito *et al.* [25]. In general, liver fractions are applied for metabolism studies of non-peptidic molecules with prevalent hepatic metabolism. The *in vitro* metabolism of peptides is generally studied using human serum or recombinant amidase models [25]. In this study the application of HLM and S9 fractions for the metabolism of small peptides was reported for the first time. Therefore HLM and S9 (both liver and kidney) fractions were incubated (without cofactors) with peptides including desmopressin, TB-500 (Thymosin- β 4), growth hormone-releasing peptide (GHRP)-2, GHRP-6, hexarelin, luteinizing hormone-releasing hormone (LHRH) and leuprolide. For each peptide several metabolites were detected after incubation with HLM and S9 fractions. The observed metabolites were similar to those after incubation with serum and indicated the presence of endopeptidase and exopeptidase activity. Deaminase activity was not demonstrated in the HLM, S9 fractions and serum. Hence, liver microsomes and S9 fractions can also be considered as a valuable tool to perform metabolism studies of small peptides.

3 Detection and identification of metabolites

A similar approach as suggested by Pozo *et al.* was applied for the detection and further characterization of metabolites (Chapter 1: Figure 1.9 and 7.2.4 *Sample preparation and analysis of in vitro and in vivo metabolism samples*).

For the initial identification of metabolites full scan mass spectra were obtained by GC-MS (after TMS-derivatization) and/or LC-MS. From these mass spectra the molecular mass of the metabolites could be derived. The observed mass differences in comparison to the molecular mass of the parent compound can be indicative for possible metabolic modifications. This modification can be verified by HRMS analysis by determining the mass deviations of the proposed chemical formulas.

Further structural characterization can be obtained by performing product ion scans of metabolites. Study of product ion scan mass spectra of parent compounds can also be helpful to determine typical, diagnostic fragment ions. Presence of these diagnostic or modified diagnostic fragment ions can indeed facilitate the identification of positions of the modifications. HRMS analysis can in this case also be useful to correlate observed product ions to structure specific fragments of the compounds.

Authentic reference standards are needed to unequivocally identify the structures of detected metabolites. However, only for a limited number of compounds such standards are commercially available. Ultimately, NMR analysis can be applied to unequivocally identify structures of parent compound and metabolites. However, the higher amount (mg range) of

metabolites needed to perform NMR analysis restricted the use of this technique during our *in vitro* and *in vivo* metabolic studies.

References

1. Rodchenkov G, Sobolevsky T, and Sizoi V (2006). New designer anabolic steroids from internet, In *Recent Advances in Doping Analysis (14)*, Proceedings of the 24th Cologne Workshop on dope analysis (Schänzer, W., Geyer, H., Gotzmann, A., and Mareck-Engelke, U., Eds.), pp 141-150, Sport & Buch Strauss, Cologne, Germany.
2. Kazlauskas R (2006). Miscellaneous projects in sports drug testing at the National Measurement Institute, Australia, 2005, In *Recent Advances in Doping Analysis (14)*, Proceedings of the 24th Cologne Workshop on dope analysis (Schänzer, W., Geyer, H., Gotzmann, A., and Mareck-Engelke, U., Eds.), pp 129-140, Sport & Buch Strauss, Cologne, Germany.
3. Yum T, Lee J, Paeng K, and Kim Y (2011). Determination of metabolites of prostanazol in human urine by LC/ESI/MS and GC/TOF-MS. *Analytical Science and Technology* 24, 173-182.
4. Shimada Y, Yoritaka A, Tanaka Y, Miyamoto N, Ueno Y, Hattori N, and Takao U (2012). Cerebral Infarction in a Young Man Using High-dose Anabolic Steroids. *J. Stroke Cerebrovasc. Dis.* 21.
5. Jasiurkowski B, Raj J, Wisinger D, Carlson R, Zou LX, and Nadir A (2006). Cholestatic jaundice and IgA nephropathy induced by OTC muscle building agent superdrol. *Am. J. Gastroenterol.* 101, 2659-2662.
6. Nasr J, and Ahmad J (2009). Severe Cholestasis and Renal Failure Associated with the Use of the Designer Steroid Superdrol (TM) (Methasteron (TM)): A Case Report and Literature Review. *Dig. Dis. Sci.* 54, 1144-1146.
7. Singh V, Rudraraju M, Carey EJ, Byrne TJ, Vargas HE, Williams JE, Balan V, Douglas DD, and Rakela J (2009). Severe Hepatotoxicity Caused by a Methasteron-containing Performance-enhancing Supplement. *J. Clin. Gastroenterol.* 43, 287-287.
8. Government of the United States. Designer anabolic steroid control act of 2012 (2012). <https://www.govtrack.us/congress/bills/112/s3431/text> (access date 04/04/2014).
9. Masse R, and Goudreault D (1992). Studies on anabolic-steroids. 11. 18-hydroxylated metabolites of mesterolone, methenolone and stenbolone - New steroids isolated from human urine. *J. Steroid Biochem. Mol. Biol.* 42, 399-410.
10. Fragkaki AG, Angelis YS, Tsantili-Kakoulidou A, Koupparis M, and Georgakopoulos C (2009). Schemes of metabolic patterns of anabolic androgenic steroids for the estimation of metabolites of designer steroids in human urine. *J. Steroid Biochem. Mol. Biol.* 115, 44-61.
11. Goudreault D, and Masse R (1991). Studies on anabolic-steroids. 6. Identification of urinary metabolites of stenbolone acetate (17-beta-acetoxy-2-methyl-5-alpha-androst-1-en-3-one) in human by gas-chromatography mass-spectrometry. *J. Steroid Biochem. Mol. Biol.* 38, 639-655.
12. Cavalcanti GD, Leal FD, Garrido BC, Padilha MC, and Neto FR (2012). Detection of designer steroid methylstenbolone in "nutritional supplement" using gas chromatography and tandem mass spectrometry: elucidation of its urinary metabolites. *Steroids* 78, 228-233.
13. Parr MK, Opfermann G, and Schänzer W (2006). Detection of new 17-alkylated anabolic steroids on WADA 2006 list, In *Recent Advances in Doping Analysis (14)*, Proceedings of the 24th Cologne Workshop on dope analysis (Schänzer W, Geyer H, Gotzmann A, and Mareck-Engelke U, Eds.), pp 249-258, Sport & Buch Strauss, Cologne, Germany.

14. Bylina DV, Gryn SV, and Tkachuk AA (2012). Detection of the methasterone and its metabolite in human urine by the gas chromatography/high resolution mass spectrometry (HRMS) method. *Methods and objects of chemical analysis* 7, 87-93.
15. Gauthier J, Goudreault D, Poirier D, and Ayotte C (2009). Identification of drostanolone and 17-methylandrostanolone metabolites produced by cryopreserved human hepatocytes. *Steroids* 74, 306-314.
16. Ayotte C, Goudreault D, Cyr D, Gauthier J, Ayotte P, Larochelle C, and Poirier D (2006). Characterisation of chemical and pharmacological properties of new steroids related to doping of athletes, In *Recent Advances in Doping Analysis (14)* , Proceedings of the 24th Cologne Workshop on dope analysis (Schänzer, W., Geyer, H., Gotzmann, A., and Mareck-Engelke, U., Eds.), pp 151-160, Sport & Buch Strauss, Cologne, Germany.
17. Parr MK, Geyer H, Gütschow M, Haenelt N, Opfermann G, Thevis M, and Schänzer W (2008). New steroids on the "supplement" market, In *Recent Advances in Doping Analysis (16)* , Proceedings of the 26th Cologne Workshop on dope analysis (Schänzer W, Geyer H, Gotzmann A, and Mareck-Engelke U, Eds.), pp 73-82, Sport & Buch Strauss, Cologne, Germany.
18. Scarth JP, Clarke AD, Teale P, and Pearce CM (2010). Comparative in vitro metabolism of the 'designer' steroid estra-4,9-diene-3,17-dione between the equine, canine and human: Identification of target metabolites for use in sports doping control. *Steroids* 75, 643-652.
19. De Brabanter N, Esposito S, Geldof L, Lootens L, Meuleman P, Leroux-Roels G, Deventer K, and Van Eenoo P (2013). In vitro and in vivo metabolisms of 1-pentyl-3-(4-methyl-1-naphthoyl)indole (JWH-122). *Forensic Toxicol.* 31, 212-222.
20. De Brabanter N, Esposito S, Tudela E, Lootens L, Meuleman P, Leroux-Roels G, Deventer K, and Van Eenoo P (2013). In vivo and in vitro metabolism of the synthetic cannabinoid JWH-200. *Rapid Commun. Mass Spectrom.* 27, 2115-2126.
21. Sobolevsky T, Dikunets M, Dudko G, and Rodchenkov G (2015). Metabolism study of selective androgen receptor modulator LGD-4033, In Poster presented at Manfred Donike Workshop - 33rd Cologne workshop on dope analysis (01/03/2015-06/03/2015).
22. Thevis M, Lagojda A, Kuehne D, Thomas A, Dib J, Hansson A, Hedeland M, Bondesson U, Wigger T, Karst U, and Schänzer W (2015). Characterization of a non-approved selective androgen receptor modulator drug candidate sold via the Internet and identification of in vitro generated phase-I metabolites for human sports drug testing. *Rapid Commun. Mass Spectrom.* 29, 991-999.
23. Sobolevsky T, Dikunets M, and Rodchenkov G (2015). Metabolism study of GSK4122, SR9009 and SR9011, new "exercise-in-a-pill" drug candidates, In Poster presented at Manfred Donike Workshop - 33rd Cologne workshop on dope analysis (01/03/2015-06/03/2015).
24. Geldof L, Deventer K, and Van Eenoo P (2014). In vitro generated synthetic cannabinoid-metabolites as an alternative for excretion urines, In Poster presented at Manfred Donike Workshop - 32nd Cologne workshop on dope analysis (31/03/2014-04/04/2014).
25. Esposito S, Deventer K, Geldof L, and Van Eenoo P (2015). In vitro models for metabolic studies of small peptide hormones in sport drug testing. *J. Pept. Sci.* 21, 1-9.

Chapter 11

Conclusions and future perspectives

1 Conclusions

Several exogenous AAS or designer steroids, such as prostanazol, dimethazine and estradienedione, were detected in black market products purchased over the internet. As these products are available to athletes, both recreational as well as professional, the risk for misuse is high and realistic. Hence, preventive anti-doping research, and especially metabolism studies, is essential to develop efficient screening methods. By anticipating this potential misuse, the ethics of sports and the health of athletes can be safeguarded. In case of designer steroids ethical objections limit the use of human volunteers for these metabolism studies. Moreover, contamination issues and incorrect labeling, as observed for the steroid product labelled to contain only methylstenbolone, give rise to additional concerns about their safety. To ensure a fast response to evolutions of performance enhancing substances in black market products, alternative models for metabolism studies are required.

In this study the use of *in vitro* (HLM / S9 liver fractions) and *in vivo* (chimeric mouse) models was examined as alternative for human administration studies of doping related compounds. HLM and S9 liver fractions showed to be valuable tools for metabolism studies with designer steroids. The uPA^{+/+}-SCID chimeric mouse model has already proven its applicability for metabolism studies with steroids. In this study the chimeric mouse model was also a valid tool for metabolism studies with designer steroids. The observed metabolic pathways for the designer steroids in both models were similar to human administration studies reported in literature.

Therefore, an integrated approach of both models can be applied as alternative for metabolism studies of performance enhancing substances, for which ethical and safety aspects limit the use of human volunteers. This approach has also the advantage that the number of animal experiments for the metabolism studies can be reduced.

HLM were successfully applied to produce *in vitro* glucuronide conjugates as alternative for human excretion urine samples. These samples can be useful for comparative purposes (e.g. method development or to establish metabolic nature) when no reference standard is available. The yield however limits the use of this *in vitro* approach to produce high amounts of reference material.

HLM and S9 liver fractions allow a fast response to new performance enhancing substances with even less ethical objections than the use of the chimeric mouse model. The test compounds for the *in vitro* metabolism studies were extended to other classes of performance enhancing substances including SARMs (e.g. LGD-4033) and REV-ERB agonists (SR9009 and SR9011). The observed metabolic pathways were also in accordance with reported metabolism studies in

human subjects. Therefore, the *in vitro* model based on HLM and S9 liver fractions is also a valid tool for these classes of substances.

Retrospective data analysis can also help to close the gap between the appearance of new doping substances and the incorporation into screening methods by doping control laboratories.

2 Future perspectives

These *in vitro* (and *in vivo*) models are valuable and ethically acceptable alternatives for human metabolism studies of non-pharmaceutical grade substances. Although these alternative models allow a fast response to new doping threats, preventive anti-doping research requires also vigilance for evolutions of performance enhancing substances. Monitoring of black market products and cooperation with customs can be helpful for this early detection of new doping threats. As observed in this study for designer steroids, SARMs and REV-ERB agonists, new emerging performance enhancing substances, from both established and potential new classes, might be expected in the future. For example, recently, small molecule ESAs, i.e. hypoxia-inducible factor (HIF) stabilizers, were introduced in black market products [1, 2]. Although still under clinical investigation, a first positive doping case of a HIF stabilizer was reported [3]. Therefore, application of the alternative metabolism models might also be helpful to improve detection windows of these substances.

In this study the primary focus of the *in vitro* procedure were phase I and phase II (UGT) pathways. The *in vitro* protocol should also be optimized in the future to study sulfate conjugation (and potentially also epimerization reactions). Since SULTs are characterized by a 'high affinity - low capacity' pathway and are susceptible for product inhibition, the production of sulfate conjugates by S9 liver fractions is complicated. To obtain a more complete study of the metabolic pathways, combined incubations with HLM and S9 liver fractions and eventually addition of NAD as cofactor should also be tested [4].

Homogenized horse livers were successfully applied for the generation of phase I and phase II metabolites as an alternative for horse liver microsomes by Wong *et al.* [5, 6]. This model has the advantage over the liver microsomes that a more simple preparation procedure can be applied and the addition of cofactors is not required. Homogenized human livers were also applied before [7, 8] for phase I metabolism studies. Although more ethical issues are related to the supply of human liver tissue, it would be interesting to investigate the use of homogenized human liver for phase I and II metabolism studies for doping control purposes.

The low production rate of metabolites observed in the *in vitro* incubation samples limits the further characterization of the metabolites by NMR analysis and the application of these *in vitro*

models to biologically synthesize reference standards. Scaling up of the *in vitro* production can be helpful to overcome these low yields [9, 10]. Other scaling up strategies using recombinant expressed enzymes such as supersomes [11, 12] and chemical enzyme-induced animal tissues [13, 14] for phase I and phase II metabolites have been reported. Other approaches based on microbial (fungus) assays, for example *Cunninghamella elegans*, have also been described to produce higher amounts of metabolites [15]. The presence of CYP450 enzymes and phase II (UGT and SULT) enzymes in these fungus species enables to mimic mammalian drug biotransformations [15-20]. These fungus based models could therefore be applied for a large-scale synthesis of potentially relevant human metabolites identified in other metabolism studies [15]. The application of *in vitro* models for the synthesis of metabolites has the advantage that no knowledge of the structure is needed in advance and stereospecific conjugation is performed [9, 13]. The produced metabolites can be separated by preparative high performance liquid chromatography (HPLC) fraction collection [9].

For the synthesis of reference standards, alternative production processes (e.g. chemical synthesis) are recommended if higher amounts, than for comparative purposes, are needed.

References

1. Jelkmann W (2009). Erythropoiesis Stimulating Agents and Techniques: A Challenge for Doping Analysts. *Curr. Med. Chem.* 16, 1236-1247.
2. Beuck S, Schänzer W, and Thevis M (2012). Hypoxia-inducible factor stabilizers and other small-molecule erythropoiesis-stimulating agents in current and preventive doping analysis. *Drug Test. Anal.* 4, 830-845.
3. Cyclingnews.com. <http://www.cyclingnews.com/news/taborre-positive-for-novel-epo-stimulating-drug-fg-4592/> (access date 04.10.2015).
4. Scarth JP, Spencer HA, Timbers SE, Hudson SC, and Hillyer LL (2010). The use of in vitro technologies coupled with high resolution accurate mass LC-MS for studying drug metabolism in equine drug surveillance. *Drug Test. Anal.* 2, 1-10.
5. Wong JKY, Tang FPW, and Wan TSM (2011). In vitro metabolic studies using homogenized horse liver in place of horse liver microsomes. *Drug Test. Anal.* 3, 393-399.
6. Wong JK, Chan GH, Leung DK, Tang FP, and Wan TS (2015). Generation of phase II in vitro metabolites using homogenized horse liver. *Drug Test Anal.*
7. Bailey DN (1995). Cocapropylene (propylcocaine) formation by human liver in vitro. *J Anal Toxicol* 19, 1-4.
8. Ammon S, von Richter O, Hofmann U, Thon KP, Eichelbaum M, and Mikus G (2000). In vitro interaction of codeine and diclofenac. *Drug Metab Dispos* 28, 1149-1152.
9. Levesque JF, Gaudreault M, Aubin Y, and Chauret N (2005). Discovery, biosynthesis, and structure elucidation of new metabolites of norandrostenedione using in vitro systems. *Steroids* 70, 305-317.
10. Levesque JF, Templeton E, Trimble L, Berthelette C, and Chauret N (2005). Discovery, biosynthesis, and structure elucidation of metabolites of a doping agent and a direct analogue, tetrahydrogestrinone and gestrinone, using human hepatocytes. *Anal. Chem.* 77, 3164-3172.
11. Kuuranne T, Kurkela M, Thevis M, Schänzer W, Finel M, and Kostianen R (2003). Glucuronidation of anabolic androgenic steroids by recombinant human UDP-glucuronosyltransferases. *Drug Metab. Dispos.* 31, 1117-1124.
12. Vail RB, Homann MJ, Hanna I, and Zaks A (2005). Preparative synthesis of drug metabolites using human cytochrome P450s 3A4, 2C9 and 1A2 with NADPH-P450 reductase expressed in *Escherichia coli*. *J Ind Microbiol Biotechnol* 32, 67-74.
13. Hintikka L, Kuuranne T, Aitio O, Thevis M, Schänzer W, and Kostianen R (2008). Enzyme-assisted synthesis and structure characterization of glucuronide conjugates of eleven anabolic steroid metabolites. *Steroids* 73, 257-265.
14. Rao GS, Haueter G, Rao ML, and Breuer H (1976). Improved assay for steroid glucuronyltransferase in rat-liver microsomes. *Anal Biochem.* 74, 35-40.
15. Asha S, and Vidyavathi M (2009). *Cunninghamella* - A microbial model for drug metabolism studies - A review. *Biotechnol. Adv.* 27, 16-29.

Chapter 11 – Conclusions and future perspectives

16. Marvalin C, and Azerad R (2011). Microbial production of phase I and phase II metabolites of propranolol. *Xenobiotica* 41, 175-186.
17. Wackett LP, and Gibson DT (1982). Metabolism of xenobiotic compounds by enzymes in cell-extracts of the fungus *Cunninghamella elegans*. *Biochem. J.* 205, 117-122.
18. Choudhary MI, Khan NT, Musharraf SG, Anjum S, and Atta ur R (2007). Biotransformation of adrenosterone by filamentous fungus, *Cunninghamella elegans*. *Steroids* 72, 923-929.
19. Guddat S, Fussholler G, Beuck S, Thomas A, Geyer H, Rydevik A, Bondesson U, Hedeland M, Lagojda A, Schänzer W, and Thevis M (2013). Synthesis, characterization, and detection of new oxandrolone metabolites as long-term markers in sports drug testing. *Anal. Bioanal. Chem.* 405, 8285-8294.
20. Thevis M, Lagojda A, Kuehne D, Thomas A, Dib J, Hansson A, Hedeland M, Bondesson U, Wigger T, Karst U, and Schänzer W (2015). Characterization of a non-approved selective androgen receptor modulator drug candidate sold via the Internet and identification of in vitro generated phase-I metabolites for human sports drug testing. *Rapid Commun. Mass Spectrom.* 29, 991-999.

Summary

Summary

Over the last years, doping control laboratories worldwide have put enormous efforts into preventive anti-doping research. This type of research is important for doping control purposes to anticipate new doping threats. Hence, these investigations can help to close the gap between doping control laboratories and doped athletes. Effective detection methods contribute to deter the use of performance enhancing substances. Therefore they are of great significance to warrant the ethics of sports and the health of athletes. Metabolism studies are essential for efficient screening methods for these substances, as metabolites can improve detection (windows). New performance enhancing substances can be available as pharmaceutical preparations or as black market products, often prior to their clinical approval. Therefore there is a quest for ethically acceptable alternatives for human metabolism studies of non-pharmaceutical grade substances.

In this study the use of alternative *in vitro* and *in vivo* models for metabolism studies was evaluated. The *in vitro* models included human liver microsomes (HLM) and S9 liver fractions. The *in vivo* model involved an uPA^{+/+}-SCID mouse model transplanted with human hepatocytes. This chimeric mouse model has already proven to be a valuable tool for metabolism studies of anabolic androgenic steroids [1].

Several designer steroids including prostanazol, methylstenbolone, methasterone, dimethazine and estradienedione were detected in black market products purchased over the internet. An integrated approach of the *in vitro* and *in vivo* models was applied to elucidate the metabolism of these designer steroids (Part 2). The obtained results showed a good correlation with reported human excretion studies. Therefore, both models can be considered as valuable tools for designer steroids. The advantages of this integrated approach include that the initial application of *in vitro* models can refine the number of animal experiments and the chimeric mouse model complements the *in vitro* experiments with a more complete overview of phase I and phase II metabolic pathways in an intact organism.

The applicability of the *in vitro* model to produce reference material of non-commercially available substances (glucuronide conjugates) was also examined (Part 2 - Chapter 7). Glucuronide conjugates were successfully produced *in vitro* for gestrinone, tetrahydrogestrinone, trenbolone, 4 β -hydroxystanozolol and 16 β -hydroxystanozolol. This *in vitro* production of reference material is useful for comparative purposes (e.g. to establish metabolic nature and for the development of detection methods), however due to the limited yield, production of high amounts of reference standards by these *in vitro* models is not efficient.

Since the number and type of performance enhancing substances are continuously evolving, the test compounds were extended to other classes of potential performance enhancing substances (Part 3). *In vitro* (HLM and/or S9 liver fractions) incubations were applied to elucidate the

metabolism of selective androgen receptor modulators (SARMs; LGD-4033) and REV-ERB agonists (SR9009 and SR9011). These *in vitro* metabolism studies allow a fast response, with even less ethical constraints than the chimeric mouse model. Comparison with human excretion studies indicates that the *in vitro* model, based on HLM and S9 liver fractions, is also a valuable alternative for metabolism studies of these substances.

In conclusion, both the *in vitro* model and the integrated approach can be considered as valuable tools for metabolism studies of compounds for which ethical and safety constraints limit the use of human volunteers. Therefore, the application of these models might also improve the response to new doping threats in the future.

References

1. Lootens, L. (2010) The mouse with the humanized liver: A new model for metabolic studies of anabolic steroids in man, In *Faculty of Medicine and Health Sciences*, Ghent University, PhD thesis, Ghent.

Samenvatting

Gedurende de voorbije jaren hebben dopingcontrolelaboratoria wereldwijd sterk geïnvesteerd in preventief anti-doping onderzoek. Dit type van onderzoek is immers belangrijk in het kader van dopingcontrole om adequaat te reageren op nieuwe dopingproducten. Deze onderzoeken kunnen dus helpen om de kloof te dichten van dopingcontrolelaboratoria ten opzichte van gedopeerde atleten.

Het bestaan van effectieve detectiemethodes heeft een ontradend effect op het gebruik van prestatiebevorderende substanties zodat ze van groot belang zijn om de ethiek van de sport en de gezondheid van de atleten te beschermen. Voor het ontwikkelen van efficiënte screening methodes voor deze substanties zijn metabole studies essentieel aangezien metaboliëten de detectie(tijden) kunnen verbeteren. Nieuwe prestatiebevorderende middelen kunnen zowel als farmaceutische preparaten als 'zwarte markt' producten, beschikbaar zijn, vaak vóór hun goedkeuring voor klinisch gebruik. Hierdoor wordt er gezocht naar ethisch aanvaardbare alternatieve modellen voor humane metabole studies met substanties waarvoor geen preparaten van farmaceutische kwaliteit voor handen zijn.

In deze studie werd het gebruik van alternatieve *in vitro* en *in vivo* modellen voor metabole studies nagegaan. Het onderzochte *in vitro* model omvatte humane lever microsomen (HLM) en S9 lever fracties. Het *in vivo* model werd gebaseerd op een uPA^{+/+}-SCID muismodel met getransplanteerde humane hepatocyten. Dit chimeer muismodel werd reeds als waardevol model beschouwd voor metabole studies met anabole androgene steroïden [1].

Verscheidene designer steroïden zoals prostanazol, methylstenbolone, methasterone, dimethazine en estradiendione werden gedetecteerd in 'zwarte markt' producten die aangekocht werden via het internet. Een integrale benadering met de *in vitro* en *in vivo* modellen werd toegepast om het metabolisme van deze designer steroïden op te helderen (Deel 2). De verkregen resultaten vertoonden een goede correlatie met humane excretiestudies gerapporteerd in de literatuur. Beide modellen kunnen bijgevolg als waardevolle hulpmiddelen voor metabole studies met designer steroïden beschouwd worden. De voordelen van deze integrale benadering is dat de initiële toepassing van *in vitro* modellen het aantal dierenexperimenten kan beperken en dat het chimeer muismodel de *in vitro* experimenten aanvult met een meer compleet overzicht van fase I en fase II metabole pathways in een intact organisme.

De toepasbaarheid van het *in vitro* model om referentiemateriaal, van niet-commercieel beschikbare substanties (glucuronide conjugaten), te produceren, werd ook onderzocht (Deel 2 - Hoofdstuk 7). Glucuronide conjugaten werden succesvol geproduceerd *in vitro* voor gestrinone, tetrahydrogestrinone, trenbolone, 4 β -hydroxystanozolol en 16 β -hydroxystanozolol. Het *in vitro* genereren van referentiemateriaal is zeker bruikbaar voor het toepassen van vergelijkende doeleinden (zoals het bepalen van de metabole aard en opstellen van methodes).

Het beperkte rendement zorgt er echter voor dat het gebruik van deze *in vitro* modellen voor het produceren van grote hoeveelheden referentiestandaarden niet zo efficiënt is.

Aangezien het aantal en de aard van de prestatiebevorderende middelen blijft evolueren, werden de te onderzoeken substanties uitgebreid naar andere klassen van potentiële prestatiebevorderende middelen (Deel 3). *In vitro* (HLM en/of S9 lever fracties) incubaties werden toegepast om het metabolisme van selectieve androgeen receptor modulators (SARMs; LGD-4033) en REV-ERB agonisten (SR9009 and SR9011) op te helderen. Deze *in vitro* metabole studies laten immers een snelle respons toe, met zelfs minder ethische bezwaren dan het chimeer muis model. Vergelijking met humane excretiestudies gaf aan dat het *in vitro* model, gebaseerd op HLM en S9 leverfracties als een waardig alternatief kan beschouwd worden voor metabole studies met deze substanties.

Tot besluit, zowel het *in vitro* model als de integrale strategie kunnen beschouwd worden als waardevolle hulpmiddelen voor het uitvoeren van metabole studies van substanties waarvoor ethische bezwaren en aspecten omtrent hun veiligheid de administratie aan humane vrijwilligers verhinderen. Het toepassen van deze modellen zou dan ook in de toekomst de reactie op nieuwe bedreigingen op vlak van doping kunnen verbeteren.

Referenties

1. Lootens, L. (2010) The mouse with the humanized liver: A new model for metabolic studies of anabolic steroids in man, In *Faculty of Medicine and Health Sciences*, Ghent University, PhD thesis, Ghent.

Curriculum Vitae

1 Personal information

Lore Geldof

Born on April 25th, 1988 in Roeselare

Belgian nationality

Contact Address Doping Control Laboratory
Ghent University
Department of Clinical Biology, Microbiology and Immunology
Faculty of Medicine and Health Sciences
Technologiepark 30B
9052 Zwijnaarde
Belgium
+32 9 331 32 92

E-mail-address: Lore.Geldof@UGent.be

2 Education

2011-2016	Ghent University – Doping Control Laboratory (DoCoLab) PhD student Promotor: Prof. Dr. ir. Peter Van Eenoo Co-Promotor: Dr. Leen Lootens
2006-2011	Ghent University Master in Biomedical Sciences Thesis: 'Detection of methandienone in urine using GC-triple quadrupole MS'
2000-2006	Burgerschool Roeselare Sciences-Mathematics

3 Scientific contributions

3.1 Papers

De Brabanter N, Van Gansbeke W, **Geldof L**, and Van Eenoo P (2012). An improved gas chromatography screening method for doping substances using triple quadrupole mass spectrometry, with an emphasis on quality assurance, *Biomedical Chromatography* 26, 1416-1435.

De Brabanter N, Esposito S, **Geldof L**, Lootens L, Meuleman P, Leroux-Roels G, Deventer K, and Van Eenoo P (2013). *In vitro* and *in vivo* metabolisms of 1-pentyl-3-(4-methyl-1-naphthoyl)indole (JWH-122), *Forensic Toxicology* 31, 212-222.

Geldof L, Lootens L, Polet M, Eichner D, Campbell T, Nair V, Botrè F, Meuleman P, Leroux-Roels G, Deventer K, Van Eenoo P (2014). Metabolism of methylstenbolone studied with human liver microsomes and the uPA^{+/+}-SCID chimeric mouse model, *Biomedical Chromatography* 28, 974-985.

Tudela E., Deventer K., **Geldof L.**, Van Eenoo P. (2014). Urinary detection of conjugated and unconjugated anabolic steroids by dilute-and-shoot liquid chromatography-high resolution mass spectrometry. *Drug Testing and Analysis* 7, 95-108.

Esposito S, Deventer K, **Geldof L**, Van Eenoo P (2014). *In vitro* models for metabolic studies of small peptide hormones in sport drug testing. *Journal of Peptide Science* 21, 1-9.

Geldof L, Pozo OJ, Lootens L, Morthier W, Van Eenoo P, Deventer K (2015). *In vitro* metabolism study of a black market product containing SARM LGD-4033. *Drug Testing and Analysis* (In press; DOI: 10.1002/dta.1930).

Geldof L, Tudela E, Lootens L, Van Lysebeth J, Meuleman P, Leroux-Roels G, Van Eenoo P and Deventer K (2015). *In vitro* and *in vivo* metabolism studies of dimethazine. *Biomedical Chromatography* (In press; DOI: 10.1002/bmc.3668).

Geldof L, Lootens L, Decroix L, Botrè F, Meuleman P, Leroux-Roels G, Deventer K and Van Eenoo P (2016). Metabolic studies of prostanazol with the uPA-SCID chimeric mouse model and human liver microsomes. *Steroids* (In press; DOI: 10.1016/j.steroids.2016.01.005).

Geldof L, Deventer K, Tudela E and Van Eenoo P (2016). *In vitro* metabolism studies of REV-ERB α agonists SR9009 and SR9011. (To be submitted).

Geldof L, Lootens L, Van Lysebeth J, Meuleman P, Leroux-Roels G, Deventer K and Van Eenoo P (2016). *In vitro* and *in vivo* metabolism studies with a steroid product containing estra-4,9-diene-3,17-dione. (To be submitted).

3.2 Proceedings

Lootens L, **Geldof L**, Decroix L, Deventer K, Botrè F, Leroux-Roels G, Meuleman P and Van Eenoo P (2012). Metabolic study of prostanazol using human liver microsomes and humanized mice. *Recent Advances in Doping Analysis* (20). Proceedings of the 30th Manfred Donike Workshop on Dope Analysis, Cologne, 58-64.

De Brabanter N, Van Gansbeke W, **Geldof L** and Van Eenoo P (2012). Improvements in GC-QqQ-MS screening, 1 year of experience, *Recent Advances in Doping Analysis* (20). Proceedings of the 30th Manfred Donike Workshop on Dope Analysis, Cologne, 73.

Geldof L, Lootens L, Deventer K, Polet M, Eichner D, Botrè F, Meuleman P, Leroux-Roels G and Van Eenoo P (2013). *In vitro* and *in vivo* metabolism studies of a nutritional supplement containing methylstenbolone, *Recent Advances in Doping Analysis* (21). Proceedings of the 31st Manfred Donike Workshop on Dope Analysis, Cologne, 41.

Tudela E, Deventer K, **Geldof L**, Van Eenoo P (2013). Detection and identification of glucuronidated stanozolol metabolites by liquid chromatography-tandem mass spectrometry, *Recent Advances in Doping Analysis* (21). Proceedings of the 31st Manfred Donike Workshop on Dope Analysis, Cologne, 27-32.

Lootens L, **Geldof L**, Tudela E, Meuleman P, Leroux-Roels G, Botrè F, Deventer K, Van Eenoo P (2013). Metabolic study of oxabolone using human liver microsomes and humanized mice, *Recent Advances in Doping Analysis* (21), Proceedings of the 31st Manfred Donike Workshop on Dope Analysis, Cologne, 42-47.

De Brabanter N, Esposito S, **Geldof L**, Lootens L, Deventer K and Van Eenoo P (2013). Phase I and phase II metabolism of synthetic cannabinoids, the Ghent strategy, Recent Advances in Doping Analysis (21). Proceedings of the 31st Manfred Donike Workshop on Dope Analysis, Cologne, 17.

Geldof L, Tudela Palomar E, Lootens L, Van Lysebeth J, Meuleman P, Leroux-Roels G, Deventer K, Van Eenoo P (2014). Metabolic study of a steroid product containing dimethazine using human liver microsomes and a chimeric mouse model, Recent Advances in Doping Analysis (22). Proceedings of the 32nd Manfred Donike Workshop on Dope Analysis, Cologne, 226.

Tudela E, Deventer K, **Geldof L**, Van Eenoo P. Detection of conjugated and unconjugated anabolic steroids in urine by dilute-and-shoot liquid chromatography-high resolution mass spectrometry (2014). Recent Advances in Doping Analysis (22). Proceedings of the 32nd Manfred Donike Workshop on Dope Analysis, Cologne, 232.

Esposito S, Deventer K, **Geldof L**, Van Eenoo P (2014). Doping control analysis of small peptides hormones: an update, Recent Advances in Doping Analysis (22). Proceedings of the 32nd Manfred Donike Workshop on Dope Analysis, Cologne, 36-41.

Geldof L, Tudela E, Van Gansbeke W, Lootens L, Morthier W, Deventer K, Van Eenoo P (2015). *In vitro* metabolism studies of black market products. Recent Advances in Doping Analysis (23). Proceedings of the 33rd Manfred Donike Workshop on Dope Analysis, Cologne, 238.

3.3 Lectures

Geldof L, Lootens L, Polet M, Eichner D, Campbell T, Nair V, Botrè F, Meuleman P, Leroux-Roels G, Deventer K, Van Eenoo P (2013). *In vitro* and *in vivo* metabolism studies of a nutritional supplement containing methylstenbolone 31st Manfred Donike workshop on dope analysis, Cologne.

Geldof L, Tudela Palomar E, Lootens L, Van Lysebeth J, Meuleman P, Leroux-Roels G, Deventer K, Van Eenoo P (2014). Metabolic study of a steroid product containing dimethazine using human liver microsomes and a chimeric mouse model. 32nd Manfred Donike workshop on dope analysis, Cologne.

Geldof L, Tudela E, Van Gansbeke W, Lootens L, Morthier W, Deventer K, Van Eenoo P (2015). *In vitro* metabolism studies of black market products. 33rd Manfred Donike workshop on dope analysis, Cologne.

Geldof L, Deventer K, Tudela E and Van Eenoo P (2016). *In vitro* metabolism studies of REV-ERB α agonists SR9009 and SR9011. 34th Manfred Donike workshop on dope analysis, Cologne.

3.4 Posters

Geldof L, Deventer K, Van Eenoo P (2014). *In vitro* generated synthetic cannabinoid-metabolites as an alternative for excretion urines. 32nd Manfred Donike workshop on dope analysis, Cologne.

4 Seminars

Research Institute of Chromatography (RIC) seminar: Chemische analysis.

Kortrijk, Belgium

22/01/2013

